Establishment of *in vitro* and *in vivo* models with underlying mitochondrial dysfunction for testing idiosyncratic drug toxicity

Inauguraldissertation

zur

Erlangung der Würde eines Doktors der Philosophie

vorgelegt der

Philosophisch-Naturwissenschaftlichen Fakultät

der Universität Basel

von

Patrizia Hägler

aus Langenbruck (BL)

Basel, 2015

Originaldokument gespeichert auf dem Dokumentenserver der Universität Basel
edoc.unibas.ch

Dieses Werk ist lizenziert unter einer Creative Commons Namensnennung - Nicht kommerziell - Keine Bearbeitungen 4.0 International Lizenz.

Genehmigt von der Philosophisch-Naturwissenschaftlichen Fakultät

auf Antrag von

Prof. Dr. Stephan Krähenbühl

Prof. Dr. Jörg Huwyler

Basel, den 15. September 2015

Prof. Dr. Jörg Schibler

Dekan der Philosophisch-

Naturwissenschaftlichen

Fakultät

Acknowledgements

My foremost thanks must go first to Prof. Stephan Krähenbühl for giving me the opportunity to work in his lab and to profit from his extensive knowledge. His encouragement supported me to advance in my scientific but also personal development. Thank you for your purposive lead and valuable advice how to reach my scientific goals.

My sincere gratitude also goes to my PhD supervisor Jamal Bouitbir. Throughout my thesis I highly appreciated your helpfulness in any way and your preconceived suggestions how to handle scientific questions and difficulties. Our discussions always motivated me to give my best throughout my PhD studies. Merci beaucoup!

After my scientific tutors, I would like to thank my best friend Linda. Although you were miles away and not around in the lab, I greatly enjoyed our almost weekly Skype sessions, where we shared our daily lab experiences and other amusing stories. Your friendship and support be it on a scientific or personal matter was invaluable for succeeding my PhD thesis. Thank you so much!

It was a pleasure to supervise the master thesis of David. I enjoyed working with you and I appreciated our common coffee breaks. Thank you for your great contribution.

Riccardo: The best workplace neighbor I could imagine. It was so much fun to sit next to you. I enjoyed our scientific discussions, but even more our passionate chats about any kind of things in life and our hilarious competitions! Thank you for bringing me closer to the Italian culture and kitchen!

A big thank goes to each of the Clinical Pharmacology & Toxicology members! Anna, Bea, Benji, Urs, Franziska, Gerda, François, Dino: It was great to get to know you all and to work in such a inspiring and pleasant environment. To all other members of the lab, past and present, representing a great group, of which I could be part of, thank to you all.

Last but not least I would like to express my deepest gratefulness towards my beloved family. Only through your indefatigable support, encouragement, and helpfulness in every way has brought me this far where I am standing now. Thank you for your support throughout my life!

All those above have contributed that I could conduct my thesis with joy and productivity, but all of this would not have been possible without the help of you, Nello. Sei stato al mio fianco. Mi hai aiutato in tutti i modi possibili e hai trovato sempre le parole giuste da dirmi nel momento in cui ne ho avuto più bisogno. Mi hai mostrato come affrontare la vita con leggerezza e gioia! Ti amo!

Table of contents

Abbreviations

ALT	Alanine aminotransferase
ATP	Adenosine triphosphate
CYP	Cytochrome P450
DILI	Drug-induced liver injury
DMSO	Dimethyl sulfoxide
ETC	Electron transport chain
$FADH_2$	Flavin adenine dinucleotide
FAO	Fatty acid oxidation
FCCP	Carbonyl cyanide-*4*-(trifluoromethoxy)phenylhydrazone
GSH, GSSG	Reduced glutathione, glutathione disulfide
HCCL	Hydroxyl-cobalamin [c-lactam]
HPLC	High-performance liquid chromatography
IMM	Inner mitochondrial membrane
MMA	Methylmalonic acid
MPTP	Mitochondrial permeability transition pore
mtDNA	Mitochondrial DNA
NADH	Nicotinamide adenine dinucleotide
NADPH	Nicotinamide adenine dinucleotide phosphate
OMM	Outer mitochondrial membrane
OXPHOS	Oxidative phosphorylation
ROS	Reactive oxygen species
RT-PCR	Real-time polymerase chain reaction
SOD2	Superoxide dismutase 2
TCA cycle	Tricarboxylic acid cycle

Summary

Idiosyncratic hepatotoxicity is an adverse reaction that can be evoked by certain drugs. The characteristic of this rare event is its occurrence at therapeutic doses that are usually well tolerated by the patients, and most importantly, this toxicity frequently becomes manifested in a specific population of subjects. These motifs point towards underlying or acquired genetically and/or environmental risk factors rendering some patients more susceptible to idiosyncratic adverse reactions. Although the mechanisms of drug-induced liver injuries are not completely understood, mitochondrial dysfunction and/or formation of toxic metabolites have been recognized as major contributors in many cases of idiosyncratic hepatotoxicity. Moreover, predisposing mitochondrial dysfunction has been suspected to be one of the factors enhancing the risk for idiosyncratic toxicity. Therefore, severe inhibition of cellular metabolic functions, maintained by the mitochondria, an organelle crucial for proper energy homeostasis and delivery for the cell, may induce oxidative stress that in turn can result in cell death and ultimately to liver dysfunction and death. The lack of reliable methods to identify substances with the risk for idiosyncratic mitochondrial toxicity represents a major issue for the pharmaceutical industry, since unpredicted idiosyncratic toxicity can consequence in withdrawal of the drug from the market or in warnings by health authorities. It is thus an important need to characterize drugs that are related to idiosyncratic toxicity for a better understanding of implicated mechanisms and also to develop suitable in vitro and in vivo systems that can be applied to test drugs for their idiosyncratic potential.

This thesis includes three papers that have been published or submitted for publication and a short report as pilot project. The first two projects and the short report present the development of an *in vitro* and *in vivo* system with underlying mitochondrial defects that could serve as tool to uncover drugs with an increased risk for idiosyncratic toxicity, whereas the third project addresses the molecular mechanisms of hepatotoxicity *in vitro* of the antimitotic agents of azoles.

Our first paper describes a newly developed *in vitro* model in HepG2 cells induced by the chemical hydroxy-cobalamin [c-lactam] (HCCL), a vitamin B_{12} analog. The model exhibits subtle changes in the respiratory chain function and slight increase of oxidative stress leading to mitochondrial swelling. HCCL is known to competitively inhibit proper processing of substrates of the propionate pathway and causes similar defects as seen for the inherited metabolic disorder methylmalonic aciduria. We showed that subtoxic concentrations of HCCL could impair mitochondrial function and thus used this model that should reflect preexisting mitochondrial diseases of patients rendering them more susceptible to mitochondrial toxicants. In this context, we demonstrated that known mitochondrial toxicants applied on our HCCL model exert increased toxicity, which supports the hypothesis that risk factors such as underlying mitochondrial defects

predispose for idiosyncratic toxicity of compounds that have a known adverse mechanisms on mitochondrial function such as dronedarone, benzbromarone, and ketoconazole.

Our second paper aimed to expand the results obtained from the HCCL in vitro study into a mouse model. We showed that daily i.p. treatment of HCCL over three weeks induced an elevation of methylmalonic acid, a marker of methylmalonic aciduria. Moreover, slight decrease of complex I of the electron transport chain in liver homogenates were observed. Histopathological analysis revealed enhanced glycogen content and fat accumulation in the liver explaining the observed elevation of liver weight. Besides that, we did not find any increased oxidative stress or other dysfunctions of the mitochondria due to HCCL exposure. Because of the metabolic changes found in this study were minor, we did not further pursue the exploration of this model in order to test idiosyncratic drugs on it.

The third paper focused on the discovery of the molecular mechanisms of hepatotoxicity of antifungal azoles. Cytotoxicity experiments in HepG2 cells uncovered dose-dependent toxicity of ketoconazole and posaconazole, whereas fluconazole and voriconazole did not affect the cells. Toxicity studies in HepaRG cells did not point at any implication of metabolites for all four tested azoles. Our functional examination on mitochondrial function of ketoconazole and posaconazole depicted a strong inhibitory potential on the respiratory chain function, accompanied by oxidative stress and apoptosis, suggesting mitochondrial dysfunction responsible for azole-induced hepatotoxicity. The exposure of these two mitochondrial toxins on our previously created HCCL in vitro model evidenced an increased toxicity already at therapeutic concentrations, strongly supporting the assumption that preexisting mitochondrial defects can lower the threshold level of a drug's toxicity and thereby a manifestation of idiosyncratic hepatotoxicity.

Lastly, the short report readopts the subject of the establishment of in vitro models with mitochondrial dysfunction, implementing it as system for testing idiosyncratic toxicity. With siRNA we depleted two different essential mitochondrial enzymes, SIRT3 or SOD2, in HepG2 cells. We hypothesized to find an increase in cytotoxicity and enhanced oxidative stress after exposure to known mitochondrial toxicants if cells either present depletion in the deacetylation of mitochondrial proteins or a silencing of one of the major antioxidant defense systems. However, our results did not reflect this assumption and did not reveal any enhanced toxicity of HepG2 cells lacking specific mitochondrial functions compared to normal HepG2 cells. Furthermore, induction of a second stress factor such as the removal of glutathione in SOD2 siRNA cells did not increase the susceptibility of these cells to mitochondrial toxicants. Nevertheless, with this study we presented interesting basic approaches how to establish models to test idiosyncratic toxicity in vitro.

Background

1. Drug-induced liver injury (DILI)

The liver, as principle site of drug metabolism, has been considered as the most important organ in drug toxicity. The liver is responsible for drug metabolism, and therefore for the elimination of drugs from the body. At the same time, these features render the liver as preferential target for drug toxicities. Drug-associated hepatotoxicity is involved in more than 50% of all cases of acute liver failure in the US, with idiosyncratic drug-induced liver injury as the most common cause of toxicity [1, 2]. Hepatotoxicity has been the major reason of post-marketing drug withdrawal in the last past decades [3]. Moreover, many drug warnings, failures, or withdrawals have been ascribed to mitochondrial toxicity [4-6]. Since drug-induced hepatotoxicity occurs very rarely it often remains undetected during drug development, as only a few thousand subjects participate in the clinical phases.

Although DILI has low estimated incidence rates of 1/100'000 to 1/10'000 exposed patients [3], in reality, the incidence cases are most-likely underestimated, due to the lack of reporting or surveillance systems, standardized nomenclature or causality assessment methods, but also because of the difficulty to evaluate the number of patients additionally taking over the counter or herbal medicines, beside the prescribed medications [7]. Therapeutic drug classes including antibiotics, antinflammatory, antipsycotics, and antimycotics, as well as herbal products and dietary supplements are implicated with DILI [8-10].

1.1. Definition

DILI can show different clinical patterns, starting from asymptomatic or transient elevation of liver biomarkers, to jaundice or severe acute liver failure, and rarely ending in chronic liver diseases. Many different terminologies of DILI made accurate clinical diagnosis difficult; therefore Aithal et al. communicated a standardized synopsis in terms of threshold criteria for identification, pattern of injury, causality assessment, and severity to facilitate the diagnosis of DILI [11]. Originally, the clinically relevant threshold level for DILI was defined as the elevation of serum concentration of either alanine aminotransferase (ALT) and/or aspartate aminotransferase (AST), alkaline phosphatase (ALP), and bilirubin exceeding twice the upper limit of normal (ULN). These definitions were adjusted due to unspecific elevations of transaminases that would be counted as DILI.

Thus the threshold level was set at AST or ALT > 5 X ULN without symptoms, or rise in ALP > 2 X ULN, or rise in bilirubin > 2 X ULN with any increase in AST and ALT concentration [10, 11].

DILI can be classified as either hepatocellular, cholestatic or mixed types, based on the degree of elevation of transaminases and ALP and the ratio of increased baseline ALT to baseline ALP (R= (ALT/ULN)/(ALP/ULN)) (see ***Table 1***). The severity of DILI does not correlate with the level of liver enzymes elevation, however, the pattern gives information about the immediate and long-term consequences [10, 11].

Table 1: **Liver injury patterns and examples of hepatotoxic drugs adapted from Weiler et al. [12]**

Type of liver injury	**Hepatocellular**	**Mixed**	**Cholestatic**
	Injury predominantly to hepatocytes	Hepatocellular and cholestatic injury	Injury to bile ducts or affecting bile flow
R-Value [R=(ALT/ULN)/(ALP/ULN)]	≥5	>2 and <5	≤2
Examples of drugs classes			
Antiinfectives	Isoniazid, ketoconazole, tetracylines	Erythromycin, amoxicillin/clavulanic acid, cotrimoxazole	Amoxicillin/clavulanic acid, erythromycin
Pain reliefers	Acetylsalicylic acid, acetaminophen		
Cardiovascular and metabolic drugs	Lorsartan, statins, allopurinol	Enalapril, verapamil	Clopidogrel
Neurologic/Psychiatric drugs	Valproic acid	Carbamazepine, phenytoin	Chlorpromazine, tricyclic antidepressants

ALT, alanine aminotransferase; ALP, alkaline phosphatase; R, ratio; ULN, upper limit normal

1.2. Discriminative terms: Intrinsic vs. idiosyncratic reactions

The basic mechanism of DILI can be distinguished in two different types; a) intrinsic "type A reaction" or b) idiosyncratic "type B reaction" (***Table 2***). Drugs that cause liver injury in a dose-dependent manner are typically referred to as intrinsic. They are predictable in humans or in animal models [6]. The most prominent drug with high potential of intrinsic DILI is the widely used pain reliever acetaminophen (APAP) [13]. Although APAP is very safe at therapeutic doses, APAP induces massive hepatocellular necrosis, when overdosed (> 4 g/d). The mechanism behind this phenomenon is the toxic metabolite N-acetyl-p-benzoquinone imine (NAPQI), which is formed during drug metabolism depleting the antioxidant glutathione content in cells

resulting in mitochondrial dysfunction culminating in cell death and subsequent acute liver failure [13, 14]. Unlike intrinsic toxicity, the idiosyncratic phenotype occurs very rarely, is unexpected, not strictly dose-dependent, affects only a small proportion of patients (< 1%), and cannot either be predicted by its pharmacology or from conventional clinical toxicology tests [8]. This implies that idiosyncratic toxic adverse reaction usually appear at therapeutic doses and in a specific population of patients [10]. In most cases, clinical features are visible within 5-90 days after the causative medication was started [7]. It is difficult to explain the underlying mechanisms why certain patients seem to be more susceptible to idiosyncratic DILI than others. As the mechanisms of intrinsic DILI can be understood and explained with animal models, to date there are no established preclinical *in vivo* or *in vitro* models successfully predicting idiosyncratic toxicity for new drug entities. Therefore, idiosyncratic DILI represents a major issue not only for the patients' safety but also in perspective of the pharmaceutical industry [3].

Table 2: **Characteristics of type A and type B adverse reactions, adapted from Pessayre D [15].**

Characteristics	**Type A (intrinsic)**	**Type B (idiosyncratic)**
Dose dependency	Yes	No simple relationship
Predictable from known pharmacology	Yes	Usually no
Host factors	Genetic factors are less important	Dependent on susceptibility factors (e.g. genetic factors, drug interactions)
Incidence	High	Low
Severity	Variable, dose dependent	Variable, more severe
Latency period	Short (days)	Few days-months
Clinical burden	High morbidity, possible mortality	High morbidity and mortality
Experimental reproducibility	Yes, animal models	Only few animal and cell models
Examples of drugs	Acetaminophen	Phenytoin, cotrimoxazole

1.3. Risk factors implicating idiosyncratic toxicity

Although idiosyncratic DILI are traditionally defined as not clearly dose-dependent, recent studies showed that just as daily doses over 50 mg, greater lipophilicity of drugs, and/or extensive hepatic metabolism usually predispose for DILI [16, 17]. Moreover, increased risk associated with idiosyncratic DILI was observed in females with an incidence of 65% [18]. Also underlying liver diseases could account for a higher susceptibility for DILI, but conflicting reports and studies render this determinant indistinct [7]. However, more likely the combination of drug-drug interactions, reactive metabolites, environmental, and genetic factors are believed to account for idiosyncratic DILI (see ***Figure 1***) [19].

The genetic susceptibility may be one of the most important factors leading to DILI. One prominent example for idiosyncratic DILI is the allele HLA-B*5701, a subclass of the human leucocyte antigen (HLA) system. Daly et al. [20] have examined in a European cohort study that the possession of a HLA-B* allele attributed to a 80-fold increased risk for flucloxacillin-induced liver toxicity. Many genetic polymorphisms of enzymes have been extensively studied the last few years and have helped to characterize pathogenic mechanisms of DILI in individual patients. Nevertheless, genome-wide association studies of pooled cases could not clearly relate genetic factors with idiosyncratic DILI [21].

Further, underlying defective health conditions, such as preexisting inborn mitochondrial cytopathies affecting metabolic function are supposed additive triggering factors, leading to drug-induced idiosyncratic hepatotoxicity that possibly is not manifested in healthy subjects [15].

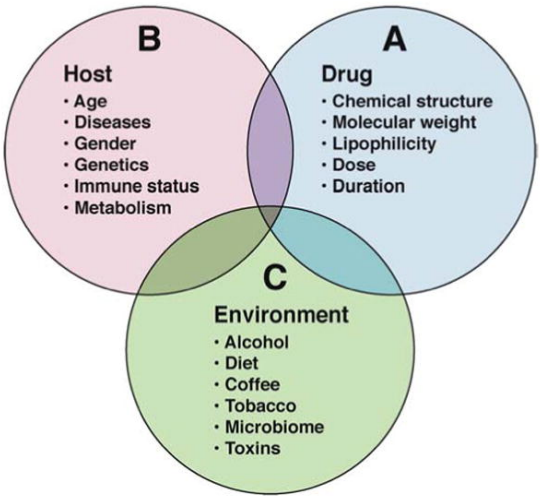

Figure 1: **Potential risk factors implicated in the pathogenesis of "Idiosyncratic" DILI as illustrated by Fontana et al. [8].** A) Drug-drug or drug-disease interactions could alter the concentration of a drug or reactive metabolite at a cellular level involved in the initiation, maintenance or resolution of liver injury. B) Clinical host risk factors such as age, body weight, and BMI can enhance the development of DILI. C) Diverse micro and macroenvironment of individuals receiving medications can potentiate the hepatotoxic risk of a drug.

1.4. Mechanistic classification of DILI

Commonly, idiosyncratic adverse reactions are either classified as immune- or metabolic-mediated DILI. The first is often referred as an allergic or 'hypersensitivity' reaction. General features of the immune-mediated adverse reactions are its early onset (1-6 weeks) and its fast reinjury with reexposure. Often hypersensitive reactions are implicated with anticonvulsive drugs (phenytoin, carbamazepine), where typical symptoms and signs of the adaptive immune system such as fever, rash, and formation of autoantibodies appear [10]. In contrast, metabolic-mediated DILI, assumed to be evoked by reactive metabolites, typically have a later onset (1-52 weeks), variable response rate, no manifestation of hypersensitivity, and usually no recurrence after rechallenge [7]. This traditional classification is probably too simplistic due to the multistep process of idiosyncratic DILI involving not only immune-and metabolic-mediated, but also genetic and environmental factors.

Hence, Russmann et al. [22] postulated a three-step working model that restricts its principle mechanism to three main ways of initial injury, emphasizing the importance of unspecific downstream events following drug-specific initial upstream hepatic injury considering genetic and environmental risk factors. According to his model, illustrated in ***Figure 2***, drugs or their metabolites initially cause direct cell stress (intrinsic pathway), trigger immune reactions (extrinsic pathway), and/or directly impair mitochondrial function. Second, after this primary hit, mitochondrial permeability transition may occur, which can initiate in a third step, apoptosis or necrosis. All these levels can be influenced by environmental or genetic factors, which in turn, in their complex interaction, function as triggering risk factors inducing idiosyncratic DILI. This means that normally one single risk factor may be not sufficient to initiate DILI. Underlying mild liver damage is probably not strong enough to disturb the fragile balance between impairing and protective factors on a cellular level, whereas another co-factor can amplify the effect and thus lead to severe idiosyncratic hepatotoxicity. This threshold theory of cumulative damages to mitochondrial targets could explain the late onset of idiosyncratic DILI [1, 23]. Therefore, the delayed onset of liver injury is most likely due to the prolonged injury to the mitochondria. Oxidative stress or impairment of mitochondrial function has first to pass a given threshold before apoptosis and necrosis, and resulting liver damages get manifested [1].

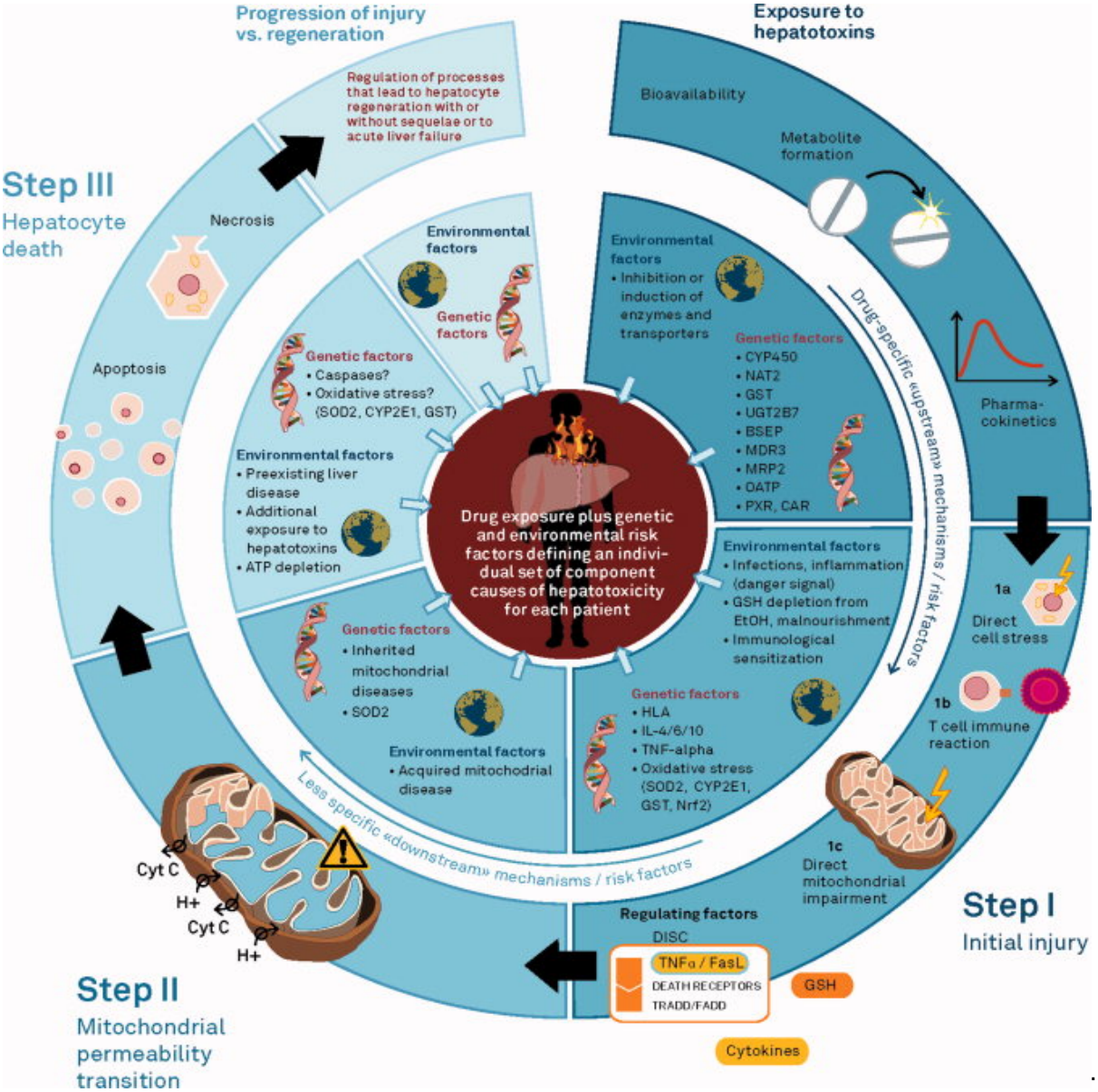

Figure 2: **Integration of genetic and environmental risk factors derived from the three-step mechanistic working model of DILI with a pie model of disease causation as explained and illustrated by Russmann et al. [24].** Some risk factors may exert their effects on different consecutive hepatotoxic mechanisms and are therefore shown more than once. Multiple causes and their complex interactive contribution to DILI vary for different drugs and between individual patients, and remain poorly understood. In addition, it is also likely that there are other currently unknown risk factors. This model also implies that environmental factors play an important and sometimes even necessary triggering role. Genetic risk factors alone may therefore not be sufficient to predict a high absolute risk of DILI in individual patients. CAR, constitutive androstane receptor; DISC, death-inducing signaling complex; EtOH, ethanol; Nrf2, nuclear factor (erythroid-derived 2)-related 2.

2. Principles of mitochondrial function and drug-induced mitochondrial toxicity

In recent years, the mitochondrion has been more widely recognized as important drug biosensor, being a key off-target of drugs inducing idiosyncratic DILI. A lot of compounds causing metabolic failure are highly associated with impaired mitochondrial function [4, 25, 26]. Thus, mitochondrial toxicity has become a major issue in drug development, being the reason of many drug candidate failures, black box warnings or withdrawal from the market (see ***Table 3***) [27].

Table 3: **Drugs associated with idiosyncratic hepatotoxicity by inhibition of mitochondrial function.**

Drug	Indication	Market status
troglitazone	antidiabetic	withdrawn
carbamezepine	anticonvulsant	black box warning
benzbromarone	uricosuric	withdrawn
diclofenac	nonsteroidal inflammatory	black box warning
ketocoanzole	antifungal	black box warning/restriction
ibufenac	nonsteroidal inflammatory	withdrawn
valproic acid	antieptileptic	black box warining
ticlopidine	antiplatelet	black box warning

Given that, as explained in the 3-step working model by Russmann et al. [22], the mitochondria play a pivotal role in the regulation of cellular function such as the supply of 90% of the overall cellular energy through processes of oxidative phosphorylation (OXPHOS), it is evident that a damage at a specific or different mitochondrial targets lead to multitissue toxicity. Particularly, mitochondria-rich organs such as the heart, brain, and/or liver that are highly working under aerobic conditions and relying on the energy-producing metabolism of the mitochondria render to be susceptible to mitochondrial toxicants [28]. Mitochondrial dysfunction thus can be induced by xenobiotics (or drugs) via a direct interaction of mitochondrial function or by an interference with mitochondrial transcription/translation and/or by increased superoxide anion production leading to oxidative stress [4, 29].

In the following paragraphs, basic principles of mitochondrial physiology and different mechanisms leading to an impairment of mitochondrial function will be described in detail.

2.1. Morphology

Mitochondria are constituted of two membrane systems, the outer and the inner mitochondrial membranes, both formed of phospholipid bilayers that are occasionally linked to each other like gap junction to form contact sites. The mitochondria are differentiated into distinct composi-

tional and functional regions, where diverse transporting and enzymatic proteins are integrated. The space between these two membranes is called the intermembrane space, in which essential proteins (e.g. cytochrome C, creatine kinase) are located, playing a major role in cell homeostasis and mitochondrial energetics. The outer membrane, separating the mitochondrial from the cytosol is permeable for ions or molecules up to 6 kDa. This smooth membrane is rich in cholesterol and contains enzymes such as palmitoyl-CoA synthase, CPT1, and the mitochondrial permeability transition pore (MPTP) [30].

In contrast, the inner mitochondrial membrane is largely impermeable and cholesterol-free, separating the mitochondrial matrix from the cytosolic environment. This partition acts as chemical barrier maintaining the electron gradient across the membrane that enables ATP generation. Moreover, in the inner mitochondrial membrane, multiple invaginations (cristae) increase the surface area, which are formed into the matrix compartment that houses assembled respiratory complexes, and proteins for ATP synthesis and transport. These important constituents are the major targets of mitochondrial toxins [31]. Among the components of the matrix are several soluble enzymes essential for the citric acid cycle, β-oxidation, or urea synthesis [15, 32].

2.2. Dynamics

Mitochondria are organized as large branched structures, building a network that is always in constant movement to regulate fission or fusion, and therefore reorganizing the mitochondrial morphology either to highly fragmented or networked (see ***Figure 3***) [33]. The mitochondrial form and function are thus closely linked to each other and are integrated into cellular signaling processes in a highly regulated way. Mitochondrial fusion is mediated by the two families of dynamin-like proteins mitofusin-1 (mfn1) and mitofusin-2 (mfn2) located in the OMM, and optic atrophy-1 (opa-1) located in the IMM. These proteins are responsible for the lengthening and the tethering of proximate mitochondria to build a network [34]. On the other hand, fission is involved in the division of mitochondria, mediated by the dynamin-related proteins drp-1 and fis-1. The splitting occurs in a manner that drp-1, by forming helical structures, is coiling around the mitochondria. Under healthy conditions, enhanced fusion creates mitochondrial tubular networks, whereas oxidative stress or other defects prevail mitochondrial fission, evoking a break up of the filamentous networks into fragmented mitochondria. Mitochondrial dysfunction is therefore tightly associated to the status of dynamics, at which mitochondrial fusion can buffer stress on the mitochondria [35].

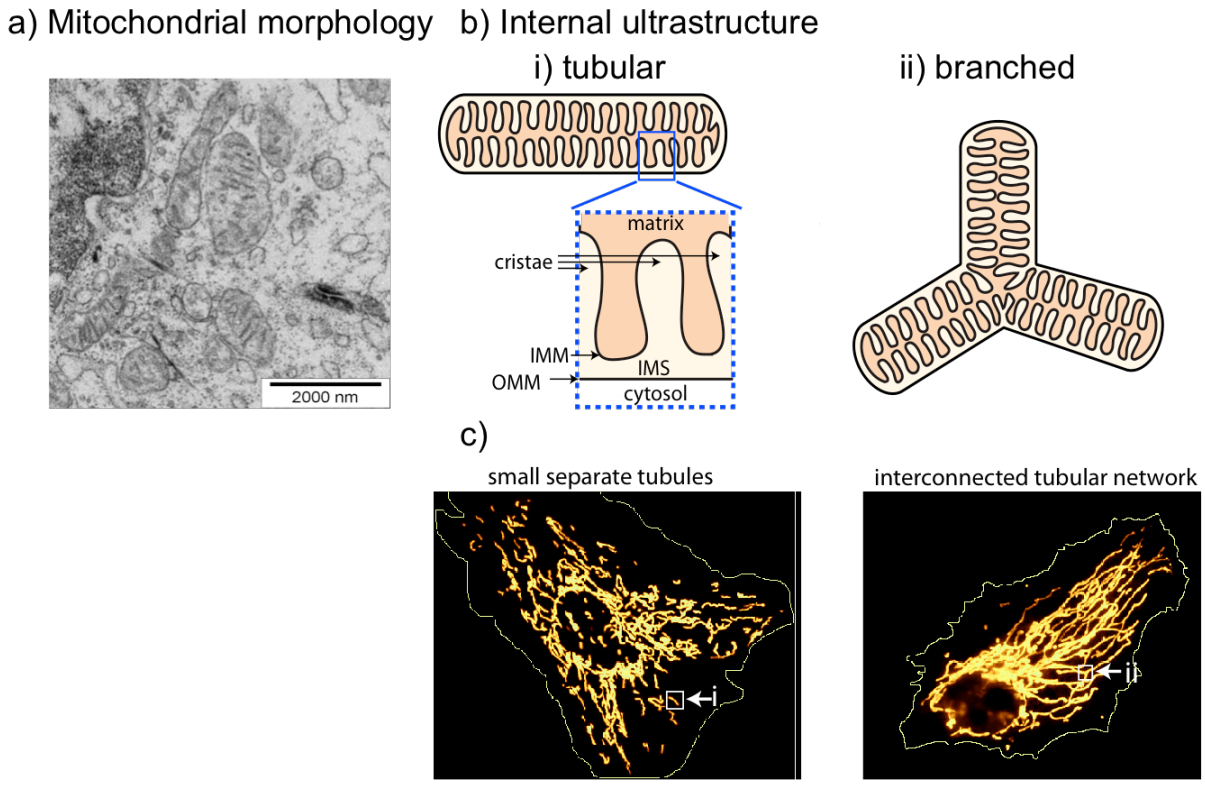

Figure 3: **Mitochondrial structure and network adapted from Rafelski et al. [36].** Examples of mitochondrial networks at the micron and nanometer scales. (a) Separate mitochondria in HepG2 cells visualized by electron microscopy. (b) Diagram of the organization of the mitochondrial membranes (ultrastructure) at the nanoscale for (i) a tubule and (ii) a tubule branch. Abbreviations in (i) include the outer and inner mitochondrial membrane (OMM and IMM, respectively) and the intermembrane space (IMS). Mitochondrial networks can vary from separated structures to interconnected networks. (c) Indian Muntjac deer skin fibroblast (left) and BPAE (bovine pulmonary artery endothelial) cell (right), both expressing a pEYFP-mitochondrial plasmid vector to label mitochondria (yellow-orange). The thin yellow line is an approximate outline of the cell. White arrows point to small boxes indicating either a tubule (left) or tubule branch (right) that are illustrated in (b).

2.3. Genome

Mitochondria, only maternal inherited, are the unique organelles outside the nucleus, possessing their own genome with the singularity of self-replication independently of the nuclear genome [37]. The mitochondrial mtDNA consists of smaller double-stranded circular chromosomes (16 569 bp) encoding only a fraction of 13 essential proteins of which all are components of the electron transport chain (ETC) [38]. Other proteins, required for proper mitochondrial function are encoded by the nuclear genome and then translocated to the mitochondria [39]. The 24 other genes present on the mtDNA (2 rRNAs and 22 tRNAs) are all expressed to further synthesize the 13 essential proteins of the OXPHOS [40].

The mtDNA has a single DNA polymerase with base excision repair activity that ensures a precise replication of the mtDNA. However, the mutation rate of mtDNA is 5 to 20-fold higher than in nuclear DNA [38]. This discrepancy can be explained by the lack of protective proteins and less repairing pathways in the mtDNA, and moreover due to its proximity to the ETC, where

the majority of reactive oxygen species (ROS) is produced [41, 42]. Additionally, in contrast to the nuclear genome, the mtDNA is mostly irreparable or slowly repairable in terms of damage or stress. The only functional buffering system against stressors is the high copy number of mtDNA and renders thereby the mtDNA as fundamental biomarker for oxidative stress [41] .

2.4. Principles of mitochondrial bioenergetics

Mitochondria play a crucial role in oxidative metabolism and energy production, as they convert the energy (NADH and $FADH_2$) produced by the oxidation of pyruvate-and free fatty acids, but also from the TCA cycle into ATP through OXPHOS [15, 43, 44]. Following sections discuss the three main energy-producing pathways of the mitochondria as illustrated in ***Figure 4***.

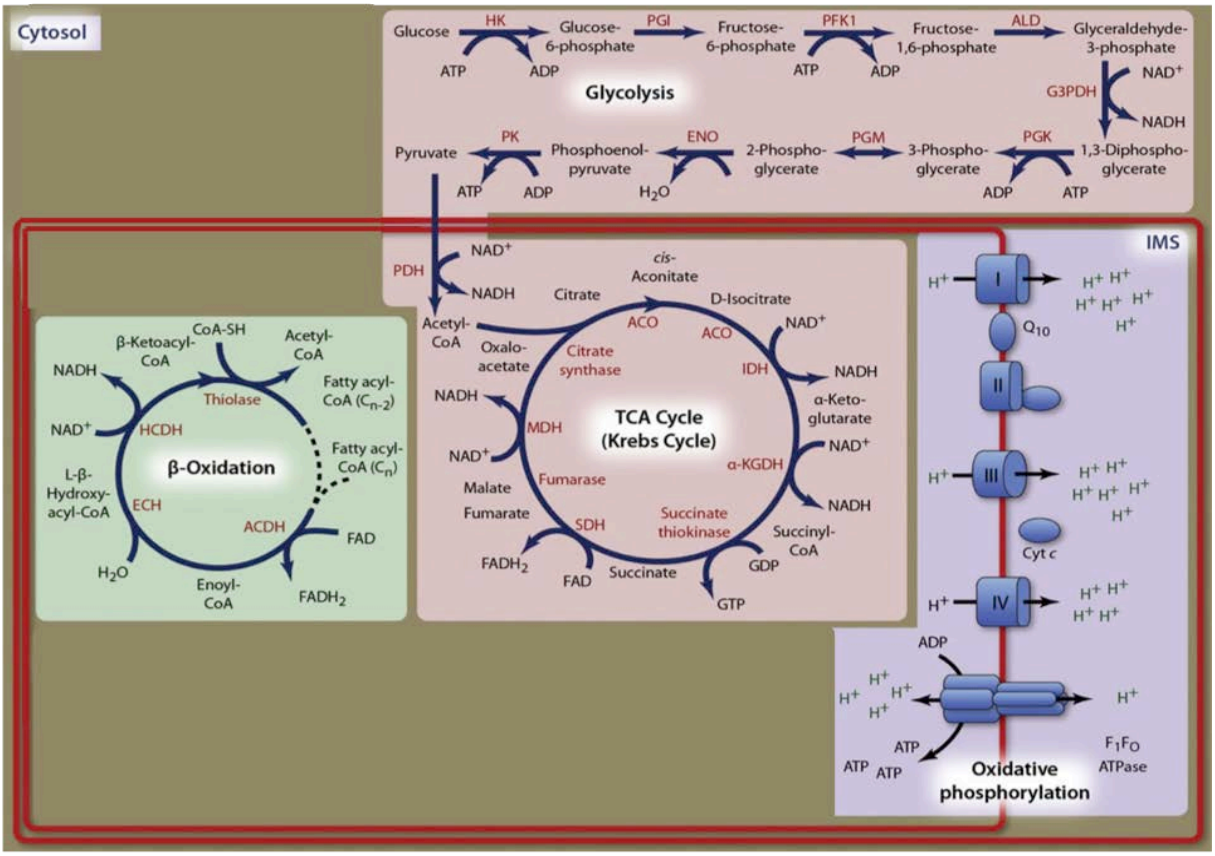

Figure 4: **Bioenergetic functions of mitochondria adapted from Galluzzi et al,[45].** Critical bioenergetic circuitries mediated by the mitochondria, including the tricarboxylic acid (TCA) cycle, OXPHOS, and cycle, β oxidation. Despite glycolysis takes place in the cytosol, its intermediates are crucial for processes in mitochondrial bioenergetics. Note that several intermediate reactions and all transporters have been purposely omitted. α-KGDH indicates α-ketoglutarate dehydrogenase; ACDH, acyl-CoA dehydrogenase; ACO, aconitase; ALD, aldolase; ASL, argininosuccinate lyase; CoA, coenzyme A; Cyt c, cytochrome c; ECH, enoyl-CoA hydratase; ENO, enolase; G3PDH, glyceraldehyde-3-phosphate dehydrogenase; HCDH, 3-hydroxyacyl-CoA dehydrogenase; HK, hexokinase; IDH, isocitrate dehydrogenase; IMS, mitochondrial intermembrane space; MDH, malate dehydrogenase; PDH, pyruvate dehydrogenase; PFK1, phosphofructokinase-1; PGI, phosphoglucose isomerase; PGK, phosphoglycerate kinase; PGM, phosphoglycerate mutase; PK, pyruvate kinase; SDH, succinate dehydrogenase; Q_{10}, Q_{10} coenzyme.

2.4.1. β-Oxidation

The degradation of fatty acids mainly occurs in the mitochondria and accounts for more than 90% of the overall cellular β-oxidation; the residual 10% are credited to the peroxisomal pathway. β-oxidation occurs in the mitochondrial matrix in four steps, at which four distinct enzymes classes with broad specificity towards CoA-esters catalyze this reaction. In the first step an acyl CoA-ester is dehydrogenated to form a trans-2-enoyl-CoA, followed by a hydration of the double bond producing L-3-hydroxy-acyl-CoA. The third step leads to a dehydrogenation to 3-keto-acyl-CoA. At last, a thiolytic binding of 3-keto-acyl-CoA yields a two-carbon chain-shortened acyl-CoA and one acetyl-CoA (see ***Figure 4***). Therefore, each cycle has a net production of acyl-CoA plus acetyl-CoA. Acyl-CoA undergoes another loop of β-oxidation while acetyl-CoA can directly enter the TCA cycle. In addition to the CoAs produced in each cycle, two reducing equivalents, NADH and $FADH_2$, are formed and further processed by the ETC where NADH is oxidized by Complex I and $FADH_2$ provides electrons to reduce coenzyme Q in Complex III. Thus, these two electron carriers display a direct junction of the β-oxidation and respiratory chain [46].

An important mechanism of β-oxidation is the specific carnitine shuttle system that transports long-chain (C14-C18) fatty acids across the mitochondrial inner membrane into the mitochondrial matrix, where they are converted to the respective acyl-CoA an can be beta-oxidized. In contrast, short-chain (C4-C6) and medium-chain (C6-C14) fatty acids are able to freely cross the mitochondrial membranes [47].

2.4.2. Odd-chain fatty acid β-oxidation

When fatty acids with odd numbered carbons undergo β-oxidation, or during the oxidation of branched chain amino acids including isoleucine, valine, and methonine the result is acetyl-CoA and propionyl-CoA instead of the usually formed acetyl-CoA from the oxidation of even numbered fatty acids. Propionyl-CoA in contrast to acetyl-CoA, first has to be catabolized into succinyl-CoA in order to enter the TCA cycle. This conversion occurs via carboxylation of propionyl-CoA into D-methylmalonyl-CoA. Then, D-methylmalonyl-CoA is transformed to L-methylmalonyl-CoA through methylmalonyl-CoA epimerase. At the last step, methyl-malonyl-CoA mutase, a vitamin B_{12}-dependent enzyme, catalyzes the rearrangement of L-methylmalonyl-CoA to succinyl-CoA, which is finally taken up by the TCA cycle and is converted to oxaloacetate (see ***Figure 5***). Compared to even numbered fatty acids, odd numbered fatty acids occur in an irregular way. Nevertheless, the utilization of the propionate metabolism by several amino acids and cholesterol remain essential for proper metabolic functions [48, 49].

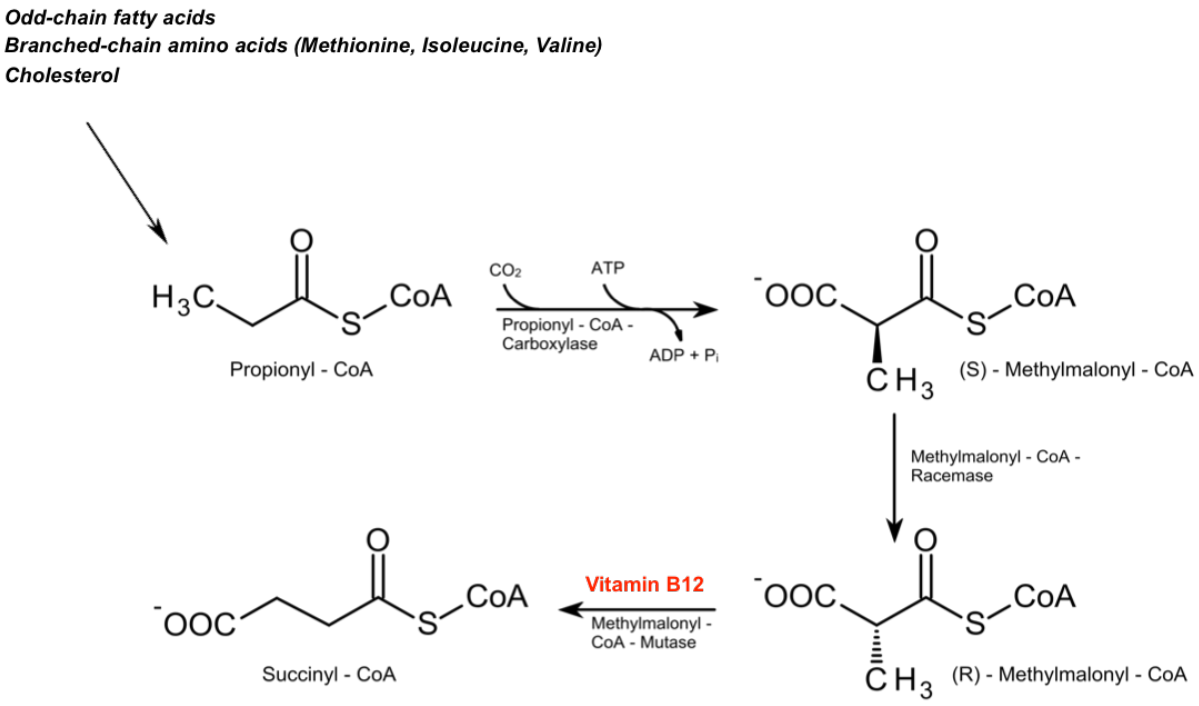

***Figure 5**:* **Scheme of propionate pathway.**

2.4.3. Tricarboxylic (TCA) cycle

The TCA cycle, better known as Krebs' cycle, represents the gateway to aerobic metabolism. In a series of eight subsequent oxidation and reduction reactions (see ***Figure 4***), two carbon molecules are oxidized to acetyl groups or dicarboxylic acids. This cycle is not only important providing precursors such as NADH and $FADH_2$ for the transformation into ATP by the utilization of acetyl-CoAs delivered from β-oxidation or glycolysis; it also serves as basic element of different molecules such as amino acids, cholesterol, porphyrin, or nucleotide bases [50].

2.4.4. Oxidative phosphorylation

Through the process of OXPHOS, mitochondria produce cellular energy via ATP. The OXPHOS consists of two distinct, functionally independent processes by which 1) reduced substrates are oxidized by the ETC and 2) ADP is converted to ATP by inorganic phosphates via phosphorylation. As the OXPHOS metabolism of one molecule of glucose yields up to 36 molecules of ATP, it is much more efficient than glycolysis yielding only two ATP. The pathway of OXPHOS is constituted of five complexes (see ***Figure 6***):

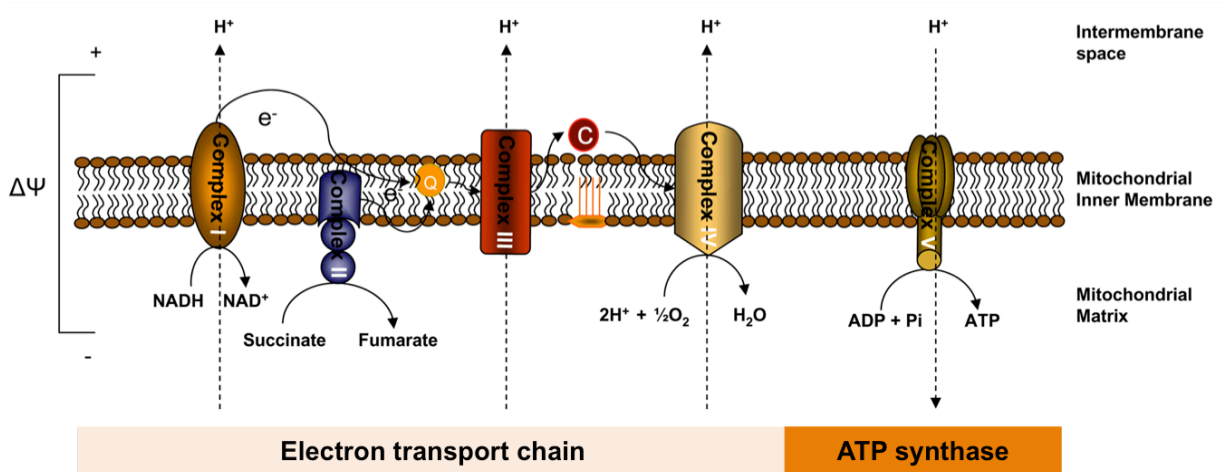

Figure 6: **Mitochondrial energy production adapted from Bayir and Kagan [51].** The mitochondrial ETC is composed of five multimeric complexes. Electron transport between complexes I to IV is coupled to extrusion of protons from complexes I, III and IV into the intermembrane space, creating an electrochemical gradient (Δψ) across the inner mitochondrial membrane. Protons then flow through complex V (ATP synthase), which utilizes the energy to synthesize ATP from ADP. C, cytochrome c; Q, ubiquinone.

Complex I to IV compose the ETC, whereas complex V represents the ATP synthase. The complexes of the OXPHOS are embedded in the inner mitochondrial membrane and consist of various individual protein subunits, encoded either by the nucleus or the mitochondrial genome. The two reducing equivalents NADH and $FADH_2$ derived from the TCA cycle are used by the OXPHOS to generate ATP [52].

Complex I, also known as NADH:ubiquinone oxidoreductase carries electrons from NADH to ubiquinone. Afterwards, Complex II (succinate:ubiquinone oxidoreductase) that is part of the TCA cycle further transfers the electrons from succinate to ubiquinone via FAD. At the stage of Complex III (ubiquinol:cytochrome c oxidoreductase), electrons from ubiquinol are transmitted to cytochrome c. At the ultimate step of the ETC, namely in Complex IV (cytochrome c oxidase), molecular oxygen (O_2) is reduced to H_2O by four electrons. This process of subsequent oxidation of reduced NADH in the ETC is coupled with oxidative phosphorylation by an electrochemical gradient (chemiosmotic potential) reaching a potential up to - 200 mV (Δψ) and a pH gradient across the mitochondria inner membrane. This efflux of protons to the intermembrane space enables a driving force of the F_0F_1 ATP synthase to generate ATP through ADP and inorganic phosphates, which is referred as Complex V [53].

2.5. Production of reactive oxygen species and detoxifying systems

The ETC is the major site of ROS formation, since 90% of cellular ROS is estimated to arise from mitochondrial ETC [54]. ROS, simply describing reactive molecules that are derived from O_2 can appear as free radicals (O_2-), hydroxyl radicals (OH^-), and/or as non-radical hydrogen peroxide

(H_2O_2). The production of ROS is an elementary process of aerobic life, thereby mediating cellular function not only by promoting redox-sensitive signal transduction cascades or stimulating gene expression of antioxidant enzymes, but also inducing apoptosis or necrosis. ROS are generated as byproducts of the ETC; although under healthy conditions most of the electrons are transferred along the ETC in a regular manner, there is a constant amount (1-2%) of electrons intercepted by molecular oxygen and reduced to superoxide anion. Complex I and Complex III of the mitochondrial ETC have been identified as the major site of ROS production [55, 56].

Cellular antioxidant defense enzymes are able to metabolize accumulated ROS (see ***Figure 7***). The most prominent enzymatic scavenger systems are superoxide dismutase (SOD), catalase, or hydroxyl peroxidases such as glutathione peroxidase [57]. Acting as a radical interceptor, SOD is catalyzing the dismutation of two superoxide anion radicals in the reaction with hydrogen in order to form H_2O_2 ($2O_2^- + 2H^+ \rightarrow H_2O_2 + O_2$). This enzyme appears in different isoforms. SOD1 or CuZN-SOD is located in the cytoplasm and mitochondrial intermembrane space, whereas the manganese SOD2, or better known as MnSOD is exclusively located in the mitochondrial matrix. SOD3, a Cu/Zn SOD resides in extracellular compartments [58]. It has been shown that mice lacking SOD2 survive only several days after birth, implicating that SOD2 represents as critical mediator for cell survival controlling a dense level of mitochondrial superoxide anion [59].

Once H_2O_2 is formed, it can easily diffuse through mitochondrial membranes, in contrast to the superoxide radicals that have limited permeability and a short half-life. Therefore other protective mechanisms have to remove H_2O_2, which can form highly reactive radicals through the spontaneous reaction with ferrous ions (Fe2+) affecting proteins, DNA, or lipids. Catalase, mainly expressed in peroxisomes is able to detoxify H_2O_2 to H_2O and O_2. Alternatively, glutathione peroxidase uses reduced GSH that serves as electron donator leading to an oxidation to cysteine disulfide bonds (GSSG) to reduce H_2O_2 to water. Afterwards, GSSG is reduced back to GSH in presence of nicotamide adenine dinucleotide phosphate (NADPH). GSH-based systems, highly expressed in the liver, constitute the most substantial redox buffer in the cytosol, where the GSH/GSSG predominates compared to other pathways involved in susbstrate reduction. After the exclusive biosynthesis in the cytosol, GSH is transported into intracellular organelles including the nucleus, endoplasmatic reticulum, and mitochondria. GSH in the mitochondria is mainly found in its reduced form, where it only represents a small fraction of 10-15% of the total cellular GSH pool. Considering the volume of the mitochondrial matrix, mitochondrial GSH concentrations can reach similar milimolar ranges (~10 mM) as in the cytosol [43, 60-63].

.

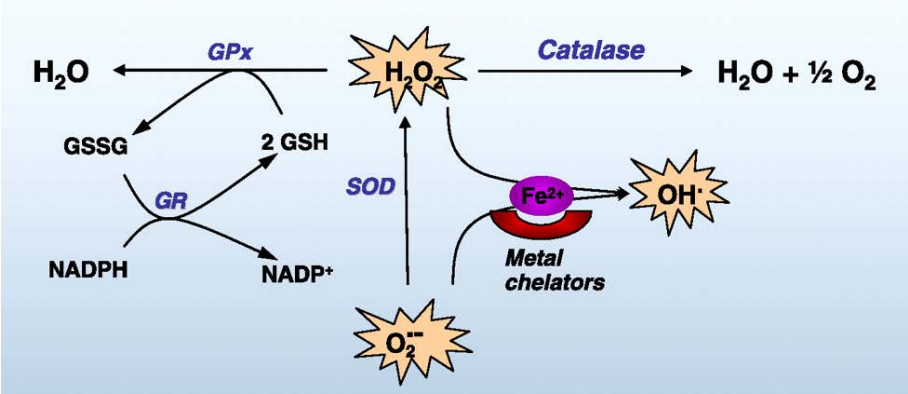

***Figure 7**:* **Major ROS detoxifying systems adapted from Bashan [64].** The major enzymes of ROS detoxification are shown in blue. GPx, glutathione peroxidase; GR, glutathione reductase; GSH, reduced glutathione; GSSG, oxidized glutathione; SOD, superoxide dismutase.

2.6. Mitochondrial signaling

In recent years, the signaling pathway mediated by the sirtuin (SIRT) family has gained much attention in regulating cellular energy metabolism. SIRT proteins are highly conserved and possess NAD^+-dependent deacetylase and/or ADP-ribosyltransferase activities. The NAD^+ dependence is linking the SIRT activity to the metabolic condition of the cell, and thereby ascribed to be a pivotal metabolic sensor of mitochondrial function [65]. The seven members of the SIRT family are differentially distributed within the mammalian cells. SIRT1, SIRT2, and SIRT6 are mainly found in the nucleus, and SIRT7 in the cytosol, whereas SIRT3-5 are located in the mitochondria where they bind and deacetylate several metabolic enzymes related to energy homeostasis [66, 67].

It has been reported that SIRT3 is directly involved in regulation of ATP-production through the respiratory chain. Knockout of SIRT3 in mice resulted in decreased cellular ATP of nearly 50% in tissues that normally express high levels of ATP (e.g. liver, heart, and kidney) compared to wild-type mice. Moreover, a depletion of SIRT3 in HepG2 cells revealed a dysfunction in the ETC resulting in a dissipation of the mitochondrial membrane potential and in an increase of ROS production [68, 69]. The decrease in ATP, but also disruption of ETC function can be explained by the augmented acetylation status of complex I in $SIRT3^{-/-}$ mice and the involvement of SIRT3 in the deaceylation of subunits of different complexes of the respiratory chain [68]. Recent studies also showed that SOD2 activity is strongly dependent on its deacetylation status at several lysine residues. Consequently, overexpression of SIRT3 increased SOD2 activity and led to decreased cellular ROS [70, 71]. Beyond the impairment of mitochondrial energy metabolism induced by a lack of SIRT3 [72], spectrometry studies demonstrated that metabolic proteins of the TCA cycle (isocitrate dehydrogenase 2; IDH2) and β-oxidation are less deacetylated in case of metabolic stress [73, 74]. These findings are strongly underscored by the relation of SIRT3

deacetylation state of long-chain acyl-CoA dehydrogenase (LCAD) and diminished fatty acid oxidation (FAO) in the liver. SIRT3$^{-/-}$ mice depicted low FAO and thereby developed fatty liver, decreased ATP production and defective thermogenesis [75]. Besides the uncovered importance of sirtuins modulatory capabilities (see ***Figure 8***), other involvement regarding apoptosis are currently discussed, but further studies are needed to get a comprehensive picture of sirtuins spectrum of influence.

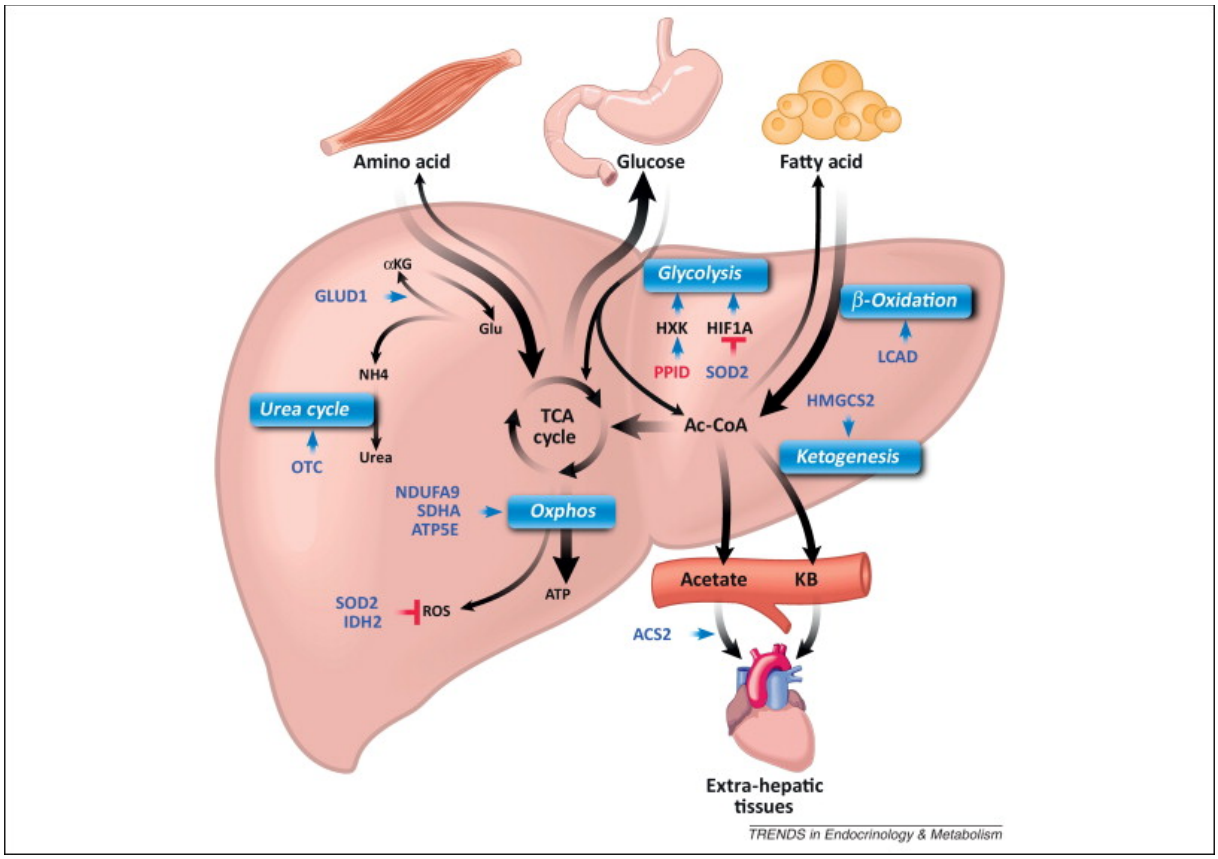

Figure 8: **The SIRT3-mediated regulation in the liver illustrated by He et al. [76].** SIRT3 regulates many of the enzymes involved in mitochondrial metabolism. Proteins in blue, activated by SIRT3. In red, deactivated by SIRT3.

2.7. Pathophysiology: Oxidative stress and mitochondrial targets of vulnerability

The term oxidative stress describes a state where massive amounts of ROS predominate in the mitochondria. More precisely, if an initial increase of ROS is relatively low, antioxidant capacities may be sufficient enough to counteract for the increased ROS, thus cellular imbalance can be recovered to baseline conditions. However, if a certain threshold is exceeded, the antioxidant systems are no longer able to compensate excessive ROS. Oxidative stress can lead to dysfunction (DNA damage, oxidation of lipids and proteins) of the mitochondria, thereby

possibly initiating cellular death [78]. Oxidative stress and/or mitochondrial dysfunction can be triggered via toxins or drugs inhibiting specific functions of the mitochondria (see ***Figure 9***).

Following paragraphs discuss most common drug off-targets, at which the mitochondria can be impaired [4, 26, 29, 39].

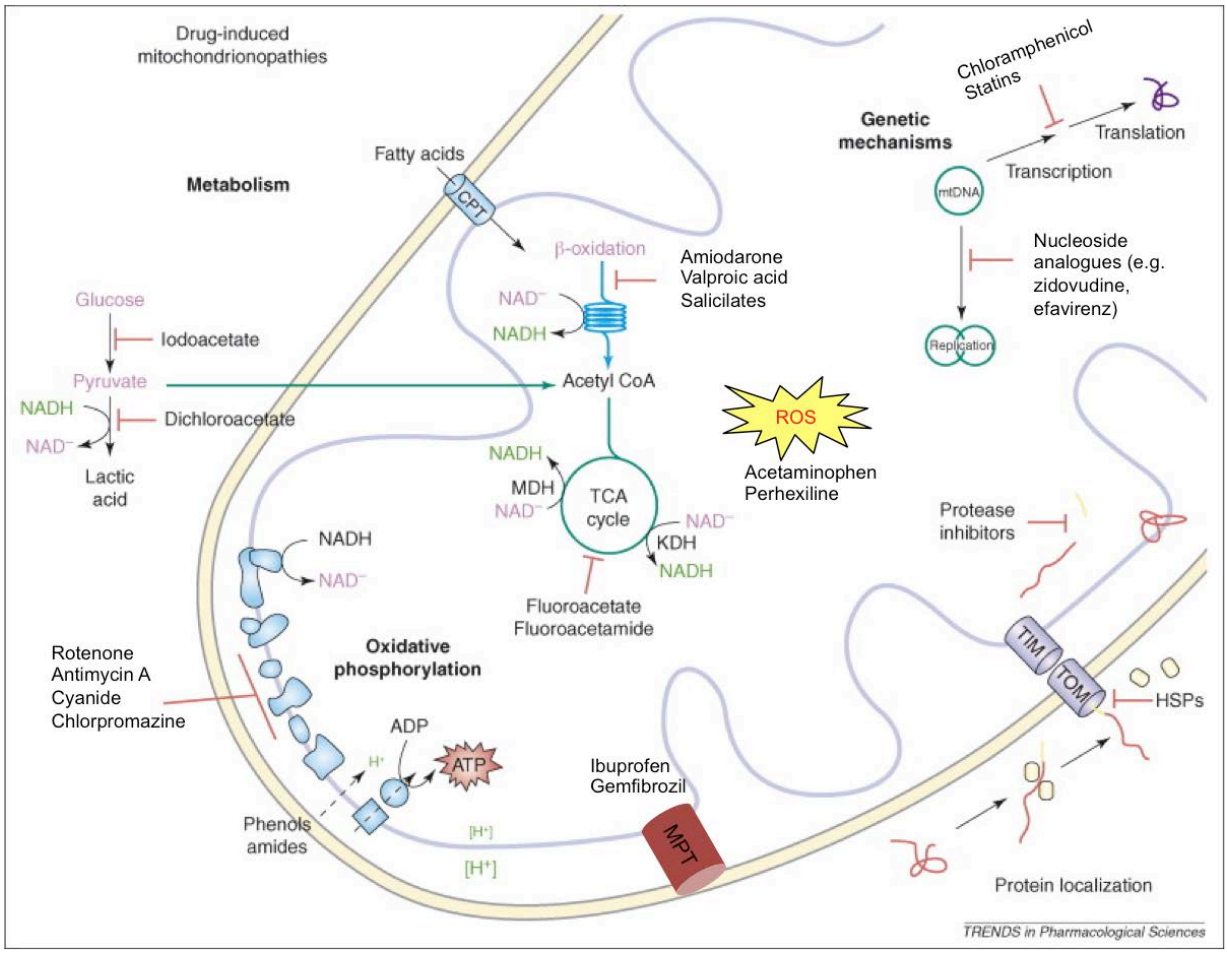

Figure 9: **Graphic representation of various molecular off-targets that have been implicated in drug-induced mitochondrial toxicities, adapted from Wallace et al. [39].** Abbreviations: carnitine palmitoyl transferase, CPT; α-ketoglutarate dehydrogenase, KDH; malate dehydrogenase, MDH; transporter outer membrane, TOM; transporter inner membrane, TIM.

1. *Electron transport chain & uncoupling of oxidative phosphorylation*

A well-defined mechanism of drug-induced mitochondrial dysfunction is the direct inhibition of the different complexes of the ETC, resulting in a diminished oxidation of substrates and oxygen consumption, finally resulting in impaired mitochondrial ATP production. In the presence of glucose, this can be compensated by glycolysis, possibly leading to lactic acidosis. Classical examples, blocking one of the five complexes of the respiratory chain include rotenone, malonate, antimycin A, cyanids, and oligomycin in the order starting from CI to CV [4]. In contrast to inhibitors of the ETC, uncouplers collaps the pH gradient and the electric potential across the IMM and thus increasing substrate

oxidation and oxygen consumption. The proton gradient across the IMM is dissipated as heat instead of ATP. Uncouplers are usually characterized as weak acids or bases (e.g. phenols or amids, respectively) with protonophoric activity, in order to carry protons into the mitochondrial matrix due to their permeability through the IMM (***Figure 10***). Laboratories performing pharmacological analysis of mitochondrial bioenergetics routinely use these known inhibitors to evaluate respiratory capacities [39].

The impairment of the OXPHOS often results in an impairment of β-oxidation due of the lack of oxidation of NADH, which is formed during β-oxidation, but also to mtDNA damage [26].

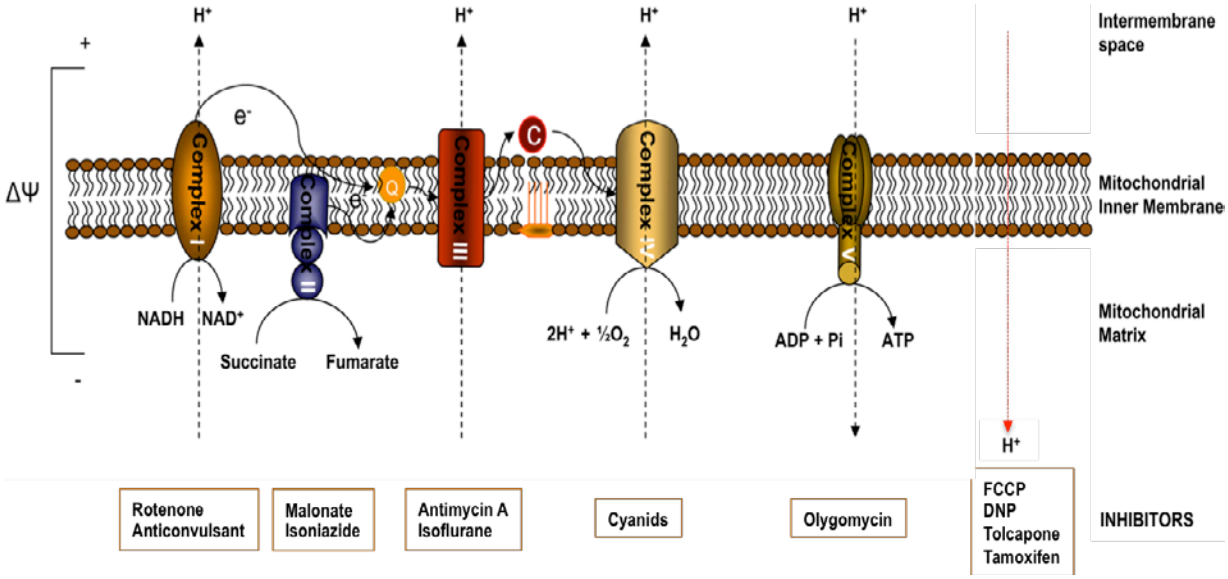

Figure 10: **Mitochondrial energy production machinery and common inhibitors of the respective complexes of the respiratory chain adapted from Bayir and Kagan [51].** C, cytochrome c; Q, ubiquinone.

2. *Inhibition of mitochondrial substrate oxidation (FAO and Krebs' cycle)*

The FAO and the Krebs'-cycle are favorite targets to be affected by many drugs that mostly mimic natural substrates. Their properties render themselves as competitive inhibitors of the respective reaction [39, 79].

As a result of the inhibition of the FAO, accumulated free fatty acids and triglycerides in the cytoplasma form small vesicles that not only influence the respiratory chain, but also inhibit the synthesis of ATP or ketone body formation, accounting for steatosis in patients. Direct inhibitors of the FAO are for example amiodarone, ibuprofen and tamoxifen. Others, such as valproic acid (VPA) or salicylic acid reach a repression via the generation of coenzyme A or L-carnitine esters leading to reduced levels of these cofactors. As opposed to direct inhibitors of the FAO, perhexiline, which is protonated in the acidic intermembrane space,

enters the mitochondrial matrix and thereby uncouples OXPHOS and inhibits complexes I and II of the ETC via indirect inhibition [39].

By reasons of the diversity of vulnerable target mechanisms in substrate oxidation, FAO is supposed to be one of the main causes for DILI. Therefore, several black box warnings (e.g. amiodarone, benzbromarone, tolcapone) have been raised [26].

Regarding the TCA cycle, the structural analogs fluroacetate and fluroacetamide react with oxaloacetate to form fluorocitrate, which in turn is a potent inhibitor of the aconitase enzyme in the TCA cycle. This leads then to a disturbance in the generation and delivery of reducing equivalents into the mitochondria ETC [39].

Consequently, the oxidation of incorrect substrates finally induces the same metabolic deficiency as the impairment of the ETC function through direct inhibitors. Highly metabolically active tissues or organs are therefore affected the most to misleading substrate oxidation [39] .

3. *Impairment of mitochondrial synthesis and biogenesis*

Several drugs have been reported to influence mtDNA and its processing such as replication and transcription [39, 43]. Most of them interact mainly with the mitochondrial polymerase γ, such as antiviral drugs (e.g. NRTIs, protease inhibitors, non NRTI) do. Some antiviral drugs can interrupt the viral life cycle by inhibiting the reverse transcription of invading viral RNA, but they may also have a high affinity to the mitochondrial polymerase γ. This in turn results in a reduction of mitochondrial DNA copies [41]. Topoisomerase inhibitors such as amsacrin and etopside can affect not only nuclear, but also mtDNA, possibly leading to mtDNA depletion. In addition, the antibiotic compound chloramphenicol inhibits mitochondrial protein synthesis due to high similarity of mitochondrial ribosomal RNA to eubacterial rRNA [26]. In general, mtDNA is more vulnerable to oxidative damage than nDNA due to the absence of histones and efficient repairing mechanisms in mtDNA. Additionally, the proximity of mtDNA to ROS-producing ETC renders the mitochondrial genome likely susceptible to drugs that block the respiratory chain and therefore increase mitochondrial ROS production [41].

2.8. Mitochondria-mediated cell death: apoptosis and necrosis

An impairment of mitochondrial function by oxidative stress or other factors can ultimately lead to apoptosis or necrotic cell death, as described in ***Figure 11***. The cell can undergo cell death after the triggering of one of the two following distinct pathways, the intrinsic or extrinsic pathway,

both leading to a mitochondrial permeability transition (MPT). The extrinsic pathway is initiated by binding of a ligand to death receptors (e.g. TNF members) at the cell surface, whereas the intrinsic pathway originates from the mitochondria, activated mainly through oxidative stress. Excessive ROS can attack phospholipid components of the inner mitochondrial membrane thus leading to the release of cytochrome C from the mitochondria into the cytosol and thereby to an initiation of proapopotic signaling cascades [80, 81].

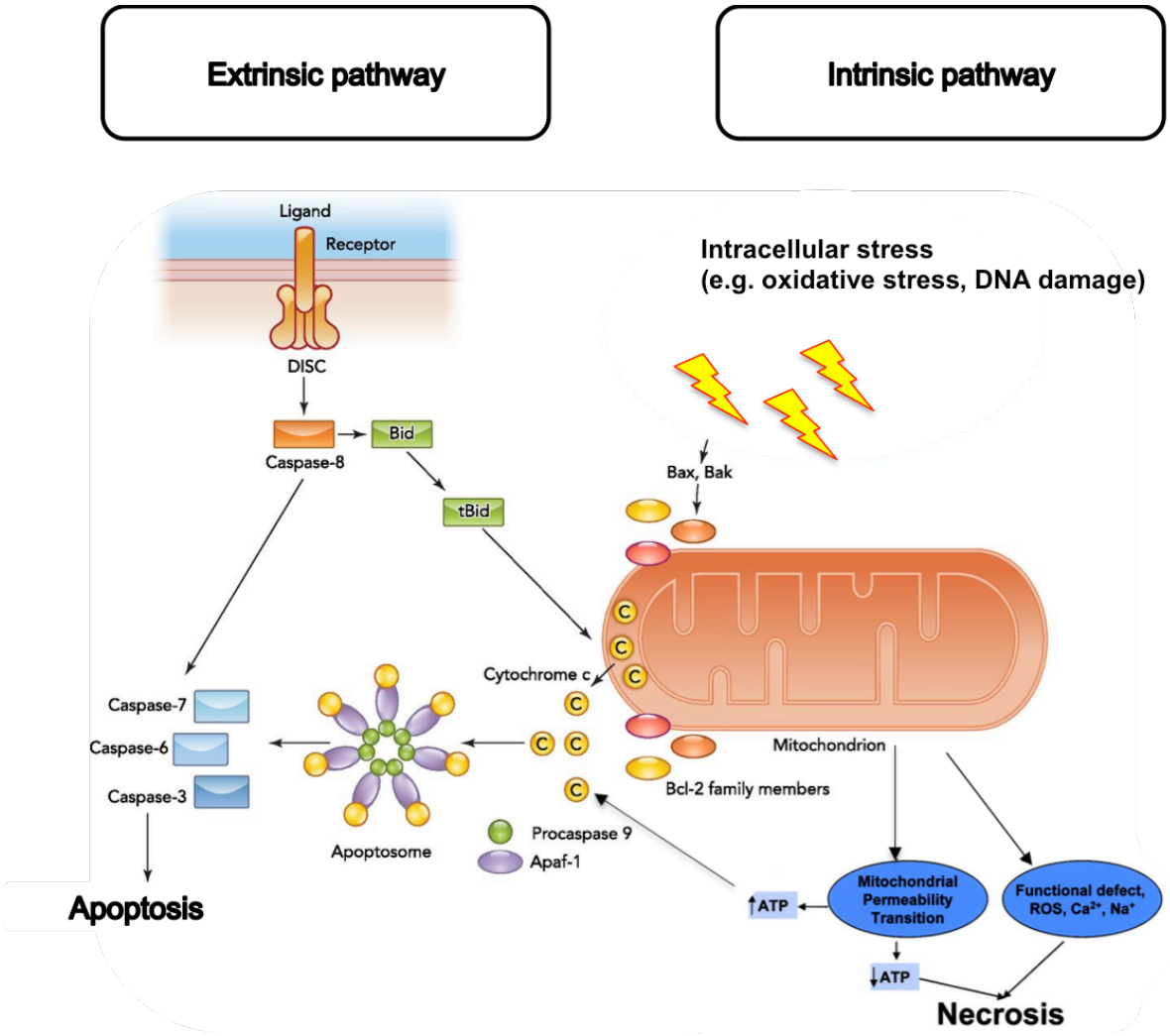

Figure 11: **Overview of the two cell-death signaling pathways apoptosis and necrosis adapted from Sendoel et al. [82] and Bhatia et al. [83].** Depending on variables such as ATP levels, ROS and/or MPT, apoptosis or necrosis can be initiated. Two distinct pathways can activate apoptosis; the binding of a death ligand to the death receptor initiates the extrinsic pathway resulting in an activation of the death-inducing signaling complex (DISC). Caspase-8 then either directly activates the downstream caspases or needs an amplification step via cleavage of Bid. In contrary, the intrinsic apoptotic signaling occurs in response to physiological signals or cellular stressors such as oxidative stress and DNA damage. Upon activation, the balance between antiapoptotic and proapoptotic Bcl-2 members on the mitochondrial membrane shifts and results in outer mitochondrial membrane permeabilization and cytochrome c release. Cytosolic cytochrome c binds to the apoptotic caspase activating factor (Apaf1) and recruits procaspase-9 to form the apoptosome complex. Activated caspase-9 within the apoptosome can then promote activation of downstream caspases.

The MPT plays a crucial role in the activation of cell death. Factors such as oxidative stress can trigger an opening of the MPTP. The MPTP is formed by an assembly of cyclophilin D, located in the matrix, adenine nucleotide translocase (ANT) residing in the inner membrane, and porin at the outer membrane. During the opened state of this pore, molecules up to 1.5 kDa can freely pass the inner mitochondrial membrane, hence causing an excessive reentry of protons through the IMM with the result of an arrest of ATP synthesis, mitochondrial swelling and rupture of the OMM [15, 43, 84, 85].

Apoptosis occurs when cytochrome C that is located on the outer surface of the inner mitochondrial membrane, is released to the cytosol and binds to a cytoplasmic scaffold (apaf-1) and pro-caspase 9. These three proteins are forming a complex referred as apoptosome, which triggers the caspase 9 signaling downstream cascade. This involves a subsequent activation of caspase 3 and other effector caspases. Moreover activated caspase 3 binds poly (ADP-ribose) polymerase (PARP), acting as DNA repair enzyme and finally is split into small fragments. All of these down-stream effector proteins signals induce apoptotic cell death, by which resulting fragments are vanished by phagocytosis [15, 52, 86]. The control of apoptotic cascade initiation occurs via antiapoptotic proteins such as Bcl-2 that reside in the outer mitochondrial membrane and prevent cytochrome C effusion, whereas proapoptotic signals like Bax are located in the cytosol and translocate to the mitochondria in presence of death stimuli. Depending on the predominance of either Bax or Bcl, cytochrome C efflux is promoted [22].

The activation of caspases is an ATP-dependent process, where a certain functioning of the mitochondria is still required, which means that MPT has not occurred rapidly and simultaneously in all mitochondria. In contrast, the process of uncontrolled cell damage or necrosis occurs in a rapid manner simultaneously in many mitochondria, which often happens with hepatotoxins that evoke such quick cell stress. Consequently, prompt and acute depletion of mitochondrial ATP and osmotic imbalance of intra- and extracellular fluids lead to cellular swelling, a disruption of the plasma membrane, and finally to cell lysis [86].

Importantly, one has to be aware that apoptosis and necrosis are not two completely distinct processes rather than overlapping events. The extent of mitochondrial damage determines whether cell undergoes either the controlled pathway of apoptosis or necrosis, in the presence of enough ATP, apoptosis is dominant and vice versa when cellular ATP concentrations are low. Cell homeostasis can also be maintained by mitochondrial autophagy, which eliminates malfunctioning mitochondria specifically [52].

2.9. Mitochondrial adaptions to drugs – limiting mitochondrial injury and dysfunction

Mitochondria have the ability to adapt to dysfunction or injury caused by toxicants or other conditions. One common mechanism to counteract oxidative stress is the enhanced expression of diverse mitochondrial antioxidant enzymes such as MnSOD and GSH peroxidase [87].

Besides that, mitochondrial biogenesis defined as the process where mitochondria are re-organized, can modulate their growth and division according to the implemented stress [88]. The proliferator-activated receptor gamma coactivator-1alpha (PGC-1α) thereby plays a crucial role as transcriptional adaptive response to injury [31]. PGC1α is involved in the expression of antioxidant proteins but it can also bind to the peroxisome proliferator-activated receptor alpha (PPARα) and thus induces the transcriptional activation of nuclear genes encoding fatty acid metabolizing enzymes such as CPT1 or medium-chain acyl-CoA dehydrogenase (MCAD) [89]. Importantly, PGC1α is also able not only to stimulate the synthesis of nuclear encoded polypeptide of the respiratory chain during oxidative stress, but as well the transcription and replication of mitochondrial DNA [43].

The reassembly of mitochondrial morphology represents a further modulatory mechanism to mitochondrial dysfunction. As already mentioned in the section Dynamics, mitochondria constantly undergo fusion and fission in order to exchange mitochondrial content such as respiratory-chain complexes or mtDNA. In terms of injury, enhanced fusion of mitochondria may reduce oxidative stress [90, 91].

Another mechanism referred as mitochondrial hormesis has been discussed, at which constant low amounts of ROS and thus slight oxidative stress ameliorates mitochondrial biogenesis [92]. This hypothesis is supported by diverse studies revealing that caloric restriction in rodents enhanced antioxidant defense capacities [93, 94].

As a last option to counteract the mitochondrial damage to prevent cell death, impaired and affected mitochondria can be eliminated by self-digestion induced via mitochondrial autophagy (illustrated in ***Figure 12***) [80, 95].

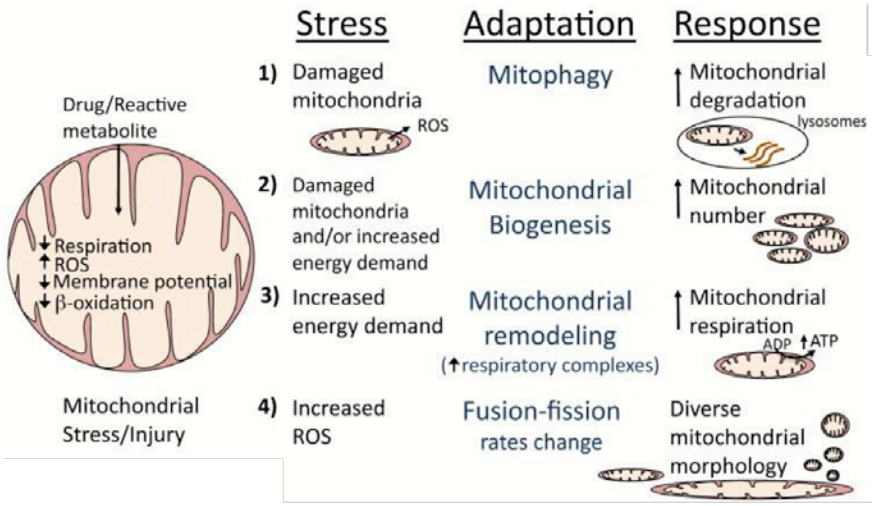

***Figure 12**:* **Various adaption mechanisms during cellular stress, adapted from Han et al. [88].**

3. Current prediction methodologies for the investigation of mitochondrial DILI

Predictable pharmacokinetic properties, avoidance of drug-drug interactions, and metabolic stability are possible concerns in drug development for pharmaceutical industry to keep patients safe from unexpected adverse reactions. Nevertheless, drug-induced hepatic dysfunction still accounts for many drug failures during clinical trials or the post-marketing phase, leading to drug withdrawals. Since susceptibility factors are important for idiosyncratic adverse drug reactions, this type of toxicity can usually not be detected in preclinical animal studies. Other than animal studies, mechanism-based in vitro toxicity assays have been established aiming to provide reliable models uncovering potential idiosyncratic toxicity in the preclinical phase. To date, no suitable standardized methods or biomarkers are available predicting idiosyncratic DILI. Only Hy's law (drugs associated with clinically relevant ALT and concomitant bilirubin elevation) is commonly applied as standard procedure in clinical phases [96, 97], but this does not cover the early detection of potential drug hepatotoxicity. Therefore, it is an important need to find new approaches providing an easy-to-use and standardized method for detecting idiosyncratic DILI in preclinical drug investigation.

In the following paragraph, state-of-the-art *in vivo* and *in vitro* methods and common endpoint measurements to identify mitochondrial toxicity (depicted in ***Figure 13***) by potentially hepatotoxic drugs will be discussed.

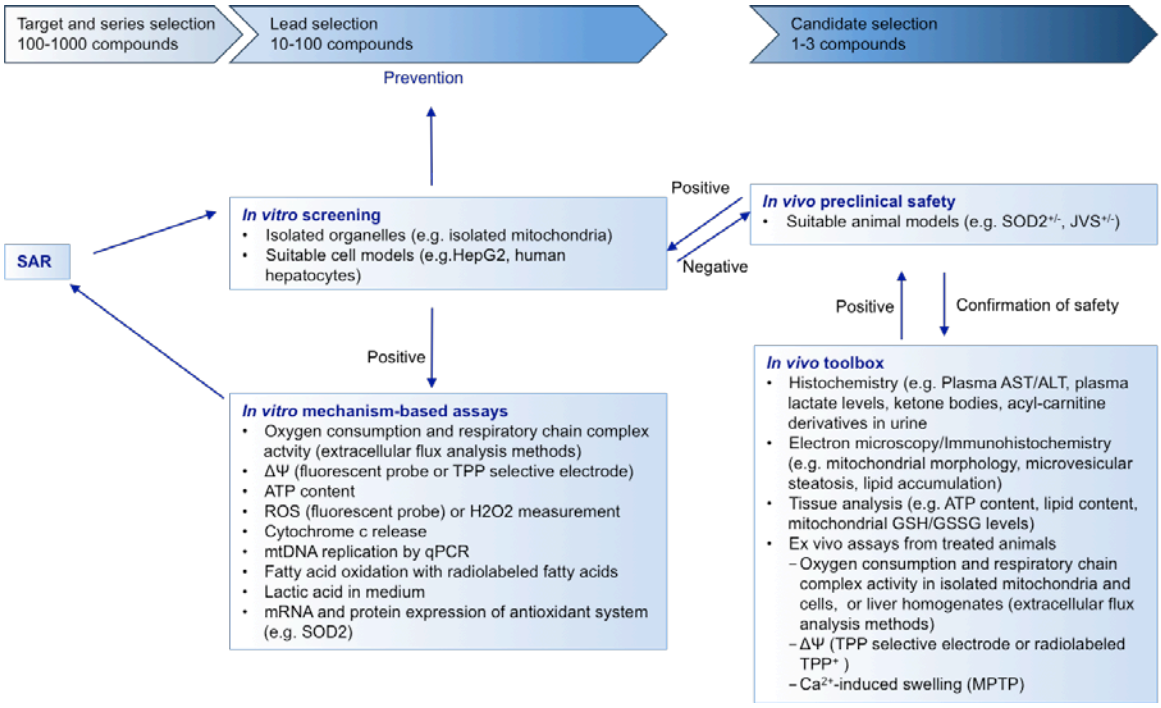

***Figure 13**:* **Model of mitochondrial toxicity screening explained and illustrated by Dykens et al. [25].** Early identification of mitochondrial toxicity during compound series selection and lead selection using in vitro screens allows for structure–activity relationship (SAR) studies to circumvent it. Cell-based screening assays are available for initial identification of general cytotoxicity. If a mitochondrial etiology is suspected, assessment of isolated mitochondrial function can also be performed in screening mode. If positive, additional in vitro mechanistic studies can examine effects on OXPHOS respiration, permeability transition, reactive oxygen and nitrogen centered (ROS), membrane potential (ΔΨ), and mitochondrial DNA (mtDNA) status, among others. Such data enable structure–activity relationship (SAR) studies necessary to circumvent mitochondrial toxicity. Mitochondrial assessment should be completed before a compound moves into further development and is elevated to drug candidate level but should certainly also be triggered if a compound has a negative response in an animal model. Classical assays such as electron microscopy and enzyme-linked assays of the individual respiratory complexes are available for assessing mitochondrial status in tissues. In addition, advanced histochemical and immunohistochemical techniques are being developed that will help illuminate mechanism of mitochondrial impairment. Fostered by the organelle and cell studies, animal models are also being developed to better reveal mitochondrial toxicity, and hence to better predict clinical outcome.

3.1. In vivo models

Animal models are, despite the efforts to meet the 3R's aiming to reduce, replace, and refine the use of animals in research, still essential for biomedical research as they allow controlling parameters that may be involved in the metabolism of compounds leading to adverse reaction. Above all they are favorable due to the fact that they are living organisms whereas cellular models typically lack the complex *in vivo* cell-cell interactions. Many attempts have been made in developing animal models for idiosyncratic DILI [98-100]. However, a lot of impediments including the lack of understanding the exact mechanisms of idiosyncratic DILI, marked inter species differences, but also the rarity of these adverse reactions led to failure in finding convincing standard approaches. Generally, normal healthy wild-type animals are used in preclinical safety studies of drug discovery but exactly these conditions do not consider the

inter-individual discrepancies such as genetic or environmental predispositions. Given that a toxic insult becomes pathological only if a certain critical threshold (as during oxidative stress in the mitochondria) has been reached, the chances to detect those in healthy wild-type animals equals zero. Therefore, different models have been emerged taking these factors into account by using the approach of generating transgenic animals with mitochondrial dysfunctions [101-104] or by utilizing chemicals inducing modifications of the mitochondrial function such as the mouse model with carnitine impairment. A deficiency induced by chronic exposure to the carnitine analog trimethylhydrazinium propionate results in an inhibition of fatty acid β-oxidation and hepatic steatosis [105-107].

The most promising mouse models so far specifically for idiosyncratic DILI are described as:

1) the heterozygous juvenile visceral steatosis ($jvs^{+/-}$) mice exerting a carnitine deficiency generated by impaired renal reabsorption. This dysfunction led to an enhanced hepatotoxicity when mice were treated during 14 days with the antiepileptic drug valproic acid, which results in elevated levels of serum ALT, defects in the ETC, and impaired mitochondrial β-oxidation, finally leading to microvesicular steatosis. Solely ($jvs^{+/-}$) mice showed this phenotype, whereas valproic acid-treated wild-type mice seemed to be unaffected [108, 109].

2) the heterozygous mitochondrial superoxide dismutase knockout mouse ($SOD2^{+/-}$) with approximately 50% reduced SOD2 activity. While homozygous SOD2 mutant mice die within several days after birth due to dilated cardiomyopathy, the heterozygous strains grow normally, but showing a phenotype characteristically for mitochondrial dysfunction namely by exhibiting increased oxidative damage [101]. With this model, several drugs could be unmasked as mitochondrial toxicants such as troglitazone, nimesulide, and flutamide inducing idiosyncratic DILI [103, 110]. The observed elevation of ALT and concurrent increase in oxidative stress causing histopathological changes (hepatic necrosis) only in $SOD2^{+/-}$ but not in wild-type mice indicates that animals with a preexisting dysfunction of the mitochondria have a higher susceptibility to mitochondrial toxicants.

Although these two models were successful in uncovering drugs with mitochondrial idiosyncratic potency, they also bear problems such as lack of reproducibility, development of only modest liver injury, or the necessity of long-term exposure to animals. Nonetheless, the concept of generating animal models with underlying dysfunctions in order to mimic the situation in patients with predisposed diseases or dysfunction appears to be the right direction in the understanding and detection of idiosyncratic DILI.

3.2. In vitro models

In early drug development stages, researchers are committed to detect hepatotoxicity before testing compounds in animal studies or clinical settings. Cell-based screening models reflecting human *in vivo* toxicity are therefore indispensable. In the following section, cellular models, which are applied currently, will be reviewed.

Human hepatocytes

Primary human hepatocytes in monolayer cultures are considered as the 'gold standard 'of *in vitro* toxicity testing and drug metabolism assessment due to their expression of P450 enzymes and therefore drug metabolism capacities. Nevertheless, the use of primary human hepatocytes have limitations including their instable phenotype, the large variability of hepatic function of different donors, their short viability, and their high cost and scarcity of availability [111].

Isolated mitochondria

Another approach in the evaluation of xenobiotics' toxic mechanism is the use of isolated mitochondria (from different species). They are suitable to measure constitutional activities of oxidative phosphorylation and other mitochondrial functions based on an acute exposure to drugs [111-114]. However, one has to be cautious in interpreting results obtained from isolated mitochondria since they do not have an interaction with a physiological environment, and moreover lack the direct contact to other organelles and plasma membrane.

Hepatoma cell lines

Several hepatoma cell lines such as HepG2, HepaRG, Huh7, and Hep3b have been proposed in the study of hepatotoxicity to circumvent some disadvantages of human hepatocytes. The ease of use, the high availability, low-cost, and particularly the unlimited lifespan of immortalized cell lines render them much more favorable than using primary human hepatocytes. However, the major obstacles of these tumor-derived cell lines are on one hand the poor expression of key-metabolic enzymes making it impossible to uncover metabolizing drugs, and on the other hand the typically attribute of rapid unregulated growth of tumor cells [111, 115]. Among the human hepatoma cell lines, HepG2 cells, the most widely used and characterized system in human hepatotoxicity investigation, as well as the novel hepatoma HepaRG cells expressing subtle levels of different CYPs, are the most relevant *in vitro* systems in the elucidation of drug–induced mitochondrial dysfunction and toxicity (see ***Figure 14***)[116, 117].

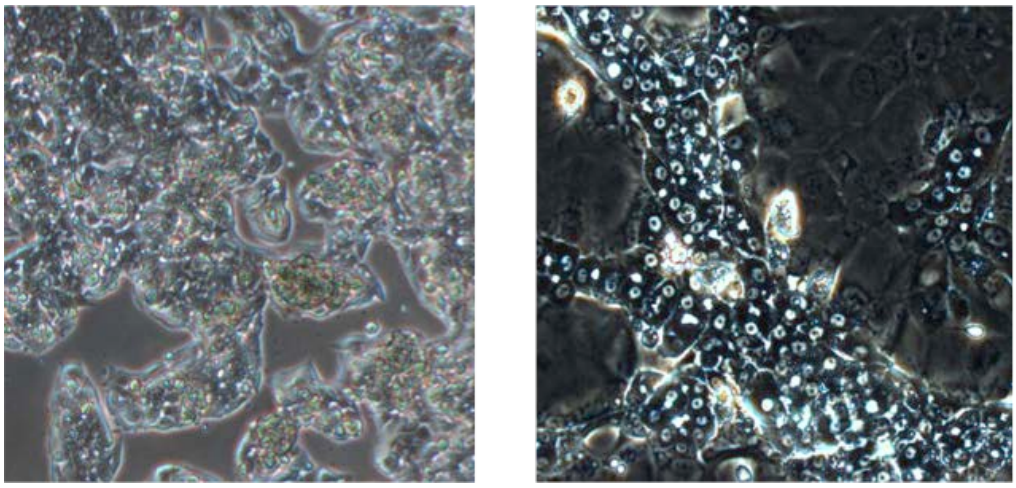

***Figure 14**:* **Light microscopy pictures of HepG2 cells (left) and differentiated HepaRG cells (right).** HepG2 cells, usually agglomerating to small colonies, possess an epithelial morphology. HepaRG cells demonstrate the typical phenotype of clustered hepatocyte-like cells surrounded by biliary-endothelial-like cells.

HepG2 cells

A variety of hepatotoxic compounds have been identified in HepG2 cells through mechanistic studies of determinants related to mitochondrial functions. Although HepG2 cells have similar characteristic to normal hepatocytes, the lack of relevant liver cytochrome P450 enzymes leads to misdetections or wrongly predicted cytotoxicity results [118]. Thus, a lot of effort has been made in constructing 3D systems of HepG2 cells that cover better functionalities with features including repolarization, metabolism, and transport activities that are usually lacking in classical 2D cultures [111, 115]. Since the rapid growth of the tumor-derived HepG2 cells is mostly accounted to the Crabtree effect [119], which means that they have limited mitochondrial production of ATP, which is replaced by increased glycolysis. This effect leads to a decreased vulnerability of HepG2 cells to mitochondrial toxicants. Therefore, a novel strategy has been developed to circumvent this problem. Normally, HepG2 cells are cultered in high-glucose medium (25 mM), which enables them to produce energy via glycolysis. If the culture media is replaced with galactose (10 mM), cells are forced to generate ATP mostly through OXPHOS. This makes them more susceptible to drugs with potential inhibitory effects on mitochondrial metabolism [120, 121]. For that reason, it is recommended to pay attention to the choice of culture media in order to avoid misleading results when researchers intend to screen for substances that possibly affect mitochondrial function.

HepaRG cells

Similar to HepG2 cells, HepaRG cells are also tumor-derived and therefore immortal cells. Since proliferating HepaRG cells do not exhibit any hepatic functions, they first need to be differentiated for two weeks in DMSO-containing medium so that they transform into a hepatocyte or cholangiocyte-like phenotype, which resemble closely the characteristics of

human hepatocytes. Unlike any other hepatoma cell line, HepaRG express 81-92% of the genes active in human hepatocytes and exert increased levels of metabolizing enzymes of phase I and II [122]. This cell line has therefore gained much attention because it allows to perform studies with drugs potentially causing toxic effects through the formation of reactive metabolites [116]. Besides these specific features, HepaRG cells can also be utilized for long-term toxicity studies due to their maintenance of metabolic function over several weeks providing important results for chronic toxicity assessment [123, 124]. Currently, HepaRG cells can be regarded as the best surrogate for primary human hepatocytes [111].

3.3. Other approaches of hepatotoxicity testing

Animal and cellular models represent the general approach to gain knowledge in drug-induced hepatotoxicity. Nevertheless, in recent years, a couple of new approaches have been developed with the aim to find relevant biomarkers or to explain mechanisms of toxic side effects [125-127].

Similar to transgenic animals, cell lines are modified via stable or transient knockdown with shRNA or siRNA, respectively [128-130], of essential genetic factors that are possibly associated with drug-induced toxicity. This technology creates conditions to comprehensively study genetic requirements in the context of drug toxicity mechanisms at which cells present deletions of genes that usually are pivotal for proper mitochondrial- or cellular functions.

The application of 'omics' technologies including genomics, proteomics, and metabolomics in toxicology has increased in the last few years. This field mainly describes microarray-based approaches assessing alterations in gene- or protein expression profiles induced by possible toxicants. In contrast to conventional methods, 'omics' provide more efficient strategies to investigate complex biological interactions and responses after exposure to toxicants [126]. Moreover they are claimed to consider strongly the interplay of genome, toxicants, and organ dysfunction, but also identify diagnostic and therapeutic fingerprints [131]. Metabolomics appears to be a promising approach to find biomarkers for hepatotoxicity due to the advantage of non-invasive sample collection and analysis [125]. Nonetheless, these technologies are still in the early stages and additional knowledge and studies are needed to judge whether these approaches will be of use as standard methods to predict toxicology in drug discovery.

4. Mitochondrial toxicants

4.1. Hydroxy-cobalamin [c-lactam] (HCCL) – A vitamin B_{12} analog

HCCL is a vitamin B_{12} analog that acts as a functional vitamin B_{12} antagonist [132]. This substance has been used to better understand morphological and functional changes occurring in the disease state of the inherited autosomal recessive disorder methylmalonic aciduria. This disease is associated with impaired activity of the enzyme methylmalonyl-Co A mutase, which may be due to mutations affecting the protein itself or due to deficient vitamin B_{12} transport, processing or metabolism, potentially resulting in severe metabolic-or multiorgan failure [133, 134]. It has been shown that subcutaneous administration of HCCL over several weeks in rats depicted similar pathological defects as observed in methylmalonic aciduria [135]. The competitive inhibition of hepatic L-methylmalonyl-CoA mutase leads to an impairment of propionate utilization, at which succinyl-CoA is formed and further used in the Krebs' cycle. Propionyl-CoA and methylmalonyl-CoA are thereby increased, leading to an accumulation of toxic compounds such as urinary excreted methylmalonic acid or propionyl-derived 2-methylcitrate [132, 136]. Krahenbuhl et al. have uncovered that HCCL induces in hepatocytes of treated rats changes in mitochondrial function such as an inhibition of complexes III and IV of the mitochondrial respiratory chain. The mechanism of this inhibition is supposed to be due to defective mitochondrial RNA processing [136]. Moreover, HCCL treatment in rats has shown increased hepatic mitochondrial capacities due to mitochondrial proliferation and enlarged mitochondria [135]. HCCL appears to be an interesting compound since it chemically inhibits specific mitochondrial functions without affecting major cellular functions. HCCL may therefore represent a useful tool in establishing a cellular model or animal model with underlying mitochondrial defects to investigate mechanisms of idiosyncratic adverse drug reactions of mitochondrial toxicants.

4.2. Azoles

Azoles, a class of heterocyclic synthetic compounds, represent the most commonly used medications against fungal infections [137]. All azole derivatives, including the imidazole ketoconazole and the more recently developed triazoles such as fluconazole, posaconazole, and voriconazole share the same mechanism of action by targeting the fungal P450-dependent enzyme 14α-lanosterol-demethylase that is essential in the ergosterol biosynthesis of the fungal membrane [137-139]. Despite the specificity against fungal infections, adverse effects and drug-drug interaction due to high affinity to human CYPs have been implicated with azole treatment. Clinically used azoles are highly associated with the development of hepatocellular injury [9, 139, 140]. However, exact underlying mechanisms evolving the hepatotoxic etiology of azoles still

remain to be discovered. Some evidence about the involvement of mitochondrial toxicity leading to hepatocellular side effect is documented for ketoconazole and fluconazole [141-145]. Nevertheless, no information exists about the toxic mechanisms of the more recently released triazoles such as posaconazole and voriconazole.

In the following paragraphs, the azoles used in our studies will be presented. ***Figure 15*** depicts the chemical structures of azoles.

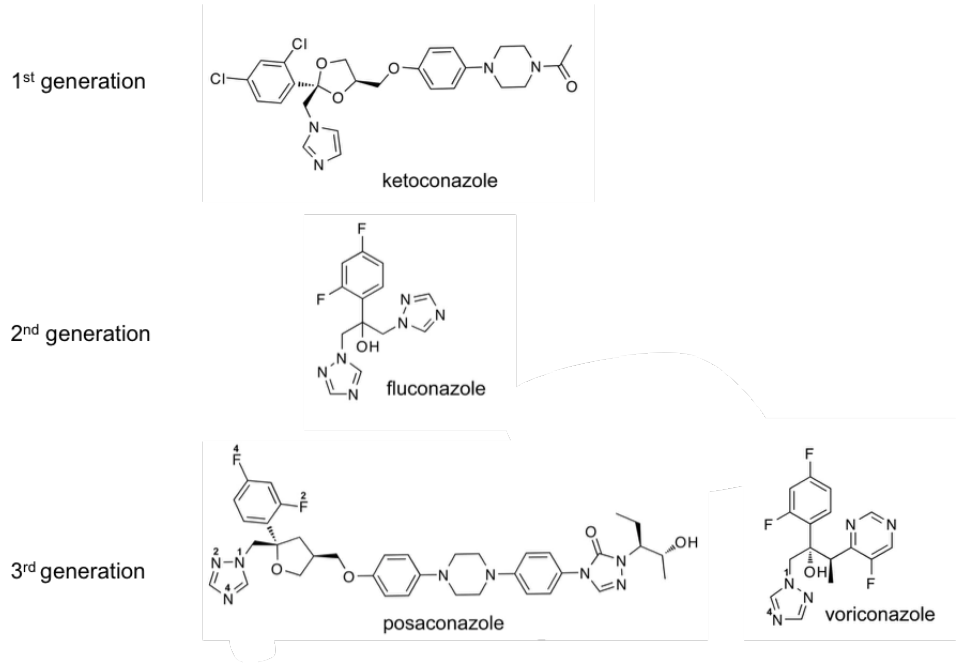

Figure 15: **Chemical structures of the three generations of systemic azoles adapted from Mast et al. [146].** The numbering of some of the heteroatoms in posaconazole and voriconazole is also shown.

Ketoconazole

As the first antifungal agent with imidazole structure, ketoconazole was introduced to the market in the 80's. Besides the antifungal properties, ketoconazole is a well-known inhibitor of various CYP450 isoforms [147]. Within five years after ketoconazole's market release, increasing reports of hepatocellular adverse effects ranging from asymptomatic elevation of transaminases to fatal hepatitis became widely recognized [148, 149]. As a sanction of rising case reports of liver injury associated with ketoconazole, the FDA limited its oral use in 2013 [147].

Fluconazole

The triazole-based antifungal fluconazole was launched with an improved safety profile compared to ketoconazole. Generally, it is well tolerated and is rarely associated to hepatotoxicity [139]. Studies in rat hepatocytes have clearly shown that fluconazole's hepatotoxic potential is only given at high concentrations, at which also impaired ETC function has been observed similar

to those seen with ketoconazole treatment, but with the main discrepancy that ketoconazole inhibited already at lower concentrations and with a greater extent than fluconazole [144].

Voriconazole

The second-generation triazole voriconazole has been developed with advanced properties. The low-molecular weight and water-soluble compound combines the broad spectrum of activity of itraconazole and increased bioavailability of fluconazole. Voriconazole has been recommended as the first-line therapy against invasive aspergillosis. Its indication requires caution due to significant drug-drug interactions, mainly evoked from the strong inhibitory potential against various CYPs. Therapeutic drug monitoring is necessary to control for variable plasma concentrations [140, 150].

Posaconazole

Posaconazole is the newest triazole, approved by the FDA in 2006. It shows lipophilic features and is structurally derived from itraconazole, thus revealing potent broad-spectrum activities against fungal infections. Its safety profile is similar to fluconazole and it has become an alternative to voriconazole. Nonetheless, posaconazole is implicated with hepatocellular injury [139, 151]. Since it is the most recently launched azole, little is known about the associated mechanisms of liver injury.

4.3. Benzofuran derivatives

Many reports have associated this class of drugs with hepatotoxicity. They are known to impair mitochondrial function that has been postulated as the major factor leading to severe hepatotoxicity [79].

Amiodarone, an antiarrhythmic drug was identified as potent inhibitor of mitochondrial fatty acid β-oxidation causing micro-and macrovesicular steatosis as well as dysfunction of the ETC and thus increased ROS production [47, 114]. These adverse properties result from amiodarone's lipophilic characteristics, which results in accumulation in tissues such as hepatocytes. Therefore, several black box warnings from the FDA were announced [79]. Dronedarone is a follow-up compound of amiodarone, but possesses a non-iodinated benzofuran structure with additional methylsulfonamide side chain, reducing its lipophilicity [114, 152]. Despite the structural improvements dronedarone showed hepatic toxicities in the post-marketing phase with the result of a black box warning by the FDA [153]. *In vivo*-and *in vitro* studies by Felser et al. have uncovered similar mechanisms for the structural derivative of amiodarone. Impairment of

mitochondrial fatty acid β-oxidations is thus most likely the primary mechanism leading to the adverse effect of dronedarone [114].

Like dronedarone, benzbromarone represents a structural analog of amiodarone, but has been used as uricosuric drug. Due to reports of hepatocellular liver injury, benzbromarone was withdrawn from the market in 2003 in several countries [154]. The mechanism of its toxicity remains not fully understood. However it is also associated with mitochondrial impairment, including β-oxidation, activation of MPT, and mitochondrial structural changes like mitochondrial fragmentation [155].

Objectives

The goal of this thesis was to contribute to an improved understanding of the molecular mechanisms of drug-induced mitochondrial dysfunction. Therefore we aimed to create models *in vitro* and *in vivo* with mitochondrial defects, either chemically induced or with siRNA serving as a sophisticated system to test potential hepatotoxic drugs, mimicking patients with underlying metabolic disease that are more prone to develop idiosyncratic drug-induced mitochondrial dysfunction. Another aim of the thesis was to elucidate the toxicity and associated molecular mechanisms of clinically relevant azoles that are suspected to cause idiosyncratic liver injuries as side effect.

The purpose of the first study was to establish a cellular model with subtle changes in mitochondrial function such as the respiratory chain function and to characterize beyond that the molecular mechanism of these functional impairments. We induced the dysfunction by exposing HepG2 cells to the structural vitamin B_{12} analog hydroxy-cobalamin [c-lactam] (HCCL) since in previous studies HCCL impaired mitochondrial bioenergetics and showed histopathological liver changes without disturbing main cellular function by competitively inhibiting major determinants of the propionate pathway.

In the second study we wanted to clarify whether the changes induced by HCCL treatment previously detected in both, rat and our newly generated cell model can also be obtained in a mouse model, which would offer considerable advantages in respect of *in vivo* toxicological studies.

If treatment with HCCL were successful and therefore confirm our hypothesis, we planned to induce specific mitochondrial dysfunction in HepG2 cells by knocking down diverse genes involved in mitochondrial energy metabolism or oxidative defense. The short report representing a pilot project hypothesized that silencing of genes, encoding for important enzymes of the mitochondria, leads to an increased liability to DILI.

The goal of the third project was to elucidate the hepatotoxicity and thereby underlying mechanisms of antifungal azole derivatives as they all feature an adverse potential of causing idiosyncratic liver injuries. In a second step, we aimed to test the hypothesis that mitochondrial toxicants are more toxic in cells with mitochondrial dysfunction (e.g. cells treated with HCCL or with knockdown of genes coding for specific mitochondrial proteins).

Paper 1

Impaired mitochondrial function in HepG2 cells treated with hydroxy-cobalamin[c-lactam]: A cell model for idiosyncratic toxicity

P Haegler[1,2], D Grünig[1,2], B Berger[1,2], S Krähenbühl[1,2,3], J Bouitbir[1,2,3]

[1] Clinical Pharmacology & Toxicology, University Hospital Basel, Switzerland

[2] Department of Biomedicine, University of Basel, Switzerland

[3] Swiss Centre of Applied Human Toxicology (SCAHT)

In press, accepted Manuscript

Toxicology, 2015, doi:10.1016/j.tox.2015.07.015

Toxicology 336 (2015) 48–58

Contents lists available at ScienceDirect

Toxicology

journal homepage: www.elsevier.com/locate/toxicol

Impaired mitochondrial function in HepG2 cells treated with hydroxy-cobalamin[c-lactam]: A cell model for idiosyncratic toxicity

Patrizia Haegler[a,b], David Grünig[a,b], Benjamin Berger[a,b], Stephan Krähenbühl[a,b,c,*], Jamal Bouitbir[a,b,c]

[a] Division of Clinical Pharmacology & Toxicology, University Hospital, 4031 Basel, Switzerland
[b] Department of Biomedicine, University of Basel, Switzerland
[c] Swiss Centre of Applied Human Toxicology, SCAHT, Switzerland

ARTICLE INFO

Article history:
Received 6 May 2015
Received in revised form 9 July 2015
Accepted 19 July 2015
Available online 26 July 2015

Keywords:
Vitamin B12 deficiency
Hydroxy-cobalamin[c-lactam]
Mitochondrial toxicity
Idiosyncratic hepatotoxicity

ABSTRACT

The vitamin B12 analog hydroxy-cobalamin[c-lactam] (HCCL) impairs mitochondrial protein synthesis and the function of the electron transport chain. Our goal was to establish an in vitro model for mitochondrial dysfunction in human hepatoma cells (HepG2), which can be used to investigate hepatotoxicity of idiosyncratic mitochondrial toxicants.

For that, HepG2 cells were treated with HCCL, which inhibits the function of methylmalonyl-CoA mutase and impairs mitochondrial protein synthesis. Secondary, cells were incubated with propionate that served as source of propionyl-CoA, a percursor of methylmalonyl-CoA. Dose-finding experiments were conducted to evaluate the optimal dose and treatment time of HCCL and propionate for experiments on mitochondrial function.

50 μM HCCL was cytotoxic after exposure of HepG2 cells for 2 d and 10 and 50 μM HCCL enhanced the cytotoxicity of 100 or 1000 μM propionate. Co-treatment with HCCL (10 μM) and propionate (1000 μM) dissipated the mitochondrial membrane potential and impaired the activity of enzyme complex IV of the electron transport chain. Treatment with HCCL decreased the mRNA content of mitochondrially encoded proteins, whereas the mtDNA content remained unchanged. We observed mitochondrial ROS accumulation and decreased mitochondrial SOD2 expression. Moreover, electron microscopy showed mitochondrial swelling. Finally, HepG2 cells pretreated with a non-cytotoxic combination of HCCL (10 μM) and propionate (100 μM) were more sensitive to the mitochondrial toxicants dronedarone, benzbromarone, and ketoconazole than untreated cells.

In conclusion, we established and characterized a cell model, which could be used for testing drugs with idiosyncratic mitochondrial toxicity.

© 2015 Elsevier Ireland Ltd. All rights reserved.

1. Introduction

Methylmalonic aciduria is a severe autosomal recessive inborn error of metabolism characterized by intermittent metabolic instability and multiorgan pathology (Deodato et al., 2006; Horster and Hoffmann, 2004). While the prognosis for short- and long-term survival has improved over the last years, progressive neurocognitive deterioration is still a common finding in affected patients (Dionisi-Vici et al., 2006). The disorder can be caused by deficient enzymatic activity of methylmalonyl-CoA (MM-CoA) mutase or defective intracellular transport, processing and/or metabolism of cobalamin (Vitamin B_{12}) (Takahashi-Iniguez et al., 2012). Vitamin B_{12} deficiency is associated with decreased activity of the cobalamin-requiring enzymes MM-CoA mutase and methionine synthetase (Stabler, 2013). MM-CoA mutase is an important mitochondrial enzyme in propionate metabolism and converts L-methylmalonyl-CoA into succinyl-CoA, a Krebs cycle intermediate (Fig. 7). A block at this enzymatic step results in elevated plasma levels and urinary excretion of methylmalonic acid as well as in the accumulation of other propionyl-CoA-derived metabolites such as 2-methylcitrate (Lehotay and Clarke, 1995).

Abbreviations: $\Delta\psi_m$, mitochondrial membrane potential; BSA, bovine serum albumin; Cbl, cobalamin; DMEM, Dulbecco's Modified Eagle Medium; DMSO, dimethyl sulfoxide; EGTA, ethylene glycol tetraacetic acid; FCCP, carbonyl cyanide *p*-(trifluoromethoxyl)-phenyl-hydrazone; HCCL, hydroxy-cobalamin[c-lactam]; HPLC, high-performance liquid chromatography; HEPES, 4-(2-hydroxyethyl)-1-piperazineethanesulfonic acid; MTT, methylthiazolyldiphenyl-tetrazolium bromide; MM-CoA, methylmalonyl-CoA; ROS, reactive oxygen species; SDS, sodium dodecyl sulfate; SOD, superoxide dismutase; TMPD, N, N,N′,N′-tetramethyl-*p*-phenylenediamine; TMRM, tetramethylrhodamine methyl ester.

* Corresponding author at: Clinical Pharmacology & Toxicology, University Hospital, 4031 Basel, Switzerland.
E-mail address: kraehenbuehl@ubs.ch (S. Krähenbühl).

http://dx.doi.org/10.1016/j.tox.2015.07.015
0300-483X/© 2015 Elsevier Ireland Ltd. All rights reserved.

Interestingly, liver mitochondria from animals and patients with vitamin B_{12} deficiency (Frenkel et al., 1976) and from animals or humans with lacking or impaired MM-CoA mutase activity (Chandler et al., 2009) have morphological and/or functional alterations. In order to better understand the mechanisms of these alterations, rats have been treated with the vitamin B_{12} analog hydroxy-cobalamin[c-lactam] (HCCL), which antagonizes the function of vitamin B_{12} regarding MM-CoA mutase (Brass et al., 1990; Stabler et al., 1991). After several weeks of continuous subcutaneous infusion with HCCL, rats developed methylmalonic aciduria and this treatment was associated with hepatic mitochondrial proliferation (Krahenbuhl et al., 1990) and impaired function of complexes III and IV of the electron transport chain of liver mitochondria (Krahenbuhl et al., 1991). The mechanism for the impaired function of enzyme complexes of the electron transport chain in the presence of HCCL is most likely a defect in the processing of mitochondrial RNA, leading to a decreased mRNA content of mitochondrially encoded proteins (Leeds and Brass, 1994). Regarding the effect of HCCL on cultured cells, treatment of oligodendrocytes (Sponne et al., 2000) or proximal tubular kidney cells (Okun et al., 2002) was associated with increased cellular methylmalonate concentrations, but did not impair the activity of enzyme complexes of the mitochondrial electron transport chain.

Our research group is interested in establishing cell and animal models for studying mechanisms of idiosyncratic adverse drug reactions. Idiosyncratic adverse drug reactions are rare and occur at therapeutic drug doses, implying the presence of susceptibility factors. Since adverse hepatic drug reactions often affect mitochondrial function (Krahenbuhl, 2001), preexisting mitochondrial dysfunction could represent a susceptibility factor. This has been demonstrated for valproate-associated liver failure, where mitochondrial dysfunction, as for instance caused by mutations in the gene coding for DNA polymerase γ, is an established susceptibility factor (Krahenbuhl et al., 2000; Stewart et al., 2010). Since, as described above, HCCL is associated with mitochondrial dysfunction affecting complexes of the electron transport chain, cell cultures or experimental animals treated with HCCL could represent suitable models for studying idiosyncratic mitochondrial toxicants. The principle aims of this project were therefore (1) to characterize the metabolic effects of HCCL on HepG2 cells (a well-characterized human hepatoma cell line) and (2) to study the cytotoxicity of known idiosyncratic toxicants on cells treated with HCCL.

2. Materials and methods

2.1. Chemicals

HCCL was synthesized on request from ReseaChem (Burgdorf, Switzerland). The manufacturer confirmed the structure by ^{1}H-NMR analysis and declared a 99% purity of HCCL by high-performance liquid chromatography (HPLC). Stock solutions were prepared in water and stored at −20 °C. All other chemicals used were purchased from Sigma-Aldrich or Fluka (Buchs, Switzerland), except where indicated.

2.2. Cell culture and determination of methylmalonate

The human hepatoma cell line HepG2 was provided by ATCC (Manassas, USA) and maintained in Dulbecco's Modified Eagle Medium (DMEM) low glucose (1.0 g/L), containing 4 mM L-glutamine and 1 mM pyruvate from Invitrogen (Basel, Switzerland). The culture medium was supplemented with 10% (v/v) heat-inactivated fetal calf serum, 2 mM GlutaMax, 10 mM HEPES buffer, and non-essential amino acids. Cell culture supplements were all purchased from GIBCO (Paisley, UK). We kept the cells at 37 °C in a humidified 5% CO_2 cell culture incubator. A Neubauer hemacytometer was used to determine the cell number and viability using the trypan blue exclusion method.

The determination of methylmalonic acid was accomplished by the LC–MS/MS analysis using the ClinMass® Complete Kit (Recipe Chemicals + Instruments GmbH, Munich, Germany). Chromatographic separation was performed using a Shimadzu HPLC (Shimadzu AG, Reinach, Switzerland). The LC system was interfaced with a triple quadrupole mass spectrometer (API4000, AB Sciex, Concord, Canada) equipped with an electrospray ionization (ESI) source. Methylmalonic acid and methylmalonic acid-d3 were detected by selected reaction monitoring (SRM) with a transition of 116.9 → 72.8/54.9 *m/z* and 119.9 → 76.0 *m/z*, respectively. Inter-assay accuracy (determined as the percentage bias) for control samples ranged from −4.1% to 7.2%, and inter-assay precision (determined as the relative standard deviation) was lower than 7.9%. The lower limit of quantification (LLOQ) was 2.48 ng/mL for methylmalonic acid.

2.3. MTT (methylthiazolyldiphenyl-tetrazolium bromide) cell viability assay

Cytotoxicity was detected with a colorimetric assay measuring the number of viable cells by the cleavage of tetrazolium salts added to the culture medium. We seeded cells at 7500 cells/well on a 96-well plate 24 h before drug treatment. Cells were incubated with HCCL and/or other relevant compounds at time points and concentrations indicated. After the incubation period, 10 μL of MTT (5 mg/mL dissolved in DMEM) was added to each well. After 3 h, the medium was removed, and 20 μL 3% SDS and 100 μL isopropanol-HCl (334 μL 37% HCl in 100 mL isopropanol) were added to the wells. The plate was then placed on an orbital shaker at room temperature for 20 min. The absorbance of the dye was measured at a wavelength of 570 nm with background subtraction at 630–690 nm using a Tecan M200 Pro Infinity plate reader (Tecan, Männedorf, Switzerland).

2.4. Cytotoxicity

Cytotoxicity was assessed by using the ToxiLight assay from Lonza (Basel, Switzerland) according to the manufacturer's manual. This assay measures the release of adenylate kinase (AK), which results from the loss of cell membrane integrity. Cells were seeded at 10,000 cells/well in a 96-well plate and treated with HCCL and/or propionate as well mitochondrial toxicants at the concentrations indicated. 0.1% Triton X was used as a positive control. 20 μL of supernatant was transferred to a new 96-well plate and 50 μL assay buffer was added per well. After incubation in the dark for 5 min, the luminescence was measured using a Tecan M200 Pro Infinity plate reader (Männedorf, Switzerland).

2.5. Intracellular ATP content

Cells were seeded at 10,000 cells/well in a 96-well plate and treated with HCCL and/or other substances at the concentrations and for the periods of time indicated. Intracellular ATP was determined using the CellTiter Glo Luminescent cell viability assay (Promega, Wallisellen, Switzerland), in accordance with the manufacturer's instructions. Briefly, 100 μL of assay buffer was added to each 96-well containing 100 μL culture medium. We used Triton X 0.1% as a positive control. After incubation in the dark for 12 min, luminescence was measured using a Tecan M200 Pro Infinity plate reader.

2.6. Mitochondrial membrane potential

HepG2 cells were seeded in a 12-well plate at 100,000 cells/well 24 h prior treatment. Treatment with HCCL and/or other compounds was conducted for the periods of time and at the concentrations indicated. The mitochondrial membrane potential was assessed using the fluorescent cationic dye TMRM from LifeTechnologies (Zug, Switzerland). First, cells were trypsinized and the cell pellet resuspended in DPBS. TMRM was dissolved in DMSO, and added to the resuspended cells at a final concentration of 50 nM. Cells were incubated on a shaker at 37 °C for 20 min. Afterwards, cells were centrifuged and the pellet was resuspended in DPBS. Samples were then assayed by flow cytometry (BD FACSCalibur™, Becton Dickinson AG, Allschwil, Switzerland) on the FL2-H channel. FCCP (10 μM) added to control cells before the addition of TMRM served as positive control. Data were analyzed using CellQuest Pro software (BD Bioscience, Allschwil, Switzerland).

2.7. Activity of the enzyme complexes of the mitochondrial electron transport chain

The activity of the enzyme complexes of the electron transport chain was analyzed using an Oxygraph-2k high-resolution respirometer equipped with DatLab software (Oroboros Instruments, Innsbruck, Austria). HepG2 cells were seeded in T75 cell culture flasks and treated for 4 d with HCCL and/or other relevant compounds before respiration measurement. Then, HepG2 cells were trypsinized and resuspended in MiR06 (mitochondrial respiration medium containing 0.5 mM EGTA, 3 mM $MgCl_2$, 60 mM K-lactobionate, 20 mM taurine, 10 mM KH_2PO_4, 20 mM HEPES, 110 mM sucrose, 1 g/L fatty acid-free bovine serum albumin [BSA] and 280 U/mL catalase, pH 7.1) before being transferred to the pre-calibrated oxygraph chambers.

The activities of complexes I, II, III and IV were assessed in HepG2 cells permeabilized with digitonin (10 μg/1 million cells). In a first run, complexes I and III were analyzed using L-glutamate/malate (10 and 5 mM, respectively) as substrates followed by the addition of ADP (2 mM) before inhibition of complex with rotenone (0.5 μM). Afterwards, duroquinol (500 μM, Tokyo Chemical Industry, Tokyo, Japan) was added to investigate complex III, followed by the addition of the complex III inhibitor antimycin A (2.5 μM). In a second run, complexes II and IV were analyzed using succinate (10 mM) as substrate in the presence of rotenone (0.5 μM) to block complex I. This was followed by the addition of ADP (2 mM) and the complex III inhibitor antimycin A (2.5 μM). Subsequently, N,N,N′,N′-tetramethyl-p-phenylenediamine (TMPD)/ascorbate (0.5 mM and 2 mM, respectively) were added to investigate complex IV activity before the addition of the complex IV inhibitor KCN (1 mM).

To assure the integrity of the outer mitochondrial membrane, the absence of a stimulatory effect of exogenous cytochrome c (10 μM) on respiration was demonstrated before the addition of KCN. We used the Pierce bicinchoninic acid (BCA) protein assay kit from Merck (Darmstadt, Germany) to determine the protein concentrations. Respiration rates are expressed in picomoles O_2 per second per mg protein.

2.8. Mitochondrial superoxide anion accumulation

Mitochondrial superoxide anion production was assessed with the fluorogenic, mitochondria-specific dye MitoSOX™ Red reagent (Molecular Probes, Eugene, OR, USA). Cells were seeded at 15,000 cells/well in a 96-well plate. After 4 d of treatment with HCCL and/or other relevant compounds, medium was removed, and HepG2 cells were stained with MitoSOX red (dissolved in DPBS) at a final concentration of 2 μM. We used amiodarone 50 μM as a positive control. After addition of MitoSOX™ Red reagent, the plate was incubated in the dark at 37 °C for 15 min, afterwards fluorescence was measured at an excitation wavelength of 510 nm and an emission wavelength of 580 nm using a Tecan Infinite pro 200 microplate reader. We normalized the results to the protein content using the Pierce BCA Protein Assay Kit according to manufacturer's instruction.

Table 1
Primers list.

Gene	Sequence 5′ → 3′
MTCYB	CAA TGG CGC CTC AAT ATT CT
	CAG GAG GAT AAT GCC GAT GT
MTCO1	CGC ATG AGC TGG AGT CCT A
	TAC AAA TGC ATG GGC TGT G
MTCO2	CGC CCT CAT AAT CAT TTT CC
	GCG GGC AGG ATA GTT CAG
MTCO3	GCA GGA TTT TTC TGA GCC TTT
	GGG ATT TAG CGG GGT GAT
SOD1	TGGCCGATGTGTCTATTGAA
	ACCTTTGCCCAAGTCATCTG
SOD2	GGTTGTTCACGTAGGCCG
	CAGCAGGCAGCTGGCT
MM-CoA mutase	TCA GAC ATC TGG ATG GTC ACT TA
	GCT GCC ATT GCT TCT ATT GC
GAPDH	TGG TAT CGT GGA AGG ACT CA
	GGG CCA TCG ACA GTC TTC
ND-1	ATG GCC AAC CTC CTA CTC CT
	CTA CAA CGT TGG GGC CTT T
36B4	GGA ATG TGG GCT TTG TGT TC
	CCC AAT TGT CCC CTT ACC TT

2.9. Quantitative RT-PCR

Cells were seeded in 12-well plates 24 h prior treatment with HCCL and other compounds of interest. After 4 d of incubation, cells were lysed with 350 μL RLT buffer (Qiagen, Hombrechtikon, Switzerland) and the cell lysate was transferred to Qiashredder columns and spinned for 2 min at 13,000 rpm. From the eluate, total RNA was extracted according to the manufacturer's protocol (Qiagen RNeasy Mini Extraction kit). We assessed the RNA quality with the NanoDrop 2000 (Thermo Scientific, Wohlen, Switzerland). Qiagen Omniscript system was used to reverse transcribe the isolated RNA to cDNA. For quantitative real-time RT-PCR, 10 ng cDNA was used. The expression of mRNA was evaluated using SYBR Green real-time PCR (Roche Diagnostics, Rotkreuz, Basel). Real-time RT-PCR was performed in triplicate on an ABI PRISM 7700 sequence detector (PE Biosystems, Rotkreuz, Switzerland) and quantification was carried out using the comparative-threshold cycle method. Forward and reverse primers for genes of interest and GAPDH as endogenous reference control (see Table 1 for primers) were purchased from Microsynth (Balgach, Switzerland).

2.10. Mitochondrial DNA content

To measure the mitochondrial DNA content, we determined the ratio of one mitochondrial gene to a nuclear gene using quantitative real-time RT-PCR as described previously with some modifications (Pieters et al., 2013). Total DNA was extracted using the DNeasy Blood and Tissue Kit (Qiagen) following the manufacturer's instructions (Quick-Start Protocol). The concentration of the extracted DNA was measured spectrophotometrically at 260 nm with the NanoDrop 2000 (Thermo Scientific, Wohlen, Switzerland). Afterwards, DNA was diluted in RNase free water to a final concentration of 10 ng/μL. The analysis of the mitochondrial and the nuclear genes was performed using SYBR Green real-time PCR (Roche Diagnostics, Rotkreuz, Switzerland) on an ABI PRISM 7700 sequence detector

(PE Biosystems, Rotkreuz, Switzerland). Quantification was performed using the comparative-threshold cycle method. Forward and reverse primers for genes of interest and GAPDH as endogenous reference control (see Table 1 for primers) were purchased from Microsynth (Balgach, Switzerland).

2.11. Transmission electron microscopy

We used the standard Epon embedding method for electron microscopy. In detail, HepG2 cells were seeded in T12.5 flask and treated with HCCL and/or other compounds for 4 d. After the incubation, the medium was removed and cells fixed with Karnofski paraformaldehyde 3% and glutaraldehyde 0.5% in PBS 10 mM pH 7.4 for 1 h. Afterwards, cells were washed with PBS and post-fixed with reduced osmium tetroxide 1% for 40 min (reduction with 1.5% potassium ferrocyanide) before treatment with osmium tetroxide 1% for 40 min. Afterwards, cells were washed and serially dehydrated in EtOH and embedded in epoxy resin. Thin sections (60 nm) were obtained with a microtome Ultracut E from Leica (Biosystems Switzerland AG). Sections were stained with 6% uranyl acetate for 60 min, and then stained with lead acetate for 2 min. A Moragagni electron microscope from FEI (Hillsboro, OR, USA) at 80 kV was used.

2.12. Statistical methods

Data are given as the mean ± standard deviation (s.d.) of at least three independent experiments. Statistical analyses were performed using GraphPad Prism 6 (GraphPad Software, La Jolla, CA, US). One-way analysis of variance (ANOVA) was used for comparisons of more than two groups, followed by Dunnett's post-test procedure. p-Values <0.05 (*), <0.01 (**) or <0.001 (***) were considered as significant.

3. Results

3.1. Cytotoxicity of HCCL

Cytotoxicity was assessed using different concentrations of HCCL in combination with different propionate concentrations and various incubation times. As shown in Fig. 1A, 100 μM propionate was not cytotoxic over 5 d, whereas 1000 μM propionate was cytotoxic already after 2 d. HCCL alone was not cytotoxic at 10 μM (Fig. 1B) but started to be cytotoxic after 2 d at a concentration of 50 μM (Fig. 1C). Co-treatment with HCCL (10 and 50 μM) and propionate (100 and 1000 μM) showed a more pronounced cytotoxicity than the individual treatments with HCCL or propionate (Fig. 1B and C).

These results indicated that HCCL is associated with hepatocellular injury, stimulating us to carry out an in-depth investigation of the mechanisms of this toxicity. According the cytotoxicity results, we decided to treat cells at 10 μM HCCL in combination with 100 μM or 1000 μM propionate for 4 d for the following experiments.

3.2. Effects of HCCL on the expression of methylmalonyl-CoA mutase

Since HCCL is an inhibitor of the MM-CoA mutase co-factor vitamin B_{12} (Stabler et al., 1991), we examined the effect of HCCL on the mRNA expression of MM-CoA mutase in HepG2 cells.

In the absence of propionate, the methylmalonate concentration in the incubation was below the limit of quantification of the assay used. In the presence of propionate, 10 μM HCCL roughly doubled the methylmalonate concentration compared to incubations without HCCL (4.5 ± 0.1 vs. 2.1 ± 0.1 μM in the presence of 100 μM propionate and 5.7 ± 0.5 vs. 3.0 ± 0.1 μM in the presence of 1000 μM propionate; data not shown).

As shown in supplemental Fig. 1, exposure of HepG2 cells to 10 μM HCCL for 4 d was associated with a 20% decrease MM-CoA mutase mRNA expression. Co-treatment with propionate (100 and 1000 μM) did not further decrease the MM-CoA mutase mRNA expression.

3.3. Mitochondrial membrane potential ($\Delta\psi_m$) and activity of the electron transport chain

Since HCCL is an established mitochondrial toxicant (Krahenbuhl et al., 1991), we next assessed the impact of HCCL exposure on oxidative metabolic function of HepG2 cells. The mitochondrial membrane potential ($\Delta\psi_m$) is an important parameter of mitochondrial integrity, since the electrical potential across the inner mitochondrial membrane is built up mainly by the proton gradient generated by the activity of the complexes of the electron transport chain (Kaufmann et al., 2006). While individual treatment with HCCL 10 μM or propionate 100 or 1000 μM for 4 d did not significantly affect $\Delta\psi_m$, co-treatment (HCCL 10 μM and propionate 1000 μM) decreased $\Delta\psi_m$ significantly by 35% ($p < 0.01$; Fig. 2A). The positive control FCCP 10 μM showed the expected marked reduction in the mitochondrial membrane potential.

In order to find out possible reasons for the effect on the mitochondrial membrane potential, we next assessed the activity of complexes I–IV of the electron transport chain by measuring the oxygen consumption in the presence of different substrates (Fig. 2B). After 4 d treatment with 10 μM HCCL, the activity of complex IV was significantly reduced by approximately 30% with or without propionate. In comparison, treatment with HCCL with or without propionate reduced the activities of complex III and complex II only numerically, without reaching statistical significance. The activity of complex I was not affected.

3.4. HCCL impairs the transcription of mitochondrial genes

Since we have shown that the activity of the enzyme complex IV was significantly reduced by HCCL treatment in HepG2 cells (with a numerical decrease of complex III activity), we wanted to investigate whether this is due impaired mitochondrial protein synthesis. We therefore assessed expression of the genes encoding the mitochondrial subunits of complexes III and IV. Complex III contains one mitochondrially encoded subunit (cyt B), whereas complex IV contains 3 mitochondrial subunits (MTCO1, MTCO2 and MTCO3). As shown in Fig. 3A, quantitative RT-PCR after 4 d of treatment with 10 μM HCCL revealed a 19% down-regulation of cyt B mRNA compared to control cells ($p < 0.01$). Treatment with 100 μM or 1000 μM propionate was associated with a 38% or 23% up-regulation of cyt B mRNA, respectively. This up-regulation was prevented by 10 μM HCCL in the presence of 100 μM propionate, but not in the presence of 1000 μM propionate. Almost identical results were obtained for MTCO1 and MTCO3, two mitochondrially encoded subunits of complex IV (Fig. 3B and D). Again, treatment with 10 μM HCCL was associated with a 20% and 28% decrease of mRNA expression of MTCO1 and MTCO3, respectively. Both concentration of propionate investigated increased mRNA expression of MTCO1 and MTCO3, whereas co-treatment with HCCL partially abolished this increase. In contrast, mRNA expression of MTCO2 was not suppressed by HCCL alone, but increased by propionate. This increase could partially be prevented by HCCL (Fig. 3C).

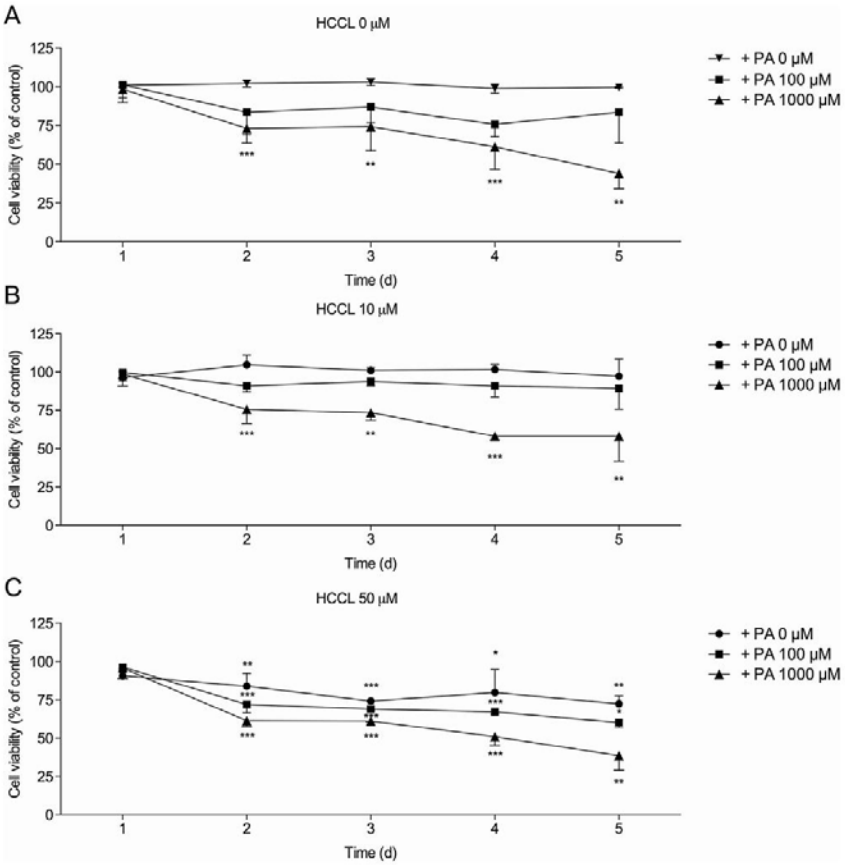

Fig. 1. Cytotoxicity of HCCL and propionate. Cytotoxicity at different concentrations of HCCL and propionate on HepG2 cells was assessed at different exposure times. Cell viability was tested by spectrophotometric measurement of the reductive conversion of MTT (Thiazolyl Blue Tetrazolium Bromide) to a water-insoluble colored formazan derivative. HCCL: hydroxy-cobalamin[c-lactam], PA: propionate. Data are expressed as mean ± s.d. of at least three independent experiments. $^{*}p < 0.05$, $^{**}p < 0.01$, $^{***}p < 0.001$ vs. control.

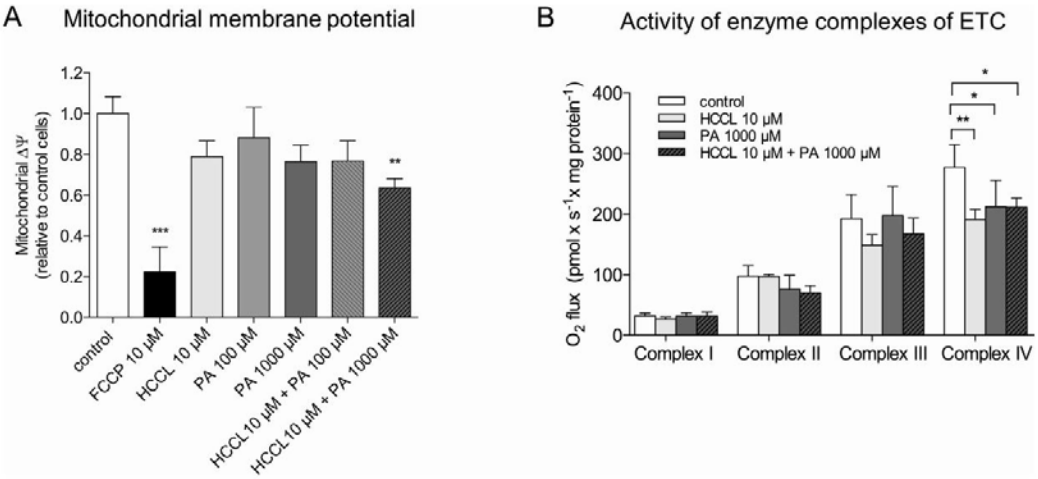

Fig. 2. Mitochondrial function. (A) Mitochondrial membrane potential of HepG2 cells after 4 d of treatment with HCCL and/or propionate. Mitochondria were labeled with the fluorescent probe TMRM and analyzed with flow cytometry. FCCP was added to control cells and was used as a positive control. (B) Respiratory capacity through complex I, II, III, IV after 4 d treatment. HepG2 cells were first permeabilized. After addition of substrates and inhibitors of the different complexes, complex activities were determined on a Oxygraph-2k high-resolution respirometer. HCCL: hydroxy-cobalamin[c-lactam], PA: propionate, FCCP: carbonyl cyanide 4 (trifluoromethoxy)phenylhydrazone, TMRM: tetramethylrhodamin-methylester. Data are expressed as mean ± s.d. of at least three independent experiments. $^{*}p < 0.05$, $^{**}p < 0.01$, $^{***}p < 0.001$ vs. control.

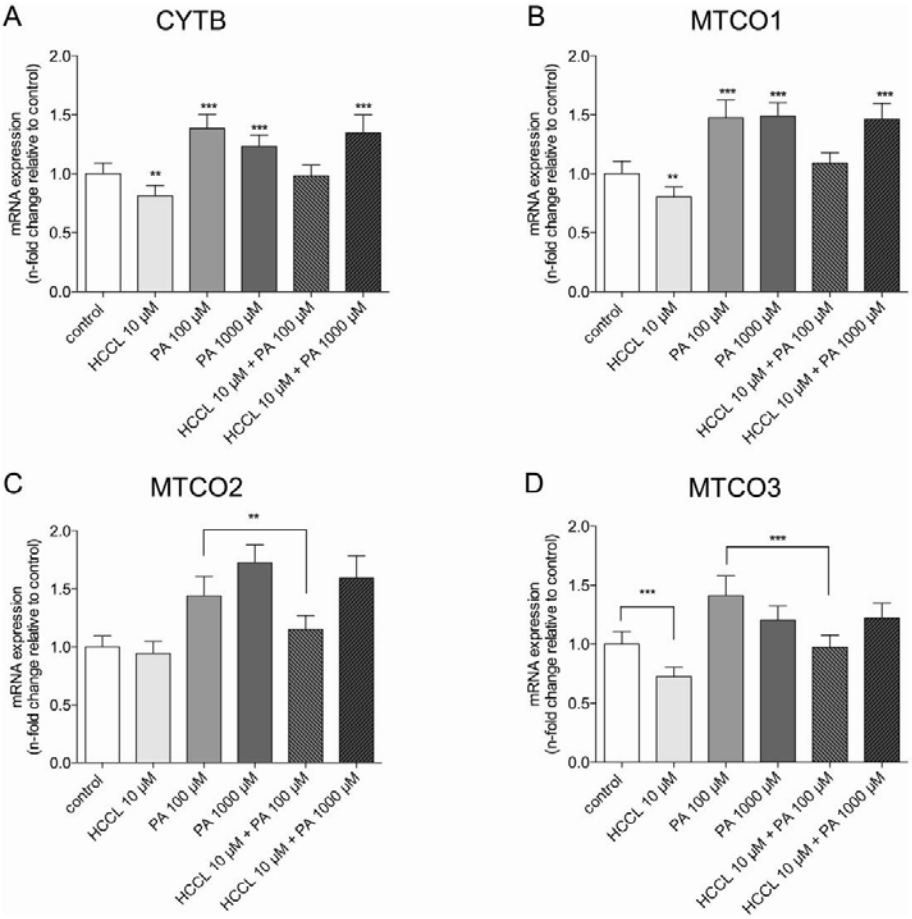

Fig. 3. mRNA expression of mitochondrial subunits in complexes III and IV. Total RNA was extracted from HepG2 cells after treatment with HCCL and/or PA for 4 d. mRNA expression of mitochondrially encoded subunits of complex III (Cyt b) and complex IV (MT-CO1, MT-CO2, and MT-CO3) was determined by qRT-PCR with GAPDH as endogenous control (A–D). Results are expressed relative to untreated control cells. HCCL: hydroxy-cobalamin[c-lactam], PA: propionate. Data are expressed as mean ± s.d. of at least three independent experiments. $^{**}p < 0.01$, and $^{***}p < 0.001$.

3.5. HCCL induces ROS accumulation in HepG2 cells

It is well established that the damage of the electron flow across the mitochondrial electron transport chain is associated with cellular ROS accumulation (Balaban et al., 2005). As expected, we detected a 20% increase of superoxide anion accumulation in the presence of 10 µM HCCL with or without 1000 µM propionate after 4 d incubation ($p < 0.01$ and $p < 0.05$, respectively; Fig. 4A). A similar increase superoxide anion accumulation was also detectable in the presence of 50 µM amiodarone, which served as a positive control (data not shown).

As shown in Fig. 4B, HCCL did not affect mRNA expression of the cytosolic SOD1, but significantly decreased the expression of mitochondrial SOD2 ($p < 0.05$). In contrast, 100 µM propionate was associated with a significant increase in mRNA expression of both SOD1 and SOD2, whereas 1000 µM propionate increased the mRNA expression of SOD1, but had no significant effect on SOD2. When combined with propionate, HCCL at least partially prevented the stimulatory effect of propionate on the mRNA expression of SOD1 and SOD2.

Accumulating ROS can be degraded by the glutathione antioxidant system, which is an effective scavenger of free radicals and reactive superoxide. A decrease in cellular glutathione levels is associated with oxidative stress as well as apoptosis and cell death. For that reason, we determined the cellular reduced glutathione content in HCCL-treated HepG2 cells. We found that HepG2 cells treated with HCCL 10 µM or propionate (100 and 1000 µM) alone or with HCCL combined with propionate was not associated with a significant decrease in the cellular GSH content compared to control cells (Supplementary Fig. 2). As expected, the cellular GSH content was reduced by approximately 90% in the presence of the positive control BSO.

3.6. HCCL does not affect mitochondrial DNA content but disturbs mitochondrial morphology

The ratio of the mtDNA to the nuclear DNA provides a measure of the mitochondrial DNA homeostasis and represents a marker of mitochondrial proliferation. As shown in Fig. 5A, qRT-PCR analysis of HepG2 cells treated for 4 d with HCCL alone (10 µM), propionate alone (100 and 1000 µM) or the combination did not show significant alterations in the ratio of mtDNA/nDNA.

To investigate the possibility that the observed metabolic alterations in mitochondria of HepG2 cells treated with HCCL are accompanied with morphological changes, we performed a detailed electron microscopic analysis (Fig. 5B). The most evident

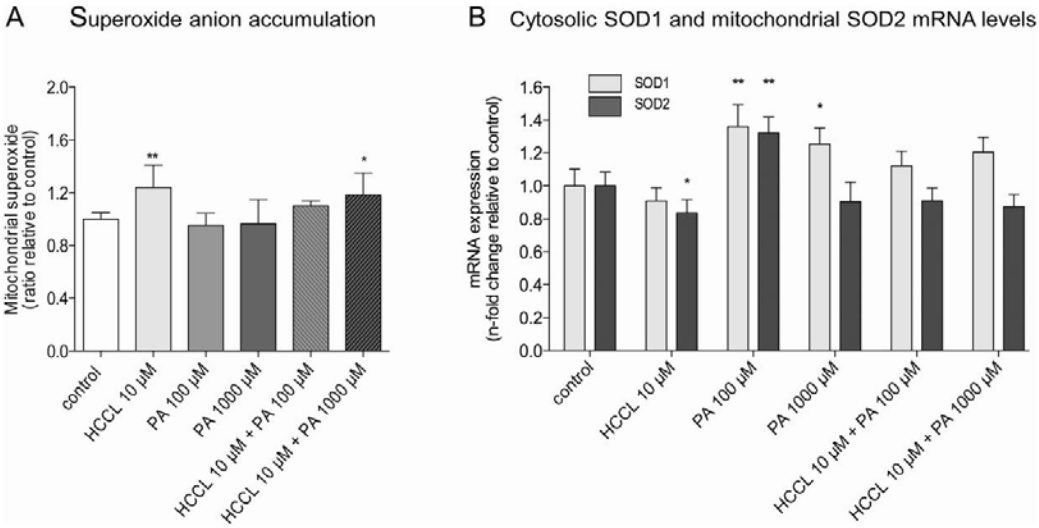

Fig. 4. Redox status. (A) Superoxide formation relative to untreated control cells. Mitochondrial superoxide production was measured with MitoSOX™ Red reagent after 4 d treatment of HepG2 cells with HCCL and/or propionate. Data were obtained from a microplate reader (510/580 nm) after incubation with 2 µM MitoSOX™ Red reagent for 10 min. (B) mRNA expression of cytosolic SOD1 and mitochondrial SOD2. Expression was measured by qRT-PCR with GAPDH as endogenous control. HCCL: hydroxy-cobalamin[c-lactam], PA: Propionate. Results are expressed relative to untreated control cells as mean ± s.d. of at least three independent experiments. $^{*}p < 0.05$, $^{**}p < 0.01$ vs. control.

finding was mitochondrial swelling in HepG2 cells treated with 10 µM HCCL and 1000 µM propionate (indicated as a black arrow). In agreement with the unchanged mtDNA/nDNA ratio, mitochondrial proliferation was not apparent.

3.7. Mitochondrial toxicants are more toxic on HepG2 cells pretreated with HCCL and propionate

In order to test the hypothesis that a preexisting mitochondrial dysfunction renders cells more susceptible to mitochondrial toxicants, we exposed HepG2 cells with non-cytotoxic concentrations of HCCL (10 µM) and/or propionate (100 µM) for 4 d and then we assessed the effect on cytotoxicity and cellular ATP in the absence and in the presence of 20 µM dronedarone or 50 µM benzbromarone or 20 µM ketoconazole for 24 h. Dronedarone, benzbromarone and ketoconazole are established mitochondrial toxicants that impair oxidative phosphorylation (Felser et al., 2013, 2014a; Rodriguez and Acosta, 1996). As shown in Fig. 6, the AK release (i.e. cytotoxicity) of cells treated with 10 µM HCCL, the combination 10 µM HCCL/100 µM propionate, or 20 µM dronedarone (Fig. 6A), 50 µM benzbromarone (Fig. 6C) or 20 µM ketoconazole (Fig. 6E) was not significantly different from untreated control cells. Moreover, in cells pretreated with 10 µM HCCL alone or with 10 µM HCCL/100 µM propionate, the addition of 20 µM dronedarone

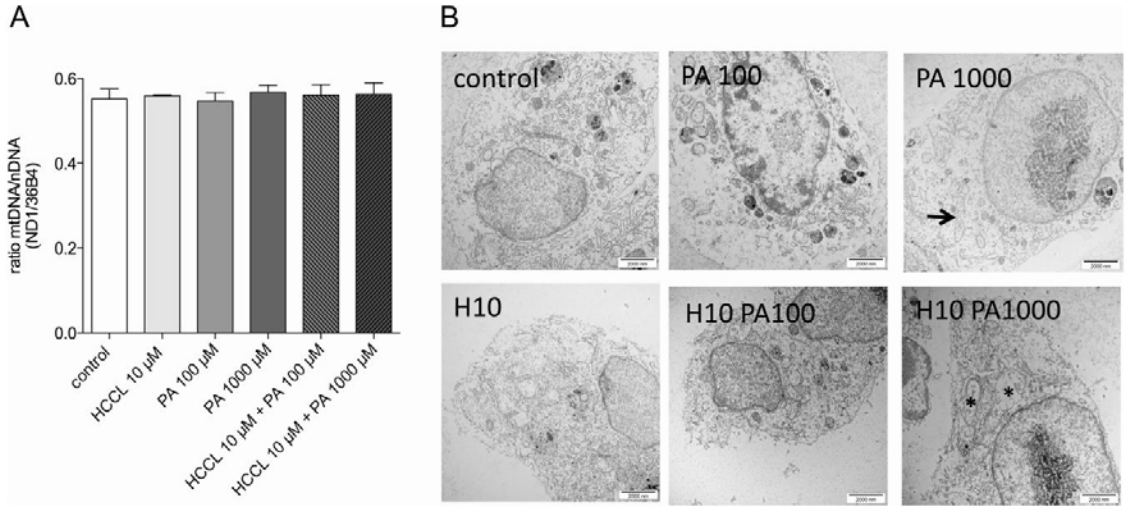

Fig. 5. Mitochondrial DNA content and morphology. (A) mtDNA content in HepG2 cells after treatment for 4 d with HCCL and/or propionate. Total DNA was extracted from cells after treatment with HCCL and/or propionate. DNA expression of a mitochondrial (ND-1) and a nuclear gene (36B4) was determined by qRT-PCR. The graph shows the expression ration of these two genes. (B) Transmission electron microscopy pictures from each group. The black arrows indicate swollen mitochondria. Results are expressed relative to untreated control cells. HCCL: hydroxy-cobalamin[c-lactam], PA: propionate. Data are expressed as mean ± s.d. of at least three independent experiments.

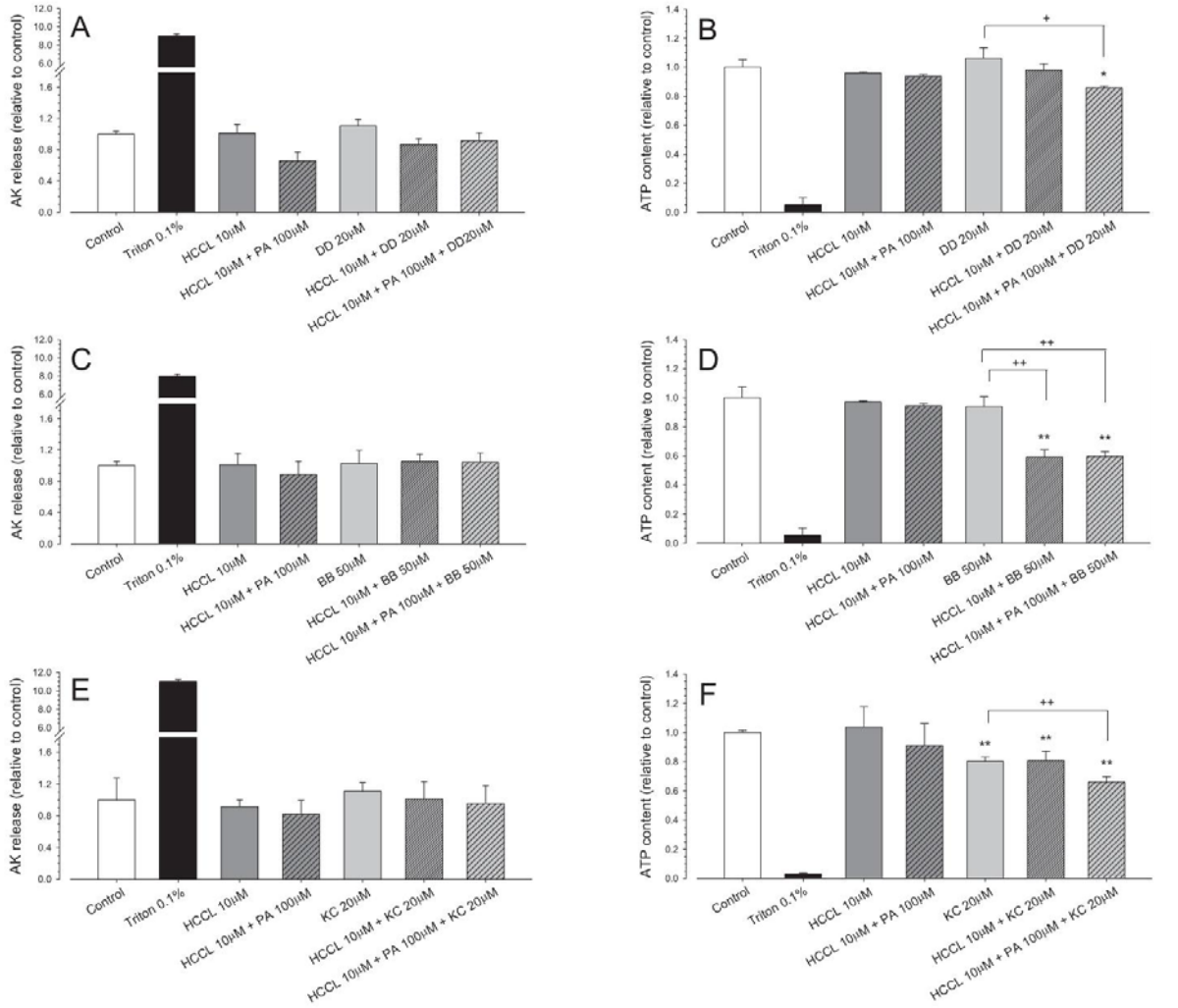

Fig. 6. Application of the HCCL cell model for the detection of idiosyncratic mitochondrial toxicity. Adenylate kinase (AK) release (marker for cytotoxicity) and intracellular ATP content (marker for mitochondrial function and energy metabolism) in HepG2 cells were determined. Exposure with HCCL/propionate was performed for 4 d and with dronaderone, benzbromarone or ketoconazole for 24 h. 0.1% Triton X served as a positive control. (A and B) Cytotoxicity and cellular ATP content, respectively, in the presence of 20 µM dronedarone in cells with and without pretreatment with HCCL/propionate. (C and D) Cytotoxicity and cellular ATP content, respectively, in the presence of 50 µM benzbromarone in cells with and without pretreatment with HCCL/propionate. (E and F) Cytotoxicity and cellular ATP content, respectively, in the presence of 20 µM ketoconazole in cells with and without pretreatment with HCCL/propionate. HCCL: hydroxy-cobalamin[c-lactam], PA: propionate. DD: dronedarone. BB: benzbromarone. KC: ketoconazole. Data are expressed as mean ± s.d. of at least three independent experiments. $^{*}p < 0.05$, $^{**}p < 0.01$ vs. control incubations and $^{+}p < 0.05$, $^{++}p < 0.01$ vs. incubations containing the toxicant only.

(Fig. 6A), 50 µM benzbromarone (Fig. 6C) or 20 µM ketoconazole (Fig. 6E) for 24 h was also not cytotoxic.

The ATP content of HepG2 cells treated with 10 µM HCCL, the combination 10 µM HCCL/100 µM propionate, 20 µM dronedarone (Fig. 6B) or 50 µM benzbromarone (Fig. 6D) was not significantly different from control cells, whereas 20 µM ketoconazole was associated with a significant drop in the ATP content (Fig. 6F). In cells pretreated with 10 µM HCCL alone, 50 µM benzbromarone significantly decreased the cellular ATP content by approximately 40% compared to control incubations and incubations containing 50 µM benzbromarone alone (Fig. 6D). In comparison, 20 µM dronedarone or ketoconazole did not significantly decrease the cellular ATP content under these conditions. In cells pretreated with 10 µM HCCL/100 µM propionate, 20 µM dronedarone, 50 µM benzbromarone and 20 µM ketoconazole significantly decreased the cellular ATP content if compared to control incubations and incubations containing the mitochondrial toxicants alone (Fig. 6B, D, F), indicating that treatment with HCCL/propionate renders HepG2 cells more sensitive to mitochondrial toxicants.

4. Discussion

The principle aims of the current investigations were to characterize the effect of HCCL on mitochondrial function and morphology in HepG2 cells and to use this cell model to test the hypothesis that HepG2 cells with impaired mitochondrial function are more susceptible to mitochondrial toxicants. The current study showed that HCCL affects the function of specific enzyme complexes of the electron transport chain of liver mitochondria and is associated with changes in mitochondrial morphology. Similar to previous

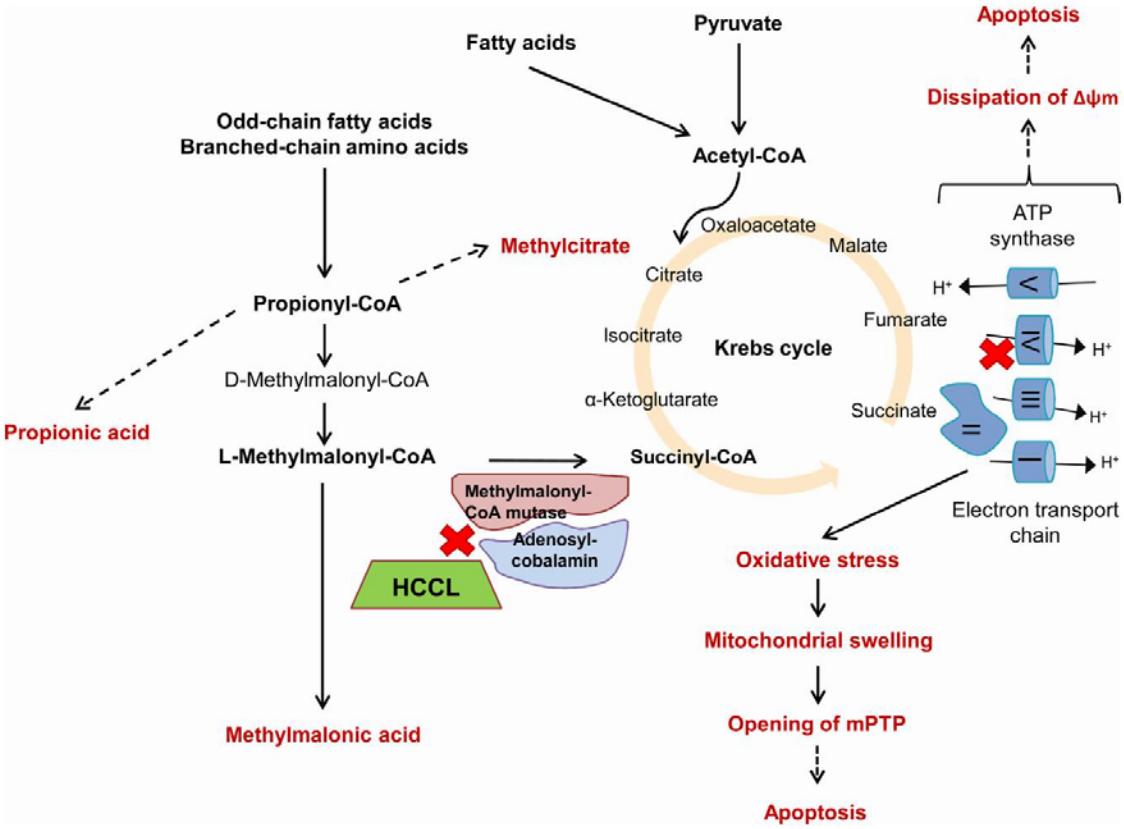

Fig. 7. Schematic illustration of the effects of HCCL on propionate metabolism. HCCL blocks the action of vitamin B_{12}, which inhibits the conversion of methylmalonyl-CoA to succinate. This leads to the formation of propionate, methylmalonate and methylcitrate, which can be excreted. HCCL blocks by a currently unknown mechanism the processing of polycistronic mtRNA, which reduces the expression mitochondrially encoded proteins. This impairs the function of enzyme complexes of the electron transport chain, mainly of complex IV. This is associated with dissipation of the mitochondrial membrane potential and production of ROS, eventually leading to cell death by apoptosis.

studies (Krahenbuhl et al., 1990; Leeds and Brass, 1994), we found that inhibition of processing of mitochondrial RNA is an important mechanism of mitochondrial toxicity associated with HCCL. Our studies also show that HepG2 cells pre-treated with HCCL are more susceptible to mitochondrial toxicants.

HCCL itself was only slightly cytotoxic, but cytotoxicity was increased in the presence of propionate. This is not surprising, since propionate itself was cytotoxic (see Fig. 1) and HCCL impairs propionate metabolism by competing with vitamin B12, prolonging exposure to propionate and propionate metabolites. In order to understand the mechanisms associated with cytotoxicity of HCCL, we focused on mitochondrial function, because HCCL is a known mitochondrial toxicant (Krahenbuhl et al., 1991). Exposure to HCCL significantly inhibited the activity of enzyme complex IV of the mitochondrial electron transport chain of HepG2 cells after 4 d of exposure and numerically reduced the activity of complex II and III (Fig. 2). This is in line with previous studies in rat liver mitochondria and isolated rat hepatocytes, where treatment with HCCL was associated with an impaired function of enzyme complexes III and IV and with a numerical reduction of complex II activity (Krahenbuhl et al., 1991). The current findings disagree with data reported from human proximal tubular kidney cells treated with HCCL and propionate, where the activity of the enzyme complexes of the electron transport chain was not impaired (Sauer et al., 2009). Since only the liver appeared to be affected in rats treated with HCCL (Krahenbuhl et al., 1990), this discrepancy is best explained by organ-specific toxicity of HCCL.

These alterations in mitochondrial function were associated with the dissipation of the electric potential across the inner mitochondrial membrane and with mitochondrial accumulation of ROS. The proton pump generated by the activity of complexes I, III and IV of the electron transport chain basically maintains the mitochondrial membrane potential. Any perturbation of these enzyme complexes and/or uncoupling of oxidative phosphorylation can therefore be expected to dissipate the mitochondrial membrane potential. The mitochondrial membrane potential can therefore be regarded as a marker of mitochondrial function and integrity (Felser et al., 2013). Since impaired activity of the electron transport chain can be associated with increased mitochondrial production of ROS (Balaban et al., 2005), mitochondrial accumulation of ROS was an expected finding. The results of our study are also in agreement with findings in skin fibroblasts of patients with methylmalonic aciduria, where an increased ROS production has been described (Richard et al., 2009). Cellular accumulation of methylmalonate may therefore be a second possible mechanism for the observed increase in the mitochondrial ROS content in HepG2 cells. As HCCL decreased mRNA expression of SOD2, the mitochondrial form of superoxide dismutase (but not the expression of the cytosolic form SOD1), mitochondrial accumulation of ROS may also have been caused by impaired ROS metabolism.

Both a decrease in the mitochondrial membrane potential and mitochondrial accumulation of ROS can lead to mitochondrial membrane permeabilization (Antico Arciuch et al., 2012), which is considered to be a point of no return for initiating apoptotic cell death (Zamzami and Kroemer, 2003). Mitochondrial membrane permeabilization can culminate in rupture and, therefore, in a loss of barrier function of the outer mitochondrial membrane with consequent release of apoptosis-inducing proteins (e.g. cytochrome c) from the mitochondrial intermembrane space (Kaufmann et al., 2006). Cell death associated with HCCL with or without propionate can be explained by this mechanism.

Persistent opening of the mitochondrial permeability transition pore is followed by a release of Ca^{2+} from the mitochondrial matrix, termination of oxidative phosphorylation and matrix swelling with inner membrane unfolding before rupture of the outer mitochondrial membrane (Lejay et al., 2014). In our transmission electron microscopy pictures, we observed a remarkable size variability of mitochondria and mitochondrial swelling after exposure to HCCL and propionate, which supports this mechanism. Similar alterations in mitochondrial morphology have been described in rats treated with HCCL (Tandler et al., 1991) and also in liver mitochondria of patients with methylmalonic aciduria (Wilnai et al., 2014).

The observed decrease in the mRNA content of mitochondrially encoded proteins associated with HCCL is consistent with the study of Leeds and Brass (Leeds and Brass, 1994), who described accumulation of polycistronic mitochondrial RNA in livers of rats treated with HCCL. As suggested by Leeds and Brass (1994), these findings are consistent with impaired processing of polycistronic RNA, leading to reduced abundance of certain mRNA species in the mitochondrial matrix. This can translate into changes in the protein composition and therefore also into an altered activity of enzyme complexes of the respiratory chain, as observed in the current and previous studies (Krahenbuhl et al., 1990, 1991).

A second aim of the current investigations was to find out whether subtle changes in the function of the electron transport chain would make HepG2 cells more susceptible for mitochondrial toxicants, simulating idiosyncratic mitochondrial toxicity. We chose benzbromarone, dronedarone and ketoconazole as test drugs. We have recently reported mitochondrial toxicity in HepG2 cells exposed with benzbromarone and dronedarone (Felser et al., 2013, 2014a). Also ketoconazole is a mitochondrial toxicant, since it decreased complex I and II activities of the electron transport chain in isolated rat liver mitochondria (Rodriguez and Acosta, 1996). As shown in Fig. 6, 20 μM dronedarone, 50 μM benzbromarone and 20 μM ketoconazole were not cytotoxic (no significant release of adenylate kinase), also not in HepG2 cells treated with HCCL/propionate. However, the mitochondrial toxicants tested were associated with a significant drop in the ATP content of HepG2 cells treated with HCCL (only ketoconazole) or the combination HCCL/propionate (all 3 toxicants investigated). The concentrations of the toxicants tested were deliberately chosen in a subtoxic or only slightly toxic range in order to be able to differentiate between effects on the cellular ATP content (reflecting a mitochondrial function) and cytotoxicity. These findings are consistent with studies in humans with severe valproate-associate hepatotoxicity (Stewart et al., 2010) and/or mice with hepatotoxicity related with valproate (Knapp et al., 2008) or dronedarone (Felser et al., 2014b). The underlying mitochondrial dysfunction lowers the concentration at which these drugs start to be hepatotoxic.

It is interesting to note that the combination HCCL/propionate rendered HepG2 cells more sensitive to the mitochondrial toxicants tested than HCCL alone, while HCCL alone caused by trend more mitochondrial damage than HCCL/propionate. This may be explained by a more accentuated accumulation of propionate and propionate metabolites in the presence of HCCL/propionate, which are considered to be hepatotoxic (Horster and Hoffmann, 2004).

It is important to realize, however, that HepG2 cells are not a suitable model for all toxicological investigations. For instance, idiosyncratic toxicities involving immune mechanisms cannot be studied with HepG2 cells alone and, since cytochrome P450 enzymes are almost completely absent in HepG2 cells (Donato et al., 2008), they are not suitable for studies where metabolites play a major role. Treatment with HCCL/propionate should therefore also be investigated in primary human hepatocytes and hepatoma cell lines with a higher cytochrome p450 content than HepG2 cells.

In conclusion, we developed and characterized a cell model with chemically induced dysfunction of enzyme complexes of the mitochondrial electron transport chain. Such cells are more susceptible for mitochondrial toxicants, rendering them suitable for testing drugs for idiosyncratic mitochondrial toxicity. Due to the almost complete absence of cytochrome P450 enzymes in HepG2 cells, this model is not suitable for testing drugs with reactive metabolites.

Funding

This work was supported by a grant to Stephan Krähenbühl from the Swiss National Science Foundation (31003A_156270).

Conflicts of interest

None of the authors reports a conflict of interest with this work.

Transparency document

The Transparency document associated with this article can be found in the online version.

Acknowledgements

We would like to thank Ursula Sauder for her kind assistance of the transmission electron microscopy.

Appendix A. Supplementary data

Supplementary data associated with this article can be found, in the online version, at http://dx.doi.org/10.1016/j.tox.2015.07.015

References

Antico Arciuch, V.G., Elguero, M.E., Poderoso, J.J., Carreras, M.C., 2012. Mitochondrial regulation of cell cycle and proliferation. Antioxid. Redox Signal. 16, 1150–1180.
Balaban, R.S., Nemoto, S., Finkel, T., 2005. Mitochondria, oxidants, and aging. Cell 120, 483–495.
Brass, E.P., Allen, R.H., Ruff, L.J., Stabler, S.P., 1990. Effect of hydroxycobalamin[c-lactam] on propionate and carnitine metabolism in the rat. Biochem. J. 266, 809–815.
Chandler, R.J., Zerfas, P.M., Shanske, S., Sloan, J., Hoffmann, V., DiMauro, S., Venditti, C.P., 2009. Mitochondrial dysfunction in mut methylmalonic acidemia. FASEB J. 23, 1252–1261.
Deodato, F., Boenzi, S., Santorelli, F.M., Dionisi-Vici, C., 2006. Methylmalonic and propionic aciduria. Am. J. Med. Genet. C Semin. Med. Genet. 142C, 104–112.
Dionisi-Vici, C., Deodato, F., Roschinger, W., Rhead, W., Wilcken, B., 2006. 'Classical' organic acidurias, propionic aciduria, methylmalonic aciduria and isovaleric aciduria: long-term outcome and effects of expanded newborn screening using tandem mass spectrometry. J. Inherit. Metab. Dis. 29, 383–389.
Donato, M.T., Lahoz, A., Castell, J.V., Gomez-Lechon, M.J., 2008. Cell lines: a tool for in vitro drug metabolism studies. Curr. Drug Metab. 9, 1–11.
Felser, A., Blum, K., Lindinger, P.W., Bouitbir, J., Krahenbuhl, S., 2013. Mechanisms of hepatocellular toxicity associated with dronedarone – a comparison to amiodarone. Toxicol. Sci. 131, 480–490.
Felser, A., Lindinger, P.W., Schnell, D., Kratschmar, D.V., Odermatt, A., Mies, S., Jeno, P., Krahenbuhl, S., 2014a. Hepatocellular toxicity of benzbromarone: effects on mitochondrial function and structure. Toxicology 324, 136–146.
Felser, A., Stoller, A., Morand, R., Schnell, D., Donzelli, M., Terracciano, L., Bouitbir, J., Krahenbuhl, S., 2014b. Hepatic toxicity of dronedarone in mice: role of mitochondrial beta-oxidation. Toxicology 323, 1–9.

Frenkel, E.P., Mukherjee, A., Hackenbrock, C.R., Srere, P.A., 1976. Biochemical and ultrastructural hepatic changes during vitamin B12 deficiency in animals and man. J. Biol. Chem. 251, 2147–2154.

Horster, F., Hoffmann, G.F., 2004. Pathophysiology, diagnosis, and treatment of methylmalonic aciduria-recent advances and new challenges. Pediatr. Nephrol. (Berlin, Germany) 19, 1071–1074.

Kaufmann, P., Torok, M., Zahno, A., Waldhauser, K.M., Brecht, K., Krahenbuhl, S., 2006. Toxicity of statins on rat skeletal muscle mitochondria. Cell. Mol. Life Sci. 63, 2415–2425.

Knapp, A.C., Todesco, L., Beier, K., Terracciano, L., Sagesser, H., Reichen, J., Krahenbuhl, S., 2008. Toxicity of valproic acid in mice with decreased plasma and tissue carnitine stores. J. Pharmacol. Exp. Ther. 324, 568–575.

Krahenbuhl, S., 2001. Mitochondria: important target for drug toxicity? J. Hepatol. 34, 334–336.

Krahenbuhl, S., Brandner, S., Kleinle, S., Liechti, S., Straumann, D., 2000. Mitochondrial diseases represent a risk factor for valproate-induced fulminant liver failure. Liver 20, 346–348.

Krahenbuhl, S., Chang, M., Brass, E.P., Hoppel, C.L., 1991. Decreased activities of ubiquinol:ferricytochrome c oxidoreductase (complex III) and ferrocytochrome c: oxygen oxidoreductase (complex IV) in liver mitochondria from rats with hydroxycobalamin[c-lactam]-induced methylmalonic aciduria. J. Biol. Chem. 266, 20998–21003.

Krahenbuhl, S., Ray, D.B., Stabler, S.P., Allen, R.H., Brass, E.P., 1990. Increased hepatic mitochondrial capacity in rats with hydroxy-cobalamin[c-lactam]-induced methylmalonic aciduria. J. Clin. Invest. 86, 2054–2061.

Leeds, F.S., Brass, E.P., 1994. Hepatic cobalamin deficiency induced by hydroxycobalamin[c-lactam] treatment in rats is associated with decreased mitochondrial mRNA contents and accumulation of polycistronic mitochondrial RNAs. J. Biol. Chem. 269, 3947–3951.

Lehotay, D.C., Clarke, J.T., 1995. Organic acidurias and related abnormalities. Crit. Rev. Clin. Lab. Sci. 32, 377–429.

Lejay, A., Meyer, A., Schlagowski, A.I., Charles, A.L., Singh, F., Bouitbir, J., Pottecher, J., Chakfe, N., Zoll, J., Geny, B., 2014. Mitochondria: mitochondrial participation in ischemia-reperfusion injury in skeletal muscle. Int. J. Biochem. Cell Biol. 50, 101–105.

Okun, J.G., Horster, F., Farkas, L.M., Feyh, P., Hinz, A., Sauer, S., Hoffmann, G.F., Unsicker, K., Mayatepek, E., Kolker, S., 2002. Neurodegeneration in methylmalonic aciduria involves inhibition of complex II and the tricarboxylic acid cycle, and synergistically acting excitotoxicity. J. Biol. Chem. 277, 14674–14680.

Pieters, N., Koppen, G., Smeets, K., Napierska, D., Plusquin, M., De Prins, S., Van De Weghe, H., Nelen, V., Cox, B., Cuypers, A., Hoet, P., Schoeters, G., Nawrot, T.S., 2013. Decreased mitochondrial DNA content in association with exposure to polycyclic aromatic hydrocarbons in house dust during wintertime: from a population enquiry to cell culture. PLOS ONE 8, e63208.

Richard, E., Jorge-Finnigan, A., Garcia-Villoria, J., Merinero, B., Desviat, L.R., Gort, L., Briones, P., Leal, F., Perez-Cerda, C., Ribes, A., Ugarte, M., Perez, B., 2009. Genetic and cellular studies of oxidative stress in methylmalonic aciduria (MMA) cobalamin deficiency type C (cblC) with homocystinuria (MMACHC). Hum. Mutat. 30, 1558–1566.

Rodriguez, R.J., Acosta Jr., D., 1996. Inhibition of mitochondrial function in isolated rate liver mitochondria by azole antifungals. J. Biochem. Toxicol. 11, 127–131.

Sauer, S.W., Opp, S., Haarmann, A., Okun, J.G., Kolker, S., Morath, M.A., 2009. Long-term exposure of human proximal tubule cells to hydroxycobalamin[c-lactam] as a possible model to study renal disease in methylmalonic acidurias. J. Inherit. Metab. Dis. 32, 720–727.

Sponne, I.E., Gaire, D., Stabler, S.P., Droesch, S., Barbe, F.M., Allen, R.H., Lambert, D.A., Nicolas, J.P., 2000. Inhibition of vitamin B12 metabolism by OH-cobalamin c-lactam in rat oligodendrocytes in culture: a model for studying neuropathy due to vitamin B12 deficiency. Neurosci. Lett. 288, 191–194.

Stabler, S.P., 2013. Clinical practice. Vitamin B12 deficiency. N. Engl. J. Med. 368, 149–160.

Stabler, S.P., Brass, E.P., Marcell, P.D., Allen, R.H., 1991. Inhibition of cobalamin-dependent enzymes by cobalamin analogues in rats. J. Clin. Invest. 87, 1422–1430.

Stewart, J.D., Horvath, R., Baruffini, E., Ferrero, I., Bulst, S., Watkins, P.B., Fontana, R.J., Day, C.P., Chinnery, P.F., 2010. Polymerase gamma gene POLG determines the risk of sodium valproate-induced liver toxicity. Hepatology (Baltimore, MD) 52, 1791–1796.

Takahashi-Iniguez, T., Garcia-Hernandez, E., Arreguin-Espinosa, R., Flores, M.E., 2012. Role of vitamin B12 on methylmalonyl-CoA mutase activity. J. Zhejiang Univ. Sci. B 13, 423–437.

Tandler, B., Krahenbuhl, S., Brass, E.P., 1991. Unusual mitochondria in the hepatocytes of rats treated with a vitamin B12 analogue. Anat. Rec. 231, 1–6.

Wilnai, Y., Enns, G.M., Niemi, A.K., Higgins, J., Vogel, H., 2014. Abnormal hepatocellular mitochondria in methylmalonic acidemia. Ultrastruct. Pathol. 38, 309–314.

Zamzami, N., Kroemer, G., 2003. Apoptosis: mitochondrial membrane permeabilization – the (w)hole story? Curr. Biol. 13, R71–R73.

Paper 2

Inhibition of cobalamin metabolism by hydroxy-cobalamin[c-lactam] in mice

P Haegler[1,2], D Grünig[1,2], B Berger[1,2], L Terracciano[3,4,], S Krähenbühl[1,2,3], J Bouitbir[1,2,3]

[1]Clinical Pharmacology & Toxicology, University Hospital Basel, Switzerland

[2]Department of Biomedicine, University of Basel, Switzerland

[3]Swiss Centre of Applied Human Toxicology (SCAHT)

[4]Department of Molecular Pathology, Institute for Pathology, University Hospital Basel

Draft manuscript

Inhibition of cobalamin metabolism by hydroxy-cobalamin[c-lactam] in mouse liver

Patrizia Hägler[1,2], David Grünig[1,2], Benjamin Berger[1,2], Luigi Terracciano[3,4], Stephan Krähenbühl[1,2, 3], Jamal Bouitbir[1,2,3]

[1]Division of Clinical Pharmacology & Toxicology, University Hospital, Basel, Switzerland

[2]Department of Biomedicine, University of Basel

[3]Swiss Centre of Applied Human Toxicology, SCAHT

[4]Department of Molecular Pathology, Institute for Pathology, University Hospital Basel

Running title: Vitamin B12 deficiency and mouse liver

Correspondence

Stephan Krähenbühl, MD, PhD

Clinical Pharmacology & Toxicology

University Hospital

4031 Basel

Switzerland

Phone: +41 61 265 4715

Fax: +41 61 265 4560

E-mail: kraehenbuehl@ubs.ch

Abbreviations

- Δψm: Mitochondrial membrane potential
- DMSO: Dimethyl sulfoxide
- HCCL: Hydroxyl-cobalamin[c-lactam]
- HPLC: High-performance liquid chromatography
- MMA: Methylmalonic acid
- MM-CoA mutase: Methylmalonyl-CoA mutase
- ROS: Reactive oxygen species
- SOD: Superoxide dismutase
- TMPD: N, N, N', N'-tetramethyl-p-phenylenediamine

Abstract

The vitamin B12 analog hydroxy-cobalamin[c-lactam] (HCCL) impairs mitochondrial protein synthesis and the function of the electron transport chain. Our goal was to establish an *in vivo* model for mitochondrial dysfunction in mice, which could be used to investigate hepatotoxicity of idiosyncratic mitochondrial toxicants.

In a first step, we performed a dose-finding study in mice with HCCL at 0.4 mg/kg and 4 mg/kg i.p. for two, three, and four weeks. We measured plasma methylmalonic acid (MMA) concentration at these timepoints and uncovered a strong increase of plasma MMA concentration at 4 mg/kg after three weeks of treatment.

Due to the observed elevation of MMA, mice were treated in a second step with 4 mg/kg HCCL for three weeks to characterize mitochondrial function and possible liver changes. We first found an increase of absolute and relative liver weight. This increase correlated with the accumulation of lipid droplets and glycogen in liver of treated mice. We discovered also an inhibition of the complex I enzyme activity of the electron transport chain in liver homogenate. However, this inhibition was not followed by the accumulation of mitochondrial superoxide anion. Moreover, reduced GSH as well as lipid peroxidation were similar in both groups. Finally, the mitochondrial DNA content was not altered with the HCCL treatment.

In conclusion, the establishment of the mouse model with HCCL serving as a suitable model for idiosyncratic reactions was partially successful. Further studies are needed for developing an animal model for testing idiosyncratic reactions.

Keywords: vitamin B12 deficiency; liver; HCCL; glycogen; mitochondrial toxicity.

Introduction

Methylmalonic aciduria is an inherited disorder characterized by a disability of the body to process certain proteins and lipids properly [1-3]. The symptoms of methylmalonic aciduria usually appear in early babyhood and can vary from mild to life-threatening. Affected infants can experience recurrent vomiting, dehydration, and muscle weakness. Moreover, once babies start to eat more proteins, this disease can culminate in developmental delay, excessive tiredness, an enlargement of the liver, and failure to thrive [4, 5]. Without treatment, this disorder can lead to coma and death [6]. Currently, the main treatment for affected patients is dietary restriction of propiogenic amino acids in order to reduce the accumulation of toxic metabolites such as methylmalonic acid (MMA) and methylcitric acid [5]. Liver and/or combined liver/kidney transplantation has been performed in a limited number of patients with methylmalonic aciduria with the aim to improve metabolic stability through the provision of organ-specific enzymatic activity [7, 8].

The etiology of this disorder can originate from deficient enzymatic activity of methylmalonyl-CoA (MM-CoA) mutase or defective intracellular transport, processing and/or metabolism of cobalamin (Vitamin B12). Vitamin B12 deficiency is associated with decreased activity of the cobalamin-requiring enzymes MM-CoA mutase and methionine synthetase [6]. MM-CoA mutase is an important mitochondrial enzyme in propionyl-CoA metabolism and converts L-methylmalonyl-CoA into succinyl-CoA, a Krebs' cycle intermediate [9]. A block at this enzymatic step results in elevated plasma levels and urinary excretion of MMA, and as well in an accumulation of other propionyl-CoA-derived metabolites such as 2-methylcitrate [6].

Interestingly, liver mitochondria from patients with methylmalonic aciduria display morphological and/or functional alterations [10]. In order to characterize and to understand the mechanism of these alterations, Krahenbuhl et *al.* established an animal model of vitamin B12 deficiency by treating rats with the inhibitory vitamin B12 analog hydroxy cobalamin[c-lactam] (HCCL) [6, 11]. After several weeks of continuous subcutaneous infusion with HCCL, rats developed methylmalonic aciduria and this treatment was associated with mitochondrial proliferation and an impaired function of complexes III and IV of the mitochondrial respiratory

chain in isolated liver mitochondria. However our knowledge about the mechanisms and the consequences underlying these observed effects is still unclear.

The maintenance of mitochondrial integrity is crucial for preservation of cellular energy homeostasis. Mitochondria are also responsible for production of the majority of reactive oxygen species (ROS) in cells [12]. Indeed, complex I and III are the major site of superoxide formation. This formation occurs when unpaired electrons escape the electron transport chain and react with molecular oxygen to generate superoxide [13]. Superoxide is rapidly dismutated into hydrogen peroxide (H_2O_2) by superoxide dismutase (MnSOD or SOD2). H_2O_2 can be further reduced to water by catalase or by glutathione peroxidase, but it can be also transformed to a hydroxyl radical in the presence of reduced copper or iron [14]. The effects of ROS on DNA, protein, and lipid oxidation can cause irreversible cellular damage associated with the underlying pathogenesis of a wide variety of diseases [15]. However, the effects of HCCL treatment in animals regarding oxidative stress are still unknown.

Considering this lack of information, we aimed to get a more comprehensive knowledge of this animal model and decided to establish it in mice. In fact the mouse, in general, appears to be more clinically relevant than the rat model and has largely supplanted other rodents as the experimental model of choice for the study of physiology, toxicology and disease [16].

In the present study we sought to establish the vitamin B12-deficient model in mice in order to better characterize new mechanistic insights into the hepatotoxicity of this disease.

Materials and Methods

Chemicals

HCCL was synthesized on request from ReseaChem (Burgdorf, Switzerland). The manufacturer declared a 99% purity of HCCL by high-performance liquid chromatography (HPLC) and confirmed the structure by ^{1}H-NMR analysis. Stock solutions were prepared in water and stored at -20 °C. All other chemicals used were purchased from Sigma-Aldrich or Fluka (Buchs, Switzerland), except where indicated.

Animals

Experiments were reviewed and accepted by the cantonal veterinary authority and were performed in agreement with the guidelines for care and use of laboratory animals (License 2623). Male C57BL/6 mice were purchased from Charles River Laboratories (Sutzfeld, Germany) and were adult age-matched (7-weeks old). They housed in a standard facility with 12h light-dark cycles and controlled temperature (21-22°C). The mice were fed with a standard pellet chow and water *ad libitum*.

Dose finding study

After one week of acclimatization, 36 animals were randomly assigned to one of the treatment groups. The mice were treated intraperitoneally for 2 weeks (n=12), 3 weeks (n=12) or 4 weeks (n=12) with two different doses of HCCL (0.4mg/kg/d and 4mg/kg/d) or saline.

Determination of MMA

The determination of MMA was accomplished by the LC-MS/MS analysis using the ClinMass® Complete Kit (Recipe Chemicals + Instruments GmbH, Munich, Germany). Chromatographic separation was performed using a Shimadzu HPLC (Shimadzu AG, Reinach, Switzerland). The LC system was interfaced with a triple quadrupole mass spectrometer (API4000, AB Sciex, Concord, Canada) equipped with an electrospray ionization (ESI) source. MMA and methylmalonic acid-d3 were detected by selected reaction monitoring (SRM) with a transition of 116.9 → 72.8/54.9 m/z and 119.9 → 76.0 m/z, respectively. Inter-assay accuracy (determined as the percentage bias) for control samples ranged from -4.1 to 7.2 %, and inter-assay precision (determined as the relative standard deviation) was lower than 7.9 %. The lower limit of quantification (LLOQ) was 2.48 ng/mL for MMA.

HCCL treatment

After one week of acclimatization, the mice were divided into two groups: 1) 12 mice (HCCL group) treated with HCCL by intraperitoneal injection at 4 mg/kg body weight/day for 3 weeks and 2) 10 mice (saline group) treated with the same amount of saline and served as a control. Animals and food intakes were weighted every two days.

Sample collection

After the 21 days of treatment, mice were anaesthetized with an intraperitoneal application of ketamine (100 mg/kg) and xylazine (10 mg/kg). Blood was collected into heparin-coated tubes by an intracardiac puncture. Plasma was separated by centrifugation at 3,000g for 15 min. One part of the liver was collected and conserved in ice-cold MiR06 (mitochondrial respiration medium containing 0.5 mM EGTA, 3 mM $MgCl_2$, 60 mM K-lactobionate, 20 mM taurine, 10 mM KH_2PO_4, 20 mM HEPES, 110 mM sucrose, 1 g/L fatty acid-free bovine serum albumin [BSA] and 280 U/ml catalase, pH 7.1) before being transferred to the pre-calibrated oxygraph chambers.

The other part of liver was frozen in liquid nitrogen immediately after excision. Since the mice were anesthetized, tissues were obtained from living animals, and the time between sampling and freezing was only a few seconds. Samples were kept at − 80 °C until analysis.

Plasma parameters

AST and total bilirubin were analysed using a commercially available colorimetric assay kit (Abcam, Cambridge, UK).

Histological analysis of liver tissue

Cross sections (10 µm) of liver cut with a cryostat microtome were fixed with paraformaldehyde 4%. All sections were then incubated in 0.5% periodic acid for 8 min, washed in running water for 5 min and in distilled water twice for several seconds. They were incubated in Schiff 's solution for 10 min, followed by 0.5% sodium metabisulfite 3 times for 3 min each. Finally, cover slips were placed on glass slides with a mounting medium and

observed under a light microscope.

Lipid accumulation was investigated by Oil red O staining. Oil red O was freshly diluted (3:2 in distilled water) from a stock solution in isopropanol (0.5 g in 100 ml) and sections were incubated for 15 min. After incubation, the slides were rinsed with 60% isopropanol, counterstained with haematoxylin and coverslipped in aqueous mountant. The stained sections were examined by light microscopy and investigated for pathological changes in the liver.

Isolation of liver mitochondria

Fresh liver tissue was quickly removed and immersed in ice-cold isolation buffer (200 mM mannitol, 50 mM sucrose, 1 mM Na4EDTA, 20 mM HEPES, pH 7.4). Liver mitochondria were isolated by differential centrifugation as described previously [17]. The mitochondrial protein content was determined using the bicinchoninic acid protein assay reagent from Thermo Scientific (Wohlen, Switzerland).

Liver homogenate

Liver homogenate (250 mg fresh liver) was prepared with the PBI-Schredder HRR set (Oroboros instruments, Austria) according to the manufacturer's instruction [18].

Mitochondrial Membrane Potential

The mitochondrial membrane potential ($\Delta\psi_m$) was determined using the [phenyl-^{3}H]-tetra-phenylphosphonium bromide uptake assay. Freshly isolated mouse-liver mitochondria (200 μg/mL) were washed with incubation buffer (137.3 mM sodium chloride, 4.74 mM potassium chloride, 2.56 mM calcium chloride, 1.18 mM potassium phosphate, 1.18 mM magnesium chloride, 10 mM HEPES, 1 g/l glucose, pH 7.4). Mitochondria were then incubated at 37°C in buffer containing 0.5 μl/ml [phenyl-^{3}H]-tetra-phenylphosphonium bromide (40 Ci/mmol, Anawa trading SA, Wangen, Switzerland). After 15 min, the suspension was centrifuged and the mitochondrial pellet resuspended in fresh non-

radioactive incubation buffer with test compounds inside. Non-radioactive tetra-phenylphosphonium was used as a positive control. Mitochondria were treated for 15 min at 37°C. Afterwards, mitochondria were centrifuged and resuspended in non-radioactive buffer. The radioactivity of the samples was measured on a Packard 1900 TR liquid scintillation analyzer.

Activity of the enzyme complexes of the mitochondrial electron transport chain

The activity of the enzyme complexes of the electron transport chain was analyzed using an Oxygraph-2k high-resolution respirometer equipped with DatLab software (Oroboros Instruments, Innsbruck, Austria). Fresh liver homogenate (20 µl /chamber) was diluted with mitochondrial respiration medium MiR06 (mitochondrial respiration medium containing 0.5 mM EGTA, 3 mM $MgCl_2$, 60 mM K-lactobionate, 20 mM taurine, 10 mM KH_2PO_4, 20 mM HEPES, 110 mM sucrose, 1 g/L fatty acid-free bovine serum albumin [BSA] and 280 U/ml catalase, pH 7.1) before being transferred to the pre-calibrated oxygraph chambers.

In a first run, complexes I and III were analyzed using L-glutamate/malate (10 and 5 mM respectively) as substrates followed by the addition of ADP (2 mM). Then, we added oligomycin (2.5 µM) for the determination of the leak-state respiration. This was followed by the addition of FCCP (1 µM) to reach a full stimulation of the ETC. After that, we added rotenone, an inhibitor of complex I. (0.5 µM). Then, duroquinol (500 µM, Tokyo Chemical Industry, Tokyo, Japan) was added to investigate complex III, followed by the addition of the complex III inhibitor antimycin A (2.5 µM). In a second run, complexes II and IV were analyzed using succinate (10 mM) as substrate in the presence of rotenone (0.5 µM) to block complex I. This was followed by the addition of ADP (2 mM). Then, we added oligomycin (2.5 µM) for the determination of the leak-state respiration. This was followed by the addition of FCCP (1 µM) to reach a full stimulation of the ETC. Then, we added antimycin A (2.5 µM) in order to block the electron transport between complex II and IV and finally N, N ,N′ ,N′ tetramethyl-p-phenylenediamine dihydrochloride (TMPD) and ascorbate (0.5 and 2 mM, respectively) as artificial substrates of complex IV before the addition of the complex IV

inhibitor KCN (1 mM).

To assure the integrity of the outer mitochondrial membrane, the absence of a stimulatory effect of exogenous cytochrome c (10 µM) on respiration was demonstrated before the addition of KCN. We used the Pierce bicinchoninic acid (BCA) protein assay kit from Merck (Darmstadt, Germany) to determine the protein concentrations. Respiration rates are expressed in picomoles O_2 per second per mg protein.

Mitochondrial superoxide anion accumulation

Mitochondrial superoxide anion production was assessed with the fluorogenic, mitochondria-specific dye MitoSOX™ Red reagent (Molecular Probes, Eugene, OR, USA). Isolated mitochondria (200 µg) were stained with MitoSOX red (dissolved in DPBS) at a final concentration of 2 µM. After addition of MitoSox, the plate was incubated in the dark at 37°C for 15 min, afterwards fluorescence was measured at an excitation wavelength of 510 nm and an emission wavelength of 580 nm using a Tecan Infinite pro 200 microplate reader. We normalized the results to the protein content using the Pierce BCA Protein Assay Kit according to manufacturer's instruction.

Reduced GSH content

The reduced GSH content was determined using the luminescent GSH-Glo Glutathione assay (Promega, Wallisellen, Switzerland) according to the manufacture's manual. Liver tissue was homogenized with a Micro-dismembrator during 1 min at 2,000 rpm (Sartorius Stedim Biotech, Göttingen, Germany). 100 µl GSH-Glo Reagent was added to 50 mg liver and incubated for 30 min in the dark. Afterwards, 100 µl Luciferin Detection Reagent was added to each 96-well and the luminescence was measured after 15 min in the dark using a Tecan M200 Pro Infinity plate reader (Männedorf, Switzerland).

Measurement of Thiobarbituric Acid-Reactive Substances.

The measurement of plasma thiobarbituric acid-reactive substances (TBARS) was based on

the formation of malondialdehyde using a commercially available TBARS Assay Kit (Cayman Chemical, USA), according to the manufacturer's instructions.

Mitochondrial DNA content

To measure the mitochondrial DNA content, we determined the ratio of one mitochondrial gene to a nuclear gene using quantitative real-time RT-PCR as described previously with some modifications [19]. Total DNA was extracted using the DNeasy Blood and Tissue Kit (Qiagen) following the manufacturer's instructions (Quick-Start Protocol). The concentration of the extracted DNA was measured spectrophotometrically at 260 nm with the NanoDrop 2000 (Thermo Scientific, Wohlen, Switzerland). Afterwards, DNA was diluted in RNase free water to a final concentration of 10 ng/µL. The analysis of the mitochondrial ND1 and the nuclear 36B4 genes was performed using SYBR Green real-time PCR (Roche Diagnostics, Rotkreuz, Switzerland) on an ABI PRISM 7700 sequence detector (PE Biosystems, Rotkreuz, Switzerland). Quantification was performed using the comparative-threshold cycle method. Forward and reverse primers for genes of interest and GAPDH as endogenous reference control (see Table 2 for primers) were purchased from Microsynth (Balgach, Switzerland).

Statistical Methods

Data are given as the mean ± standard deviation (S.D.). Statistical analyses were performed using the Student t-test using GraphPad Prism 6 (GraphPad Software, La Jolla, CA, US). P-values <0.05 (*), <0.01 (**) or <0.001 (***) were considered as significant.

Results

Dose finding range

The goal of this first part was to determine the dose and the duration of HCCL treatment with the measurement of plasma MMA concentration. We showed that the treatment with HCCL

for 3 weeks at 4mg/kg/d increased 3-fold the plasma MMA concentration compared to the saline treatment ($p<0.01$; Fig. 1). However we could already see a non-significant increase of plasma MMA concentration after 2 weeks treatment with HCCL at 4 mg/kg/d. After 4 weeks, the MMA concentration was still higher after the treatment with HCCL compared to the saline treatment ($p<0.001$; Fig. 1). According that, we decided to perform the following animal study with HCCL at 4 mg/kg/d for 3 weeks.

Characterization of the animals

The absolute liver weight was increased in the HCCL-treated animals when compared to saline (1421 ± 139 *vs*. 1275 ± 123 mg wet liver respectively; $p<0.05$; Fig. 2A). This liver increase was maintained when liver weight was expressed relative to the body weight (49.94 ± 4.60 *vs*. 53.79 ± 3.88 mg wet liver per gram body weight respectively; $p<0.05$; Fig. 2B).

Daily food consumption was not different between the saline and HCCL groups (3.64 ± 0.08 *vs.* 3.46 ± 0.06 g per day respectively; Fig. 2C).

AST and Total bilirubin levels were higher in the HCCL treated mice compared to the saline treatment, without reaching the statistical significance (Table 1).

Histological changes in the liver

The presence of glycogen in the cytoplasm of hepatocytes was detected and quantified using the periodic acid-Schiff (PAS) staining in mouse liver tissues. PAS staining was observed as a strong red-purple color in the cytoplasm of hepatocytes in treated mice (Fig. 2D)

Neutral hepatic lipids, mainly triacylglycerols, were detected and quantified in frozen liver sections using the oil red O stain (Fig. 2D). Similar to the results of hepatic glycogen, triacylglycerols content was higher in liver mice treated with HCCL compared to the controls.

Mitochondrial membrane potential ($\Delta\psi_m$) *and activity of the electron transport chain*

Since HCCL is an established mitochondrial toxicant [11], we next assessed the impact of HCCL treatment on oxidative metabolic function of HepG2 cells. The mitochondrial

membrane potential ($\Delta\psi_m$) is an important parameter of mitochondrial integrity, as the electrical potential across the inner mitochondrial membrane is built up mainly by the proton gradient generated by the activity of the complexes of the electron transport chain [20]. We observed that HCCL treatment did not significantly affect $\Delta\psi_m$ (Fig. 3A).

We next assessed the activity of complexes I-IV of the electron transport chain by measuring the oxygen consumption in the presence of different substrates (Fig. 3B). The treatment with HCCL reduced significantly the activity of complex I ($p<0.05$). The activity of complex II and III was also reduced only numerically without reaching statistical significance.

Oxidative stress evaluation

It is well established that the damage of the electron flow across the mitochondrial electron transport chain is associated with cellular ROS accumulation [12]. Superoxide anion accumulation was similar in both groups (Fig. 4A).

Accumulating ROS can be degraded by the glutathione antioxidant system, which is an effective scavenger of free radicals and reactive superoxide. A decrease in cellular glutathione levels is associated with oxidative stress as well as apoptosis and cell death. For that reason, we determined the cellular reduced glutathione content. We found that HCCL treatment was not associated with a decrease in the cellular GSH content compared to saline group (Fig. 4B). As indicated by the accumulation of TBARS, lipid peroxides were similar in the livers of saline and HCCL treated mice (Fig. 4C).

HCCL does not affect mitochondrial DNA content.

The ratio of the mtDNA to the nuclear DNA provides a measure of the mitochondrial DNA homeostasis and represents a marker of mitochondrial proliferation. As shown in Fig. 5, qRT-PCR analysis did not show significant alterations in the ratio of mtDNA/nDNA after HCCL treatment.

Discussion

In the current study, we showed that HCCL treatment for 3 weeks at 4 mg/kg/d i.p. in mice 1) caused an elevated plasma concentration of MMA, 2) increased significantly the liver weight, which was correlated with an increase of lipid droplets and glycogen content, and 3) altered mitochondrial function through an inhibition of the complex I activity in liver homogenate.

We sought to translate the established rat HCCL model [6, 11, 21] into a mouse model since mice are more clinically relevant regarding toxicology and diseases studies and provide the possibility to further enlarge the gained knowledge into knockout-or transgenic mice, whereas this is impeded in rats [16, 22, 23]. Moreover, with the HCCL mouse model we wanted to better understand the involvement of hepatocellular alterations associated with vitamin B12 deficiency since the use of the cobalamin antagonist HCCL has provided a facile model of the human methylmalonic acidurias [6].

In a first step, we performed a dose-finding study in which we treated mice with HCCL at two different concentrations (0.4mg/kg and 4mg/kg) for three different durations (two, three and four weeks). We measured the accumulation of MMA in plasma as a biomarker of vitamin B12 deficiency. We showed that the accumulation of MMA reached the highest level with a HCCL treatment of 3 weeks at 4mg/kg i.p. According to that, we decided to perform a second animal study with this concentration and duration in order to better characterize this model.

In the current study, we showed that HCCL 4mg/kg for 3 weeks increased significantly the liver weight. This increase was maintained when the liver weight was normalized to the body weight. PAS and Oil red O stainings showed an accumulation of glycogen and lipid droplets in liver HCCL-treated mice. We could explain this elevation with a significant increase in volume of peroxisomes as a percentage of cytoplasmic area, thus indicating that peroxisomes were increased in size. The combination of these findings suggests that HCCL-induced hepatomegaly could be associated with peroxisomal changes. Compounds (for instance ibuprofen) that elicit peroxisome proliferation are associated with the induction of hepatocellular hypertrophy, proliferation, and hepatocellular neoplasia in rodents [24].

Our research group is interested in establishing animal models for studying mechanisms of

idiosyncratic adverse drug reactions. Idiosyncratic adverse drug reactions are rare and occur at therapeutic drug doses, implying the presence of susceptibility factors. Since adverse hepatic drug reactions often affect mitochondrial function [25], preexisting mitochondrial dysfunction could represent a susceptibility factor. This has been demonstrated for valproate associated liver failure, where mitochondrial dysfunction, as for instance caused by mutations in the gene coding for DNA polymerase gamma, is an established susceptibility factor [26]. Since, as described above, HCCL is associated with mitochondrial dysfunction affecting complexes of the electron transport chain, animals treated with HCCL could represent suitable models for studying idiosyncratic mitochondrial toxicants. The application of this mouse model with treatment of HCCL could therefore provide a useful model for testing idiosyncratic mitochondrial toxicity. This is underlined by the findings of Krahenbuhl et al, showing that HCCL administration to rats is associated with hepatic mitochondrial proliferation as assessed by enzyme activities per gram of liver or per hepatocyte, hepatocyte oxidative capacity, and ultrastructural morphology [27]. In addition, liver mitochondria from rats treated with HCCL for 6 weeks manifested specific defects (per mg of mitochondrial protein) in the activity of the electron transport chain enzymes ubiquinol:cytochrome c oxidoreductase and cytochrome c oxidase while other enzyme activities were normal [11].

Our studies in mice partially confirmed these findings; We showed that HCCL treatment at 4 mg/kg for 3 weeks inhibited the enzyme activity of complex I of the mitochondrial electron transport chain and numerically reduced the activity of complex II and III in liver homogenate whereas Krahenbuhl et al. showed an inhibition of complex III and IV in isolated liver mitochondria. These different observations can be explained by interspecies differences or due to a varying application method compared to ours; HCCL infusion in rats was conducted by subcutaneous implanted mini-pumps over 6 weeks, leading to a higher impact of affection on mitochondrial energy function than only 3 weeks of i.p. treatment in mice. Additionally, we did not monitor steady-state levels of HCCL in the plasma of treated mice. Irregular HCCL concentrations therefore may be a reason that we found minor defects on mitochondrial

function.

As impaired activity of the electron transport chain can be associated with increased mitochondrial production of ROS [12], mitochondrial accumulation of ROS was an expected finding. However, we were surprised to find no changes in mitochondrial superoxide accumulation. The results of our study are not in agreement with findings in skin fibroblasts of patients with methylmalonic aciduria, where an increased ROS production has been described [28]. Moreover, recently, we showed that exposure to HCCL on HepG2 cells increased mitochondrial ROS accumulation [29]. One explanation for this discrepancy could be the absence of mitochondrial substrates (i.e. glutamate/malate or succinate) in our assay, which could allow measuring the maximal ROS production. Apart from that, we also measured reduced GSH and lipid peroxidation as a marker for oxidative stress. However, we did not find any alterations. These results suggest that HCCL treatment did not induce oxidative stress despite the inhibition of the enzyme complex I activity. We thus speculate that the dose and duration were not sufficient to induce a strong impairment of mitochondrial function.

The current study showed that mice exposed to HCCL 4 mg/d for 3 weeks presented similar pathological signs including elevated MMA concentrations and metabolic changes as commonly observed in vitamin B12-deficient patients. However these changes were only minor and let us to the conclusion, that our proposed mouse model was not efficient enough to further us it in the determination of idiosyncratic hepatotoxic drugs. Nevertheless, an interesting finding was that HCCL increased the liver weight correlated with the increase of lipids and glycogen contents emphasizing its potency to induce subtle changes in the liver and thus allowing a better understanding of the implicated mechanisms in vitamin B12 deficiency.

Funding source

This study was supported by a grant to Stephan Krähenbühl from the Swiss National Science Foundation (31003A_156270).

Conflicts of interest

None of the authors reports a conflict of interest with this work.

References

1. Janata J, Kogekar N, Fenton WA. Expression and kinetic characterization of methylmalonyl-CoA mutase from patients with the mut- phenotype: evidence for naturally occurring interallelic complementation. Human molecular genetics. 1997;6(9):1457-64. Epub 1997/09/01. PubMed PMID: 9285782.

2. Sponne IE, Gaire D, Stabler SP, Droesch S, Barbe FM, Allen RH, et al. Inhibition of vitamin B12 metabolism by OH-cobalamin c-lactam in rat oligodendrocytes in culture: a model for studying neuropathy due to vitamin B12 deficiency. Neuroscience letters. 2000;288(3):191-4. Epub 2000/07/13. PubMed PMID: 10889340.

3. Wilnai Y, Enns GM, Niemi AK, Higgins J, Vogel H. Abnormal hepatocellular mitochondria in methylmalonic acidemia. Ultrastructural pathology. 2014;38(5):309-14. doi: 10.3109/01913123.2014.921657. PubMed PMID: 24933007.

4. Chandler RJ, Venditti CP. Pre-clinical efficacy and dosing of an AAV8 vector expressing human methylmalonyl-CoA mutase in a murine model of methylmalonic acidemia (MMA). Molecular genetics and metabolism. 2012;107(3):617-9. Epub 2012/10/11. doi: 10.1016/j.ymgme.2012.09.019. PubMed PMID: 23046887; PubMed Central PMCID: PMC3522145.

5. Horster F, Hoffmann GF. Pathophysiology, diagnosis, and treatment of methylmalonic aciduria-recent advances and new challenges. Pediatr Nephrol. 2004;19(10):1071-4. doi: 10.1007/s00467-004-1572-3. PubMed PMID: 15293040.

6. Krahenbuhl S, Ray DB, Stabler SP, Allen RH, Brass EP. Increased hepatic mitochondrial capacity in rats with hydroxy-cobalamin[c-lactam]-induced methylmalonic

aciduria. The Journal of clinical investigation. 1990;86(6):2054-61. Epub 1990/12/01. doi: 10.1172/JCI114942. PubMed PMID: 1701451; PubMed Central PMCID: PMC329844.

7. Chandler RJ, Zerfas PM, Shanske S, Sloan J, Hoffmann V, DiMauro S, et al. Mitochondrial dysfunction in mut methylmalonic acidemia. FASEB journal : official publication of the Federation of American Societies for Experimental Biology. 2009;23(4):1252-61. Epub 2008/12/18. doi: 10.1096/fj.08-121848. PubMed PMID: 19088183; PubMed Central PMCID: PMC2660647.

8. Deodato F, Boenzi S, Santorelli FM, Dionisi-Vici C. Methylmalonic and propionic aciduria. Am J Med Genet C Semin Med Genet. 2006;142C(2):104-12. doi: 10.1002/ajmg.c.30090. PubMed PMID: 16602092.

9. Brass EP, Allen RH, Ruff LJ, Stabler SP. Effect of hydroxycobalamin[c-lactam] on propionate and carnitine metabolism in the rat. The Biochemical journal. 1990;266(3):809-15. Epub 1990/03/15. PubMed PMID: 2327967; PubMed Central PMCID: PMC1131211.

10. Frenkel EP, Mukherjee A, Hackenbrock CR, Srere PA. Biochemical and ultrastructural hepatic changes during vitamin B12 deficiency in animals and man. The Journal of biological chemistry. 1976;251(7):2147-54. Epub 1976/04/10. PubMed PMID: 178657.

11. Krahenbuhl S, Chang M, Brass EP, Hoppel CL. Decreased activities of ubiquinol:ferricytochrome c oxidoreductase (complex III) and ferrocytochrome c:oxygen oxidoreductase (complex IV) in liver mitochondria from rats with hydroxycobalamin[c-lactam]-induced methylmalonic aciduria. The Journal of biological chemistry. 1991;266(31):20998-1003. Epub 1991/11/05. PubMed PMID: 1657942.

12. Balaban RS, Nemoto S, Finkel T. Mitochondria, oxidants, and aging. Cell. 2005;120(4):483-95. doi: 10.1016/j.cell.2005.02.001. PubMed PMID: 15734681.

13. Turrens JF. Mitochondrial formation of reactive oxygen species. J Physiol. 2003;552(Pt 2):335-44. doi: 10.1113/jphysiol.2003.049478. PubMed PMID: 14561818; PubMed Central PMCID: PMC2343396.

14. Ribas V, Garcia-Ruiz C, Fernandez-Checa JC. Glutathione and mitochondria. Frontiers in pharmacology. 2014;5:151. Epub 2014/07/16. doi: 10.3389/fphar.2014.00151. PubMed PMID: 25024695; PubMed Central PMCID: PMC4079069.

15. Alfadda AA, Sallam RM. Reactive oxygen species in health and disease. J Biomed Biotechnol. 2012;2012:936486. doi: 10.1155/2012/936486. PubMed PMID: 22927725; PubMed Central PMCID: PMC3424049.

16. Muruganandan S, Sinal CJ. Mice as clinically relevant models for the study of cytochrome P450-dependent metabolism. Clinical pharmacology and therapeutics. 2008;83(6):818-28. Epub 2008/04/05. doi: 10.1038/clpt.2008.50. PubMed PMID: 18388875.

17. Hoppel C, DiMarco JP, Tandler B. Riboflavin and rat hepatic cell structure and function. Mitochondrial oxidative metabolism in deficiency states. The Journal of biological chemistry. 1979;254(10):4164-70. Epub 1979/05/25. PubMed PMID: 571436.

18. Pecinova A, Drahota Z, Nuskova H, Pecina P, Houstek J. Evaluation of basic mitochondrial functions using rat tissue homogenates. Mitochondrion. 2011;11(5):722-8. Epub 2011/06/15. doi: 10.1016/j.mito.2011.05.006. PubMed PMID: 21664301.

19. Pieters N, Koppen G, Smeets K, Napierska D, Plusquin M, De Prins S, et al. Decreased mitochondrial DNA content in association with exposure to polycyclic aromatic

hydrocarbons in house dust during wintertime: from a population enquiry to cell culture. PloS one. 2013;8(5):e63208. Epub 2013/05/10. doi: 10.1371/journal.pone.0063208. PubMed PMID: 23658810; PubMed Central PMCID: PMC3643917.

20. Kaufmann P, Torok M, Zahno A, Waldhauser KM, Brecht K, Krahenbuhl S. Toxicity of statins on rat skeletal muscle mitochondria. Cellular and molecular life sciences : CMLS. 2006;63(19-20):2415-25. Epub 2006/10/03. doi: 10.1007/s00018-006-6235-z. PubMed PMID: 17013560.

21. Tandler B, Krahenbuhl S, Brass EP. Unusual mitochondria in the hepatocytes of rats treated with a vitamin B12 analogue. The Anatomical record. 1991;231(1):1-6. Epub 1991/09/01. doi: 10.1002/ar.1092310102. PubMed PMID: 1661107.

22. Picciotto MR, Wickman K. Using knockout and transgenic mice to study neurophysiology and behavior. Physiol Rev. 1998;78(4):1131-63. PubMed PMID: 9790572.

23. Doyle A, McGarry MP, Lee NA, Lee JJ. The construction of transgenic and gene knockout/knockin mouse models of human disease. Transgenic Res. 2012;21(2):327-49. doi: 10.1007/s11248-011-9537-3. PubMed PMID: 21800101; PubMed Central PMCID: PMC3516403.

24. Bendele AM, Hulman JF, White S, Brodhecker C, Bendele RA. Hepatocellular proliferation in ibuprofen-treated mice. Toxicol Pathol. 1993;21(1):15-20. PubMed PMID: 8378703.

25. Krahenbuhl S. Mitochondria: important target for drug toxicity? Journal of hepatology. 2001;34(2):334-6. Epub 2001/04/03. PubMed PMID: 11281565.

26. Krahenbuhl S, Brandner S, Kleinle S, Liechti S, Straumann D. Mitochondrial diseases represent a risk factor for valproate-induced fulminant liver failure. Liver. 2000;20(4):346-8. Epub 2000/08/26. PubMed PMID: 10959815.

27. Leeds FS, Brass EP. Hepatic cobalamin deficiency induced by hydroxycobalamin[c-lactam] treatment in rats is associated with decreased mitochondrial mRNA contents and accumulation of polycistronic mitochondrial RNAs. The Journal of biological chemistry. 1994;269(6):3947-51. Epub 1994/02/11. PubMed PMID: 7508436.

28. Richard E, Jorge-Finnigan A, Garcia-Villoria J, Merinero B, Desviat LR, Gort L, et al. Genetic and cellular studies of oxidative stress in methylmalonic aciduria (MMA) cobalamin deficiency type C (cblC) with homocystinuria (MMACHC). Human mutation. 2009;30(11):1558-66. Epub 2009/09/18. doi: 10.1002/humu.21107. PubMed PMID: 19760748.

29. Haegler P, Grunig D, Berger B, Krahenbuhl S, Bouitbir J. Impaired mitochondrial function in HepG2 cells treated with hydroxy-cobalamin[c-lactam]: A cell model for idiosyncratic toxicity. Toxicology. 2015. doi: 10.1016/j.tox.2015.07.015. PubMed PMID: 26219506.

Legends to figures

Fig. 1: MMA plasma concentration. MMA levels were measured with LC-MS/MS analysis using the ClinMass® Complete Kit after mice were treated with HCCL at 0.4 mg/kg/d or 4 mg/kg/d for two, three or four weeks. Data are expressed as mean ± SD. **p < 0.01, ***p < 0.001.

Fig. 2: Characterisation of the animals. (A) Liver weight, (B) Liver weight/body weight ratio. (C) Daily food intake, (D) PAS, and Oil Red O stainings. Data are expressed as mean ± SD. *p < 0.05.

Fig. 3: Mitochondrial function. (A) Mitochondrial membrane potential ($\Delta\psi_m$) was measured with the [phenyl-^{3}H]-tetra-phenylphosphonium bromide uptake assay in isolated liver mitochondria of HCCL treated mice. (B) Electron transport chain complex activities in mouse liver homogenate of HCCL treated mice. After addition of substrates and inhibitors of the different complexes, complex activities were determined on a Oxygraph-2k high-resolution respirometer. HCCL: hydroxy-cobalamin[c-lactam], FCCP: Carbonyl cyanide 4 (trifluoromethoxy)phenylhydrazone, Data are expressed as mean ± SD. *p < 0.05.

Fig. 4: Evaluation on oxidative stress. (A) Mitochondrial superoxide production was measured with MitoSOX™ Red reagent in isolated liver mitochondria in mice treated with HCCL. (B) Reduced GSH in the liver of treated mice, determined with the luminescent GSH-Glo Glutathione assay. (C) Plasma concentrations of TBARS of HCCL treated mice based on the formation of malondialdehyde. Data are expressed as mean ± SD.

Fig. 5: Mitochondrial DNA content. Total DNA was extracted from the liver after treatment with HCCL on mice. DNA expression of a mitochondrial (ND-1) and a nuclear gene (36B4)

was determined by qRT-PCR. The graph shows the expression ratio of these two genes. Data are expressed as mean ± SD.

Tables

Table 1: Plasma parameters. Aspartate aminotransferase (AST), and total bilirubin (bilirubin) were determined in mouse plasma of mice treated or not with HCCL 4mg/kg i.p. for 3 weeks.

	Saline	HCCL 4mg/kg/d
AST (U/L)	18.7±1.3	21.9±1.7
Total Bilirubin (g/L)	0.7±0.1	1.1±0.2

Table 2: Primers List

Gene	Sequence 5'--→3'
ND-1	ATG GCC AAC CTC CTA CTC CT CTA CAA CGT TGG GGC CTT T
36B4	GGA ATG TGG GCT TTG TGT TC CCC AAT TGT CCC CTT ACC TT

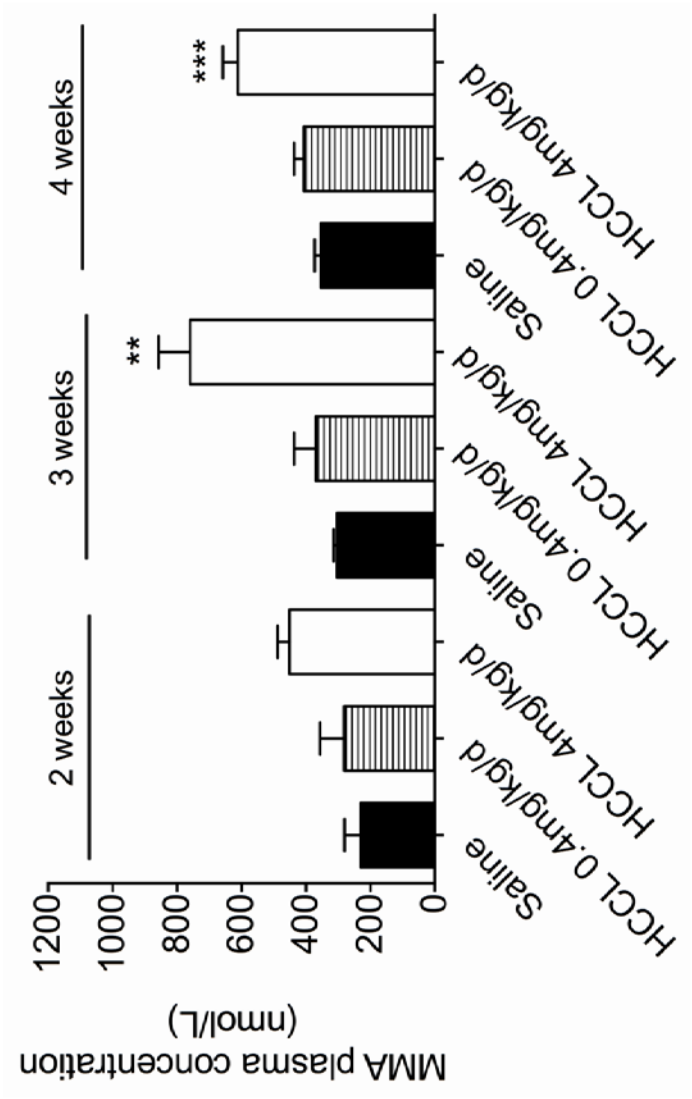
MMA plasma concentration
(nmol/L)
1200
1000
800
600
400
200
0
2 weeks
3 weeks
4 weeks
**
***
Saline
HCCL 0.4mg/kg/d
HCCL 4mg/kg/d
Saline
HCCL 0.4mg/kg/d
HCCL 4mg/kg/d
Saline
HCCL 0.4mg/kg/d
HCCL 4mg/kg/d

1

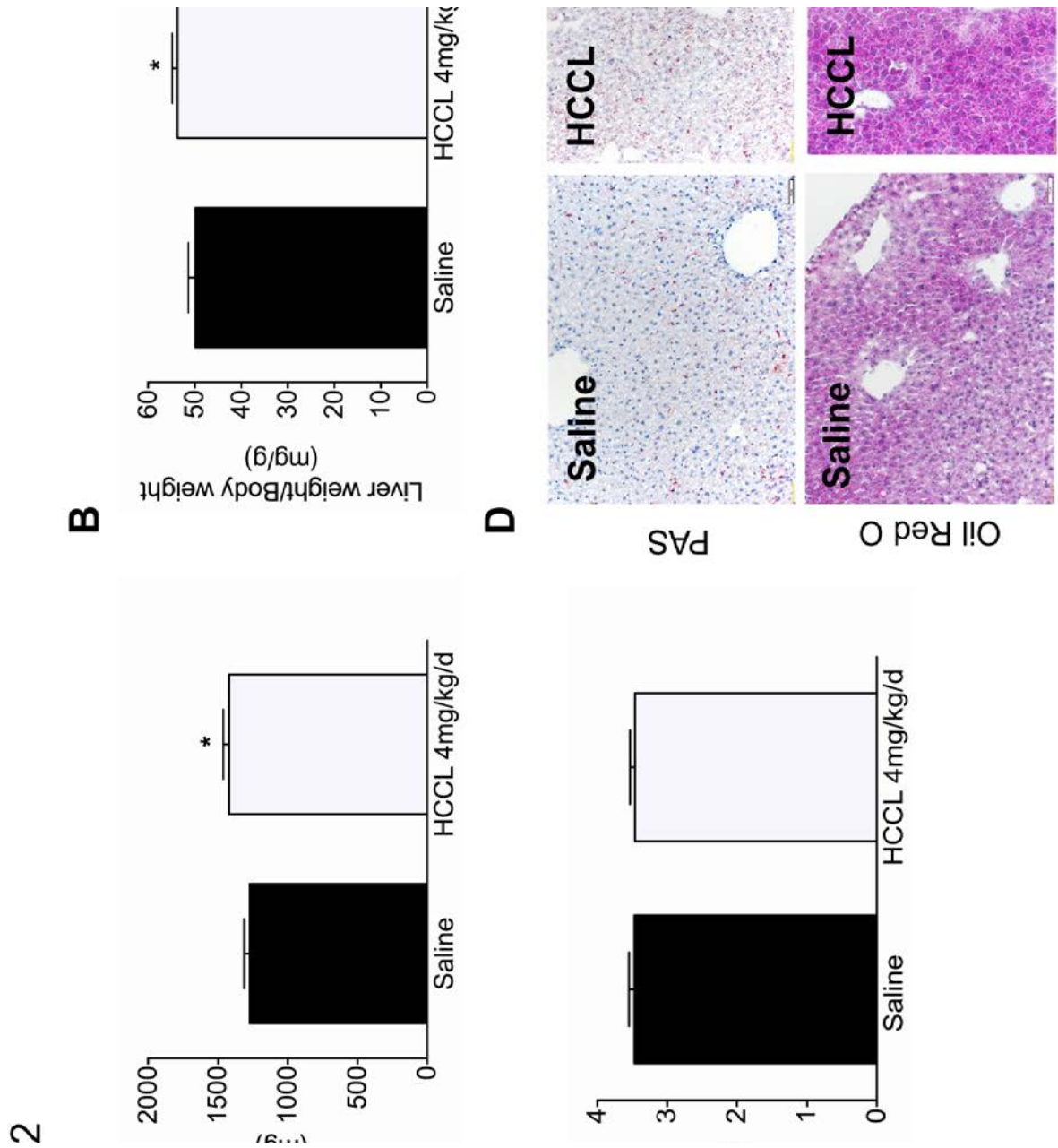
2
B
Liver weight/Body weight
(mg/g)
60
50
40
30
20
10
0
Saline
HCCL 4mg/k
*
2000
1500
1000
500
0
Saline
HCCL 4mg/kg/d
*
4
3
2
1
0
Saline
HCCL 4mg/kg/d
D
Oil Red O
PAS
Saline
HCCL
Saline
HCCL

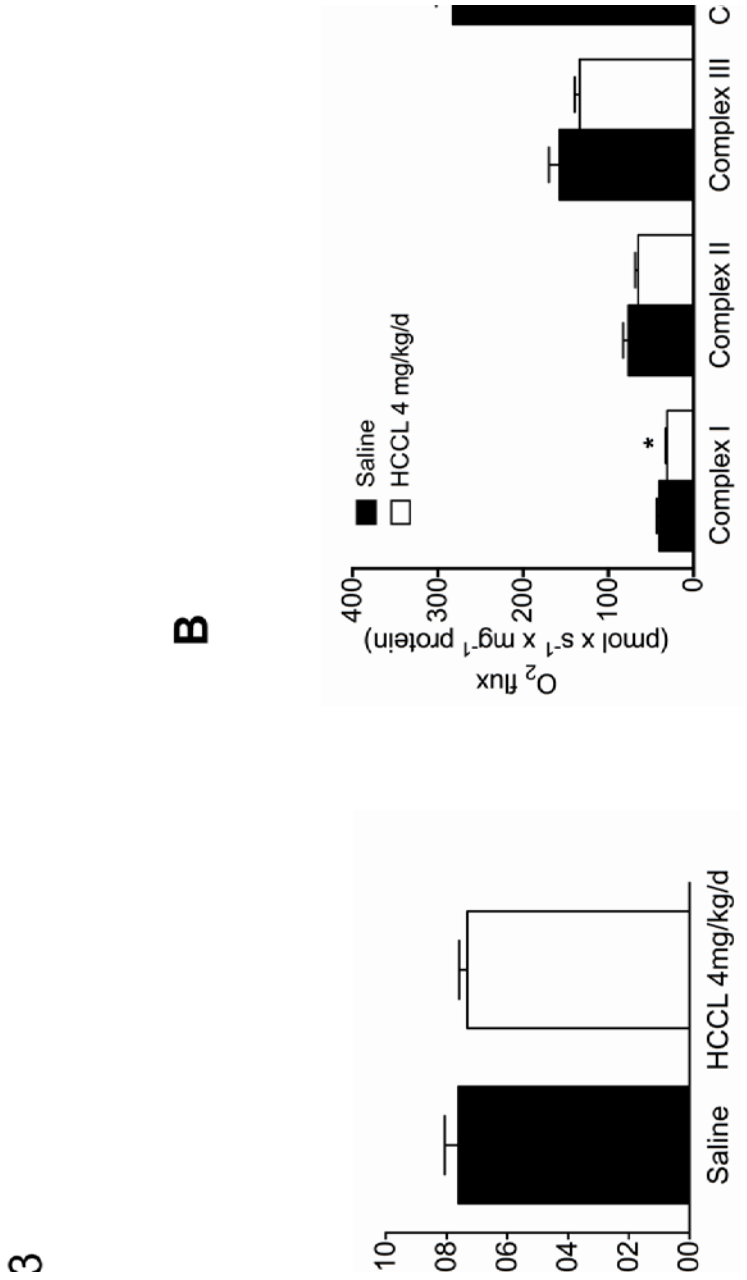
B
Saline
HCCL 4 mg/kg/d
O2 flux
(pmol x s-1 x mg-1 protein)
400
300
200
100
0
*
Complex I
Complex II
Complex III
C
3
Saline
HCCL 4mg/kg/d
10
08
06
04
02
00

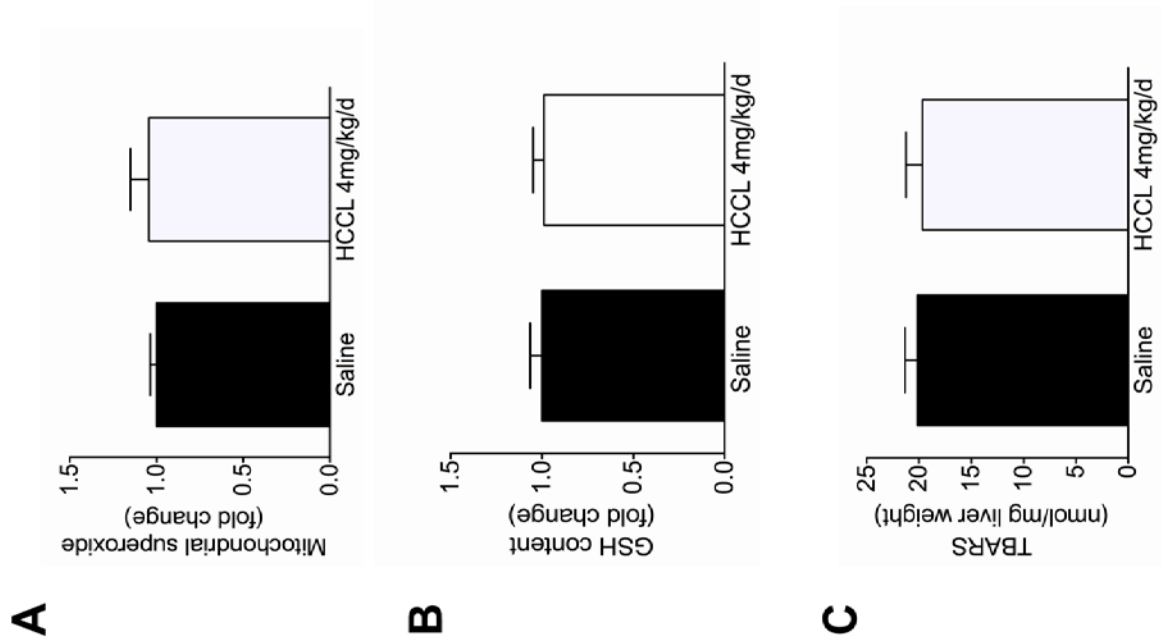
4
A
Mitochondrial superoxide (fold change)
1.5
1.0
0.5
0.0
Saline
HCCL 4mg/kg/d
B
GSH content (fold change)
1.5
1.0
0.5
0.0
Saline
HCCL 4mg/kg/d
C
TBARS (nmol/mg liver weight)
25
20
15
10
5
0
Saline
HCCL 4mg/kg/d

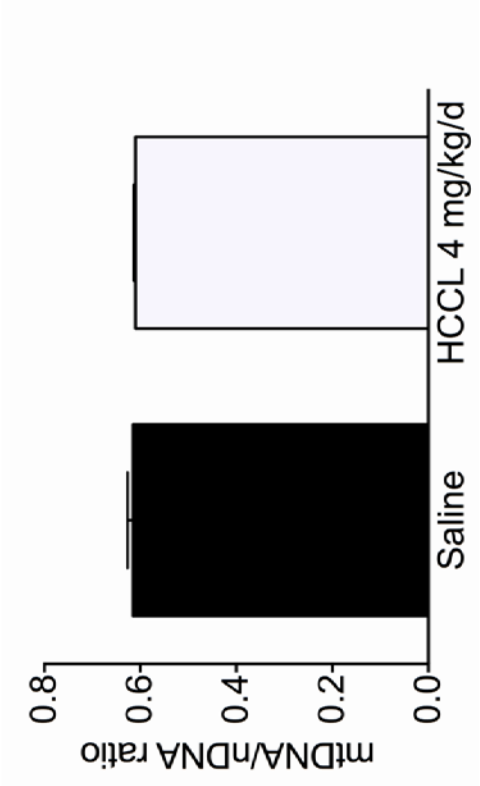

5

Paper 3

Hepatocellular toxicity of imidazole and triazole antimycotic agents

P Haegler[1,2], L Joerin[1,2], B Berger[1,2], S Krähenbühl[1,2,3], J Bouitbir[1,2,3]

[1] Clinical Pharmacology & Toxicology, University Hospital Basel, Switzerland

[2] Department of Biomedicine, University of Basel, Switzerland

[3] Swiss Centre of Applied Human Toxicology (SCAHT)

Manuscript submitted

to

Archives of Toxicology

Hepatocellular toxicity of imidazole and triazole antimycotic agents

Patrizia Hägler[1,2], Lorenz Joerin[1,2], Stephan Krähenbühl[1,2,3] and Jamal Bouitbir[1,2,3]

[1] Clinical Pharmacology & Toxicology, University Hospital Basel, Switzerland

[2] Department of Biomedicine, University of Basel, Switzerland

[3] Swiss Centre of Applied Human Toxicology (SCAHT)

Funding: This study was funded by grant 31003A_156270 of the Swiss National Science Foundation to SK

Conflict of Interest: The authors declare that they have no conflict of interest regarding this study

Correspondence:

Stephan Krähenbühl, MD, PhD

Clinical Pharmacology & Toxicology

University Hospital

4031 Basel/Switzerland

Phone: +41 61 265 4715

Fax: +41 61 265 4560

e-mail: stephan.kraehenbuehl@usb.ch

Abstract

Hepatotoxicity has been described for all antimycotic azoles currently marketed. A possible mechanism involving mitochondrial dysfunction has been postulated for ketoconazole, but not for the other azoles. The aim of the current investigations was to study the toxicity of different azoles in different cell models and to find out the mechanism of their toxicity. In HepG2 cells, posaconazole and ketoconazole were both cytotoxic starting at 50 µM and decreased the cellular ATP content starting at 5 or 10 µM in galactose or glucose-based culture media, respectively. In HepaRG cells, cytotoxicity started at 20 or 100 µM for posaconazole or ketoconazole, respectively, and was accentuated by cytochrome P450 (CYP) induction. ATP depletion was observed at 100 µM for posaconazole and voriconazole and was not increased by CYP induction. Voriconazole and fluconazole were not cytotoxic and did not deplete cellular ATP stores up to 100 µM. In HepG2 cells, both posaconazole and ketoconazole (but not fluconazole or voriconazole) decreased the mitochondrial membrane potential, impaired the function of enzyme complexes of the electron transport chain, were associated with mitochondrial superoxide accumulation and induced apoptosis. In HepG2 cells with mitochondrial dysfunction induced by the vitamin B12 antagonist hydroxy-cobalamin[c-lactam], cytotoxicity and/or ATP depletion was more accentuated than in untreated cells. We conclude that ketoconazole and posaconazole are mitochondrial toxicants starting at concentrations, which can be reached in vivo. Cytotoxicity and ATP depletion are more accentuated in cells with mitochondrial damage, suggesting that mitochondrial dysfunction is a susceptibility factor for hepatotoxicity associated with these drugs.

Key words: posaconazole, voriconazole, mitochondrial membrane potential, electron transport chain, apoptosis

Introduction

Azole antifungal drugs are the most commonly used agents for the treatment of invasive fungal infections (Castelli et al. 2014; Lass-Florl 2011). Antifungal azoles, which are heterocyclic synthetic compounds, can be divided into two classes: imidazole derivatives and the newer triazole derivatives (see supplementary Fig. 1 for chemical structures). Both classes share the same mechanism of action; they inhibit the cytochrome P450 (CYP)-dependent enzyme lanosterole 14α-demethylase, leading to ergosterol deficiency and accumulation of 14α-methylated sterols in the fungal cell membranes (Kathiravan et al. 2012; Van den Bossche et al. 1980).

More than three decades ago, ketoconazole, one of the first imidazole derivatives, was introduced to the market (Greenblatt and Greenblatt 2014). One decade later, the first generation triazole fluconazole quickly became the most widely described antifungal agent due to its improved efficacy and safety profile compared to ketoconazole (Lewis 2011). However, while fluconazole is very active against yeast, it lacks activity against aspergillus and other species (Lewis 2011). Therefore, voriconazole and posaconazole (second generation triazoles), covering a wider spectrum than fluconazole, were developed and launched (Lass-Florl 2011; Stevens 2012).

All four systemic antimycotic azoles mentioned above are associated with a risk for liver injury (DILI) (Bercoff et al. 1985; Bronstein et al. 1997; Raschi et al. 2014; Stricker et al. 1986). The reported hepatotoxicity ranges from mild, asymptomatic, mostly reversible elevation in serum transaminases to potentially fatal acute liver failure (Raschi et al. 2014). The reported incidence of azole-related DILI varies depending on the drug of interest and the definition of liver disease (Cronin and Chandrasekar 2010; Egunsola et al. 2013; Garcia Rodriguez et al. 1999). A recent review and meta-analysis estimated an overall incidence of 3.6%-4.2% for symptomatic and asymptomatic liver injury in patients treated with systemic ketoconazole (Yan et al. 2013). The actual incidence may even be higher due to underreporting. Based on these considerations, the US Food and Drug Administration limited the use of ketoconazole in 2013 and the Committee on Medicinal Products for human use of

the European Medicine Agency banned the use of systemic ketoconazole as an antifungal agent in 2013 due to a negative benefit-risk balance. The incidence of liver injury for the newer agents is less well established than for ketoconazole, but is probably lower than for ketoconazole (Kao et al. 2014).

To date, the exact mechanism of liver toxicity associated with these agents is not entirely clear. An early report demonstrated cytotoxicity of ketoconazole in cultured rat hepatocytes (Rodriguez and Acosta 1995). Later, the same authors showed that the cytotoxic effect of ketoconazole is not only associated with the parent compound, but also with N-deacetyl ketoconazole, the main metabolite of ketoconazole (Rodriguez and Acosta 1997b). Furthermore, Rodriguez and Acosta (Rodriguez and Acosta 1996) showed that ketoconazole decreased the complex I and II activities of the electron transport chain in isolated rat liver mitochondria, suggesting that mitochondria may play an important role in azole-associated hepatotoxicity.

Since mechanistic toxicological studies concerning the newer triazoles fluconazole, voriconazole and posaconazole are rare or lacking, our first goal was to study the hepatocellular toxicity of these agents in comparison to ketoconazole. For that, we used two human hepatoma cell lines, namely HepG2 and HepaRG cells. A second goal of our project was to find out possible mechanisms of hepatotoxicity, with a special focus on mitochondrial toxicity and involvement of metabolites contributing to toxicity. If mitochondrial toxicity were detected, a third aim was to test such substances in a newly created cell model with mitochondrial dysfunction (Hägler et al. 2015) with the assumption that the toxicity would be increased.

Materials and Methods

Chemicals

Ketoconazole, posaconazole, voriconazole, and fluconazole were purchased from Sigma-Aldrich (Buchs, Switzerland). Stock solutions were dissolved in DMSO and stored at -20 °C.

We used control incubations containing 0.1% DMSO and this concentration has been shown not be cytotoxic (Waldhauser et al. 2006). Hydroxy-cobalamin[c-lactam] (HCCL) was synthesized on request from ReseaChem (Burgdorf, Switzerland). The manufacturer declared a purity of 99% by high-performance liquid chromatography and confirmed the structure by ^{1}H-NMR analysis. Stock solutions of HCCL were prepared in water and stored at -20 °C. All other chemicals used were purchased from Sigma-Aldrich or Fluka (Buchs, Switzerland), except where indicated.

Cell lines and cell culture

Two cell lines were used; HepG2 cells and HepaRG cells. HepG2 cells were provided by ATCC (Manassas, USA) and cultured either in low-glucose or galactose-containing media. Highly proliferative cells normally generate ATP via glycolysis despite fully functional mitochondria (Crabtree effect), when they are fed with glucose. Substitution of glucose with galactose forces the cells to produce ATP mainly via mitochondrial oxidative phosphorylation, thereby rendering the cells more susceptible to mitochondrial toxicants (Marroquin et al. 2007). Low-glucose containing medium was prepared with Dulbecco's Modified Eagle Medium (DMEM) containing 1.0 g/L glucose, 4 mM L-glutamine, and 1 mM pyruvate from Invitrogen (Basel, Switzerland). The medium was further supplemented with 10% (v/v) heat-inactivated fetal calf serum, 2 mM GlutaMax, 10 mM HEPES buffer, and non-essential amino acids. Galactose supplemented media was composed of glucose-free Dulbecco's Modified Eagle Medium containing 4 mM L-glutamine, and supplemented with 10 mM galactose, L-Glutamine 200mM, HEPES buffer solution 1 M, sodium pyruvate 100 mM, and penicillin/streptomycin 10000 U/ml.

HepaRG cells were obtained from Dr. Christiane Guguen-Guillouzo (Rennes, France) and cultured as described (Aninat et al. 2006). These cells were cultured in the presence of glucose.

Cell culture supplements were all purchased from GIBCO (Paisley, UK). We kept the cells at 37 °C in a humidified 5% CO_2 cell culture incubator. A Neubauer hemacytometer was used to determine the cell number and viability using the trypan blue exclusion method.

Mouse liver mitochondria

Male C57BL/6 mice were kept in the animal facility of the University Hospital Basel (Basel, Switzerland) in a temperature-controlled environment with a 12-h light/dark cycle and food and water *ad libitum*. Animal procedures were conducted in accordance with the institutional guidelines for the care and use of laboratory animals. The mean mouse weight was 25±2 g and the mean liver weight 1.3±0.1 g. Mice were sacrificed by cervical dislocation. Fresh liver tissue was quickly removed and immersed in ice-cold isolation buffer (200mM mannitol, 50mM sucrose, 1mM Na_4EDTA, 20 mM HEPES, pH 7.4) and isolated by differential centrifugation as described previously (Hoppel et al. 1979). The mitochondrial protein content was determined using the bicinchoninic acid (BCA) protein assay kit from Thermo Scientific (Wohlen, Switzerland).

Cytotoxicity

Cells were seeded at 20,000 cells/well in a 96-well plate 24 h prior drug treatment. We used the ToxiLight® (Lonza, Basel, Switzerland) assay to determine the cytotoxicity of different concentrations (1, 5, 10, 20, 50, and 100 µM) and treatment times (24 h and 48 h) of the azoles indicated. We used Triton X 0.1% as a positive control. The release of adenylate kinase was measured according to the manufacturer's instructions. Briefly, ToxiLight® reaction buffer (100 µL) was mixed with 20 µL of supernatant from the treated cells. Then, the mixture was left in the dark for 5 min and the luminescence was measured with a Tecan M200 Pro Infinity plate reader (Männedorf, Switzerland).

Intracellular ATP content

Cells were seeded at 20,000 cells/well in a 96-well plate. HepG2 cells were then treated with

azoles at different concentrations (1, 5, 10, 20, 50, and 100 µM) and incubation times (24 h and 48 h). Intracellular ATP was determined using the CellTiterGlo Luminescent cell viability assay (Promega, Switzerland), in accordance with the manufacturer's instructions. Briefly, 100 µL of assay buffer was added to each 96-well containing 100 µL culture medium. After incubation in the dark for 12 min, luminescence was measured using a Tecan M200 Pro Infinity plate reader.

Mitochondrial membrane potential in cells and isolated liver mitochondria

HepG2 cells were seeded in a 12-well plate at 500,000 cells/well 24 h prior exposure to azoles at the concentrations indicated. The mitochondrial membrane potential was assessed using the fluorescent cationic dye TMRM from Life Technologies (Zug, Switzerland). First, cells were trypsinized after the indicated incubation time and the cell pellet resuspended in DPBS. TMRM was dissolved in DMSO, and added to resuspended cells at a final concentration of 50 nM. Cells were incubated on a shaker at 37°C for 20 minutes in the dark. Afterwards, cells were centrifuged and the pellet resuspended in DPBS. Samples were measured by flow cytometry (BD FACSCalibur™, Becton Dickinson AG, Allschwil, Switzerland) on the FL2-H channel. FCCP (10 µM) was added to control cells and served as positive control. Data were analyzed using CellQuest Pro software (BD Bioscience, Allschwil, Switzerland).

The mitochondrial membrane potential in isolated mouse liver mitochondria was determined as described by Kaufmann *et al.* (Kaufmann et al. 2005) with some modifications. Freshly isolated mouse liver mitochondria were washed with incubation buffer containing 137 mM sodium chloride, 4.74 mM potassium chloride, 2.56 mM calcium chloride, 1.18 mM potassium phosphate, 1.18 mM magnesium chloride, 10 mM HEPES, and 1 g/l glucose (pH 7.4). Then, mitochondria were incubated at 37°C in incubation buffer containing 0.5 µl/ml [phenyl-^{3}H]-tetraphenylphosphonium bromide (^{3}H-TPP; 40 Ci/mmol, Anawa trading SA, Wangen, Switzerland). After 15 min, the suspension was centrifuged and the mitochondrial pellet resuspended in fresh nonradioactive incubation buffer. Afterwards, mitochondria were

treated with drugs at concentrations indicated for 15min at 37°C and centrifuged. After the incubation, radioactivity of the mitochondrial pellet was measured on a Packard 1900 TR liquid scintillation analyzer.

Activities of the enzyme complexes of the mitochondrial electron transport chain in permeabilized cells and isolated mouse liver mitochondria

The activity of specific enzyme complexes of the respiratory chain was analyzed using an Oxygraph-2k high-resolution respirometer equipped with DatLab software (Oroboros Instruments, Innsbruck, Austria). HepG2 cells were seeded in T75 cell culture flasks and treated for 24 h with ketoconazole or posaconazole at the concentrations and periods of time indicated in the Result section. Then, the trypsinized HepG2 cells or freshly isolated mouse liver mitochondria were resuspended in MiR06 (mitochondrial respiration medium containing 0.5 mM EGTA, 3 mM $MgCl_2$, 60 mM K-lactobionate, 20 mM taurine, 10 mM KH_2PO_4, 20 mM HEPES, 110 mM sucrose, 1 g/L fatty acid-free bovine serum albumin (BSA), and 280 U/ml catalase, pH7.1) before being transferred to the pre-calibrated oxygraph chambers.

The activities of complexes I, II, III and IV were assessed in fresh mouse liver mitochondria and HepG2 cells permeabilized with digitonin (10µg/1 million cells). In a first run, complexes I and III were analyzed using L-glutamate/malate (10 and 5 mM respectively) as substrates followed by the addition of ADP (2 mM). Then, the oxidative leak, a marker for uncoupling, was identified by the assessment of the residual oxygen consumption after addition of oligomycin (1 µM). We elucidated the uncoupling capacity with the addition of FCCP (1 µM) followed by inhibition of complex I with rotenone (0.5 µM). Afterwards, duroquinol (500µM, Tokyo Chemical Industry, Tokyo, Japan) was added to investigate complex III and inhibited with antimycin A (2.5 µM). In a second run, complexes II and IV were analyzed using succinate (10 mM) as substrate in the presence of rotenone (0.5 µM) to block complex I. This was followed by the addition of ADP (2 mM). Again, the oxidative leak was identified by the assessment of the residual oxygen consumption after addition of oligomycin (1 µM), followed by the addition of FCCP (1 µM) in order to evaluate the uncoupling capacity. After this, the inhibitor antimycin A (2.5 µM) was added to block complex III . Subsequently, N,N,N',N'-

tetramethyl-p-phenylenediamine (TMPD)/ascorbate (0.5 mM and 2 mM respectively) were added to investigate complex IV followed by an inhibition of this complex with KCN (1 mM). To assure the integrity of the outer mitochondrial membrane, the absence of a stimulatory effect of exogenous cytochrome c (10 µM) on respiration was shown. We used the Pierce bicinchoninic acid protein assay kit from Thermo Scientific (Darmstadt, Germany) to determine the protein concentrations. Respiration rates are expressed in picomoles O_2 per second per mg protein.

Mitochondrial superoxide anion accumulation

Mitochondrial superoxide anion production was determined with the fluorogenic dye MitoSOX™ Red reagent (Molecular Probes, Eugene, OR, USA). Cells were seeded at 25,000 cells/well in a 96-well plate. After 24 h of treatment with azoles at the concentrations indicated, the medium was removed and the HepG2 cells stained with MitoSOX red (dissolved in DPBS) at a final concentration of 2 µM. We used amiodarone 50 µM as a positive control. The plate was incubated in the dark at 37°C for 15 min, afterwards fluorescence was measured at an excitation wavelength of 510 nm and an emission wavelength of 580 nm using a Tecan Infinite pro 200 microplate reader. We normalized the results to the protein content using the Pierce BCA Protein Assay Kit (Darmstadt, Germany) according to manufacturer's instruction.

Quantitative RT-PCR

Cells were seeded in 12-well plates 24 h prior treatment. After 24 h of incubation with the compounds indicated, cells were lysed with 350 uL of RLT buffer (Qiagen, Hombrechtikon, Switzerland) and the cell lysate was transferred to Qiashredder columns and spinned for 2 min at 13,000 rpm. From the eluate, total RNA was extracted according to the manufacturer's protocol (Qiagen RNeasy Mini Extraction kit). We assessed the RNA quality with a NanoDrop 2000 (Thermo Scientific, Wohlen, Switzerland). The Qiagen Omniscript system was used to reversely transcribe the isolated RNA (1 ug) to cDNA. For quantitative real-time RT-PCR, 10

ng cDNA was used. The expression of mRNA was evaluated using SYBR Green real-time PCR (Roche Diagnostics, Rotkreuz, Basel). Real-time RT-PCR was performed in triplicate on an ABI PRISM 7700 sequence detector (PE Biosystems, Rotkreuz, Switzerland) and quantification was carried out using the comparative-threshold cycle method. Forward and reverse primers for genes of interest and GAPDH as endogenous reference control (see Table 1 for primers) were purchased from Microsynth (Balgach, Switzerland).

Protein extraction and western blot analysis

Cells were seeded in 6-well plates at 10^6 cells per well, 24 h prior treatment with ketoconazole and posaconazole. After 24 h of incubation with the compounds indicated, cells were washed with ice-cold PBS and lysed with RIPA buffer (50 nM Tris-HCL, pH 7.4, 150 mM NaCl, 1% Triton X-100, 0.5% sodium deoxycholate, 0.1% sodium dodecyl sulfate, and 1 mM EDTA in water). Lysates were incubated with RIPA buffer under constant agitation for 20 min and then centrifuged at 13,000 rpm for 10 min at 4 °C. After determining the protein content with a Pierce BCA Protein Assay Kit (Darmstadt, Germany) according to the manufacturer's instructions, we separated 15 µg protein on 4-12% bis-tris gradient gels (Invitrogen, CA, U.S.A), and transferred them to polyvinyli- den difluoride membranes (Bio-rad, CA, U.S.A). Membranes were blocked with 5% nonfat dry milk in phosphate buffered saline (PBS) (Gibco, Paisley, UK) containing 0.1% Tween-20 (PBS-T) (Sigma-Aldrich, MO, USA) for 1 h at room temperature before the overnight incubation with the relevant primary antibody (Cell Signaling Technology, USA) diluted 1:1000 in blocking buffer. The day after, blots were incubated for 1 h with peroxidase-labeled secondary antibody (Santa Cruz Biotechnology, Danvers, U.S.A) diluted 1:2000 in 5% nonfat milk in PBS-T. Then, we washed the membranes and developed the immunoreactive bands using enhanced chemiluminescence (GE Healthcare, Little Chalfont, UK). We scanned the chemiluminescent images with a HP Scanjet 8300 (Hewlett-Packard Co., Palo Alto, CA) and quantified band intensities of the scanned images with the National Institutes of Health Image J program (version 1.41). To correct for loading differences, the scanning units obtained from the

probed proteins were divided by the scanning units obtained from the respective housekeeping protein GAPDH. Following primary antibodies were used: SOD2 (Cell signaling technology, Danvers, U.S.A), SIRT3 (Cell signaling technology, Danvers, U.S.A), caspase 9 (Cell signaling technology, Danvers, U.S.A), PARP (Cell signaling technology, Danvers, U.S.A), caspase 3 (Abcam, Cambridge, UK), and GAPDH (Abcam, Cambridge, UK).

Mitochondrial DNA content

As a measure of the mitochondrial DNA content, we determined the ratio of the DNA content of the mitochondrial gene ND1 and the nuclear gene 36B4 (see Table 1 for primers) using quantitative real-time RT-PCR as described with some modifications (Pieters et al. 2013). Total DNA was extracted using the DNeasy Blood and Tissue Kit (Qiagen, Hombrechtikon, Switzerland) following the manufacturer's instructions. The concentration of the extracted DNA was measured spectrophotometrically at 260 nm with the NanoDrop 2000 (Thermo Scientific, Wohlen, Switzerland). Afterwards, DNA was diluted in RNase free water to a final concentration of 10 ng/µL. The expression of the mitochondrial and nuclear genes was evaluated using SYBR Green real-time PCR (Roche Diagnostics, Rotkreuz, Basel) and was performed on an ABI PRISM 7700 sequence detector (PE Biosystems, Rotkreuz, Switzerland). Quantification was performed using the comparative-threshold cycle method.

Statistical Methods

Data are given as the mean ± standard deviation (SD) of at least three independent experiments. Statistical analyses were performed using GraphPad Prism 6 (GraphPad Software, La Jolla, CA, US). One-way analysis of variance (ANOVA) was used for comparisons of more than two groups, followed by Dunnett's post-test procedure to localize differences between the individual groups tested. Nonparametric tests were used in case of not normally distributed data. P-values <0.05 were considered as significant.

Results

Cytotoxicity and intracellular ATP content in azole-treated HepG2 cells

To elucidate the toxic effects of the four investigated azoles (ketoconazole, posaconazole, fluconazole, and voriconazole), we first assessed cytotoxicity and cellular ATP content in HepG2 cells exposed at different concentrations for two time periods (24 and 48 h) in low glucose and galactose media. After 24 h of treatment, we found an increase in adenylate kinase release in ketoconazole and posaconazole treated HepG2 cells in low glucose medium at concentrations starting from 20 µM, whereas fluconazole or voriconazole were not cytotoxic up to 100 µM (Fig. 1A). In the presence of galactose, fluconazole and voriconazole were again not cytotoxic up to 100 µM, whereas the cytotoxicity of ketoconazole and posaconazole was qualitatively similar to the glucose medium but quantitatively more accentuated (Fig. 1B). Similar to cytotoxicity, the intracellular ATP content of HepG2 cells cultured with low-glucose started to decrease at 10 µM in the presence of ketoconazole or posaconazole but was not affected by fluconazole or voriconazole (Fig.1C). In the presence of galactose, the cellular ATP content started to decrease already at 5 µM ketoconazole or posaconazole but was again not affected by fluconazole or voriconazole (Fig. 1D).

After an incubation time of 48 h in low glucose media, fluconazole and voriconazole were not cytotoxic and did not decrease the cellular ATP content up to a concentration of 100 µM (supplementary figure 2A and B). In contrast, ketoconazole started to be cytotoxic at 50 µM, and posaconazole and ketoconazole started to decrease the cellular ATP content at 5 and 10 µM, respectively (suppl. Fig. 2A and B).

In order to find out if metabolites could be responsible for the observed cytotoxicity, we conducted cytotoxicity studies in HepaRG cells in low glucose media under basal conditions and after CYP induction with rifampicin. After 24 h of incubation, there was no cytotoxicity associated with voriconazole and fluconazole up to 100 µM, whereas posaconazole and ketoconazole started to show cytotoxicity at 20 and 100 µM, respectively, and started to decrease the cellular ATP content at 100 µM (suppl. Fig. 3A and B). CYP induction by

rifampicin accentuated cytotoxicity for both ketoconazole and posaconazole but did not significantly affect ATP depletion in the presence of these toxicants.

The comparison of cytotoxicity in the presence of low-glucose or galactose in HepG2 cells revealed that ketoconazole and posaconazole were more toxic under galactose conditions. Since the presence of galactose forces cells to produce ATP with oxidative phosphorylation (and not with glycolysis), we focused on mitochondrial toxicity.

Acute effects on isolated mouse liver mitochondria and long-term effects on mitochondria in HepG2 cells

The mitochondrial membrane potential ($\Delta\psi_m$) reflects the electrical potential across the inner mitochondrial membrane which is mainly generated by the proton gradient between the mitochondrial matrix and the intermembrane space. Mitochondrial toxicants are expected to be associated with a decrease $\Delta\psi_m$, which can therefore be used as a marker of mitochondrial function and integrity (Felser et al. 2013; Kaufmann et al. 2005).

We determined $\Delta\psi_m$ using the fluorescent probe TMRM which accumulates in mitochondria depending on $\Delta\psi_m$ (Perry et al. 2011). Acute exposure (15 min) of freshly isolated mouse liver mitochondria with ketoconazole resulted in a 30% decrease in $\Delta\psi_m$ starting at 5 µM, whereas posaconazole did not affect $\Delta\psi_m$ under these conditions (Fig. 2A).

In HepG2 cells exposed for 24 h in low glucose medium, posaconazole decreased $\Delta\psi_m$ in a dose-dependent manner starting at 10 µM, whereas ketoconazole decreased $\Delta\psi_m$ already at 5 µM. However, we did not find any changes in $\Delta\psi_m$ in incubations with fluconazole or voriconazole (Fig. 2B). These results confirmed mitochondrial toxicity of ketoconazole and posaconazole and the lack of cytotoxicity of voriconazole and fluconazole.

In order to find out the reason for impaired $\Delta\psi_m$, we next investigated the function of the electron transport chain by high-resolution respirometry. Acute treatment (15 min) of isolated mouse liver mitochondria with ketoconazole revealed a significant inhibition of complex I activity at concentrations starting from 20 µM (Fig. 2C). In HepG2 cells grown under low glucose conditions and treated for 24 h, ketoconazole significantly reduced the activities of all

enzyme complexes starting at 20 µM (complex III) or 50 µM (complex I, II and IV) (Fig.2D). Under the same conditions, posaconazole reduced complex III starting at 20 µM and complex I activity at 50 µM (Fig.2E).

Possible mechanisms leading to impaired function of the electron transport chain

Since a decrease in mtDNA can be associated with impaired mitochondrial protein synthesis and therefore impaired activity of complexes I, III and/or IV (Jiang et al. 2013), we investigated the mtDNA/nuclear DNA ratio. As shown in Fig. 3A, 24 h of treatment with ketoconazole or posaconazole was associated with a numerical increase in the mtDNA/nuclear DNA ratio (without reaching statistical significance), excluding this possibility. In addition to the mtDNA/nuclear DNA ratio, we also studied expression of SIRT3. SIRT3 is a NAD^+- dependent deacetylase which regulates expression and function of mitochondrial proteins by its deacetylase activity (Houtkooper et al. 2012). Incubation with 10 µM ketoconazole or posaconazole for 24h was associated with a significantly increased mRNA expression of SIRT3, whereas increasing drug concentrations (up to 50 µM) resulted in a numerically decreased SIRT3 mRNA expression (Fig.3B). In contrast to mRNA expression, the protein content of SIRT3 was almost identical to control incubations at 10 and 20 µM and showed a numerical decrease without statistical significance at 50 µM ketoconazole or posaconazole (50 µM) (Fig. 3C and D). Impaired activity of SIRT3 is therefore also an unlikely reason for the observed decrease in enzyme complexes of the electron transport chain.

Superoxide anion accumulation

As complexes I and III of the electron transport chain are the main sites of mitochondrial superoxide anion generation (Balaban et al. 2005), we examined the accumulation of superoxide anion in HepG2 cells exposed to azoles for 24 h in glucose and galactose media. As expected, we found a significantly increased superoxide accumulation when cells were treated with ketoconazole or posaconazole, but not with voriconazole or fluconazole. Under

low-glucose conditions, treatment with ketoconazole was associated with a 1.5-fold to 2-fold increase in superoxide accumulation at concentrations from 20 to 100 µM. With posaconazole, superoxide accumulation increased 3-fold compared to control conditions between 10 and 100 µM (Fig. 4A). Similar results were found in galactose-treated HepG2 cells, but the accumulation was by trend more accentuated than in the presence of glucose (Fig. 4B).

Since SOD2 is a mitochondrial enzyme engaged superoxide anion degradation (Felser et al. 2013), it was interesting to study its mRNA expression in the presence ketoconazole and posaconazole. As shown in Fig. 4C, both ketoconazole and posaconazole significantly increased the mRNA expression of SOD2 starting at 10 µM. For ketoconazole, higher concentrations were associated with a numerical increase in SOD2 mRNA expression only, whereas posaconazole increased the mRNA expression of SOD2 up to 50 µM. In contrast to the mRNA content, the protein expression of SOD2 was not significantly different to control incubations (Fig. 4D).

Mechanisms of cell death in HepG2 cells

When oxidative stress overcomes the cellular defense mechanisms it starts to damage proteins, lipids and DNA and can induce apoptosis (Roberts et al. 2010). In order to find out whether HepG2 cell death associated with ketoconazole and posaconazole is induced by apoptosis, we examined several important markers of apoptosis. As shown in fig. 5A, we found a concentration-dependent, significant increase of the Bax/Bcl2 ratio in posaconazole-treated HepG2 cells. 10 µM posaconazole increased the Bax/Bcl-2 ratio 1.5-fold, and 20 µM and 50 µM were associated with a 2.5-fold and a 3-fold increase, respectively. In contrast, ketoconazole treatment showed only a numerical increase of this ratio, which did not reach statistical significance. In addition, we analyzed the protein expression of three key mediators of apoptosis (Fig. 5B). Treatment with ketoconazole and posaconazole for 24h was associated with concentration-dependent increases of cleaved caspase 9, cleaved caspase 3 and PARP, proving that both azoles tested induce apoptosis.

Cytotoxicity in HepG2 cells with mitochondrial dysfunction

The current toxicological characterization revealed a mitochondrially-mediated toxicity of ketoconazole and posaconazole starting at 5 to 10 µM, but not of fluconazole or voriconazole up to 100 µM. In order to test the hypothesis that a pre-existing mitochondrial deficiency renders cells more susceptible to mitochondrial toxicants, we investigated ketoconazole and posaconazole on a previously established system of mitochondrial dysfunction (Hägler et al. 2015). First, we pre-treated HepG2 cells cultured in galactose with non-toxic concentrations of the vitamin B12 analog HCCL or the combination of HCCL and propionic acid (PA) for 4 days, then for 24 h with 10 and 20 µM ketoconazole or 10 and 20 µM posaconazole. As shown in Fig. 6, HepG2 cells pretreated with HCCL or the combination HCCL/PA exposed to 10 or 20 µM posaconazole showed a more accentuated cytotoxicity (adenylate kinase release) (Fig. 6A and 6C) or drop in cellular ATP (Fig. 6B and 6D) than control cells (DMSO 0.1%) or HepG2 cells treated with posaconazole only. As shown in suppl. Fig. 4, similar results regarding cytotoxicity (suppl. Fig. 4A and C) and cellular ATP content (suppl. Fig. 4B and D) were obtained in the presence of 10 or 20 µM ketoconazole.

Discussion

Our investigations revealed that two of the four azoles investigated, the imidazole ketoconazole and the most newly launched triazole posaconazole, are potent inhibitors of important mitochondrial functions. Exposure of HepG2 cells with these azoles was associated with decreased mitochondrial membrane potential, impaired function of the mitochondrial electron transport chain, increased mitochondrial oxidative stress with activation of the antioxidant system and cytotoxicity due to apoptosis. In comparison, fluconazole and voriconazole were not toxic up to 100 µM in both human hepatoma cell lines used.

In contrast to the findings in the current study, which revealed no cytotoxicity for fluconazole and voriconazole, there are reports of hepatotoxicity in the literature for both compounds (Bronstein et al. 1997; Foo and Gottlieb 2007; Kao et al. 2014; Raschi et al. 2014). Fluconazole is mainly eliminated unchanged by the kidneys (Lewis 2011), while voriconazole undergoes extensive hepatic metabolism by CYP2C19, CYP2C9 and CYP3A4, leading to N-oxidation of the pyrimidine ring (Hyland et al. 2003). Since rifampicin induces CYPs in HepaRG cells (Gerets et al. 2012), an increased formation of the voriconazole N-oxide metabolite could have been expected under the conditions used in our experiments. Since cytotoxicity of voriconazole did not increase in rifampicin-treated HepaRG cells, voriconazole N-oxide may not be responsible for hepatotoxicity associated with voriconazole. This conclusion must be made with caution, however, since we did not determine voriconazole N-oxide and voriconazole itself showed no cytotoxicity in both cell systems used in the current studies. It is therefore possible that our in vitro systems were not suitable to detect hepatocellular toxicity associated with voriconazole and/or its major metabolite voriconazole N-oxide. For instance, these systems are not able to detect immune-mediated toxicity. Our data do agree, however, with a recent study from Somchit et al. (Somchit et al. 2012), who observed no relevant hepatic or renal toxicity in rats treated with single (up to 200 mg/kg) or repetitive doses (14 days up to 100 mg/kg) of voriconazole intraperitoneally.

Regarding fluconazole, the data of the current study are in agreement with a previous study in which fluconazole up to 1 mM was only marginally cytotoxic for primary rat hepatocytes (Rodriguez and Acosta 1995). Since fluconazole is excreted almost entirely unchanged by the kidneys (Lewis 2011), it could be expected that CYP induction by rifampicin would not increase fluconazole-associated toxicity in HepaRG cells.

As shown in Fig. 1, posaconazole and ketoconazole were by trend more toxic in cell cultures containing galactose as compared to glucose. In addition, in HepG2 cells the cellular ATP content dropped already at lower posaconazole and ketoconazole concentrations than cytotoxicity was detectable. Both of these findings suggested mitochondrial toxicity of these compounds. For ketoconazole, this has already been demonstrated in isolated rat liver

mitochondria (Rodriguez and Acosta 1996). We not only could confirm these data in HepG2 cells, but, in addition, we could also demonstrate the consequences on cell metabolism and survival.

Regarding ketoconazole, hepatocellular toxicity has been shown for the parent compound (Rodriguez and Acosta 1995) as well as for the N-deacetylated main metabolite (Rodriguez and Acosta 1997b). N-deacetyl-ketoconazole can be N-oxidized at the piperazine ring by flavin-containing monooxygenases (FMO) (Rodriguez and Acosta 1997a; Rodriguez and Miranda 2000; Rodriguez et al. 1999) and this N-oxide is also considered to be hepatotoxic (Rodriguez and Buckholz 2003). In the current study, we used the parent compound, not the N-deacetylated metabolite. Since hydrolases are ubiquitous enzymes, it can be assumed that N-deacetylation occurred in the cell models used by us. In addition, it has recently been shown that FMO1 and FMO3, the most important human enzymes for N-deacetyl-ketoconazole oxidation (Rodriguez and Miranda 2000), are functionally expressed in HepG2 cells (Fedejko-Kap et al. 2011). It can therefore be assumed that at least some of the toxicity by ketoconazole observed in the current study has been due to N-deacetyl-ketoconazole N-oxide. However, since FMOs are induced via activation of the hydrocarbon receptor (Celius et al. 2010; Celius et al. 2008), which is only weakly stimulated by rifampicin (Derungs et al. 2015), it is unlikely that increased cytotoxicity following treatment with rifampicin is explained by increased activity FMOs. As shown recently, a substantial portion of ketoconazole is also metabolized by CYP3A4 (Fitch et al. 2009), which is highly induced by rifampicin in HepaRG cells (Gerets et al. 2012). Our data therefore suggest that CYP3A4-associated metabolites of voriconazole can be cytotoxic in HepaRG cells.

The concentration-dependent hepatocellular toxicity of posaconazole is an important finding of our study. Posaconazole has been associated with liver injury in patients (Raschi et al. 2014), but there are fewer reports in the literature than for ketoconazole or voriconazole. In the current study, posaconazole decreased the cellular ATP content and the mitochondrial membrane potential after treatment for 24 h, impaired the function of complex I and III of the electron transport chain, increased mitochondrial reactive oxygen species (ROS) production

and SOD2 mRNA expression, and was associated with apoptosis. The increase in mitochondrial ROS production is most likely a consequence of the inhibition of complex I and III of the respiratory chain (Sinha et al. 2013) and a likely reason for SOD2 mRNA induction (Felser et al. 2013). Since mitochondrial accumulation of ROS is associated with mitochondrial membrane permeability transition (Balaban et al. 2005; Kaufmann et al. 2005), increased ROS production is also a likely reason for apoptotic cell death observed in HepG2 cells.

Our studies did not reveal a clear mechanism for the decrease in the activity of the enzyme complexes of the electron transport chain. We could exclude a decrease in mtDNA and also a decreased protein expression of SIRT3. For ketoconazole, which was acutely toxic on isolated mouse liver mitochondria (see Fig. 2A and 2C), a direct inhibition of complex I with subsequent stimulation ROS production, which can further impair the function of complex I and possibly of other enzyme complexes, is a likely mechanism.

Regarding posaconazole, it is interesting to compare the concentrations associated with hepatocellular toxicity with those obtained in patients. The recommended trough serum concentration for prophylaxis in immunocompromised patients is 700 µg/L (1 µM) and 1000 µg/L in patients with manifest fungal infection (Ashbee et al. 2014). In a recent study comparing serum steady state serum concentrations in patients ingesting either 600 mg posaconazole as a suspension or 300 mg posaconazole as retarded tablets, average concentrations of 390 µg/L (range 51 – 1870 µg/L) or 1781 µg/L (range 662 – 3350 µg/L) for suspension or tablets, respectively, were determined (Cumpston et al. 2015). In the tablet group, the patient with the highest steady state serum concentration (3350 µg/L, corresponding to approximately 5 µM) developed hepatocellular liver injury. At a concentration of 5 µM, we started to see hepatocellular injury in the presence of galactose (see Fig. 1), which forces the cells to produce ATP by the mitochondrial respiratory chain and not by glycolysis. This comparison shows that potentially hepatotoxic concentrations can be reached in vivo.

In the publication of Cumpston et al. (Cumpston et al. 2015) a second patient developed liver injury. This patient had a steady serum concentration of 390 µg/L (approximately 0.6 µM), which is approximately ten times lower than the lowest concentration at which we started to observe toxicity, suggesting the existence of susceptibility factors for posaconazole-associated toxicity. For mitochondrial toxicants, mitochondrial dysfunction is considered to be an important susceptibility factor for idiosyncratic toxicity (Krahenbuhl et al. 2000; Li et al. 2015; Stewart et al. 2010). We have established a hepatocyte model with a subtle damage of enzyme complexes of the mitochondrial electron transport chain which can be used as a tool to detect idiosyncratic toxicity of mitochondrial toxicants (Hägler et al. 2015). After having demonstrated that ketoconazole and posaconazole are mitochondrial toxicants, it was therefore interesting to investigate these two compounds in this cell model. Indeed, we could show that pretreatment with HCCL with or without propionate rendered HepG2 cells more sensitive to the toxic effects of posaconazole and also ketoconazole. Our results therefore support the hypothesis that certain susceptibility factors, such as preexisting defects in mitochondrial function, can be a triggering event for the manifestation of cellular and organ toxicity at drug concentrations which are not toxic in the absence of such factors.

In conclusion, our study confirms the mitochondrial toxicity of ketoconazole and shows the consequences of this toxicity for mitochondria and hepatocytes. Furthermore, we provide evidence for a similar toxicity associated with posaconazole and show that cytotoxicity is increased in a cell model with impaired mitochondrial function. Our studies are therefore relevant for the understanding of the toxicological mechanisms associated with idiosyncratic toxicants.

Literature

Aninat C, Piton A, Glaise D, et al. (2006) Expression of cytochromes P450, conjugating enzymes and nuclear receptors in human hepatoma HepaRG cells. Drug metabolism and disposition: the biological fate of chemicals 34(1):75-83 doi:10.1124/dmd.105.006759

Ashbee HR, Barnes RA, Johnson EM, Richardson MD, Gorton R, Hope WW (2014) Therapeutic drug monitoring (TDM) of antifungal agents: guidelines from the British Society for Medical Mycology. The Journal of antimicrobial chemotherapy 69(5):1162-76 doi:10.1093/jac/dkt508

Balaban RS, Nemoto S, Finkel T (2005) Mitochondria, oxidants, and aging. Cell 120(4):483-95 doi:10.1016/j.cell.2005.02.001

Bercoff E, Bernuau J, Degott C, et al. (1985) Ketoconazole-induced fulminant hepatitis. Gut 26(6):636-8

Bronstein JA, Gros P, Hernandez E, Larroque P, Molinie C (1997) Fatal acute hepatic necrosis due to dose-dependent fluconazole hepatotoxicity. Clinical infectious diseases : an official publication of the Infectious Diseases Society of America 25(5):1266-7

Castelli MV, Butassi E, Monteiro MC, Svetaz LA, Vicente F, Zacchino SA (2014) Novel antifungal agents: a patent review (2011 - present). Expert opinion on therapeutic patents 24(3):323-38 doi:10.1517/13543776.2014.876993

Celius T, Pansoy A, Matthews J, et al. (2010) Flavin-containing monooxygenase-3: induction by 3-methylcholanthrene and complex regulation by xenobiotic chemicals in hepatoma cells and mouse liver. Toxicology and applied pharmacology 247(1):60-9 doi:10.1016/j.taap.2010.05.018

Celius T, Roblin S, Harper PA, et al. (2008) Aryl hydrocarbon receptor-dependent induction of flavin-containing monooxygenase mRNAs in mouse liver. Drug metabolism and disposition: the biological fate of chemicals 36(12):2499-505 doi:10.1124/dmd.108.023457

Cronin S, Chandrasekar PH (2010) Safety of triazole antifungal drugs in patients with cancer. The Journal of antimicrobial chemotherapy 65(3):410-6 doi:10.1093/jac/dkp464

Cumpston A, Caddell R, Shillingburg A, et al. (2015) Superior Serum Concentrations with Posaconazole Delayed-Release Tablets Compared to Suspension Formulation in Hematological Malignancies. Antimicrobial agents and chemotherapy 59(8):4424-8 doi:10.1128/aac.00581-15

Derungs A, Donzelli M, Berger B, Noppen C, Krahenbuhl S, Haschke M (2015) Effects of Cytochrome P450 Inhibition and Induction on the Phenotyping Metrics of the Basel Cocktail: A Randomized Crossover Study. Clinical pharmacokinetics doi:10.1007/s40262-015-0294-y

Egunsola O, Adefurin A, Fakis A, Jacqz-Aigrain E, Choonara I, Sammons H (2013) Safety of fluconazole in paediatrics: a systematic review. European journal of clinical pharmacology 69(6):1211-21 doi:10.1007/s00228-012-1468-2

Fedejko-Kap B, Niemira M, Radominska-Pandya A, Mazerska Z (2011) Flavin monooxygenases, FMO1 and FMO3, not cytochrome P450 isoenzymes, contribute to metabolism of anti-tumour triazoloacridinone, C-1305, in liver microsomes and HepG2

cells. Xenobiotica; the fate of foreign compounds in biological systems 41(12):1044-55 doi:10.3109/00498254.2011.604743

Felser A, Blum K, Lindinger PW, Bouitbir J, Krahenbuhl S (2013) Mechanisms of hepatocellular toxicity associated with dronedarone--a comparison to amiodarone. Toxicological sciences : an official journal of the Society of Toxicology 131(2):480-90 doi:10.1093/toxsci/kfs298

Fitch WL, Tran T, Young M, Liu L, Chen Y (2009) Revisiting the metabolism of ketoconazole using accurate mass. Drug metabolism letters 3(3):191-8

Foo H, Gottlieb T (2007) Lack of cross-hepatotoxicity between voriconazole and posaconazole. Clinical infectious diseases : an official publication of the Infectious Diseases Society of America 45(6):803-5 doi:10.1086/521174

Garcia Rodriguez LA, Duque A, Castellsague J, Perez-Gutthann S, Stricker BH (1999) A cohort study on the risk of acute liver injury among users of ketoconazole and other antifungal drugs. British journal of clinical pharmacology 48(6):847-52

Gerets HH, Tilmant K, Gerin B, et al. (2012) Characterization of primary human hepatocytes, HepG2 cells, and HepaRG cells at the mRNA level and CYP activity in response to inducers and their predictivity for the detection of human hepatotoxins. Cell biology and toxicology 28(2):69-87 doi:10.1007/s10565-011-9208-4

Greenblatt HK, Greenblatt DJ (2014) Liver injury associated with ketoconazole: review of the published evidence. Journal of clinical pharmacology 54(12):1321-9 doi:10.1002/jcph.400

Hägler P, Grünig D, Berger B, Krähenbühl S, Bouitbir J (2015) Impaired mitochondrial function in HepG2 cells treated with hydroxy-cobalamin[c-lactam]: a cell model for idiosyncratic toxicity. Toxicology in press

Hoppel C, DiMarco JP, Tandler B (1979) Riboflavin and rat hepatic cell structure and function. Mitochondrial oxidative metabolism in deficiency states. The Journal of biological chemistry 254(10):4164-70

Houtkooper RH, Pirinen E, Auwerx J (2012) Sirtuins as regulators of metabolism and healthspan. Nature reviews Molecular cell biology 13(4):225-38 doi:10.1038/nrm3293

Hyland R, Jones BC, Smith DA (2003) Identification of the cytochrome P450 enzymes involved in the N-oxidation of voriconazole. Drug metabolism and disposition: the biological fate of chemicals 31(5):540-7

Jiang Z, Bao Q, Sun L, et al. (2013) Possible role of mtDNA depletion and respiratory chain defects in aristolochic acid I-induced acute nephrotoxicity. Toxicology and applied pharmacology 266(2):198-203 doi:10.1016/j.taap.2012.07.008

Kao WY, Su CW, Huang YS, et al. (2014) Risk of oral antifungal agent-induced liver injury in Taiwanese. British journal of clinical pharmacology 77(1):180-9 doi:10.1111/bcp.12178

Kathiravan MK, Salake AB, Chothe AS, et al. (2012) The biology and chemistry of antifungal agents: a review. Bioorganic & medicinal chemistry 20(19):5678-98 doi:10.1016/j.bmc.2012.04.045

Kaufmann P, Torok M, Hanni A, Roberts P, Gasser R, Krahenbuhl S (2005) Mechanisms of benzarone and benzbromarone-induced hepatic toxicity. Hepatology (Baltimore, Md) 41(4):925-35 doi:10.1002/hep.20634

Krahenbuhl S, Brandner S, Kleinle S, Liechti S, Straumann D (2000) Mitochondrial diseases represent a risk factor for valproate-induced fulminant liver failure. Liver 20(4):346-8

Lass-Florl C (2011) Triazole antifungal agents in invasive fungal infections: a comparative review. Drugs 71(18):2405-19 doi:10.2165/11596540-000000000-00000

Lewis RE (2011) Current concepts in antifungal pharmacology. Mayo Clinic proceedings 86(8):805-17 doi:10.4065/mcp.2011.0247

Li S, Guo J, Ying Z, et al. (2015) Valproic acid-induced hepatotoxicity in Alpers syndrome is associated with mitochondrial permeability transition pore opening-dependent apoptotic sensitivity in an induced pluripotent stem cell model. Hepatology (Baltimore, Md) 61(5):1730-9 doi:10.1002/hep.27712

Marroquin LD, Hynes J, Dykens JA, Jamieson JD, Will Y (2007) Circumventing the Crabtree effect: replacing media glucose with galactose increases susceptibility of HepG2 cells to mitochondrial toxicants. Toxicological sciences : an official journal of the Society of Toxicology 97(2):539-47 doi:10.1093/toxsci/kfm052

Perry SW, Norman JP, Barbieri J, Brown EB, Gelbard HA (2011) Mitochondrial membrane potential probes and the proton gradient: a practical usage guide. BioTechniques 50(2):98-115 doi:10.2144/000113610

Pieters N, Koppen G, Smeets K, et al. (2013) Decreased mitochondrial DNA content in association with exposure to polycyclic aromatic hydrocarbons in house dust during wintertime: from a population enquiry to cell culture. PLoS One 8(5):e63208 doi:10.1371/journal.pone.0063208

Raschi E, Poluzzi E, Koci A, Caraceni P, Ponti FD (2014) Assessing liver injury associated with antimycotics: Concise literature review and clues from data mining of the FAERS database. World journal of hepatology 6(8):601-12 doi:10.4254/wjh.v6.i8.601

Roberts RA, Smith RA, Safe S, Szabo C, Tjalkens RB, Robertson FM (2010) Toxicological and pathophysiological roles of reactive oxygen and nitrogen species. Toxicology 276(2):85-94 doi:10.1016/j.tox.2010.07.009

Rodriguez RJ, Acosta D, Jr. (1995) Comparison of ketoconazole- and fluconazole-induced hepatotoxicity in a primary culture system of rat hepatocytes. Toxicology 96(2):83-92

Rodriguez RJ, Acosta D, Jr. (1996) Inhibition of mitochondrial function in isolated rate liver mitochondria by azole antifungals. Journal of biochemical toxicology 11(3):127-31 doi:10.1002/(sici)1522-7146(1996)11:3<127::aid-jbt4>3.0.co;2-m

Rodriguez RJ, Acosta D, Jr. (1997a) Metabolism of ketoconazole and deacetylated ketoconazole by rat hepatic microsomes and flavin-containing monooxygenases. Drug metabolism and disposition: the biological fate of chemicals 25(6):772-7

Rodriguez RJ, Acosta D, Jr. (1997b) N-deacetyl ketoconazole-induced hepatotoxicity in a primary culture system of rat hepatocytes. Toxicology 117(2-3):123-31

Rodriguez RJ, Buckholz CJ (2003) Hepatotoxicity of ketoconazole in Sprague-Dawley rats: glutathione depletion, flavin-containing monooxygenases-mediated bioactivation and hepatic covalent binding. Xenobiotica; the fate of foreign compounds in biological systems 33(4):429-41 doi:10.1080/0049825031000072243

Krahenbuhl S, Brandner S, Kleinle S, Liechti S, Straumann D (2000) Mitochondrial diseases represent a risk factor for valproate-induced fulminant liver failure. Liver 20(4):346-8

Lass-Florl C (2011) Triazole antifungal agents in invasive fungal infections: a comparative review. Drugs 71(18):2405-19 doi:10.2165/11596540-000000000-00000

Lewis RE (2011) Current concepts in antifungal pharmacology. Mayo Clinic proceedings 86(8):805-17 doi:10.4065/mcp.2011.0247

Li S, Guo J, Ying Z, et al. (2015) Valproic acid-induced hepatotoxicity in Alpers syndrome is associated with mitochondrial permeability transition pore opening-dependent apoptotic sensitivity in an induced pluripotent stem cell model. Hepatology (Baltimore, Md) 61(5):1730-9 doi:10.1002/hep.27712

Marroquin LD, Hynes J, Dykens JA, Jamieson JD, Will Y (2007) Circumventing the Crabtree effect: replacing media glucose with galactose increases susceptibility of HepG2 cells to mitochondrial toxicants. Toxicological sciences : an official journal of the Society of Toxicology 97(2):539-47 doi:10.1093/toxsci/kfm052

Perry SW, Norman JP, Barbieri J, Brown EB, Gelbard HA (2011) Mitochondrial membrane potential probes and the proton gradient: a practical usage guide. BioTechniques 50(2):98-115 doi:10.2144/000113610

Pieters N, Koppen G, Smeets K, et al. (2013) Decreased mitochondrial DNA content in association with exposure to polycyclic aromatic hydrocarbons in house dust during wintertime: from a population enquiry to cell culture. PLoS One 8(5):e63208 doi:10.1371/journal.pone.0063208

Raschi E, Poluzzi E, Koci A, Caraceni P, Ponti FD (2014) Assessing liver injury associated with antimycotics: Concise literature review and clues from data mining of the FAERS database. World journal of hepatology 6(8):601-12 doi:10.4254/wjh.v6.i8.601

Roberts RA, Smith RA, Safe S, Szabo C, Tjalkens RB, Robertson FM (2010) Toxicological and pathophysiological roles of reactive oxygen and nitrogen species. Toxicology 276(2):85-94 doi:10.1016/j.tox.2010.07.009

Rodriguez RJ, Acosta D, Jr. (1995) Comparison of ketoconazole- and fluconazole-induced hepatotoxicity in a primary culture system of rat hepatocytes. Toxicology 96(2):83-92

Rodriguez RJ, Acosta D, Jr. (1996) Inhibition of mitochondrial function in isolated rate liver mitochondria by azole antifungals. Journal of biochemical toxicology 11(3):127-31 doi:10.1002/(sici)1522-7146(1996)11:3<127::aid-jbt4>3.0.co;2-m

Rodriguez RJ, Acosta D, Jr. (1997a) Metabolism of ketoconazole and deacetylated ketoconazole by rat hepatic microsomes and flavin-containing monooxygenases. Drug metabolism and disposition: the biological fate of chemicals 25(6):772-7

Rodriguez RJ, Acosta D, Jr. (1997b) N-deacetyl ketoconazole-induced hepatotoxicity in a primary culture system of rat hepatocytes. Toxicology 117(2-3):123-31

Rodriguez RJ, Buckholz CJ (2003) Hepatotoxicity of ketoconazole in Sprague-Dawley rats: glutathione depletion, flavin-containing monooxygenases-mediated bioactivation and hepatic covalent binding. Xenobiotica; the fate of foreign compounds in biological systems 33(4):429-41 doi:10.1080/0049825031000072243

Legends to figures

Fig. 1. *Cytotoxicity and effects on intracellular ATP content.* Cytotoxicity was assayed using the Toxilight® assay and ATP content was measured with CellTiterGlo Luminescent cell viability assay. **A.** Cytotoxicity in HepG2 cells (low-glucose medium) after drug exposure for 24 h. **B.** Cytotoxicity in HepG2 cells (galactose medium) after drug exposure for 24 h. **C.** Intracellular ATP content in HepG2 cells (low-glucose medium) after drug exposure for 24 h. **D.** Intracellular ATP content in HepG2 cells (galactose medium) after drug exposure for 24 h. Triton X was used as a positive control. Data are expressed as fold change relative to DMSO control cells. Data represent the mean ± SD of at least three independent experiments. *p < 0.05, **p < 0.01, ***p < 0.001 vs. control incubations.

Fig. 2. *Effect on mitochondrial membrane potential and enzyme complexes of the electron transport chain.* **A.** Membrane potential of freshly isolated mouse liver mitochondria after exposure to azoles for 15 min. Mitochondria were labeled with [phenyl-^{3}H]-tetraphenylphosphonium bromide and mitochondrial accumulation of radioactivity was determined. **B.** Mitochondrial membrane potential in HepG2 cells cultured under low glucose conditions exposed to azoles for 24 h. Mitochondria were labeled with the fluorescent probe TMRM and analyzed with flow cytometry. **C.** Activity of the enzyme complexes of the electron transport chain in freshly isolated mouse liver mitochondria acutely exposed to ketoconazole. **D.** Activity of the enzyme complexes of the electron transport chain in HepG2 cells exposed to ketoconazole for 24 h. **E.** Activity of the enzyme complexes of the electron transport chain in HepG2 cells exposed to posaconazole for 24 h. Data are expressed as the ratio to DMSO control (membrane potential) or oxygen consumption (pmol x sec^{-1} x mg protein^{-1}) (enzyme complex activities). Data are presented as mean ± SD of at least three independent experiments. *p < 0.05, **p < 0.01, ***p < 0.001 vs. DMSO control.

Fig. 3. *Mitochondrial DNA (mtDNA) and SIRT3 expression in HepG2 cells.* **A.** mtDNA. Total DNA was extracted from HepG2 cells after treatment with ketoconazole and posaconazole

for 24 h. The graph shows the ratio of a mitochondrial gene (ND1) and a nuclear gene (36B4) determined by qRT-PCR. **B.** SIRT3 mRNA expression. Total RNA was extracted from HepG2 cells treated with the toxicants for 24h. mRNA was quantified with qRT-PCR as described in methods using GAPDH as an endogenous control. **C.** Protein expression of SIRT3 was determined by western blotting. **D.** Quantification of the bands obtained from three individual western blots of SIRT3. Data are expressed relative to control incubations (containing DMSO 0.1%) and are presented as mean ± SD of at least three independent experiments. ***p < 0.001 vs. control.

Fig. 4. *Superoxide anion accumulation and defense mechanisms in mitochondria of azole treated cells.* **A/B.** Mitochondrial accumulation of superoxide in HepG2 cells cultured in low glucose (A) or galactose media (B). Mitochondrial superoxide production was measured with MitoSOX™ Red reagent after 24 h drug-treatment. Amiodarone (50 µM) served as a positive control (data not shown). **C.** mRNA expression of mitochondrial SOD2. Expression was measured by qRT-PCR with GAPDH as endogenous control. **D.** Protein expression of SOD determined by western blotting including quantification of the bands obtained from three individual experiments. Quantitative results are expressed relative to control incubations. Data are presented as mean ± SD of at least three independent experiments. **p < 0.01, ***p < 0.001 vs. control incubations.

Fig. 5. *Effects of ketoconazole and posaconazole on markers of apoptosis in HepG2 cells.* **A.** Ratio of mRNA expression levels of Bax/Bcl-2 after exposure to ketoconazole or posaconazole for 24 h. The mRNA expression was measured by qRT-PCR with GAPDH as endogenous control. Results are relative expressed (n-fold) to control cells. **B.** Protein expression of cleaved caspase 9, caspase 3, and PARP after treatment with ketoconazole or posaconazole for 24 h. We used staurosporine (STS) as a positive control for apoptosis at a concentration of 200 nM. GAPDH was used to confirm equal loading. Results are expressed relative to control cells. Data are shown as mean ± SD of at least three independent

experiments. **p < 0.01, ***p < 0.001.

Fig. 6. *Toxicity of posaconazole on HepG2 cells with mitochondrial dysfunction.* Mitochondrial dysfunction was induced by treatment with HCCL or the combination HCCL/propionic acid (PA). **A./B.** Cytotoxicity (A) and cellular ATP content (B) after treatment with posaconazole 10 µM for 24 h. **C/D.** Cytotoxicity (C) and cellular ATP content (D) after treatment with posaconazole 20 µM for 24 h. HCCL: hydroxy-cobalamin[c-lactam]. Triton X was used as a positive control. Data are expressed as mean ± SD of at least four independent experiments. *p < 0.05, **p < 0.01, ***p < 0.001 vs. control incubations. $^{+}$p < 0.05, $^{+++}$p < 0.001 vs. incubations containing posaconazole only.

Table 1: List of primers

Gene	Sequence 5'--→3'
SIRT3	TCC CAG TTT CTT CTT TTC GAG T GGA AAG CTT CCC CTT GTC AC
SOD2	GGT TGT TCA CGT AGG CCG CAG CAG GCA GCT GGC T
GAPDH	TGG TAT CGT GGA AGG ACT CA GGG CCA TCG ACA GTC TTC
ND-1	ATG GCC AAC CTC CTA CTC CT CTA CAA CGT TGG GGC CTT T
36B4	GGA ATG TGG GCT TTG TGT TC CCC AAT TGT CCC CTT ACC TT
BAX	GGG GAC GAA CTG GAC AGT AA CAG TTG AAG TTG CCG TCA GA
BCL-2	CTG CAC CTG ACG CCC TTC ACC CAC ATG ACC CCA CCG AAC TCA AAG A

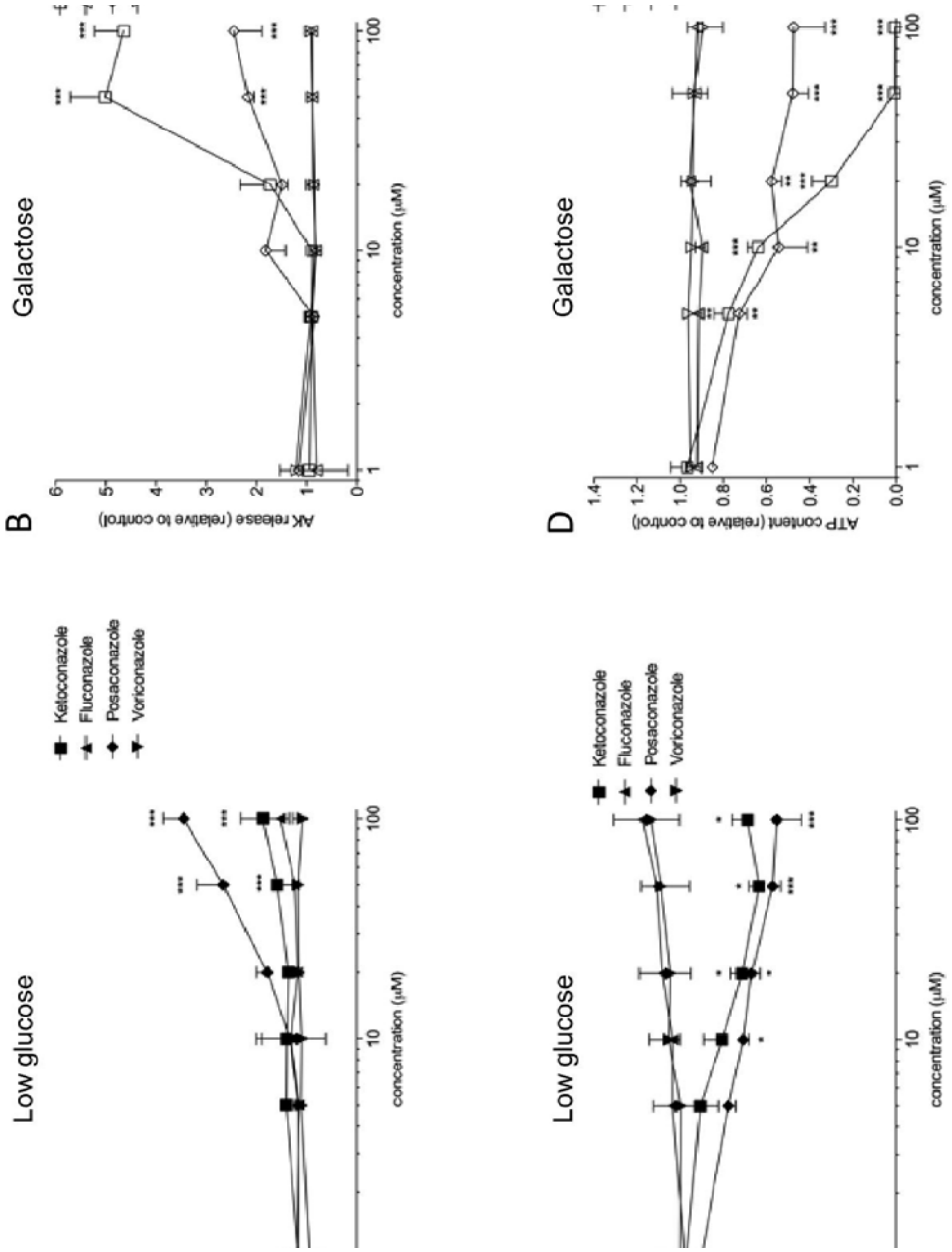
B
Galactose
AK release (relative to control)
concentration (µM)
D
Galactose
ATP content (relative to control)
concentration (µM)
Low glucose
concentration (µM)
Low glucose
concentration (µM)
Ketoconazole
Fluconazole
Posaconazole
Voriconazole

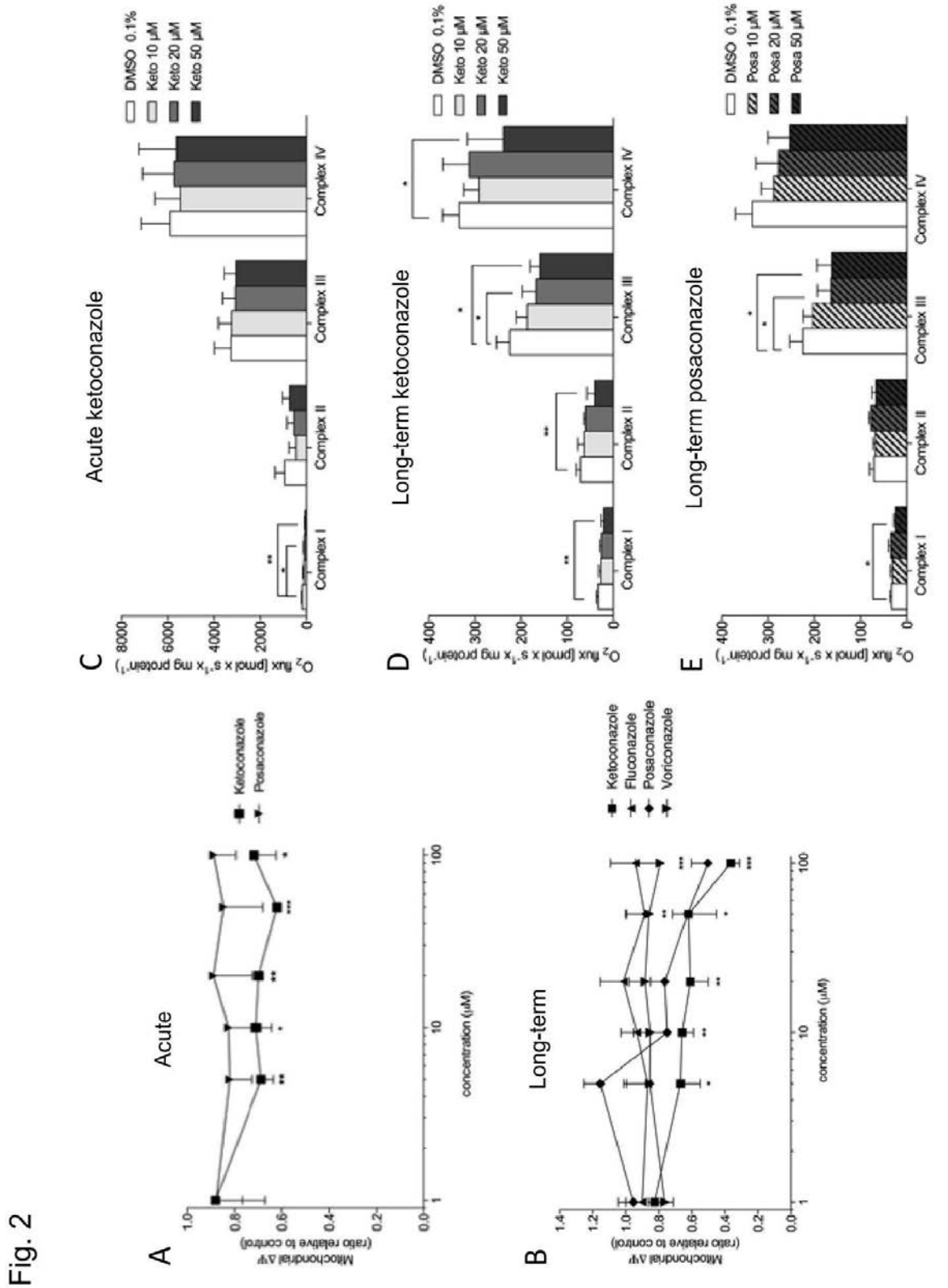
A
Acute
Ketoconazole
Posaconazole
Mitochondrial ΔΨ (ratio relative to control)
concentration (µM)
B
Long-term
Ketoconazole
Fluconazole
Posaconazole
Voriconazole
C
Acute ketoconazole
DMSO 0.1%
Keto 10 µM
Keto 20 µM
Keto 50 µM
Complex I
Complex II
Complex III
Complex IV
D
Long-term ketoconazole
E
Long-term posaconazole
Posa 10 µM
Posa 20 µM
Posa 50 µM

Fig. 2

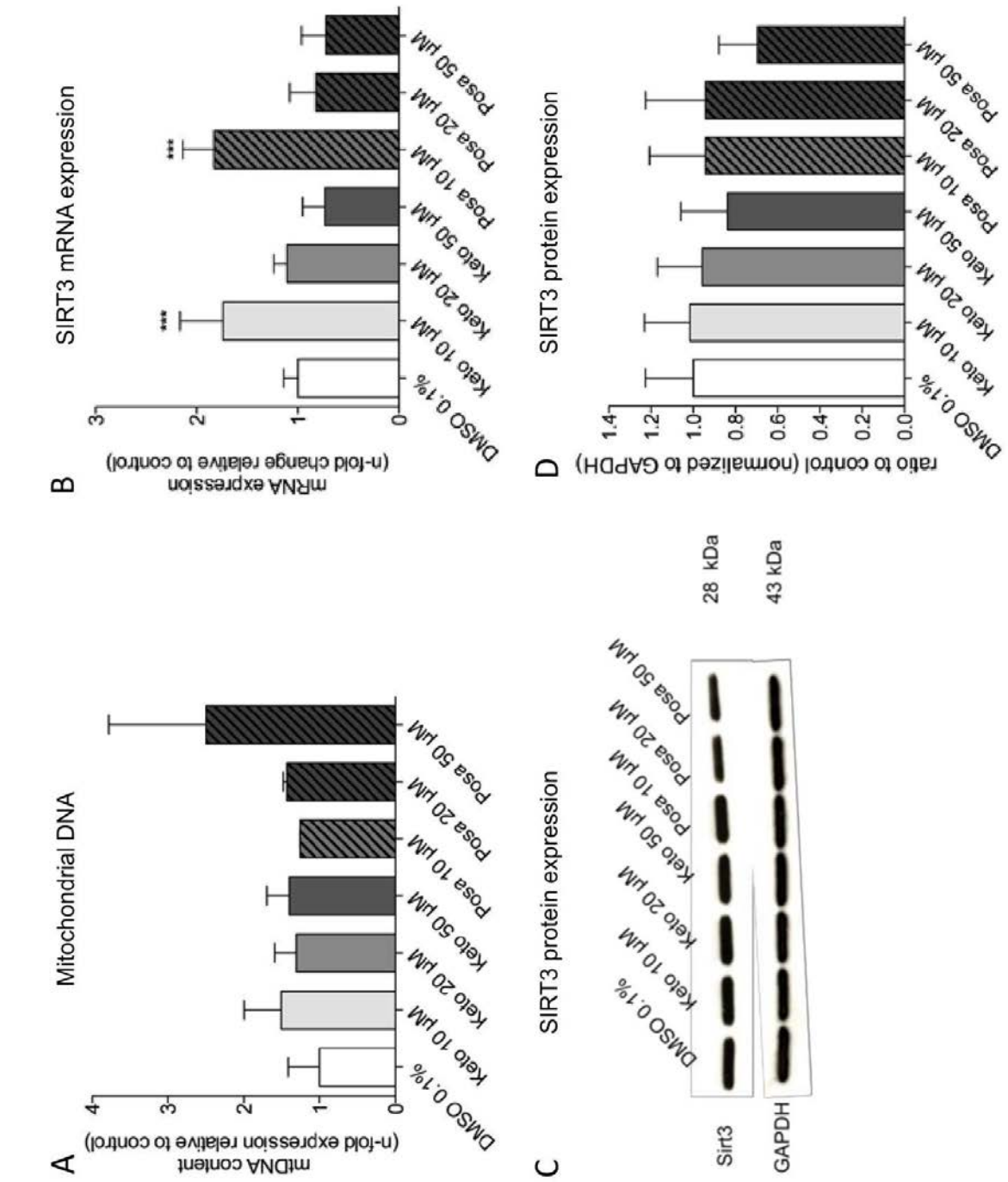
A
Mitochondrial DNA
mtDNA content
(n-fold expression relative to control)
B
SIRT3 mRNA expression
mRNA expression
(n-fold change relative to control)
C
SIRT3 protein expression
28 kDa
43 kDa
Sirt3
GAPDH
D
SIRT3 protein expression
ratio to control (normalized to GAPDH)
DMSO 0.1%
Keio 10 µM
Keio 20 µM
Keio 50 µM
Posa 10 µM
Posa 20 µM
Posa 50 µM

Fig. 3

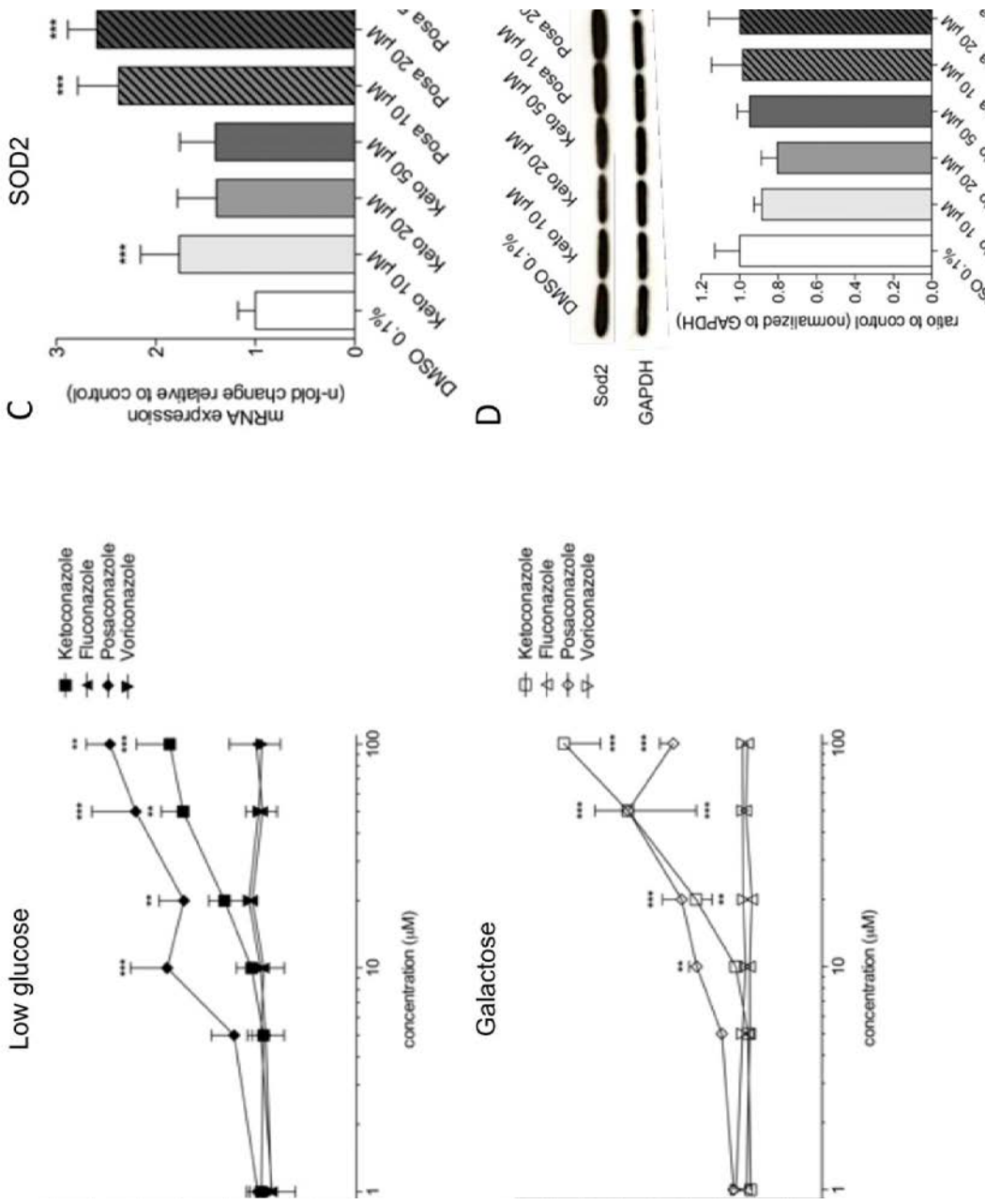
C
SOD2
mRNA expression
(n-fold change relative to control)
DMSO 0.1%
Keto 10 µM
Keto 20 µM
Keto 50 µM
Posa 10 µM
Posa 20 µM
D
Sod2
GAPDH
ratio to control (normalized to GAPDH)
Low glucose
Galactose
Ketoconazole
Fluconazole
Posaconazole
Voriconazole
concentration (µM)

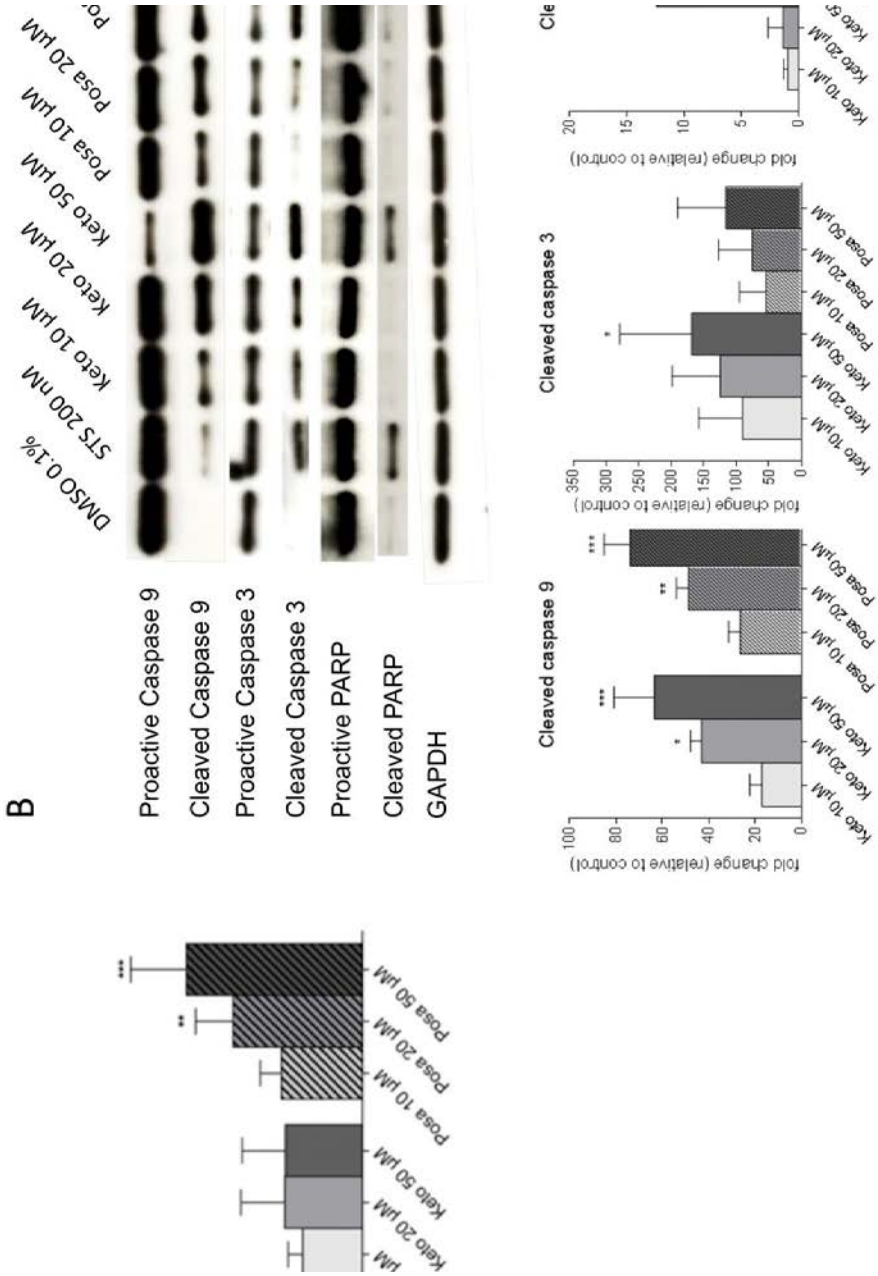
B
Proactive Caspase 9
Cleaved Caspase 9
Proactive Caspase 3
Cleaved Caspase 3
Proactive PARP
Cleaved PARP
GAPDH
DMSO 0.1%
STS 200 nM
Keto 10 µM
Keto 20 µM
Keto 50 µM
Posa 10 µM
Posa 20 µM
Cleaved caspase 9
Cleaved caspase 3
fold change (relative to control)
Keto 10 µM
Keto 20 µM
Keto 50 µM
Posa 10 µM
Posa 20 µM
Posa 50 µM

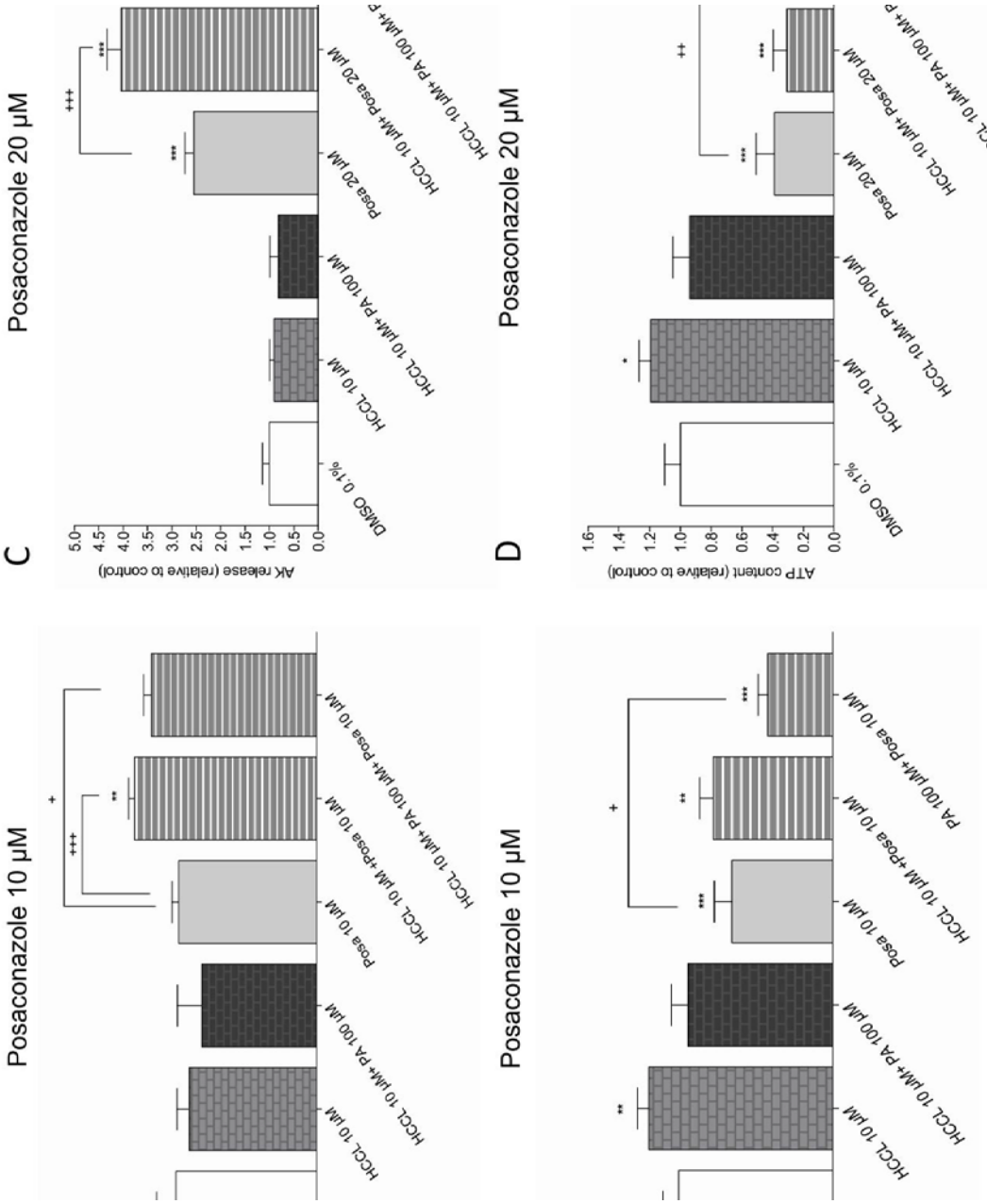
C
Posaconazole 20 µM
Posaconazole 10 µM
D
Posaconazole 20 µM
Posaconazole 10 µM
HCCL 10 µM
HCCL 10 µM+ PA 100 µM
Posa 10 µM
HCCL 10 µM+ Posa 10 µM
HCCL 10 µM+ PA 100 µM+ Posa 10 µM
PA 100 µM+ Posa 10 µM
DMSO 0.1%
Posa 20 µM
HCCL 10 µM+ Posa 20 µM
HCCL 10 µM+ PA 100 µM+ P
ATP content (relative to control)

Supplementary data

Hepatocellular toxicity of imidazole and triazole antimycotic agents

Patrizia Hägler[1,2], Lorenz Joerin[1,2], Stephan Krähenbühl[1,2,3] and Jamal Bouitbir[1,2,3]

[1] Clinical Pharmacology & Toxicology, University Hospital Basel, Switzerland

[2] Department of Biomedicine, University of Basel, Switzerland

[3] Swiss Centre of Applied Human Toxicology (SCAHT)

Funding: This study was funded by grant 31003A_156270 of the Swiss National Science Foundation to SK

Conflict of Interest: The authors declare that they have no conflict of interest regarding this study

Correspondence:

Stephan Krähenbühl, MD, PhD

Clinical Pharmacology & Toxicology

University Hospital

4031 Basel/Switzerland

Phone: +41 61 265 4715

Fax: +41 61 265 4560

e-mail: stephan.kraehenbuehl@usb.ch

Legends to supplementary figures

Suppl. Fig. 1. *Chemical structures and metabolic pathways of azoles investigated*. Ketoconazole is an imidazole derivative, and fluconazole, voriconazole and posaconazole are triazole derivatives. CYP: cytochrome P450 enzyme, FMO: Flavin-containing monooxidase.

Suppl. Fig. 2. *Cytotoxicity and effects on intracellular ATP content of HepG2 cells exposed for 48 h.* Cytotoxicity was assayed using the Toxilight® assay and ATP content was measured with CellTiterGlo Luminescent cell viability assay. **A.** Cytotoxicity in HepG2 cells (low-glucose medium) after drug exposure for 48 h. **B.** Intracellular ATP content in HepG2 cells (low-glucose medium) after drug exposure for 48 h. Triton X was used as a positive control (not shown). Data are expressed as fold change relative to DMSO control cells. Data represent the mean ± SD of at least three independent experiments. *$p < 0.05$, **$p < 0.01$, ***$p < 0.001$ vs. control incubations.

Suppl. Fig. 3. *Cytotoxicity and effects on intracellular ATP content of HepaRG cells.* Cells were CYP-induced (open bars; rifampicin 20 µM for 3 days) or not CYP-induced (closed bars). Cytotoxicity was assayed using the Toxilight® assay and ATP content was measured with CellTiterGlo Luminescent cell viability assay. **A.** Cytotoxicity in HepaRG cells (low-glucose medium) after drug exposure for 24 h. **B.** Intracellular ATP content in HepaRG cells (low-glucose medium) after drug exposure for 24 h. Triton X was used as a positive control (not shown). Data are expressed as fold change relative to DMSO control cells. Data represent the mean ± SD of at least three independent experiments. *$p < 0.05$, **$p < 0.01$, ***$p < 0.001$ vs. control incubations containing 0.1% DMSO. $^{+++}p < 0.001$ vs. respective incubations of cells not treated with rifampicin.

Suppl. Fig. 4. *Toxicity of ketoconazole on HepG2 cells with mitochondrial dysfunction.* Mitochondrial dysfunction was induced by treatment with HCCL or the combination HCCL/propionic acid (PA). **A./B.** Cytotoxicity (A) and cellular ATP content (B) after treatment with ketoconazole 10 µM for 24 h. **C/D.** Cytotoxicity (C) and cellular ATP content (D) after treatment with ketoconazole 20 µM for 24 h. HCCL: hydroxy-cobalamin[c-lactam]. Triton X was used as a positive control. Data are expressed as mean ± SD of at least four independent experiments. *$p < 0.05$, **$p < 0.01$, ***$p < 0.001$ vs. control incubations. $^{+}p < 0.05$, $^{+++}p < 0.001$ vs. incubations containing ketoconazole only.

Suppl. Fig. 1

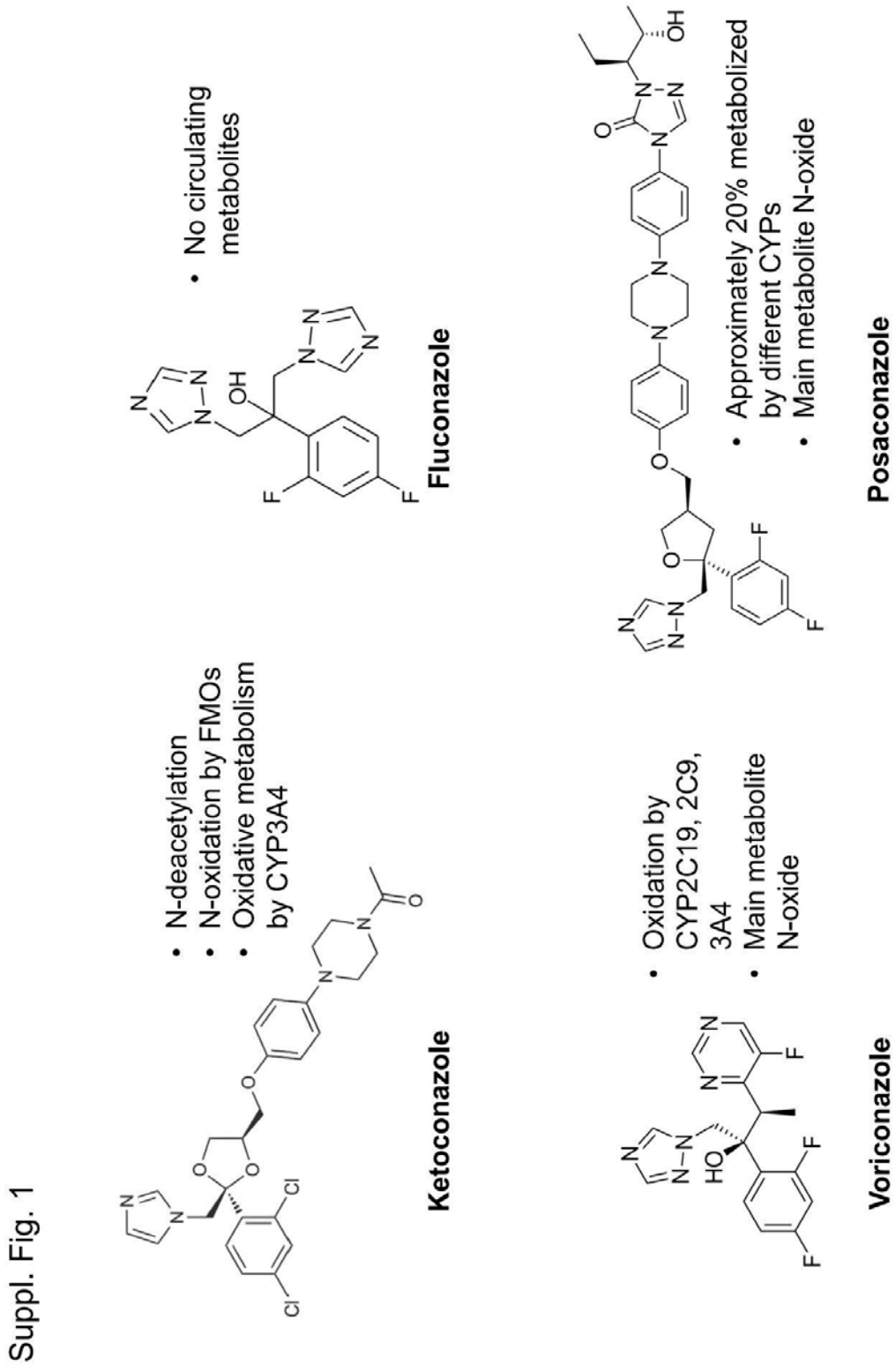
• No circulating metabolites
Fluconazole
• Approximately 20% metabolized by different CYPs
• Main metabolite N-oxide
Posaconazole
• N-deacetylation
• N-oxidation by FMOs
• Oxidative metabolism by CYP3A4
Ketoconazole
• Oxidation by CYP2C19, 2C9, 3A4
• Main metabolite N-oxide
Voriconazole

Suppl. Fig. 2

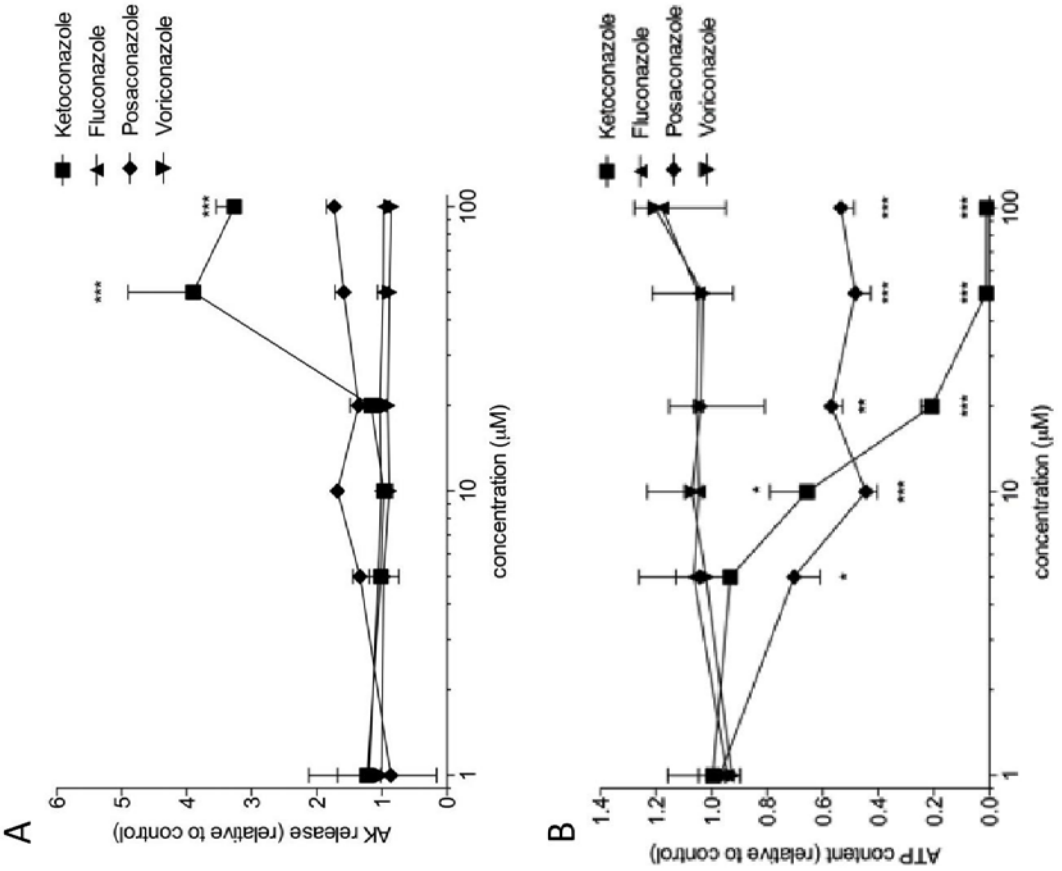
A
Ketoconazole
Fluconazole
Posaconazole
Voriconazole
AK release (relative to control)
concentration (µM)
B
ATP content (relative to control)
concentration (µM)

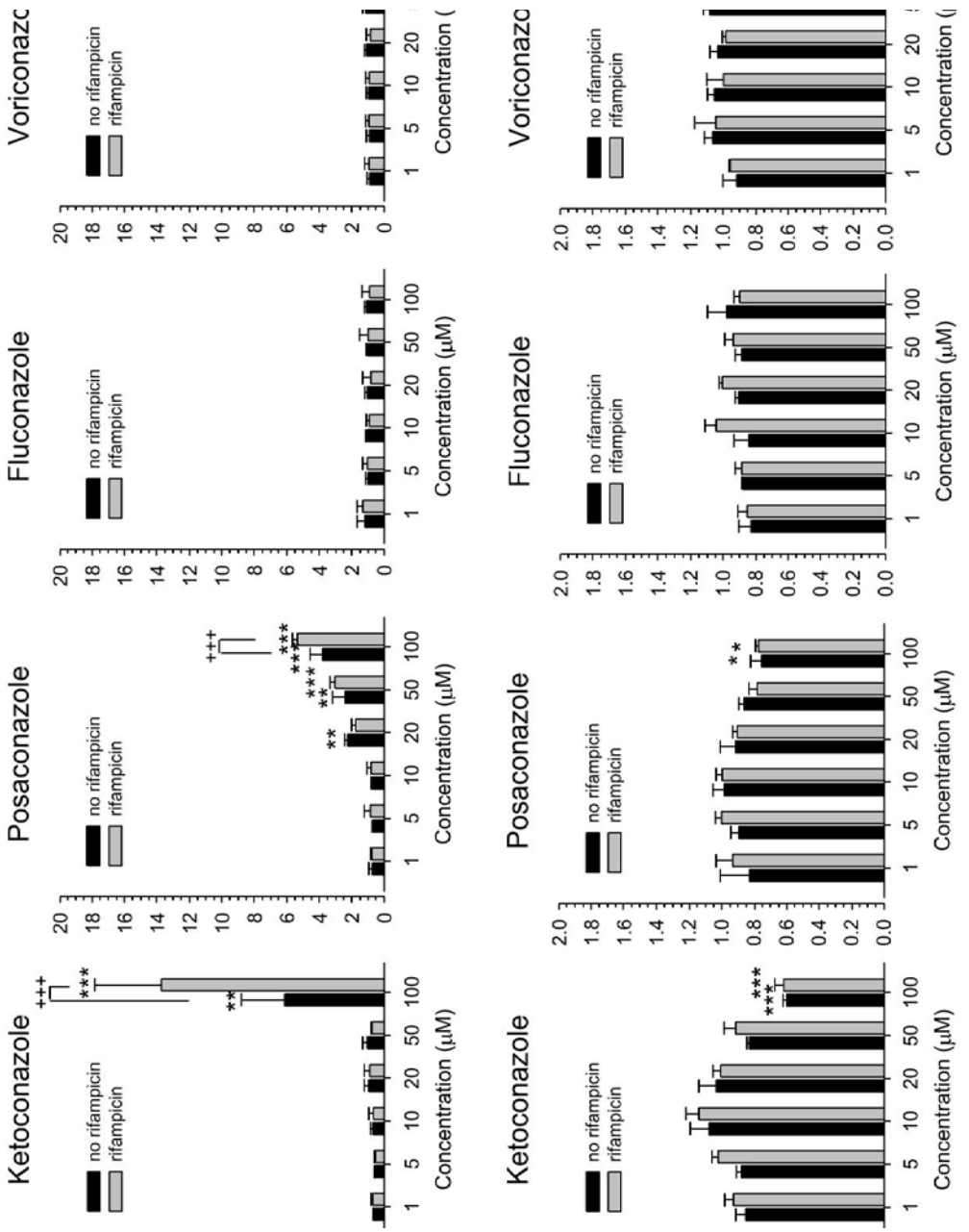
Ketoconazole
Posaconazole
Fluconazole
Voriconazo
no rifampicin
rifampicin
Concentration (µM)
+++
***
**

g. 3

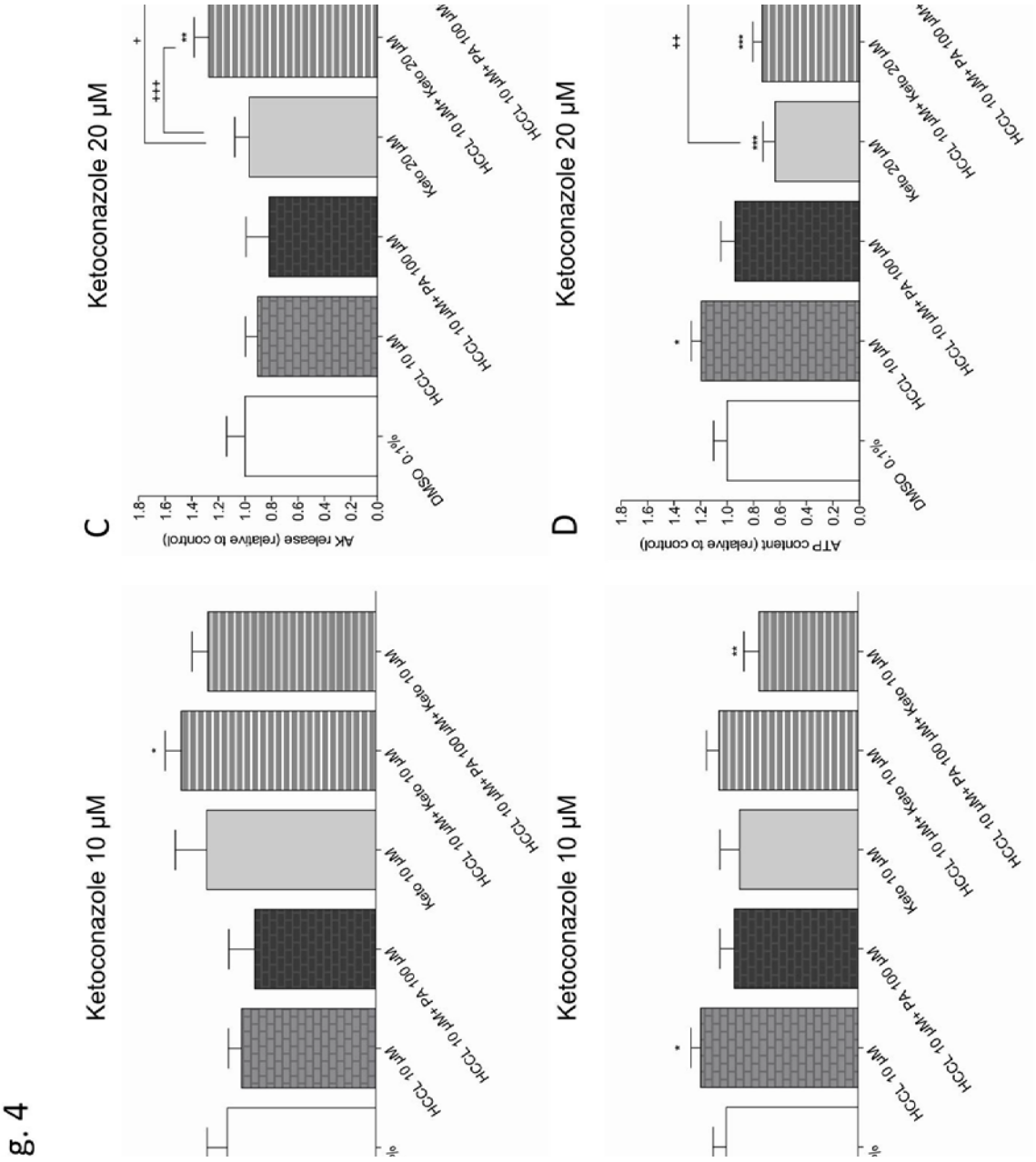
C
Ketoconazole 20 µM
AK release (relative to control)
1.8
1.6
1.4
1.2
1.0
0.8
0.6
0.4
0.2
0.0
DMSO 0.1%
HCCL 10 µM
HCCL 10 µM+ PA 100 µM
Keto 20 µM
HCCL 10 µM+ Keto 20 µM
HCCL 10 µM+ PA 100 µM
D
Ketoconazole 20 µM
ATP content (relative to control)
Ketoconazole 10 µM
HCCL 10 µM+ Keto 10 µM
Keto 10 µM
HCCL 10 µM+ PA 100 µM+ Keto 10 µM

g. 4

Report

Development of hepatocellular models lacking essential mitochondrial function to test drugs associated with idiosyncratic toxicity

P Haegler[1,2], S Krähenbühl[1,2,3], J Bouitbir[1,2,3]

[1] Clinical Pharmacology & Toxicology, University Hospital Basel, Switzerland

[2] Department of Biomedicine, University of Basel, Switzerland

[3] Swiss Centre of Applied Human Toxicology (SCAHT)

Draft manuscript

Development of hepatocellular models lacking essential mitochondrial function to test drugs associated with idiosyncratic toxicity

Patrizia Haegler[1,2], Stephan Krähenbühl[1,2,3] and Jamal Bouitbir[1,2,3]

[1] Clinical Pharmacology & Toxicology, University Hospital Basel, Switzerland

[2] Department of Biomedicine, University of Basel, Switzerland

[3] Swiss Centre of Applied Human Toxicology (SCAHT)

Abstract

The major problem implicated in the early detection of idiosyncratic hepatotoxic drugs is that often only under certain genetically or environmental conditions pathological signs of hepatotoxicity are presented pointing to underlying risk factors, which may be responsible for rendering some patients more susceptible to drug-induced liver injuries. The goal of our investigation was therefore to create suitable hepatocellular systems with specific depletion of important mitochondrial function, representing possible determinants that increase the liability to mitochondrial toxicants and thus to the manifestation of idiosyncratic toxicity.

With siRNA transfection, we depleted mRNA levels and protein expression of the antioxidant enzyme SOD2 or its deacetylator SIRT3 in HepG2 cells. Knockdown efficacy was elucidated over 72 h and assayed with RT-PCR and western blot analysis. Possible cytotoxic effects of transfection media were measured by the release of adenylate kinase. Cytotoxicity, ATP content, and generation of superoxide anion of azoles, which are known to exert mitochondrial toxic effects on the liver, were then tested on siRNA cells lacking SOD2 or SIRT3 function.

We confirmed a time-dependent decrease of knockdown of the genes of interest and related proteins from 24, 48, and 72 h to 50, 20, and 10%, respectively. After 24 h of exposure to ketoconazole and/or posaconazole, we found a dose-dependent increased toxicity and a concurrent decrease in ATP content, as well as increased ROS levels after treatment with the toxicants. However, we did not observe enhanced toxicites of siRNA cells lacking SIRT3 and/or SOD2 exposed to ketoconazole and posaconazole for 24 h compared to normal HepG2 cells.

We conclude that cells possess mechanisms to compensate lacking antioxidant functions or implicated regulation of antioxidant enzymes. Further functional toxicological experiments are needed to characterize more precisely the impact of the depletion of theses genes. The use of other mitochondrial toxicants will also enhance the validity of the proposed siRNA models.

Introduction

Drug-induced mitochondrial hepatotoxicity is a serious adverse event that has been accounted for some important drugs in clinical use such as amiodarone or valproic acid [1, 2]. The detection of suchlike adverse effects has ultimately led to black box warnings, restricted use, or even to withdrawal of some drugs from the market [3, 4]. Early prediction methods uncovering harmful compound turned out to be a difficult task, since idiosyncratic drug-induced adverse liver injuries are rarely manifested and occur often at subtoxic concentration, and usually in a specific population of patients [5, 6]. It has been assumed that underlying diseases or existing mitochondrial dysfunctions represent one of the risk factor that predispose patients to be more susceptible to mitochondrial toxic drugs [7, 8]. We therefore aimed to establish a cellular model that lacks important mitochondrial function in order to answer the question if our proposed model is useful for screening mitochondrial toxicants.

Mitochondria exhibit several defense mechanisms to counteract against oxidative stress induced by xenobiotics or intrinsic triggering factors. The most important two antioxidant systems represents the enzymatic scavenger mitochondrial manganese superoxide dismutase 2 (SOD2) or glutathione peroxidase [9]. The latter one is a crucial redox buffer in the cytosol eliminating H2O2 that easily can diffuse through the mitochondrial membrane to form toxic radicals leading to an impairment of the cell [10].

As a first line defender, SOD2 is able to scavenge oxygen radicals by reacting with hydrogen resulting in a formation of H2O2 (2O2- + 2H+ -> H2O2 + O2) [11]. Interestingly, mice lacking SOD2 only survive several days after birth, suggesting that SOD2 is a pivotal mediator for cell survival by maintaining mitochondrial superoxide anion levels [12]. The expression of SOD2 in turn is tightly connected to its deacetylation status [13]. SIRT3 belonging to the family of sirtuins has therefore been recognized as eminent key player in the regulation of cellular energy processes through its NAD+-dependent deacetylation activity [14]. Among the seven members of sirtuins, the mitochondrially located SIRT3 is highly expressed in tissues with high oxidative capacity like the liver, kidney or brain. SIRT3 activity is thus directly linked to the energetic status of a cell [15]. This means that in terms of increased energy demand as for example in the case of caloric restriction, SIRT3 is upregulated and consequently enhances the deacetylation of substrates related in the electron transport chain or as well as the antioxidant enzyme SOD2, and thereby induces a reduction of ROS and oxidative stress [16]. Bao et al. [17] have created a hepatocellular model with depleted SIRT3 function using siRNA transfection and demonstrated a disturbance of the

electron transport chain (ETC), implicating a dissipation of the mitochondrial membrane potential and a subsequent increase of ROS production. These observations are reasonably explained by the diminished deacetylation of those important proteins [18].

By reasons of the importance of SOD2 in the mitochondrial antioxidant pathway, SIRT3 mediated-regulation of mitochondrial key energy metabolic enzymes, and based on the evidences made by diverse *in vivo* and *in vitro* investigations on SIRT3 and SOD2 [19-22], we intended creating two hepatocellular models; one lacking SIRT3 function and the other with depleted SOD2 antioxidant scavenger. We purposed that the lack of such crucial enzymes of the mitochondria lead to an increased liability of these cells to mitochondrial toxicants. Thus, we aimed in a first step to establish a knockdown of SIRT3 and SOD2 in Hepg2 cells using siRNA transfection, and in a second step to test known mitochondrial toxicant on our purposed system of underlying mitochondrial dysfunction to prove the hypothesis that patients with underlying dysfunctions such as genetic abnormalities are more prone to idiosyncratic toxicity.

Material and Methods

Chemicals

Ketoconazole and posaconazole were purchased from Sigma-Aldrich (Buchs, Switzerland). Stock solutions were dissolved in DMSO and stored at -20 °C. We used control incubations containing 0.1% DMSO that has been shown to be untoxic [2]. All other chemicals used were purchased from Sigma-Aldrich or Fluka (Buchs, Switzerland), except where indicated.

Cell lines, cell culture, and treatment

The human hepatoma cell line HepG2 was provided by ATCC (Manassas, USA) and cultured in low-glucose. Low-glucose containing medium was prepared with Dulbecco's Modified Eagle Medium (DMEM) low glucose 1.0 g/L, containing 4 mM L-Glutamine, and 1 mM pyruvate from Invitrogen (Basel, Switzerland) that was supplemented with 10% (v/v) heat-inactivated fetal calf serum, 2 mM GlutaMax, 10 mM HEPES buffer, and non-essential amino acids. Cell culture supplements were all purchased from GIBCO (Paisley, UK). We kept the cells at 37 °C in a humidified 5% CO_2 cell culture incubator. A Neubauer hemacytometer was used to determine the cell number and viability using the trypan blue exclusion method.

Cells were treated with posaconazole and/or ketoconazole with concentrations indicated in the Results section for 24 h after 48 h of siRNA transfection. Total cellular GSH level was depleted by the pretreatment of BSO, a known inhibitor of GSH synthesis according to Raza, H et al. with some modifications [23]. Briefly, 24 h after transfection, cells were treated with 100 mM BSO that has been previously dissolved in culture medium for 24 h, and than treated together with toxicants for another 24 h on transfected cells.

siRNA transfection

Reverse transfection of siRNA was performed using Lipofectamine® RNAiMAX according the manufacturer`s instruction (Invitrogen, Life Technologies, Carlsbad, CA). Briefly, siRNA (30 μM) were diluted with 500 μL Opti-MEM in 6-well culture plates. Then, Lipofectamine® RNAiMAX (5 μL) was added to the wells. Cell culture plates were incubated for 20 min at room temperature before adding 250,000 cells per well to reach a final siRNA concentration of 10 nM. Cell culture plates were then kept at 37 °C in a humidified 5% CO_2 cell culture incubator. At 24, 48, and 72 h post-transfection, cells were harvested for real-time PCR or lysed for protein expression analysis. siRNA transfection for cytotoxicity and other functional experiments of known mitochondrial toxic drugs were performed in 96-well format in the concentrations according to the manufacturer`s instruction (Invitrogen, Life Technologies, Carlsbad, CA). The following validated Silencer R Select siRNAs, obtained from Ambion® (Invitrogen, Life Technologies, Carlsbad, CA), were used in this study: human negative control siRNA (sequence: sense strand: 5'- GCUCGGCAUCUGUUGGUUtt3, antisense: UAACCAACAGAUGCCGAGCtt), human siRNA SOD2 (sequences: sense 5'-UGUCAGGCCUGAUUAUCUAtt3, antisense: UAGAUAAUCAGGCCUGACAAtt), and human SIRT3 (sequences: sense 5'-GCUCGGCAUCUGUUGGUUtt3, antisense: UAACCAACAGAUGCCGAGCtt).

Cytotoxicity

Cells were seeded and transfected according to the manufacturer`s instruction (Invitrogen, Life Technologies, Carlsbad, CA) at 10,000 cells/well in a 96-well plate. We used the ToxiLight® (Lonza, Basel, Switzerland) assay to determine the cytotoxicity of different known mitochondrial toxic drugs on transfected cells (transfection period was 48 h) after 24 h of treatment at concentrations indicated. We used Triton X 0.1% as a positive control. The release of adenylate kinase was measured according to the manufacturer's instructions.

Briefly, ToxiLight® reaction buffer (100 µL) was mixed with 20 µL of supernatant from the treated cells. Then, the mixture was left in the dark for 5 min and the luminescence was measured with a Tecan M200 Pro Infinity plate reader (Männedorf, Switzerland).

Intracellular ATP content

Cells were seeded and transfected according to the manufacturer`s instruction (Invitrogen, Life Technologies, Carlsbad, CA) at 10,000 cells/well in a 96-well plate. 48 h after the transfection, medium was removed and replaced with mitochondrial toxic drugs at concentrations indicated for 24 h. Then, intracellular ATP was determined using CellTiterGlo Luminescent cell viability assay (Promega, Switzerland), in accordance with the manufacturer's instructions. Briefly, 100 µL of assay buffer was added to each 96-well containing 100 µL culture medium. We used Triton X 0.1% as a positive control. After incubation in the dark for 12 min, luminescence was measured using a Tecan M200 Pro Infinity plate reader.

Mitochondrial superoxide anion accumulation

Mitochondrial superoxide anion production was detected with the fluorogenic dye MitoSOX™ Red reagent (Molecular Probes, Eugene, OR, USA). Cells were seeded and transfected according to the manufacturer`s instruction (Invitrogen, Life Technologies, Carlsbad, CA) at 10,000 cells/well in a 96-well plate. After 72 h of transfection, mitochondrial toxic drugs were added to the wells and left on the cells for 24 h. Then, medium was removed, and HepG2 cells were stained with MitoSOX red (dissolved in DPBS) at a final concentration of 2 µM. We used amiodarone 50 µM as a positive control. Plate was incubated in the dark at 37 °C for 15 min, afterwards fluorescence was measured at an excitation wavelength of 510 nm and an emission wavelength of 580 nm using a Tecan Infinite pro 200 microplate reader. We normalized the results to the protein content using the Pierce BCA Protein Assay Kit (Darmstadt, Germany) according to manufacturer's instruction.

Quantitative RT-PCR

Cells were seeded and transfected according to the manufacturer`s instruction (Invitrogen, Life Technologies, Carlsbad, CA) at 250,000 cells/well in a 6-well plate. At 24, 48, and 72 h post-transfection, cells were harvested for real-time PCR. Cells were then lysed with 350 µL

of RLT buffer (Qiagen, Hombrechtikon, Switzerland) and the cell lysate was transferred to Qiashredder columns and spinned for 2 min at 13,000 rpm. From the eluate, total RNA was extracted according to the manufacturer's protocol (Qiagen RNeasy Mini Extraction kit). We assessed the RNA quality with the NanoDrop 2000 (Thermo Scientific, Wohlen, Switzerland). Qiagen Omniscript system was used to reverse transcribe the isolated RNA (1 µg) to cDNA. For quantitative real-time RT-PCR, 10 ng cDNA was used. The expression of mRNA was evaluated using SYBR Green real-time PCR (Roche Diagnostics, Rotkreuz, Basel). Real-time RT-PCR was performed in triplicate on an ABI PRISM 7700 sequence detector (PE Biosystems, Rotkreuz, Switzerland) and quantification was carrying out using the comparative-threshold cycle method. Forward and reverse primers for genes of interest and GAPDH as endogenous reference control (see Table 1 for primers) were purchased from Microsynth (Balgach, Switzerland).

Protein extraction and western blot analysis

Cells were seeded and transfected according to the manufacturer`s instruction (Invitrogen, Life Technologies, Carlsbad, CA) at 250,000 cells/well in a 6-well plate. At 24, 48, and 72 h post-transfection, cells were washed with ice-cold PBS and lysed with RIPA buffer (50 nM Tris-HCL, pH 7.4, 150 mM NaCl, 1% Triton X-100, 0.5% sodium deoxylcholate, 0.1% sodium dodecyl sulfate, and 1 mM ethylenediaminetetraacetic acid [EDTA] in water). Lysates were incubated with RIPA buffer under constant agitation for 20 min and then centrifuged at 13,000 rpm for 10 min at 4 °C. After determining the protein amount with Pierce BCA Protein Assay Kit (Darmstadt, Germany) according the manufacturer's instructions, we separated 15 µg protein on 4-12% bis-tris gradient gels (Invitrogen, CA, U.S.A), and transferred them to polyvinyli- dendifluoride membranes (Bio-rad, CA, U.S.A). Membranes were blocked with 5% nonfat dry milk in phosphate buffered saline (PBS) (Gibco, Paisley, UK) containing 0.1% Tween-20 (PBS-T) (Sigma-Aldrich, MO, USA) for 1 h at room temperature before the overnight incubation with the relevant primary antibody (Cell Signaling Technology, USA) diluted 1:1000 in blocking buffer. The day after, blots were incubated for 1 h with peroxidase-labeled secondary antibody (Santa Cruz Biotechnology, Danvers, U.S.A) diluted 1:2000 in 5% nonfat milk in PBS-T. Then, we washed the membranes and developed the immunoreactive bands using enhanced chemiluminescence (GE Healthcare, Little Chalfont, UK). We scanned the chemiluminescent images with a HP Scanjet 8300 (Hewlett-Packard Co., Palo Alto, CA) and quantified band intensities of the

scanned images with the National Institutes of Health Image J program (version 1.41). To correct for loading differences, the scanning units obtained from the probed proteins were divided by the scanning units obtained from the respective housekeeping protein GAPDH. Following primary antibodies were used: SOD2 (Cell signaling technology, Danvers, U.S.A) SIRT3 (Cell signaling technology, Danvers, U.S.A) and GAPDH (Abcam, Cambridge, UK).

Statistical Methods

Data are given as the mean ± standard deviation (SD) of at least three independent experiments if not specially indicated. Statistical analyses were performed using GraphPad Prism 6 (GraphPad Software, La Jolla, CA, US). One-way analysis of variance (ANOVA) was used for comparisons of more than two groups, followed by Dunnett's post-test procedure to localize differences between the individual groups tested. Nonparametric tests were used in case of not normally distributed data. P-values <0.05 were considered as significant.

Results and Discussion

siRNA transfection efficacy and toxicity

To prove whether the knockdown of SIRT3 and SOD2 in HepG2 cells was efficient, we assessed over a time course of 24, 48 to 72 h the silencing efficiency by gene expression analysis and western blotting. The data obtained from the mRNA expression experiments revealed a distinctive reduced fold change already after 24 h of transfection to less than 10% of both genes, SOD2 and SIRT3 compared to HepG2 cells that have been transfected with a control sequence, which is not changing any of the genetic information of the cell (Figs. 1A and B). Western blots showed similar results as mRNA levels; SOD2 and SIRT3 protein expression decreased gradually with the duration of transfection compared to control cells (Fig.1C). The quantitative analysis of the western blots depicted for SOD2 a time-dependent reduction in protein expression. A transfection time of 24 h resulted in a decrease of SIRT3 to 65%, whereas we determined for longer transfection periods such as 48 h and 72 h a reduction of protein expression to 20% and 10%, respectively. SOD2 silencing caused a diminished protein expression of 50% already after 24 h, followed by a stronger knockdown effect of 80% after 48 h and almost to a complete silencing (>90%) after 72 h of transfection (Fig. 1D). To assure that the transfection and the transfection components are not toxic to the cells over

the time of knockdown, we confirmed by time-dependent cytotoxicity experiments that no significant increase of adenylate kinase, a marker for leaky cells, was reached during the transfection period from 24 h to 72 h (Fig.1E). Since a transfection time of 48 h already revealed high potency in knocking down SIRT3 and/or SOD2, we decided to use this duration for all following experiments. Due to the efficient knockdown of the two genes of interest, we further used this model to identify an increased susceptibility of these cells to mitochondrial toxicants.

We enlarged these sets of experiments also in HepG2 cells kept in galactose media, where cells are forced to produce energy mainly through oxidative phosphorylation and not via glycolysis, that mainly occurs in low-glucose maintained HepG2 cells [24]. Under galactose conditions, knockdown of SIRT3 and SOD2 revealed mostly identically data as seen for HepG2 cells kept in low-glucose media (data not shown).

Cytotoxicity and oxidative stress in HepG2 cells with silenced SIRT3 or SOD2 function

To test the hypothesis if underlying mitochondrial defects such as silenced function of important enzymes of the mitochondria count to the risk factors for increased liability to mitochondrial toxicants, we assessed the toxicity and as well as the mitochondrial superoxide anion production in HepG2 cells with silenced SIRT3 or SOD2 function after exposure to known mitochondrial toxic drugs as for instance the antimycotic azoles ketoconazole and posaconazole. First, we transfected HepG2 cells within 48 h with SIRT3 or SOD2, then concentrations of 10, 20, and 50 μM of either posaconazole or ketocoanzole were incubated on cells for 24 h. As shown in Fig. 2.A-D treatment with posaconazole or ketoconazole increased the toxicity and decreased the cellular ATP content in a dose-dependent manner as shown in our previous study on azoles' hepatotoxicity. However, when comparing the impact of the treatment on different groups such as normal HepG2 cells, siCTRL cells, siSOD2, and/or SIRT3 cells, we did not see any enhanced changes towards increased toxicity or reduced ATP content in HepG2 cells with silenced SIRT3 and SOD2 function, neither for posaconazole (Figs. 2A and 2C) nor for ketoconazole (Figs. 2B and 2D). The same observation has been made for ROS production after treatment of the two antifungal drugs. They did not increase the levels of mitochondrial ROS in the groups of HepG2 cells that exhibit depleted SIRT3 or SOD2 function (Figs. 2E and 2F).

We presumed to find an increased toxicity and a concurrent decrease of the ATP content after exposure to mitochondrial toxic agents. Moreover, we supposed to see an augmentation of mitochondrial ROS levels, since we knocked down genes that are strongly involved in oxidative stress. Evidences, underlying our hypotheses that SOD2 siRNA transfection in HepG2 cells should increase the susceptibility to toxicants, are given by an existing mouse model with partially defective antioxidant function ($SOD2^{+/-}$ mice), which turned out to be a useful model in detecting idiosyncratic toxicity. Ong and colleagues [25] thereby used this mouse model to uncover if this mitochondrial abnormality is associated with troglitazone-induced hepatotoxicity. Indeed, they proved that under compromised mitochondrial function, $SOD2^{+/-}$ mice were more susceptible to troglitazone treatment (30 mg/kg/day) within a prolonged exposure of 4 weeks, manifesting elevated serum alanine aminotransferase, hepatic necrosis, and increased oxidative stress compared to wild-type mice treated with the same dose of troglitazone, which did not exert any signs of hepatic toxicity [25]. However, contrary to these observations, our cellular model lacking SOD2 did not show increased liability to mitochondrial toxicants.

The same can be assigned for SIRT3 depleted HepG2 cells. Although the study of Bao et al. [17] has demonstrated that $SIRT3^{-/-}$ mice and HepG2 cells with depleted SIRT3 are more liable to lipotoxicity, thus indicating the importance of SIRT3-mediated signaling in oxidative stress, we could not confirm that a depletion of SIRT3 function render HepG2 cells more prone to ketoconazole or posaconazole treatment. However, from our obtained results, we conclude that the affection of the silencing was not enough to make the cells more prone to the known antimycotic azoles ketoconazole and posaconzole.

The presented experiments as depicted in Figure 2 were also conducted in HepG2 cells that have been kept under galactose condition, so that they primarily produce energy via OXPHOS instead through glycolysis, which is the case if cells are maintained in low-glucose medium. Therefore, HepG2 cells cultured in galactose exhibit enhanced liability to mitochondrial toxicants [24]. Results under galactose condition however did not reveal any other outcome than observed in low-glucose cells. Although transfection and resulting knockdown of the two genes of interest were efficient, the treatment of ketoconazole and posaconazole on these cells did show any differing results than in control cells (data not shown).

Cytotoxicity and oxidative stress in transfected HepG2 cells with depleted GSH content

Nevertheless, out of our first observations, we concluded, that one stress factor such as silenced mitochondrial function may not be enough to induce an increased susceptibility of our purposed cell system to toxicants. We thus, secondarily to the depletion of SOD2, imposed a depletion of intracellular GSH in the same cells, which could act as second factor triggering idiosyncratic mitochondrial dysfunction. GSH depletion induced by L-Buthionine-sulfoximine (BSO) that irreversibly inhibits γ-glutamylcysteine synthetase, an essential enzyme for the synthesis of GSH has shown to deplete to a high extend intracellular GSH levels (80-90%) without impairing main cellular function [23, 26]. The impact of a depletion of GSH stores showed the investigations on aspirin (acetlysalicylic acid) in HepG2 cells with depleted GSH content depicting augmented cytotoxicity and oxidative stress under blunted GSH stores [23].

We therefore diminished the intracellular GSH content by treating transfected cells after 24 h with the chemical inhibitor BSO for 48 h. After 24 h of BSO treatment, fresh BSO-and azoles containing medium were applied on transfected cells. We discovered that ATP content of HepG2 cells lacking SOD2 and cellular GSH pool, exposed to ketocoanzole or posacoanzole for 24 h, were not more affected than ketoconazole and/or posaconazole-treated siCTRL or normal HepG2 cells. Moreover, when comparing normal HepG2 cells with or without BSO pretreatment, no significant changes were observed after exposure to posaconazole or ketoconazole. We only found a general reduction of ATP content and a concurrent dose-dependent increase of toxicity that we already have previously described for azoles on HepG2 cells (Fig.3.A-D). According to the experiments on ATP content and toxicity, mitochondrial ROS production was not enhanced in any of the groups; neither in HepG2 with or without depleted GSH content nor in the combination of depleted GSH and lack of SOD2, if exposed to ketoconazole and posaconazole (Figures 3E and F). Contrary to our hypothesis, we did not determine any results towards increased toxicity of azoles in HepG2 cells lacking GSH stores or both, depleted GSH and silent SOD2 function.

According to our findings, we assume that some cellular mechanisms are able to compensate silenced mitochondrial function. It is also likely that augmented toxicity can only be detected dependent on the specificity of a drug. Therefore, in a further step, we have to enlarge the set of mitochondrial toxicants, which should be applied on our created system to make a definite conclusion of this study. However, it has to be mentioned that our approach to answer the purposed question was most likely too simplistic. We did not examine for example in detail

the direct impact of the knockdown of these two genes on other mitochondrial function such as on the respiratory chain function. Hence, an in depth-characterization of HepG2 cells lacking SIRT3 or SOD2 is needed to understand involved processes in siRNA cells.

Literature

1. Felser, A., et al., *Mechanisms of hepatocellular toxicity associated with dronedarone--a comparison to amiodarone.* Toxicol Sci, 2013. **131**(2): p. 480-90.
2. Waldhauser, K.M., et al., *Hepatocellular toxicity and pharmacological effect of amiodarone and amiodarone derivatives.* J Pharmacol Exp Ther, 2006. **319**(3): p. 1413-23.
3. Chan, K., et al., *Drug-induced mitochondrial toxicity.* Expert Opin Drug Metab Toxicol, 2005. **1**(4): p. 655-69.
4. Kaplowitz, N., *Idiosyncratic drug hepatotoxicity.* Nat Rev Drug Discov, 2005. **4**(6): p. 489-99.
5. Regev, A., *Drug-induced liver injury and drug development: industry perspective.* Semin Liver Dis, 2014. **34**(2): p. 227-39.
6. Pessayre, D., et al., *Mitochondrial involvement in drug-induced liver injury.* Handb Exp Pharmacol, 2010(196): p. 311-65.
7. Chalasani, N.P., et al., *ACG Clinical Guideline: the diagnosis and management of idiosyncratic drug-induced liver injury.* Am J Gastroenterol, 2014. **109**(7): p. 950-66; quiz 967.
8. Hussaini, S.H. and E.A. Farrington, *Idiosyncratic drug-induced liver injury: an update on the 2007 overview.* Expert Opin Drug Saf, 2014. **13**(1): p. 67-81.
9. Deavall, D.G., et al., *Drug-induced oxidative stress and toxicity.* J Toxicol, 2012. **2012**: p. 645460.
10. Deponte, M., *Glutathione catalysis and the reaction mechanisms of glutathione-dependent enzymes.* Biochim Biophys Acta, 2013. **1830**(5): p. 3217-66.
11. Lee, Y.H., et al., *Proteomics profiling of hepatic mitochondria in heterozygous Sod2+/- mice, an animal model of discreet mitochondrial oxidative stress.* Proteomics, 2008. **8**(3): p. 555-68.
12. Li, Y., et al., *Dilated cardiomyopathy and neonatal lethality in mutant mice lacking manganese superoxide dismutase.* Nat Genet, 1995. **11**(4): p. 376-81.
13. Chen, Y., et al., *Melatonin protects hepatocytes against bile acid-induced mitochondrial oxidative stress via the AMPK-SIRT3-SOD2 pathway.* Free Radic Res, 2015: p. 1-10.
14. Ahn, B.H., et al., *A role for the mitochondrial deacetylase Sirt3 in regulating energy homeostasis.* Proc Natl Acad Sci U S A, 2008. **105**(38): p. 14447-52.
15. He, W., et al., *Mitochondrial sirtuins: regulators of protein acylation and metabolism.* Trends Endocrinol Metab, 2012. **23**(9): p. 467-76.
16. Qiu, X., et al., *Calorie restriction reduces oxidative stress by SIRT3-mediated SOD2 activation.* Cell Metab, 2010. **12**(6): p. 662-7.
17. Bao, J., et al., *SIRT3 is regulated by nutrient excess and modulates hepatic susceptibility to lipotoxicity.* Free Radic Biol Med, 2010. **49**(7): p. 1230-7.
18. Verdin, E., et al., *Sirtuin regulation of mitochondria: energy production, apoptosis, and signaling.* Trends Biochem Sci, 2010. **35**(12): p. 669-75.
19. Lee, Y.H., et al., *The Sod2 mutant mouse as a model for oxidative stress: a functional proteomics perspective.* Mass Spectrom Rev, 2010. **29**(2): p. 179-96.
20. Gounden, S., et al., *Increased SIRT3 Expression and Antioxidant Defense under Hyperglycemic Conditions in HepG2 Cells.* Metab Syndr Relat Disord, 2015. **13**(6): p. 255-63.
21. Ong, M.M., et al., *Nimesulide-induced hepatic mitochondrial injury in heterozygous Sod2(+/-) mice.* Free Radic Biol Med, 2006. **40**(3): p. 420-9.
22. Coleman, M.C., et al., *Superoxide mediates acute liver injury in irradiated mice lacking sirtuin 3.* Antioxid Redox Signal, 2014. **20**(9): p. 1423-35.

23. Raza, H. and A. John, *Implications of altered glutathione metabolism in aspirin-induced oxidative stress and mitochondrial dysfunction in HepG2 cells.* PLoS One, 2012. **7**(4): p. e36325.
24. Marroquin, L.D., et al., *Circumventing the Crabtree effect: replacing media glucose with galactose increases susceptibility of HepG2 cells to mitochondrial toxicants.* Toxicol Sci, 2007. **97**(2): p. 539-47.
25. Ong, M.M., C. Latchoumycandane, and U.A. Boelsterli, *Troglitazone-induced hepatic necrosis in an animal model of silent genetic mitochondrial abnormalities.* Toxicol Sci, 2007. **97**(1): p. 205-13.
26. Liebmann, J.E., et al., *Glutathione depletion by L-buthionine sulfoximine antagonizes taxol cytotoxicity.* Cancer Res, 1993. **53**(9): p. 2066-70.

Figures

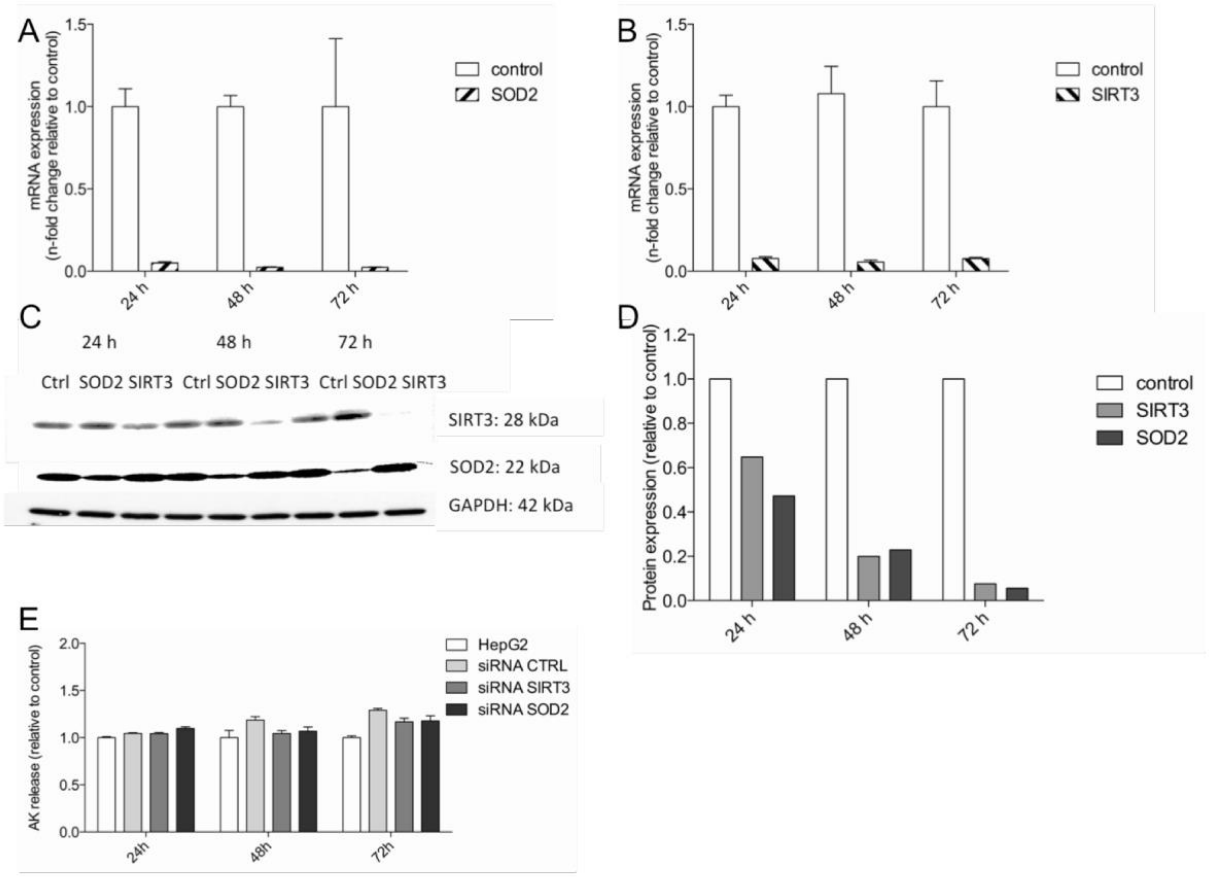

Figure 1: *mRNA and protein expression levels and cytotoxicity of transfected cells.* **A/B.** mRNA expression of mitochondrial SOD2 (A) and SIRT3 (B). Expression was measured by qRT-PCR with GAPDH as endogenous control. **C/D.** Protein expression of SOD2 and SIRT3 (C) determined by western blotting including quantification (D) of the bands obtained from three individual experiments. Quantitative results are expressed relative to control incubations. GAPDH was used to confirm equal loading **E.** Cytotoxicity was assayed using the Toxilight® assay after drug exposure for 24 h. Triton X was used as a positive control (Data not shown). Data are expressed as fold change relative to DMSO control cells and represent observations of one experiment carried out in triplicates.

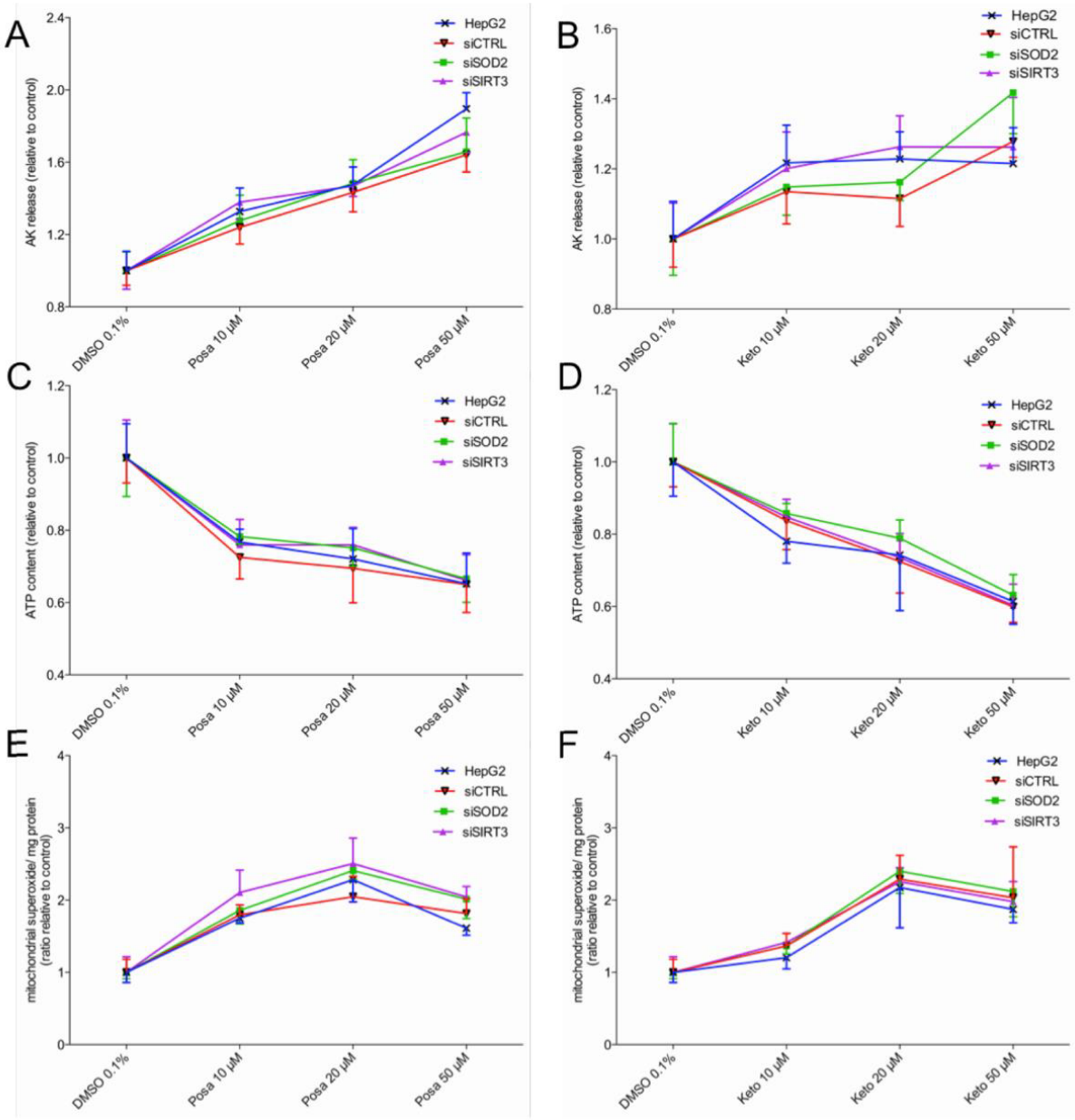

Figure 2: *Toxicity and superoxide anion accumulation of posaconazole and ketocoanzole on HepG2 cells with mitochondrial dysfunction.* Mitochondrial dysfunction was induced by a knockdown (48 h) of either SIRT3 or SOD2 in HepG2 cells. Normal HepG2 cells treated with toxicants were compared to HepG2 cells transfected with a control vector (siCTRL), and HepG2 cells transfected with either SIRT3 (siSIRT3) or SOD2 (siSOD2) treated with toxicants. **A/C**. Cytotoxicity (A) and cellular ATP content (C) after treatment with posaconazole for 24 h. **B/D**. Cytotoxicity (B) and cellular ATP content (D) after treatment with ketoconazole for 24 h. Triton X was used as a positive control (Data not shown). **E/F**. Mitochondrial accumulation of superoxide in HepG2 cells treated with posaconazole (E) or ketocoanzole (F). Mitochondrial superoxide production was measured with MitoSOX™ Red reagent after 24 h drug-treatment. Amiodarone (50 µM) served as a positive control (data not shown). Data are expressed as mean ± SD of at least three independent experiments.

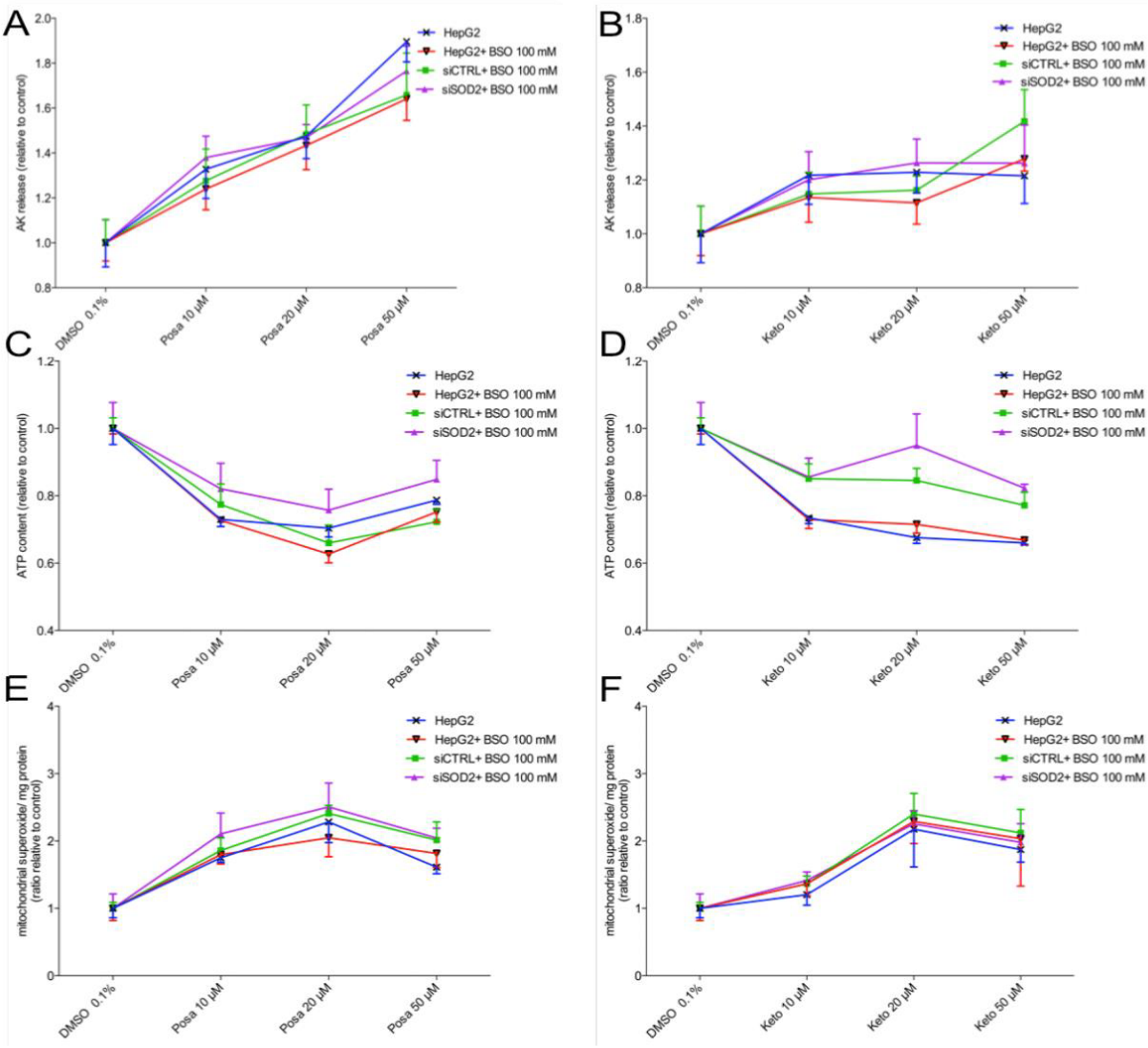

Figure 3: *Toxicity and superoxide anion accumulation of posaconazole and ketocoanzole on HepG2 cells with blunted antioxidant functions.* Mitochondrial dysfunction was induced by a knockdown (48 h) of SOD2 in HepG2 cells and a depletion of GSH stores by a pretreatment with BSO for 48 h after 24 h of transfection. Normal HepG2 cells treated w/o BSO and respective toxicants were compared to HepG2 cells, pretreated with BSO, and transfected with either a control vector (siCTRL) or HepG2 cells transfected with SOD2 (siSOD2) treated with toxicants. **A/C**. Cytotoxicity (A) and cellular ATP content (C) after treatment with posaconazole for 24 h. **B/D**. Cytotoxicity (B) and cellular ATP content (D) after treatment with ketoconazole for 24 h. Triton X was used as a positive control (Data not shown). **E/F**. Mitochondrial accumulation of superoxide in HepG2 cells treated with posaconazole (E) or ketocoanzole (F). Mitochondrial superoxide production was measured with MitoSOX™ Red reagent after 24 h drug-treatment. Amiodarone (50 µM) served as a positive control (data not shown). Data are expressed as mean ± SD of at least three independent experiments.

Table 1: Primers List

Gene	Sequence 5'-->3'
SIRT3	TCC CAG TTT CTT CTT TTC GAG T GGA AAG CTT CCC CTT GTC AC
SOD2	GGT TGT TCA CGT AGG CCG CAG CAG GCA GCT GGC T

Final discussion

Unforeseen drug-induced adverse reactions are not only one of the most feared incidences for the pharmaceutical industry but as well for health care professionals, and most importantly for patients. Such adverse reactions can lead to drug withdrawal, black box warnings and restricted use assignments [3, 11]. Although the understanding of the precise mechanisms of idiosyncratic DILI is not completely solved, research in the last few years has shown that DILI is often related with mitochondrial dysfunction [156]. Particularly preexisting or underlying mitochondrial predispositions enhance the chance of unwanted idiosyncratic toxic reactions [43]. Since no standardized guidelines exist according to which potential mitochondrial toxic drugs or new drug entities can be routinely tested, it is a need to find approaches or test systems for early discovery of idiosyncratic hepatotoxicity.

With our newly established models having subtle changes in mitochondrial function, we aimed to contribute to an increased comprehension of the complex mechanisms of mitochondrial toxicity and to the use of these models as tool of testing drugs associated with idiosyncratic mitochondrial toxicity.

HCCL induces alterations in mitochondrial function and HepG2 cells treated with HCCL serve as a model for testing drugs related to idiosyncratic mitochondrial toxicity

The chemically modified vitamin B_{12} analog HCCL competitively blocks vitamin B_{12}, which is essential for the activity of methylmalonyl-CoA mutase. MM-CoA mutase is crucial for proper catabolism of odd-chain fatty acids, and amino acids through propionate utilization [132, 135]. With HCCL, we aimed to develop a suitable cell- and mouse model with subtle mitochondrial dysfunction that can be used as a system for detecting idiosyncratic toxicity, as preexisting mitochondrial defects represent a possible risk factor that can diminish the threshold level of a mitochondrial toxicant and thus enhance the susceptibility to idiosyncratic drug reactions.

Complying with our requirements for establishing a model with specific alterations in mitochondrial function, the HCCL *in vitro* study presented inhibition of the mitochondrial respiratory chain and other functional changes of the mitochondria without affecting main cellular homeostasis. According to the findings of Krahenbuhl et al. [136] our *in vitro* findings confirmed indeed a functional decrease of several complexes (CIII and CIV) of the respiratory chain, an additionally decreased mitochondrial membrane potential ($\Delta\Psi$), and a slightly

increased oxidative stress. Moreover, we showed that HCCL implicated structural changes such as mitochondrial swelling or alterations in mitochondrial size *in vitro* which comes along with our results of the *in vivo* study where we found increased liver weight, fat inclusions and accumulation of glycogen in the liver of mice exposed to HCCL. These observations are in agreement with the study by Krahenbuhl et al. that depicted an increased hepatic capacity of rat mitochondria after exposure to HCCL [135]. Although our mouse model did not point towards mitochondrial dysfunction observed in the *in vitro* study, we could show that HCCL increased MMA levels, indicating the activity of HCCL in inducing methylmalonic aciduria. Dose finding studies showed a dose-dependent elevation of MMA in blood of HCCL treated mice and functional studies after 3 weeks of daily i.p. injections of 4 mg/kg of HCCL revealed decreased activity of complex I in liver homogenate. This is different from the fndings in rats, where complex III and IV were affected [136]. This discrepancy could be explained by interspecies differences or by the possibility that HCCL continuous exposure of rats by subcutaneous mini-pumps over 6 weeks had a higher impact on mitochondrial energy function than only 3 weeks of i.p. treatment in mice. The possibility of fluctuations in HCCL plasma and tissue levels with i.p. injection could have diminished effects on mitochondrial function.

However, since we found only minor changes in the liver and on mitochondrial function, and due to the lack of time, we abandoned the approach of the *in vivo* mouse model to test idiosyncratic toxicity and pursued the *in vitro* HCCL model for testing idiosyncratic toxicity. In fact, we clearly demonstrated that known mitochondrial toxicants including benzbromarone, dronedarone, and ketoconazole exert a higher toxicity in our proposed HCCL-cell model than in normal HepG2 cells, validating and emphasizing the assumption that underlying mitochondria-related diseases or dysfunctions may be important determinates in the development of idiosyncratic hepatotoxicity.

Methodological problems and limitations

We were confronted with several difficulties during the establishment of the HCCL model in HepG2 cells as for instance the choice of optimal conditions of HCCL treatment; we included different treatment conditions such as HCCL with and/or without propionate, since the used low-glucose media supplemented with amino acids may not be sufficient enough to serve as source of propionate in order to activate propionate metabolism, which is important for the effect of HCCL[157]. Interestingly, the combined treatment of HCCL and propionate was associated with increased sensitivity of HepG2 cells to mitochondrial toxicants but less mitochondrial damage as the treatment with HCCL alone. This could be explained by propionate's toxicity itself and the augmentation of propionate and its metabolites in the conditions HCCL/propionate, which can be associated to increased hepatotoxicity [158].

Moreover, it should be kept in mind that our model may be particularly useful in testing drugs where the mother substance and not a metabolite is mainly responsible for the toxicity, as HepG2 cells do not possess any adequate CYP450 activities. This difficulty can be circumvented, however, by using HepaRG cells after CYP induction with rifampicin.

Additionally, HepG2 cells maintained in glucose conditions may not be the ideal cell system to study mitochondrial defects due to their high glycolytic activities (crabtree-effect) and modified functions compared to human hepatocytes [115, 120, 121, 159], which may result in misleading results and potentially not reflecting the true effect in humans. The crabtree effect was circumvented by performing studies in the presence of galactose, which cannot be converted to glucose and favors mitochondrial ATP production.

Knockdown of key players of mitochondrial function – suitable systems in detecting mitochondrial toxicants?

As already mentioned, due to the paucity of models with underlying defects reflecting environmental or genetic risk factors in the development of DILI, it is a substantial necessity to create convenient models in order to understand the mechanisms of DILI and to anticipate these unwanted reactions, and above all, to early detect mitochondrial toxic agents. Although the HCCL *in vitro* model with chemically induced mitochondrial alterations appeared to be a suitable predicting model to uncover idiosyncratic toxicity, it is important to notice that there may remain the uncertainty that HCCL could implicate other unexpected cellular processes, which are not evident but still could misleadingly influence the obtained results. For this reason, we focused with the last project on the development of two cellular models with a specific knockdown of genes. The specificity of this approach should help us to understand and investigate better susceptibility factors associated with idiosyncratic toxicity.

Against our hypothesis that a depletion of important enzymes of the mitochondria leads to an increased sensitivity to idiosyncratic toxicants, the results we obtained from the cytotoxicity studies neither showed an increased toxicity after treatment with different mitochondrial toxicants on cells with a siRNA-mediated knockdown of SOD2 or SIRT3 nor depicted an elevation of ROS production compared to normal HepG2 cells. Not even the additional impairment of a second mitochondrial antioxidant defense system such as the cellular GSH content could increase the susceptibility to the applied toxicants in HepG2 cells lacking SOD2.

Since none of our proposed knockdown system showed any changes in the toxicity profile of mitochondrial toxicants, mitochondria may have additional compensatory mechanism that enable them to balance out the introduced defects. It appears that these systems have to be

reinvestigated in a more sophisticated way in order to understand better the compensatory mechanisms in cells with specific knockdown of mitochondrial enzymes or other key proteins. Furthermore, other than azole-mitochondrial toxic drugs should be tested on these models to get a larger database.

Uncovered mitochondrial toxicity for ketoconazole and the triazole posaconazole – clearing up the molecular mechanisms of azole-induced hepatotoxicity

To contribute with our knowledge about mitochondrial toxicity to clinically relevant drugs, we elucidated in the third project the problem of azole-associated hepatocellular injury. An increasing number of reports points to idiosyncratic hepatotoxicity-related side effects in many patients [9]. Mitochondrial toxicity could be a major contributor to these adverse effects. Indeed, in a few *in vitro* studies, mitochondrial impairment has clearly been identified as a mechanism of ketoconazole's hepatotoxicity [9, 141, 144, 145]. We hypothesized therefore, that the current azoles in clinical use might have the same mechanism of hepatotoxicity as observed for the structurally similar imidazole ketoconazole.

We found a strong cytotoxic potential for posaconazole and, as expected, for ketoconazole; the pronounced decrease in ATP content suggested a direct involvement of mitochondrial dysfunction. Indeed, we showed damage to several mitochondrial functions in particularly an inhibition of complexes of the ETC, but as well high levels of ROS causing oxidative stress and leading to a mitochondria-induced activation of apoptosis. Moreover, additional cytotoxicity experiments in galactose-containing media to enforce ATP production via OXPHOS, revealed increased vulnerability of HepG2 cells to the exposure of ketoconazole and posaconazole, underlining the impairment of mitochondrial energy metabolism [121].

We found that fluconazole and voriconazole did not express cytotoxic effects in HepG2 cells and HepaRG cells, although many case reports evidenced hepatotoxicity with these triazoles [9]. These observations indicate that the cell systems used in our studies are not able to detect all types of hepatotoxicity. For instance, immunological liver injury cannot be detected by our systems used.

The application of the mitochondrial-toxic azoles on the HCCL model in galactose-cultured HepG2 cells, which increased cytotoxicity, clearly showed that underlying defects in OXPHOS can act as susceptibility factors for mitochondrial toxicants [22].

In conclusion, we have expanded the knowledge on the mechanisms of azole-induced hepatotoxicity *in vitro* in particular for posaconazole, since our study is the first in characterizing the molecular mechanisms of mitochondrial toxicity of posaconazole. However, further studies in human hepatocytes should be undertaken to ensure the validity of our findings.

Promising perspectives in the early detection of DILI – future trends

Taking together, our attempts to improve the knowledge of idiosyncratic mitochondrial toxicity and the establishment of suitable systems reflecting clinical manifestations of mitochondrial dysfunction as risk factor in the development of DILI were at least partially successful.

We have shown that the chemically induced modification of mitochondrial function was successful as *in vitro* test system for the identification of increased toxicity of mitochondrial toxicants. However, chemically induced inhibition of specific functions may alter other cellular mechanisms, which may be associated with misleading results. Therefore the approach of shutting-down specific genes and knowing their impact on a cellular level may be preferable, as they minimize the chances for affecting other metabolic processes or pathways.

Despite our knockdown models were not successful to detect idiosyncratic mitochondrial toxicity, this concept remains to be further pursued and some ideas have to be reassessed. Stable knockdown of the target genes in HepG2 cells may improve the experimental setup since the foreign DNA information is integrated in the host genome, whereas siRNA only transports the RNA to the nucleus without being integrated into the genomic information [162]. With this method chances of off-target effects such as the down regulation of multiple transcripts with sequences complementary to the siRNA seed region can be reduced [163]. In addition, cells can be kept longer in this condition, enabling them to adapt their metabolism. Moreover, the use of another cell line such as HepaRG cells that are closer to human hepatocytes could also enhance the chance of creating a suitable model for testing idiosyncratic reactions. Furthermore, search for other target genes to be silenced may also improve the concept. For example the silencing of genes that are important for proper maintenance of mitochondrial function as the transcriptional factor NF-E2-related factor 2 (Nrf2) could serve as promising model for testing mitochondrial toxicants.

Our approach for the preliminary data of the siRNA model was to deplete the expression of genes that directly restore mitochondrial/cellular homeostasis. It may be of higher effectiveness to blunt Nrf2 that is a crucial nuclear factor for the activation of constitutive and inducible expression of detoxifying and antioxidant genes. Genetically modified mice that lack Nrf2 demonstrated increased susceptibility to acetaminophen-induced hepatocellular injury due to

reduced activation of Nrf2 –responsive genes, which are necessary for the promotion of antioxidant proteins [164]. Since the mitochondria are the major site of ROS production, silencing of Nrf2, be it in a cell assay approach or in a mouse model, could hold interesting insights in mitochondrial dysfunction and may be a useful test system in the screening of mitochondrial toxicants.

Other targets of interest could be the two key proteins mitochondrial transcription factor A (TFAM) and mitochondrial polymerase γ (POLG) implicated in the replication of mtDNA. The latter one is the only polymerase γ in the mitochondrial DNA holding a pivotal role in the replication and repair of mtDNA. It is well established that a mutation or defects of POLG lead to severe metabolic dysfunction because a depletion of mtDNA affects the synthesis of mitochondrial proteins and therefore the function of the respiratory chain [165]. TFAM belongs to the high mobility group proteins triggering mtDNA transcription in mammals that in turn lead to a generation of RNA primers necessary for the initiation of mtDNA replication [166, 167]. Knockout in mice of either TFAM or POLG showed a severe depletion of mtDNA and deficient respiratory chain function. Moreover polymorphisms in POLG have been clearly related with increased risk of mitochondrial toxicity with Nucleoside Reverse Transcriptase Inhibitor (NRTI) treatment [79]. On the basis of these findings, it would be of great value to apply those animal models or translating them into a cell model, which could serve as system with underlying mitochondrial defects.

Besides the approach of gene knockdown, the development or use of sophisticated cellular 3D models with organ-like interactions are more likely to provide comprehensive results with higher value, as they reflect more physiological conditions and thereby enhance the clinical relevance of *in vitro* findings. In summary, these specified strategies could help to progress in the knowledge and development of reliable prediction methods of mitochondrial dysfunction-related DILI.

In spite of all the different aspects of generating suitable screening models, it has to be mentioned that it is most unlikely to develop one single assessment method that detects mitochondrial toxicants. Rather a combination of different approaches, as already explained in **Figure 13** will enhance the predictive power to identify possible harmful drugs with high sensitivity and selectivity. To exemplify, the integrative model would subsequently incorporate data received from QSAR analysis, *in vitro* HTS toxicology studies and more in-depth functional assessment studies of mitochondrial dysfunction (e.g. siRNA models, isolated mitochondria) to specific animal models and toxicogenomics to determine mitochondrial toxic drugs [125]. However, this strategy will include a plethora of differently obtained data rendering it a major challenge to correctly conclude the outcomes and will not represent a fast screening method.

Concluding remarks

Despite some impediments, with our vision of building suitable systems with which we could identify idiosyncratic mitochondrial toxicity, we have added important new insights regarding the molecular mechanisms of mitochondrial dysfunction. Our *in vitro* HCCL model supports the assumption that mitochondrial dysfunction reflects a crucial risk factor enhancing the adverse potential of mitochondrial toxicants. We thereby reported evidence of increased toxicity of some known mitochondrial disruptors such as benzbromarone or ketoconazole under impaired energy metabolism. Above all, our established HCCL *in vitro* model showed promising potential as a tool to screen for drugs that are associated with idiosyncratic adverse effects. Beyond, we have contributed new knowledge of azole-associated adverse effects by uncovering with diverse assessment methods of mitochondrial function the mechanism of ketoconazole-and posaconazole induced idiosyncratic mitochondrial toxicity in liver cells.

This thesis highlights that mitochondrial testing needs to become a fundamental tool in preclinical research, but at the same time, the choice of cell lines, culture conditions, and assessment methods always has to be well considered in order to meet the scientific questions as accurately as possible. We have learned that HepG2 cells are suitable as a preliminary tool to screen for toxicity, but they may be inappropriate for a more complex view on interacting processes, since they are tumor-derived and do not conserve main liver functions including the CYP450 enzymes.

Nevertheless it is indispensable to take notice of studies detecting mitochondrial toxicity carried out in cells that may not exactly reflect human constitution. They all contribute to an enhanced understanding of the complexity of the rare disease state of DILI.

Above all, regulated guidelines systematically recording DILI associated with mitochondrial toxicity, as well as innovative testing system will be needed to improve the preclinical prediction of idiosyncratic toxicity.

References

1. Amacher, D.E., *The primary role of hepatic metabolism in idiosyncratic drug-induced liver injury.* Expert Opin Drug Metab Toxicol, 2012. **8**(3): p. 335-47.
2. Lee, W.M., *Drug-induced acute liver failure.* Clin Liver Dis, 2013. **17**(4): p. 575-86, viii.
3. Regev, A., *Drug-induced liver injury and drug development: industry perspective.* Semin Liver Dis, 2014. **34**(2): p. 227-39.
4. Chan, K., et al., *Drug-induced mitochondrial toxicity.* Expert Opin Drug Metab Toxicol, 2005. **1**(4): p. 655-69.
5. Kaplowitz, N., *Idiosyncratic drug hepatotoxicity.* Nat Rev Drug Discov, 2005. **4**(6): p. 489-99.
6. Roth, R.A. and P.E. Ganey, *Intrinsic versus idiosyncratic drug-induced hepatotoxicity--two villains or one?* J Pharmacol Exp Ther, 2010. **332**(3): p. 692-7.
7. Hussaini, S.H. and E.A. Farrington, *Idiosyncratic drug-induced liver injury: an update on the 2007 overview.* Expert Opin Drug Saf, 2014. **13**(1): p. 67-81.
8. Fontana, R.J., *Pathogenesis of idiosyncratic drug-induced liver injury and clinical perspectives.* Gastroenterology, 2014. **146**(4): p. 914-28.
9. Raschi, E., et al., *Assessing liver injury associated with antimycotics: Concise literature review and clues from data mining of the FAERS database.* World J Hepatol, 2014. **6**(8): p. 601-12.
10. Devarbhavi, H., *An Update on Drug-induced Liver Injury.* J Clin Exp Hepatol, 2012. **2**(3): p. 247-59.
11. Aithal, G.P., et al., *Case definition and phenotype standardization in drug-induced liver injury.* Clin Pharmacol Ther, 2011. **89**(6): p. 806-15.
12. Weiler, S., M. Merz, and G.A. Kullak-Ublick, *Drug-induced liver injury: the dawn of biomarkers?* F1000Prime Rep, 2015. **7**: p. 34.
13. Chalasani, N.P., et al., *ACG Clinical Guideline: the diagnosis and management of idiosyncratic drug-induced liver injury.* Am J Gastroenterol, 2014. **109**(7): p. 950-66; quiz 967.
14. Jaeschke, H. and M.L. Bajt, *Intracellular signaling mechanisms of acetaminophen-induced liver cell death.* Toxicol Sci, 2006. **89**(1): p. 31-41.
15. Pessayre, D., et al., *Mitochondrial involvement in drug-induced liver injury.* Handb Exp Pharmacol, 2010(196): p. 311-65.
16. Lammert, C., et al., *Relationship between daily dose of oral medications and idiosyncratic drug-induced liver injury: search for signals.* Hepatology, 2008. **47**(6): p. 2003-9.
17. Russo, M.W., et al., *Liver transplantation for acute liver failure from drug induced liver injury in the United States.* Liver Transpl, 2004. **10**(8): p. 1018-23.
18. Chalasani, N., et al., *Determinants of mortality in patients with advanced cirrhosis after transjugular intrahepatic portosystemic shunting.* Gastroenterology, 2000. **118**(1): p. 138-44.
19. Russo, M.W., et al., *Spectrum of statin hepatotoxicity: experience of the drug-induced liver injury network.* Hepatology, 2014. **60**(2): p. 679-86.
20. Daly, A.K., et al., *HLA-B*5701 genotype is a major determinant of drug-induced liver injury due to flucloxacillin.* Nat Genet, 2009. **41**(7): p. 816-9.
21. Stephens, C., M.I. Lucena, and R.J. Andrade, *Genetic variations in drug-induced liver injury (DILI): resolving the puzzle.* Front Genet, 2012. **3**: p. 253.
22. Russmann, S., G.A. Kullak-Ublick, and I. Grattagliano, *Current concepts of mechanisms in drug-induced hepatotoxicity.* Curr Med Chem, 2009. **16**(23): p. 3041-53.
23. Greil, W., et al., *Pharmacotherapeutic trends in 2231 psychiatric inpatients with bipolar depression from the International AMSP Project between 1994 and 2009.* J Affect Disord, 2012. **136**(3): p. 534-42.
24. Russmann, S., A. Jetter, and G.A. Kullak-Ublick, *Pharmacogenetics of drug-induced liver injury.* Hepatology, 2010. **52**(2): p. 748-61.
25. Dykens, J.A. and Y. Will, *The significance of mitochondrial toxicity testing in drug development.* Drug Discov Today, 2007. **12**(17-18): p. 777-85.

26. Olszewska, A. and A. Szewczyk, *Mitochondria as a pharmacological target: magnum overview.* IUBMB Life, 2013. **65**(3): p. 273-81.
27. Liguori, M.J. and J.F. Waring, *Investigations toward enhanced understanding of hepatic idiosyncratic drug reactions.* Expert Opin Drug Metab Toxicol, 2006. **2**(6): p. 835-46.
28. Wallace, K.B. and A.A. Starkov, *Mitochondrial targets of drug toxicity.* Annu Rev Pharmacol Toxicol, 2000. **40**: p. 353-88.
29. Dykens, J.A., L.D. Marroquin, and Y. Will, *Strategies to reduce late-stage drug attrition due to mitochondrial toxicity.* Expert Rev Mol Diagn, 2007. **7**(2): p. 161-75.
30. Cooper, G.M., *The Cell: A Molecular Approach. 2nd edition.* Sunderland (MA): Sinauer Associates, 2000.
31. Duchen, M.R., *Mitochondria in health and disease: perspectives on a new mitochondrial biology.* Mol Aspects Med, 2004. **25**(4): p. 365-451.
32. Wojtczak, L. and K. Zablocki, *[Mitochondria in cell life, death and disease].* Postepy Biochem, 2008. **54**(2): p. 129-41.
33. Vafai, S.B. and V.K. Mootha, *Mitochondrial disorders as windows into an ancient organelle.* Nature, 2012. **491**(7424): p. 374-83.
34. Bolisetty, S. and E.A. Jaimes, *Mitochondria and reactive oxygen species: physiology and pathophysiology.* Int J Mol Sci, 2013. **14**(3): p. 6306-44.
35. Youle, R.J. and A.M. van der Bliek, *Mitochondrial fission, fusion, and stress.* Science, 2012. **337**(6098): p. 1062-5.
36. Rafelski, S.M., *Mitochondrial network morphology: building an integrative, geometrical view.* BMC Biol, 2013. **11**: p. 71.
37. Pereira, C.V., et al., *Investigating drug-induced mitochondrial toxicity: a biosensor to increase drug safety?* Curr Drug Saf, 2009. **4**(1): p. 34-54.
38. Taylor, R.W. and D.M. Turnbull, *Mitochondrial DNA mutations in human disease.* Nat Rev Genet, 2005. **6**(5): p. 389-402.
39. Wallace, K.B., *Mitochondrial off targets of drug therapy.* Trends Pharmacol Sci, 2008. **29**(7): p. 361-6.
40. Taanman, J.W., *The mitochondrial genome: structure, transcription, translation and replication.* Biochim Biophys Acta, 1999. **1410**(2): p. 103-23.
41. Meyer, J.N., et al., *Mitochondria as a target of environmental toxicants.* Toxicol Sci, 2013. **134**(1): p. 1-17.
42. Fruehauf, J.P. and F.L. Meyskens, Jr., *Reactive oxygen species: a breath of life or death?* Clin Cancer Res, 2007. **13**(3): p. 789-94.
43. Pessayre, D., et al., *Central role of mitochondria in drug-induced liver injury.* Drug Metab Rev, 2012. **44**(1): p. 34-87.
44. Fernie, A.R., F. Carrari, and L.J. Sweetlove, *Respiratory metabolism: glycolysis, the TCA cycle and mitochondrial electron transport.* Curr Opin Plant Biol, 2004. **7**(3): p. 254-61.
45. Galluzzi, L., et al., *Mitochondrial control of cellular life, stress, and death.* Circ Res, 2012. **111**(9): p. 1198-207.
46. Houten, S.M. and R.J. Wanders, *A general introduction to the biochemistry of mitochondrial fatty acid beta-oxidation.* J Inherit Metab Dis, 2010. **33**(5): p. 469-77.
47. Fromenty, B. and D. Pessayre, *Inhibition of mitochondrial beta-oxidation as a mechanism of hepatotoxicity.* Pharmacol Ther, 1995. **67**(1): p. 101-54.
48. Beck, W.S., M. Flavin, and S. Ochoa, *Metabolism of propionic acid in animal tissues. III. Formation of succinate.* J Biol Chem, 1957. **229**(2): p. 997-1010.
49. Fenton, W.A., R.A. Gravel, and D.S. Rosenblatt, *Disorders of propionate and methylmalonate metabolism.* OMMBID- The online metabolic & molecular bases of inherited diseases, 2001.
50. Williamson, J.R. and R.H. Cooper, *Regulation of the citric acid cycle in mammalian systems.* FEBS Lett, 1980. **117 Suppl**: p. K73-85.
51. Bayir, H. and V.E. Kagan, *Bench-to-bedside review: Mitochondrial injury, oxidative stress and apoptosis--there is nothing more practical than a good theory.* Crit Care, 2008. **12**(1): p. 206.

52. Milane, L., et al., *Mitochondrial biology, targets, and drug delivery.* J Control Release, 2015. **207**: p. 40-58.
53. Alberts B, J.A., Lewis J, et al. , *Molecular Biology of the Cell*. Electron-Transport Chains and Their Proton Pumps, ed. t. edition. 2002, New York: Garland Science.
54. Balaban, R.S., S. Nemoto, and T. Finkel, *Mitochondria, oxidants, and aging.* Cell, 2005. **120**(4): p. 483-95.
55. Turrens, J.F., *Mitochondrial formation of reactive oxygen species.* J Physiol, 2003. **552**(Pt 2): p. 335-44.
56. Ott, M., et al., *Mitochondria, oxidative stress and cell death.* Apoptosis, 2007. **12**(5): p. 913-22.
57. Deavall, D.G., et al., *Drug-induced oxidative stress and toxicity.* J Toxicol, 2012. **2012**: p. 645460.
58. Liu, Y., G. Fiskum, and D. Schubert, *Generation of reactive oxygen species by the mitochondrial electron transport chain.* J Neurochem, 2002. **80**(5): p. 780-7.
59. Li, Y., et al., *Dilated cardiomyopathy and neonatal lethality in mutant mice lacking manganese superoxide dismutase.* Nat Genet, 1995. **11**(4): p. 376-81.
60. Deponte, M., *Glutathione catalysis and the reaction mechanisms of glutathione-dependent enzymes.* Biochim Biophys Acta, 2013. **1830**(5): p. 3217-66.
61. Pereira, C.V., et al., *The contribution of oxidative stress to drug-induced organ toxicity and its detection in vitro and in vivo.* Expert Opin Drug Metab Toxicol, 2012. **8**(2): p. 219-37.
62. Zahno, A., et al., *Hepatocellular toxicity of clopidogrel: mechanisms and risk factors.* Free Radic Biol Med, 2013. **65**: p. 208-16.
63. Mari, M., et al., *Redox control of liver function in health and disease.* Antioxid Redox Signal, 2010. **12**(11): p. 1295-331.
64. Bashan, N., et al., *Positive and negative regulation of insulin signaling by reactive oxygen and nitrogen species.* Physiol Rev, 2009. **89**(1): p. 27-71.
65. Choudhary, C., et al., *Lysine acetylation targets protein complexes and co-regulates major cellular functions.* Science, 2009. **325**(5942): p. 834-40.
66. Giralt, A. and F. Villarroya, *SIRT3, a pivotal actor in mitochondrial functions: metabolism, cell death and aging.* Biochem J, 2012. **444**(1): p. 1-10.
67. Houtkooper, R.H., E. Pirinen, and J. Auwerx, *Sirtuins as regulators of metabolism and healthspan.* Nat Rev Mol Cell Biol, 2012. **13**(4): p. 225-38.
68. Ahn, B.H., et al., *A role for the mitochondrial deacetylase Sirt3 in regulating energy homeostasis.* Proc Natl Acad Sci U S A, 2008. **105**(38): p. 14447-52.
69. Bao, J., et al., *SIRT3 is regulated by nutrient excess and modulates hepatic susceptibility to lipotoxicity.* Free Radic Biol Med, 2010. **49**(7): p. 1230-7.
70. Chen, Y., et al., *Tumour suppressor SIRT3 deacetylates and activates manganese superoxide dismutase to scavenge ROS.* EMBO Rep, 2011. **12**(6): p. 534-41.
71. Tao, R., et al., *Sirt3-mediated deacetylation of evolutionarily conserved lysine 122 regulates MnSOD activity in response to stress.* Mol Cell, 2010. **40**(6): p. 893-904.
72. Bause, A.S. and M.C. Haigis, *SIRT3 regulation of mitochondrial oxidative stress.* Exp Gerontol, 2013. **48**(7): p. 634-9.
73. Kim, S.C., et al., *Substrate and functional diversity of lysine acetylation revealed by a proteomics survey.* Mol Cell, 2006. **23**(4): p. 607-18.
74. Zhao, S., et al., *Regulation of cellular metabolism by protein lysine acetylation.* Science, 2010. **327**(5968): p. 1000-4.
75. Hirschey, M.D., et al., *SIRT3 regulates mitochondrial fatty-acid oxidation by reversible enzyme deacetylation.* Nature, 2010. **464**(7285): p. 121-5.
76. He, W., et al., *Mitochondrial sirtuins: regulators of protein acylation and metabolism.* Trends Endocrinol Metab, 2012. **23**(9): p. 467-76.
78. Oliveira, A.M., Nuno Machado, Telma Bernardo and Vilma Sardao *Mitochondria as a Biosensor for Drug-induced Toxicity – Is It Really Relevant?*, in *Biosensors for Health, Environment and Biosecurity*, P.P.A. Serra, Editor. 2011. p. 66-76.

79. Labbe, G., D. Pessayre, and B. Fromenty, *Drug-induced liver injury through mitochondrial dysfunction: mechanisms and detection during preclinical safety studies.* Fundam Clin Pharmacol, 2008. **22**(4): p. 335-53.
80. Elmore, S., *Apoptosis: a review of programmed cell death.* Toxicol Pathol, 2007. **35**(4): p. 495-516.
81. Kroemer, G., B. Dallaporta, and M. Resche-Rigon, *The mitochondrial death/life regulator in apoptosis and necrosis.* Annu Rev Physiol, 1998. **60**: p. 619-42.
82. Sendoel, A. and M.O. Hengartner, *Apoptotic cell death under hypoxia.* Physiology (Bethesda), 2014. **29**(3): p. 168-76.
83. Bhatia, M., *Apoptosis versus necrosis in acute pancreatitis.* Am J Physiol Gastrointest Liver Physiol, 2004. **286**(2): p. G189-96.
84. Azzolin, L., et al., *The mitochondrial permeability transition from yeast to mammals.* FEBS Lett, 2010. **584**(12): p. 2504-9.
85. Lemasters, J.J., *V. Necrapoptosis and the mitochondrial permeability transition: shared pathways to necrosis and apoptosis.* Am J Physiol, 1999. **276**(1 Pt 1): p. G1-6.
86. Malhi, H., G.J. Gores, and J.J. Lemasters, *Apoptosis and necrosis in the liver: a tale of two deaths?* Hepatology, 2006. **43**(2 Suppl 1): p. S31-44.
87. Cichoz-Lach, H. and A. Michalak, *Oxidative stress as a crucial factor in liver diseases.* World J Gastroenterol, 2014. **20**(25): p. 8082-91.
88. Han, D., et al., *Regulation of drug-induced liver injury by signal transduction pathways: critical role of mitochondria.* Trends Pharmacol Sci, 2013. **34**(4): p. 243-53.
89. St-Pierre, J., et al., *Suppression of reactive oxygen species and neurodegeneration by the PGC-1 transcriptional coactivators.* Cell, 2006. **127**(2): p. 397-408.
90. Chen, H., J.M. McCaffery, and D.C. Chan, *Mitochondrial fusion protects against neurodegeneration in the cerebellum.* Cell, 2007. **130**(3): p. 548-62.
91. Nunnari, J. and A. Suomalainen, *Mitochondria: in sickness and in health.* Cell, 2012. **148**(6): p. 1145-59.
92. Ristow, M. and K. Zarse, *How increased oxidative stress promotes longevity and metabolic health: The concept of mitochondrial hormesis (mitohormesis).* Exp Gerontol, 2010. **45**(6): p. 410-8.
93. Sreekumar, R., et al., *Effects of caloric restriction on mitochondrial function and gene transcripts in rat muscle.* Am J Physiol Endocrinol Metab, 2002. **283**(1): p. E38-43.
94. Youngman, L.D., J.Y. Park, and B.N. Ames, *Protein oxidation associated with aging is reduced by dietary restriction of protein or calories.* Proc Natl Acad Sci U S A, 1992. **89**(19): p. 9112-6.
95. Nikoletopoulou, V., et al., *Crosstalk between apoptosis, necrosis and autophagy.* Biochim Biophys Acta, 2013. **1833**(12): p. 3448-59.
96. FDA, U.F.a.D.A. *Drug-induced livery injury: premarketing clinical evaluation. In: Guidance for industry*. 2009; Available from: http://www.fda.gov/downloads/Drugs/GuidanceComplianceRegulatoryInformation/Guidances/UCM174090.pdf.
97. Temple, R., *Hy's law: predicting serious hepatotoxicity.* Pharmacoepidemiol Drug Saf, 2006. **15**(4): p. 241-3.
98. Ng, W., et al., *Animal models of idiosyncratic drug reactions.* Adv Pharmacol, 2012. **63**: p. 81-135.
99. Roth, R.A. and P.E. Ganey, *Animal models of idiosyncratic drug-induced liver injury--current status.* Crit Rev Toxicol, 2011. **41**(9): p. 723-39.
100. Boelsterli, U.A., *Animal models of human disease in drug safety assessment.* J Toxicol Sci, 2003. **28**(3): p. 109-21.
101. Boelsterli, U.A. and C.J. Hsiao, *The heterozygous Sod2(+/-) mouse: modeling the mitochondrial role in drug toxicity.* Drug Discov Today, 2008. **13**(21-22): p. 982-8.
102. Kokoszka, J.E., et al., *Increased mitochondrial oxidative stress in the Sod2 (+/-) mouse results in the age-related decline of mitochondrial function culminating in increased apoptosis.* Proc Natl Acad Sci U S A, 2001. **98**(5): p. 2278-83.

103. Ong, M.M., et al., *Nimesulide-induced hepatic mitochondrial injury in heterozygous Sod2(+/-) mice.* Free Radic Biol Med, 2006. **40**(3): p. 420-9.
104. Lee, Y.H., et al., *Troglitazone-induced hepatic mitochondrial proteome expression dynamics in heterozygous Sod2(+/-) mice: two-stage oxidative injury.* Toxicol Appl Pharmacol, 2008. **231**(1): p. 43-51.
105. Spaniol, M., et al., *Development and characterization of an animal model of carnitine deficiency.* Eur J Biochem, 2001. **268**(6): p. 1876-87.
106. Spaniol, M., et al., *Mechanisms of liver steatosis in rats with systemic carnitine deficiency due to treatment with trimethylhydraziniumpropionate.* J Lipid Res, 2003. **44**(1): p. 144-53.
107. Zaugg, C.E., et al., *Myocardial function and energy metabolism in carnitine-deficient rats.* Cell Mol Life Sci, 2003. **60**(4): p. 767-75.
108. Knapp, A.C., et al., *Toxicity of valproic acid in mice with decreased plasma and tissue carnitine stores.* J Pharmacol Exp Ther, 2008. **324**(2): p. 568-75.
109. Knapp, A.C., et al., *Effect of carnitine deprivation on carnitine homeostasis and energy metabolism in mice with systemic carnitine deficiency.* Ann Nutr Metab, 2008. **52**(2): p. 136-44.
110. Ong, M.M., C. Latchoumycandane, and U.A. Boelsterli, *Troglitazone-induced hepatic necrosis in an animal model of silent genetic mitochondrial abnormalities.* Toxicol Sci, 2007. **97**(1): p. 205-13.
111. Gomez-Lechon, M.J., et al., *Competency of different cell models to predict human hepatotoxic drugs.* Expert Opin Drug Metab Toxicol, 2014. **10**(11): p. 1553-68.
112. Brass, E.P., *Translation rates of isolated liver mitochondria under conditions of hepatic mitochondrial proliferation.* Biochem J, 1992. **288 (Pt 1)**: p. 175-80.
113. Brand, M.D. and D.G. Nicholls, *Assessing mitochondrial dysfunction in cells.* Biochem J, 2011. **435**(2): p. 297-312.
114. Felser, A., et al., *Mechanisms of hepatocellular toxicity associated with dronedarone--a comparison to amiodarone.* Toxicol Sci, 2013. **131**(2): p. 480-90.
115. Castell, J.V., et al., *Hepatocyte cell lines: their use, scope and limitations in drug metabolism studies.* Expert Opin Drug Metab Toxicol, 2006. **2**(2): p. 183-212.
116. Andersson, T.B., K.P. Kanebratt, and J.G. Kenna, *The HepaRG cell line: a unique in vitro tool for understanding drug metabolism and toxicology in human.* Expert Opin Drug Metab Toxicol, 2012. **8**(7): p. 909-20.
117. Antherieu, S., et al., *Optimization of the HepaRG cell model for drug metabolism and toxicity studies.* Toxicol In Vitro, 2012. **26**(8): p. 1278-85.
118. Pinti, M., et al., *Hepatoma HepG2 cells as a model for in vitro studies on mitochondrial toxicity of antiviral drugs: which correlation with the patient?* J Biol Regul Homeost Agents, 2003. **17**(2): p. 166-71.
119. Wojtczak, L., *The Crabtree effect: a new look at the old problem.* Acta Biochim Pol, 1996. **43**(2): p. 361-8.
120. Marroquin, L.D., et al., *Circumventing the Crabtree effect: replacing media glucose with galactose increases susceptibility of HepG2 cells to mitochondrial toxicants.* Toxicol Sci, 2007. **97**(2): p. 539-47.
121. Swiss, R. and Y. Will, *Assessment of mitochondrial toxicity in HepG2 cells cultured in high-glucose- or galactose-containing media.* Curr Protoc Toxicol, 2011. **Chapter 2**: p. Unit2 20.
122. Mueller, S.O., et al., *Drug biokinetic and toxicity assessments in rat and human primary hepatocytes and HepaRG cells within the EU-funded Predict-IV project.* Toxicol In Vitro, 2015.
123. Klein, S., et al., *Long-term maintenance of HepaRG cells in serum-free conditions and application in a repeated dose study.* J Appl Toxicol, 2014. **34**(10): p. 1078-86.
124. Mueller, D., et al., *3D organotypic HepaRG cultures as in vitro model for acute and repeated dose toxicity studies.* Toxicol In Vitro, 2014. **28**(1): p. 104-12.
125. Chen, M., et al., *Toward predictive models for drug-induced liver injury in humans: are we there yet?* Biomark Med, 2014. **8**(2): p. 201-13.
126. Bale, S.S., et al., *In vitro platforms for evaluating liver toxicity.* Exp Biol Med (Maywood), 2014. **239**(9): p. 1180-91.

127. Gaytan, B.D. and C.D. Vulpe, *Functional toxicology: tools to advance the future of toxicity testing.* Front Genet, 2014. **5**: p. 110.
128. Moore, C.B., et al., *Short hairpin RNA (shRNA): design, delivery, and assessment of gene knockdown.* Methods Mol Biol, 2010. **629**: p. 141-58.
129. Agrawal, N., et al., *RNA interference: biology, mechanism, and applications.* Microbiol Mol Biol Rev, 2003. **67**(4): p. 657-85.
130. Kiefer, J., et al., *High-throughput siRNA screening as a method of perturbation of biological systems and identification of targeted pathways coupled with compound screening.* Methods Mol Biol, 2009. **563**: p. 275-87.
131. Debnath, D.M., D.G.B.K.S. Prasad, and D.P.S. Bisen, *Omics Technology*, in *Molecular Diagnostics: Promises and Possibilities*. 2010, Springer: Netherlands. p. 11-31.
132. Stabler, S.P., et al., *Inhibition of cobalamin-dependent enzymes by cobalamin analogues in rats.* J Clin Invest, 1991. **87**(4): p. 1422-30.
133. Deodato, F., et al., *Methylmalonic and propionic aciduria.* Am J Med Genet C Semin Med Genet, 2006. **142C**(2): p. 104-12.
134. Brass, E.P., et al., *Coenzyme A metabolism in vitamin B-12-deficient rats.* J Nutr, 1990. **120**(3): p. 290-7.
135. Krahenbuhl, S., et al., *Increased hepatic mitochondrial capacity in rats with hydroxy-cobalamin[c-lactam]-induced methylmalonic aciduria.* J Clin Invest, 1990. **86**(6): p. 2054-61.
136. Krahenbuhl, S., et al., *Decreased activities of ubiquinol:ferricytochrome c oxidoreductase (complex III) and ferrocytochrome c:oxygen oxidoreductase (complex IV) in liver mitochondria from rats with hydroxycobalamin[c-lactam]-induced methylmalonic aciduria.* J Biol Chem, 1991. **266**(31): p. 20998-1003.
137. Lewis, R.E., *Current concepts in antifungal pharmacology.* Mayo Clin Proc, 2011. **86**(8): p. 805-17.
138. Kathiravan, M.K., et al., *The biology and chemistry of antifungal agents: a review.* Bioorg Med Chem, 2012. **20**(19): p. 5678-98.
139. Lass-Florl, C., *Triazole antifungal agents in invasive fungal infections: a comparative review.* Drugs, 2011. **71**(18): p. 2405-19.
140. Larru, B. and T.E. Zaoutis, *Newer antifungal agents.* Curr Opin Pediatr, 2013. **25**(1): p. 110-5.
141. Rodriguez, R.J. and D. Acosta, Jr., *Inhibition of mitochondrial function in isolated rate liver mitochondria by azole antifungals.* J Biochem Toxicol, 1996. **11**(3): p. 127-31.
142. Rodriguez, R.J. and D. Acosta, Jr., *Metabolism of ketoconazole and deacetylated ketoconazole by rat hepatic microsomes and flavin-containing monooxygenases.* Drug Metab Dispos, 1997. **25**(6): p. 772-7.
143. Rodriguez, R.J. and D. Acosta, Jr., *N-deacetyl ketoconazole-induced hepatotoxicity in a primary culture system of rat hepatocytes.* Toxicology, 1997. **117**(2-3): p. 123-31.
144. Rodriguez, R.J. and D. Acosta, Jr., *Comparison of ketoconazole- and fluconazole-induced hepatotoxicity in a primary culture system of rat hepatocytes.* Toxicology, 1995. **96**(2): p. 83-92.
145. Rodriguez, R.J. and C.J. Buckholz, *Hepatotoxicity of ketoconazole in Sprague-Dawley rats: glutathione depletion, flavin-containing monooxygenases-mediated bioactivation and hepatic covalent binding.* Xenobiotica, 2003. **33**(4): p. 429-41.
146. Mast, N., et al., *Antifungal Azoles: Structural Insights into Undesired Tight Binding to Cholesterol-Metabolizing CYP46A1.* Mol Pharmacol, 2013. **84**(1): p. 86-94.
147. Gupta, A.K. and D.C. Lyons, *The Rise and Fall of Oral Ketoconazole.* J Cutan Med Surg, 2015.
148. Lewis, J.H., et al., *Hepatic injury associated with ketoconazole therapy. Analysis of 33 cases.* Gastroenterology, 1984. **86**(3): p. 503-13.
149. Bernuau, J., F. Durand, and D. Pessayre, *Ketoconazole-induced hepatotoxicity.* Hepatology, 1997. **26**(3): p. 802.
150. Zonios, D., et al., *Voriconazole metabolism, toxicity, and the effect of cytochrome P450 2C19 genotype.* J Infect Dis, 2014. **209**(12): p. 1941-8.

151. Stevens, D.A., *Advances in systemic antifungal therapy.* Clin Dermatol, 2012. **30**(6): p. 657-61.
152. Felser, A., et al., *Hepatic toxicity of dronedarone in mice: role of mitochondrial beta-oxidation.* Toxicology, 2014. **323**: p. 1-9.
153. FDA, U.F.a.D.A., *MedWatch The FDA Safety Information and Adverse Event Reporting ProgramSafety Information.* 2014.
154. Lee, M.H., et al., *A benefit-risk assessment of benzbromarone in the treatment of gout. Was its withdrawal from the market in the best interest of patients?* Drug Saf, 2008. **31**(8): p. 643-65.
155. Felser, A., et al., *Hepatocellular toxicity of benzbromarone: effects on mitochondrial function and structure.* Toxicology, 2014. **324**: p. 136-46.
156. Tujios, S. and R.J. Fontana, *Mechanisms of drug-induced liver injury: from bedside to bench.* Nat Rev Gastroenterol Hepatol, 2011. **8**(4): p. 202-11.
157. Sauer, S.W., et al., *Long-term exposure of human proximal tubule cells to hydroxycobalamin[c-lactam] as a possible model to study renal disease in methylmalonic acidurias.* J Inherit Metab Dis, 2009. **32**(6): p. 720-7.
158. Horster, F. and G.F. Hoffmann, *Pathophysiology, diagnosis, and treatment of methylmalonic aciduria-recent advances and new challenges.* Pediatr Nephrol, 2004. **19**(10): p. 1071-4.
159. Thompson, R.A., et al., *In vitro approach to assess the potential for risk of idiosyncratic adverse reactions caused by candidate drugs.* Chem Res Toxicol, 2012. **25**(8): p. 1616-32.
160. Gubbins, P.O., *Triazole antifungal agents drug-drug interactions involving hepatic cytochrome P450.* Expert Opin Drug Metab Toxicol, 2011. **7**(11): p. 1411-29.
161. Lee, Y.H., et al., *The Sod2 mutant mouse as a model for oxidative stress: a functional proteomics perspective.* Mass Spectrom Rev, 2010. **29**(2): p. 179-96.
162. Kim, T.K. and J.H. Eberwine, *Mammalian cell transfection: the present and the future.* Anal Bioanal Chem, 2010. **397**(8): p. 3173-8.
163. Jackson, A.L. and P.S. Linsley, *Recognizing and avoiding siRNA off-target effects for target identification and therapeutic application.* Nat Rev Drug Discov, 2010. **9**(1): p. 57-67.
164. Aleksunes, L.M. and J.E. Manautou, *Emerging role of Nrf2 in protecting against hepatic and gastrointestinal disease.* Toxicol Pathol, 2007. **35**(4): p. 459-73.
165. Facucho-Oliveira, J.M., et al., *Mitochondrial DNA replication during differentiation of murine embryonic stem cells.* J Cell Sci, 2007. **120**(Pt 22): p. 4025-34.
166. Parisi, M.A. and D.A. Clayton, *Similarity of human mitochondrial transcription factor 1 to high mobility group proteins.* Science, 1991. **252**(5008): p. 965-9.
167. Garstka, H.L., et al., *Import of mitochondrial transcription factor A (TFAM) into rat liver mitochondria stimulates transcription of mitochondrial DNA.* Nucleic Acids Res, 2003. **31**(17): p. 5039-47.